Circularly polarized microstrip phased array antennas for mobile communications (a theoretical research)

Visser, H.J.

Award date:
1989

EINDHOVEN UNIVERSITY OF TECHNOLOGY
DEPARTMENT OF ELECTRICAL ENGINEERING
PROFESSIONAL GROUP ELECTROMAGNETISM AND
CIRCUIT THEORY

CIRCULARLY POLARIZED MICROSTRIP PHASED ARRAY ANTENNAS FOR MOBILE COMMUNICATIONS

(a theoretical research)

by H.J. Visser

ET- 3 - 89

This study has been performed in fulfilment of the requirements for the degree of Master of Science (Ir.) at the Eindhoven University of Technology, Department of Electrical Engineering from March 1988 until February 1989 under supervision of Dr. M.E.J. Jeuken.
Eindhoven, February 1989.

Summary

This report describes a theoretical investigation of microstrip array antennas for mobile communications. The antennas are designed for L-band use with a circular polarization of the electric field. The characteristics are compared with requirements from INMARSAT and MSATX.

The choise for the microstrip element has been made in favour of the circular patch, because of the ease in handling the far field equations of this radiating element. For practical use however, it will be necessary to broaden the VSWR-bandwidth of this patch. The patch described in this report will not do.

First different fixed beam arrays are discussed. Circular polarization is obtained by use of circularly polarized patches or by use of sequentially rotated and fed linearly polarized patches. The best compromise between performance and costs are given by: a 4x4-array composed of circularly polarized patches on a substrate with dielectric constant $\varepsilon_r = 2.33$, a 4x4-array composed of sequentially rotated and fed linearly polarized patches on the same dielectric substrate, or a 16-element circular array composed of sequentially rotated and fed linearly polarized patches on the same substrate.

After the fixed beam antennas, scanned beam antennas (phased array antennas) are discussed. The best compromise between performance and cost is given by: a 4x4-subarraylevel-scanned-array, composed of sequentially rotated and fed linearly polarized patches on a substrate with dielectric constant $\varepsilon_r = 6$.

This antenna nearly meets the MSATX-requirements. The axial ratio will be less than 4dB for a maximum scanangle $\vartheta_s = 55^0$.

Applying the sequential rotation technique can reduce the antenna gain. For small elementspacings the gain is nearly equal to the gain of an array composed of circularly polarized patches. For increasing spacing the gain loss can exceed 6dB for a 16-element array.

Wilkinson power splitters are recommended for use in the feeding network of the array. This because of the good isolation between output ports and the nearly zero reflection coefficient at the input when 90^0-phaseshifters are used in the network.

For keeping track of the satellite, the simultaneous lobe comparison technique is applied to the phased arrays.

CONTENTS

1. INTRODUCTION

Because of their thin planar configuration and their relative low cost, microstrip antennas have gained an increasing interest in scientific research, especially in the field of mobile satellite communications.
This report deals with the theoretical design of a small circularly polarized microstrip phased array antenna, that can, for example, be positioned on a truck and is suitable for L-band communication with a satellite at 1.5 GHz and 1.6 GHz. Special attention is paid to maintaining circular polarization, while scanning the hemisphere and array techniques to realize the necessary bandwidth with the inherent narrow band microstrip patches.

§1.1 - Choice of patch shape

A great variety of microstrip antenna shapes is known, of which the most important are the rectangular one and the circular one (see figure 1.1).

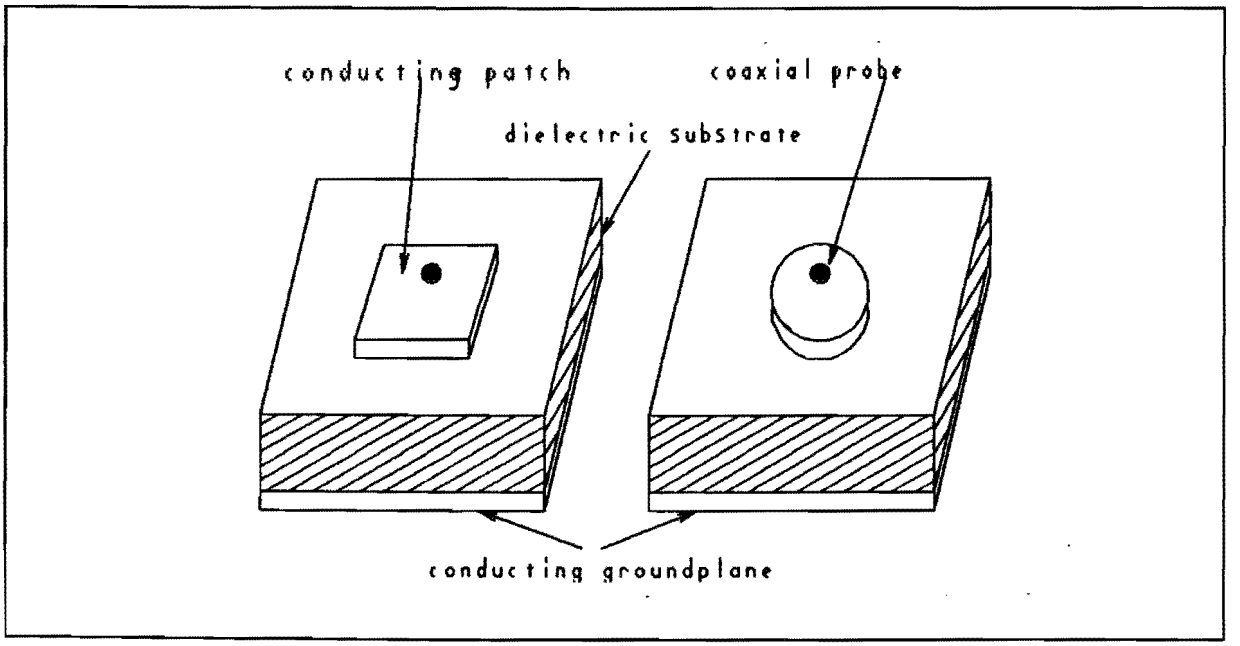

Fig. 1.1 - Microstrip patch antennas

For the theoretical analysis the choice has been made in favor of circularly shaped microstrip patches. As can be seen in table 1.1 [1-1], the electrical behavior of a rectangular microstrip patch is slightly better than that of a circular one, at the expense of a larger physical area.

Table 1.1 - Microstrip patch characteristics

Characteristic	Configuration	
	Rectangular	Circular Disk
I Radiation:		
Beam Position	Broadside	Broadside
3dB Beamwidth		
E-plane	111^0	100^0
H-plane	123^0	80^0
First Side Lobe Level		
E-plane	-	-
H-plane	-	-
Directivity	7.08dB	7.1dB
Efficiency	99.8%	94%
Gain	7.07dB	6.8dB
II Bandwidth:		
2:1 VSWR Bandwidth	2%	1.1%
III Physical Area		
Area of Patch	$28.2cm^2$	$24.3cm^2$

In spite of the above, the choice has been made for circularly shaped microstrip patches, because of the ease in handling the far field equations, which is quite cumbersome in the case of the rectangular shaped microstrip patch. The results of the analysis can, if necessary, be transformed to the case of the rectangular shaped microstrip patch. To illustrate the remarks about the ease in handling the far field equations for the circular microstrip antenna, those equations are given for a rectangular patch and for a circular patch.

The far field equations for the rectangular patch antenna are given by [1-2]:

$$E_\varphi = \frac{jke^{-jkr}}{4\pi r} \cdot 2E_0 \Delta (a+\Delta) \cos\left(\frac{k(b+\Delta)}{2} \cdot \sin\vartheta\cos\varphi\right) \cdot$$

$$\cdot \operatorname{sinc}\left(\frac{k(a+\Delta)}{2} \sin\vartheta\sin\varphi\right) \cos\vartheta\sin\varphi \cdot$$

$$\cdot \left\{ \operatorname{sinc}\left(\frac{k\Delta}{2} \sin\vartheta\cos\varphi\right) + \frac{k^2\sin^2\vartheta\cos^2\varphi}{\left(\frac{\pi}{b+\Delta} - k^2\sin^2\vartheta\cos^2\varphi\right)} \cdot \right.$$

$$\left. \cdot \operatorname{sinc}\left(\frac{k\Delta}{2} \sin\vartheta\sin\varphi\right) \right\} \qquad (1.1a)$$

$$E_\vartheta = \frac{jke^{-jkr}}{4\pi r} \cdot 2E_0 \Delta (a+\Delta) \cos\left(\frac{k(b+\Delta)}{2} \cdot \sin\vartheta\cos\varphi\right) \cdot$$

$$\cdot \operatorname{sinc}\left(\frac{k(a+\Delta)}{2} \sin\vartheta\sin\varphi\right) \cos\varphi \cdot$$

$$\cdot \left\{ \operatorname{sinc}\left(\frac{k\Delta}{2} \sin\vartheta\cos\varphi\right) \cdot \frac{k^2\sin^2\vartheta\sin^2\varphi}{\left(\frac{\pi}{b+\Delta} - k^2\sin^2\vartheta\cos^2\varphi\right)} + \right.$$

$$\left. -\operatorname{sinc}\left(\frac{k\Delta}{2} \sin\vartheta\cos\varphi\right) \right\} \qquad (1.1b)$$

with

$$\operatorname{sinc}(x) = \frac{\sin(x)}{x} \qquad (1.1c)$$

and a and b the dimensions of the patch and Δ the width of the radiating slots.

The far field equations of the circular patch antenna are given by [1-1]:

$$E_\varphi = j^n \cdot \frac{Vak_0}{2} \cdot \frac{e^{-jk_0 r}}{r} \cdot \cos\vartheta \sin(n\varphi) \cdot [J_{n+1}(k_0 a \sin\vartheta) + J_{n-1}(k_0 a \sin\vartheta)] \quad (1.2a)$$

$$E_\vartheta = j^n \cdot \frac{Vak_0}{2} \cdot \frac{e^{-jk_0 r}}{r} \cdot \cos(n\varphi) \cdot [J_{n+1}(k_0 a \sin\vartheta) - J_{n-1}(k_0 a \sin\vartheta)] \quad (1.2b)$$

with a the radius of the patch and V the voltage across the patch. Observe that for the circular shaped patch, the ϑ- and φ-dependence are separated. This is a second reason for the choise in favor of the circular shaped patch, because the technique of sequential rotation, which will be discussed in a forthcoming section, can be understood for this special case.

§1.2 - Organization of the report

The organization of the report is as follows. First of all, in chapter 2, important antenna characteristics, including the ones dealing with polarization, are defined and antenna specifications for future mobile communication projects, as required by INMARSAT and MSATX, are stated. Chapter 3 deals with methods for realizing circular polarization with a single microstrip antenna and realizing circular polarization with a microstrip array antenna. In one of the methods circular polarization is obtained by use of linearly polarized antenna elements. For the various antennas developed in this chapter, the characteristics, as defined in chapter 2, will be discussed.
In chapter 4 the theory is extended with scanning properties of microstrip array antennas. Use of new dielectric materials will make it possible to scan on 'subarray level'. This will turn out to be a phase shifter reducing invention.
In chapter 5 the microstrip antenna is analyzed using the cavity model, the results of which will be used in the analysis of the feeding network of a microstrip array antenna, which consists of microstriplines, power dividers and phase shifters.
In chapter 6 is discussed a method of keeping track of the satellite. This method is based on 'sequential lobing technique' or 'monopulse technique'.

§1.3 - References

[1-1] Bahl I.J., Bhartia P., *'Microstrip Antennas '*,
Artech House, 1980.

[1-2] Hammer P., Van Bouchaute D., Verschraeven D., Van de Capelle D., *'A Model For Calculating The Radiation Field Of Microstrip Antennas '*,
IEEE Trans. on Antennas & Propagation, Vol.AP-27, 1979, No.2, pp.267-270.

2. SPECIFICATIONS AND DEFINITIONS

Before something can be said about the antenna specifications, as asked for by INMARSAT (International Maritime Satellite Organization) and NASA for future mobile communications systems, it is necessary to pay attention to the definitions used in these specifications. In the following these definitions will be given and explained, after which the INMARSAT specifications and specifications for the NASA sponsored MSATX (Mobile Satellite Experiment) will be described.

§2.1 - Definitions

The characteristics of an antenna are described by quantities like polarization, polarization loss and axial ratio, as far as the polarization of the field is concerned and by directivity and gain in connection with the radiated or received power. These quantities will be described below, with emphasis on circular polarization because this type of polarization will be employed in the mobile satellite services. This aspect will be explained in detail in section 2.1.1.

§2.1.1 - Circular polarization

The far field equations of an antenna can, in general, be written as [2-1]:

$$\bar{E}(r,\vartheta,\varphi) = E_{\vartheta}(r,\vartheta,\varphi)\cdot\bar{a}_{\vartheta} + E_{\varphi}(r,\vartheta,\varphi)\cdot\bar{a}_{\varphi} \qquad (2.1a)$$

$$\bar{H}(r,\vartheta,\varphi) = H_{\vartheta}(r,\vartheta,\varphi)\cdot\bar{a}_{\vartheta} + H_{\varphi}(r,\vartheta,\varphi)\cdot\bar{a}_{\varphi} \qquad (2.1b)$$

The above equations are given in spherical coordinates. The two coordinate systems are depicted in figure 2.1 and the relationship between spherical and cartesian coordinates is given by the relations (2.2).

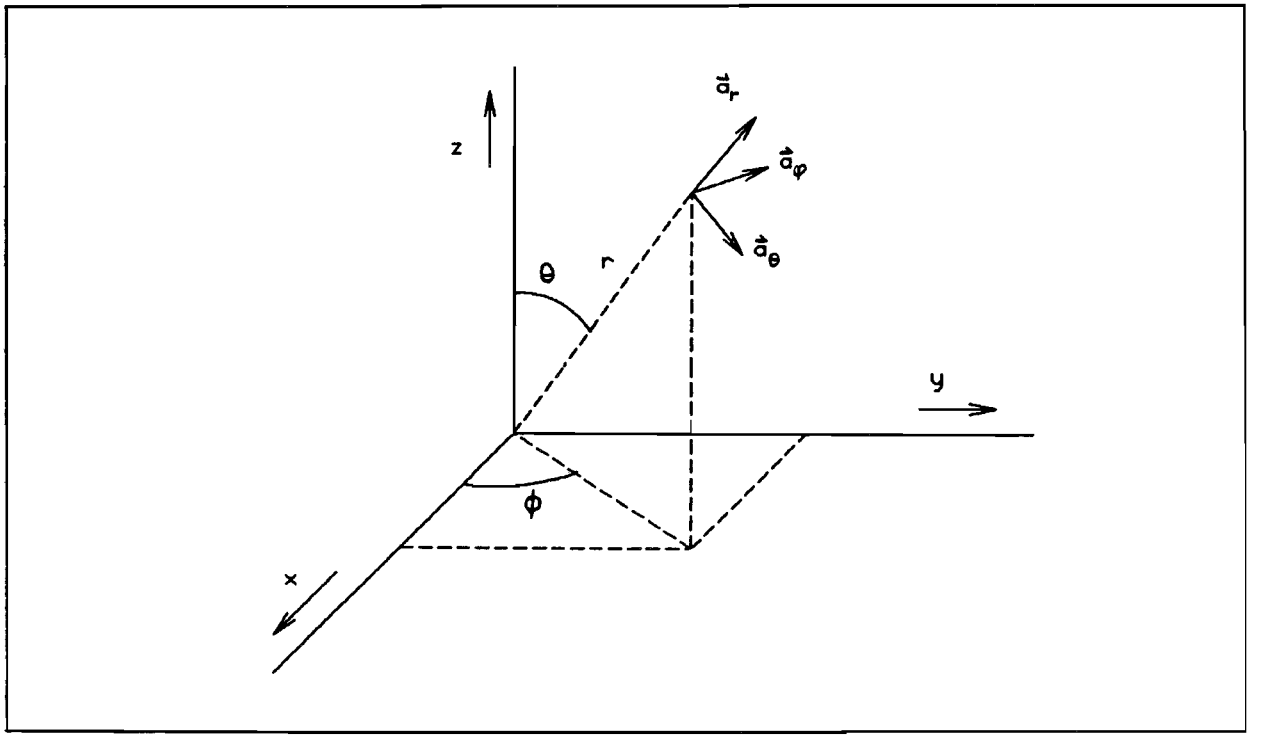

Fig.2.1 - Spherical and cartesian coordinates

$$\bar{a}_r = \sin\vartheta\cdot\cos\varphi\cdot\bar{a}_x + \sin\vartheta\cdot\sin\varphi\cdot\bar{a}_y + \cos\vartheta\cdot\bar{a}_z \qquad (2.2a)$$

$$\bar{a}_\vartheta = \cos\vartheta\cdot\cos\varphi\cdot\bar{a}_x + \cos\vartheta\cdot\sin\varphi\cdot\bar{a}_y - \sin\vartheta\cdot\bar{a}_z \qquad (2.2b)$$

$$\bar{a}_\varphi = -\sin\varphi\cdot\bar{a}_x + \cos\varphi\cdot\bar{a}_y \qquad (2.2c)$$

Returning to equation (2.1a):

$$\bar{E}(r,\vartheta,\varphi) = E_\vartheta(r,\vartheta,\varphi)\cdot\bar{a}_\vartheta + E_\varphi(r,\vartheta,\varphi)\cdot\bar{a}_\varphi \qquad (2.1a)$$

The $\bar{E}$ vector lies in the plane build up by the unit vectors $\bar{a}_\vartheta$ and $\bar{a}_\varphi$. E_ϑ and E_φ are phasor components in the direction of the unit vectors, thus having amplitude and phase:

$$E_\vartheta = |E_\vartheta| \cdot e^{j\psi_\vartheta} \tag{2.3a}$$

$$E_\varphi = |E_\varphi| \cdot e^{j\psi_\varphi} \tag{2.3b}$$

The $\bar{E}$ field can be written as:

$$\bar{E} = |E_\vartheta| \cdot e^{j\psi_\vartheta} \cdot (\bar{a}_\vartheta + \rho \cdot \bar{a}_\varphi) \tag{2.4a}$$

with

$$\rho = \frac{|E_\varphi|}{|E_\vartheta|} \cdot e^{j(\psi_\varphi - \psi_\vartheta)} \tag{2.4b}$$

If time is included in equation (2.4) the extremity of the vector $\bar{E}$ can be traced in space as a function of time. This figure is called the polarization of the wave [2-2]. The figure appears to be an ellipse in the ϑ,φ-plane with the electric field rotating either clockwise or counterclockwise (see figure 2.2). The proof of this is given in appendix A [2-1].

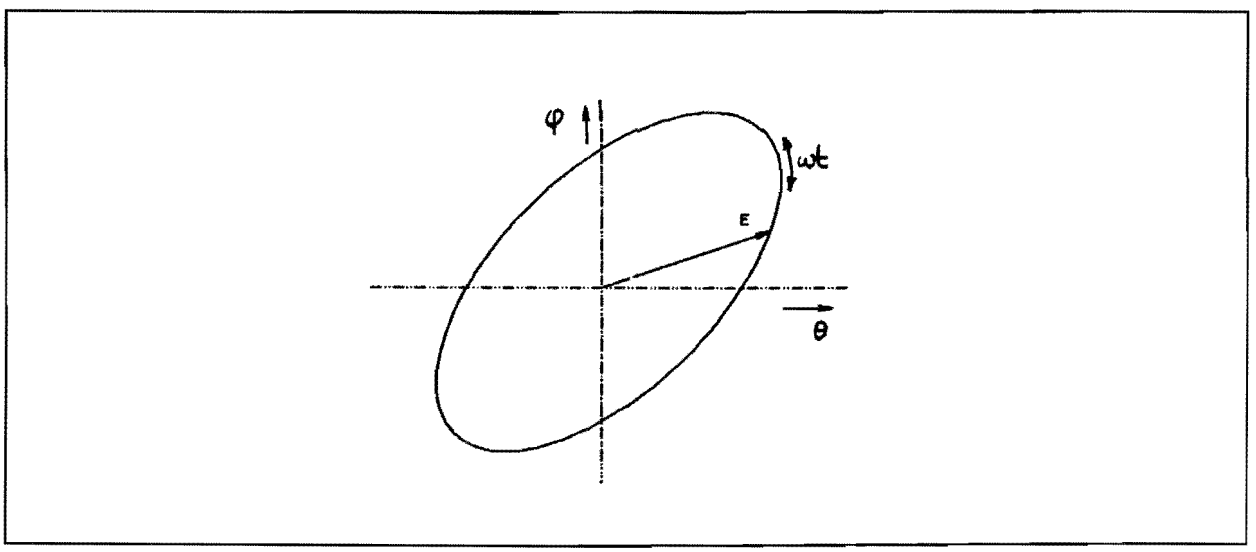

Fig.2.2 - Polarization ellipse

In general the polarization figure is an ellipse and the polarization called elliptical. If $(\psi_\varphi - \psi_\vartheta) = 0$ or $(\psi_\varphi - \psi_\vartheta) = \pi$, the electric field describes a straight line in space and time and the polarization is called linear.
If:

$$(\psi_\varphi - \psi_\vartheta) = \pm \frac{\pi}{2} \tag{2.5a}$$

$$|E_\vartheta| = |E_\varphi| \tag{2.5b}$$

equation (2.4a) can be written as:

$$\bar{E} = |E_\vartheta| \cdot e^{j\psi_\vartheta} \cdot (\bar{a}_\vartheta \pm j \cdot \bar{a}_\varphi) \tag{2.6}$$

Including the time dependence in the above equation, the $\bar{E}$-vector now describes a circle in the ϑ,φ-plane in time. For the formula with +j, when looking in the direction of propagation, the electric field rotates counterclockwise and the polarization is called Left Hand Circular (LHC). For the formula with -j, when looking in the direction of propagation, the electric field rotates clockwise and the polarization is called Right Hand Circular (RHC) [2-3]. These rotations are presented in figure 2.3.

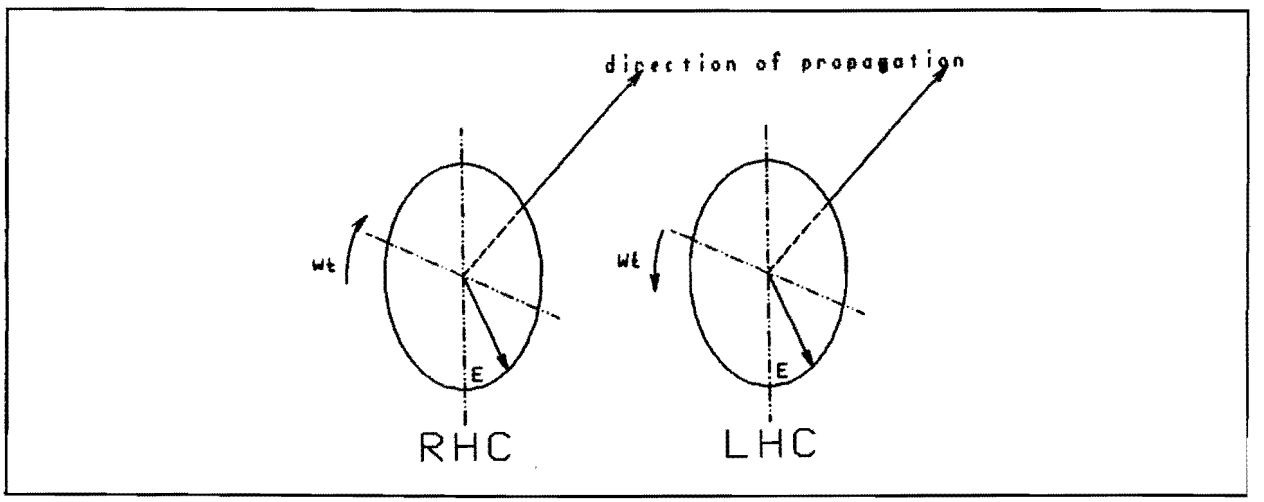

Fig.2.3 - Circular polarization

In mobile satellite communications it is this kind of polarization that is needed, because mobile satellite communications use the 1.5-1.6GHz band, where the ionosphere acts as a Faraday rotator [2-4]. That is: a linearly polarized wave rotates upon passing the ionosphere, as depicted in figure 2.4.

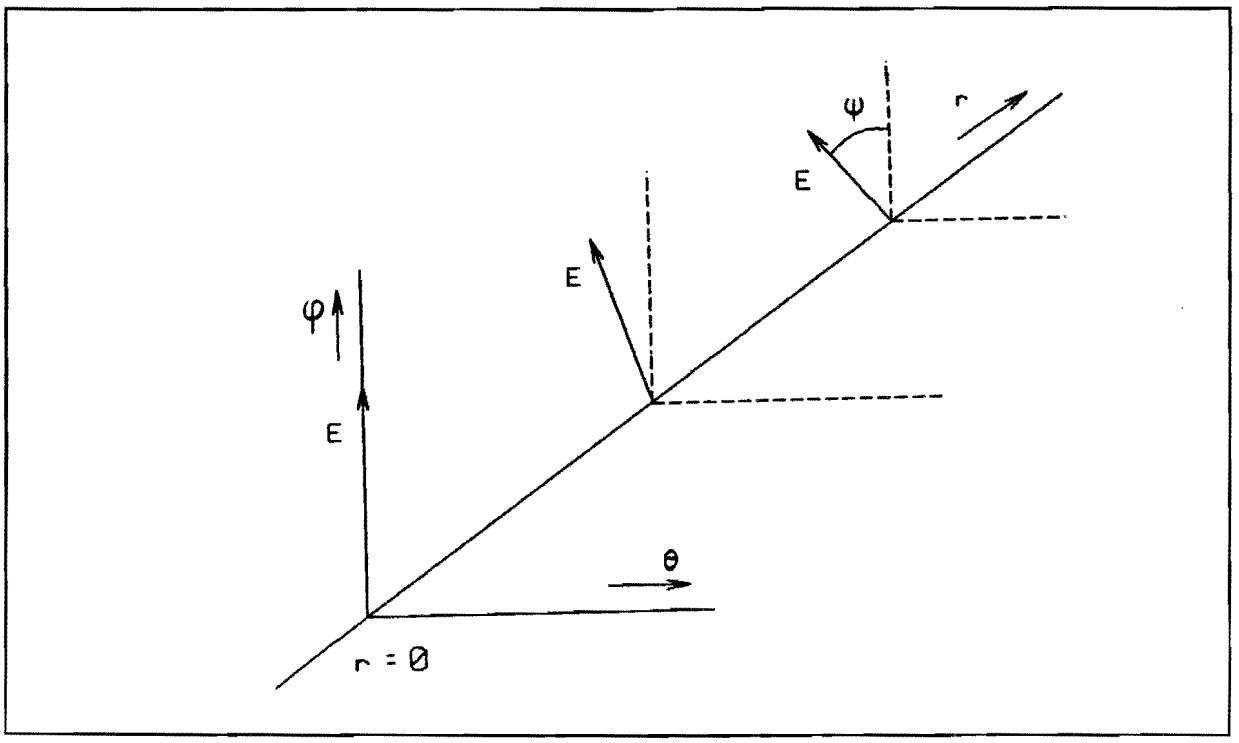

Fig.2.4 - Rotation of a linearly polarized wave in the ionosphere

If antennas for satellite communications are designed for transmitting and receiving circularly polarized waves, no disadvantageous effects of the ionosphere will be experienced.

§2.1.2 - Polarization Loss

If the polarization of transmitting antenna and receiving antenna in a communication link are not matched, an extra loss, called the polarization loss, is added to the path loss. Assuming an antenna, transmitting in the $\bar{r}$-direction (see figure 2.1), the electric field is given by:

$$\bar{E}_{tr} = E_{\vartheta} \cdot (\bar{a}_{\vartheta} + \rho_{tr} \cdot \bar{a}_{\varphi}) \tag{2.7a}$$

with:

$$\rho_{tr} = |\rho_{tr}| \cdot e^{j\delta_{tr}} \tag{2.7b}$$

The incident wave on the receiving antenna is given by:

$$\bar{E}_{re} = E_{\vartheta} \cdot (\bar{a}_{\vartheta} + \rho_{re} \cdot \bar{a}_{\varphi}) \tag{2.8a}$$

with:

$$\rho_{re} = |\rho_{re}| \cdot e^{j\delta_{re}} \tag{2.8b}$$

The response of the receiving antenna to the incident wave is given by:

$$\begin{aligned} \bar{E}_{tr} \cdot \bar{E}^{*}_{re} &= E_{\vartheta} \cdot E^{*}_{\vartheta} \cdot (\bar{a}_{\vartheta} + \rho_{tr} \cdot \bar{a}_{\varphi}) \cdot (\bar{a}_{\vartheta} + \rho^{*}_{re} \cdot \bar{a}_{\varphi}) \\ &= E_{\vartheta} \cdot E^{*}_{\vartheta} \cdot (1 + \rho_{tr} \cdot \rho^{*}_{re}) \end{aligned} \tag{2.9}$$

If the transmitted and received fields are normalized, the loss due to the polarization mismatch can be found.

$$\bar{E}'_{tr} = \frac{\bar{a}_{\vartheta} + \rho_{tr}\cdot\bar{a}_{\varphi}}{\sqrt{1 + \rho_{tr}\cdot\rho^{*}_{tr}}} \qquad (2.10a)$$

$$\bar{E}'^{*}_{re} = \frac{\bar{a}_{\vartheta} + \rho^{*}_{re}\cdot\bar{a}_{\varphi}}{\sqrt{1 + \rho_{re}\cdot\rho^{*}_{re}}} \qquad (2.10b)$$

The normalized voltage response is:

$$\frac{1 + \rho_{tr}\cdot\rho^{*}_{re}}{\sqrt{1 + \rho_{tr}\cdot\rho^{*}_{tr}}\cdot\sqrt{1 + \rho_{re}\cdot\rho^{*}_{re}}} \qquad (2.11)$$

This expression can be transformed to a power response:

$$\Gamma = \frac{1 + |\rho_{tr}|^2\cdot|\rho_{re}|^2 + 2\cdot|\rho_{tr}|\cdot|\rho_{re}|\cdot\cos(\delta_{\rho_{re}} - \delta_{\rho_{tr}})}{(1 + |\rho_{tr}|^2)\cdot(1 + |\rho_{re}|^2)} \qquad (2.12)$$

Γ is called the polarization efficiency or, somewhat misleading, the polarization loss.

§2.1.3 - Axial Ratio

Because the polarization efficiency Γ is not a quantity easy to measure, another quantity which accounts for the polarization mismatch will be discussed here. This quantity is called the axial ratio. For the discussion of the axial ratio remind figure 2.2. The polarization ellipse, depicted in this figure, can be considered to arise from the vectorial addition of two rotating vectors. One rotating clockwise and the other rotating counterclockwise. Or in other words: an elliptically polarized wave can be splitted up in a Right Hand Circularly polarized wave and a Left Hand Circularly polarized wave.

With this, equation (2.1a) can be written as:

$$\bar{E} = E_\vartheta \cdot \bar{a}_\vartheta + E_\varphi \cdot \bar{a}_\varphi = E_L \cdot \bar{a}_L + E_R \cdot \bar{a}_R \tag{2.13}$$

with unit vectors:

$$\bar{a}_L = \frac{1}{\sqrt{2}} \cdot (\bar{a}_\vartheta + j\bar{a}_\varphi) \tag{2.14a}$$

$$\bar{a}_R = \frac{1}{\sqrt{2}} \cdot (\bar{a}_\vartheta - j\bar{a}_\varphi) \tag{2.14b}$$

and:

$$E_L = \frac{1}{\sqrt{2}} \cdot (E_\vartheta - jE_\varphi) \tag{2.15a}$$

$$E_R = \frac{1}{\sqrt{2}} \cdot (E_\vartheta + jE_\varphi) \tag{2.15b}$$

E_L is the LHC component of the wave, E_R is the RHC component of the wave. The relationship between elliptical poarization and both circular polarizations is graphically represented in figure 2.5.

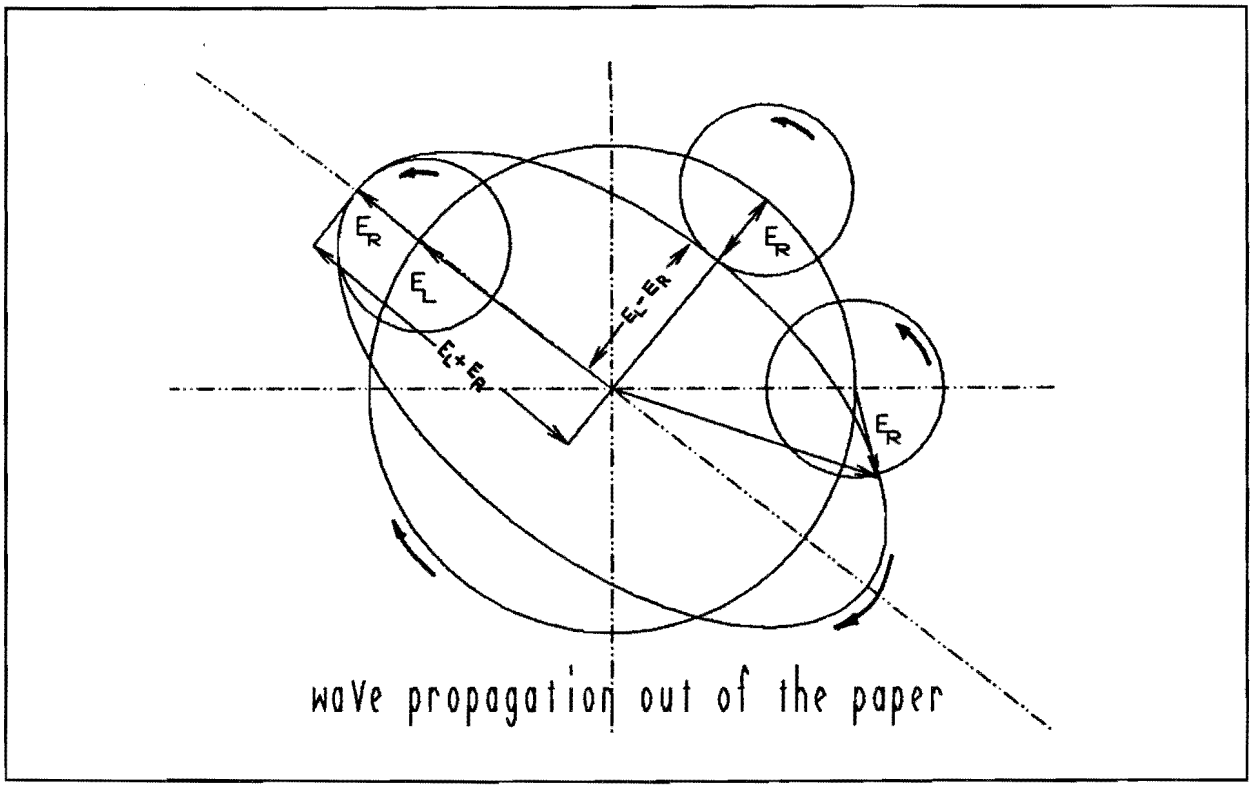

Fig.2.5 - Polarization ellipse with RHC and LHC components

In a predominately Left Hand Circularly polarized wave (as depicted in the above figure), the LHC component is called the copolarization and the RHC component is called the crosspolarization. The opposite is true for a predominately Right Hand Circularly polarized wave.
The axial ratio now is defined as [2-2]:

$$\text{Axial Ratio} = \frac{E_{max}}{E_{min}} = \frac{|E_L| + |E_R|}{|E_L| - |E_R|} \quad \text{LHC} \qquad (2.16a)$$

$$= \frac{|E_L| + |E_R|}{|E_R| - |E_L|} \quad \text{RHC} \qquad (2.16b)$$

In general:

$$\text{Axial Ratio} = \left| \frac{|E_L| + |E_R|}{|E_L| - |E_R|} \right| \qquad (2.17)$$

If the radiation pattern of an antenna is measured by the method of the ' spinning dipole ' [2-5, 2-6], the axial ratio can be extracted from the radiation pattern as indicated in figure 2.6 [2-6].

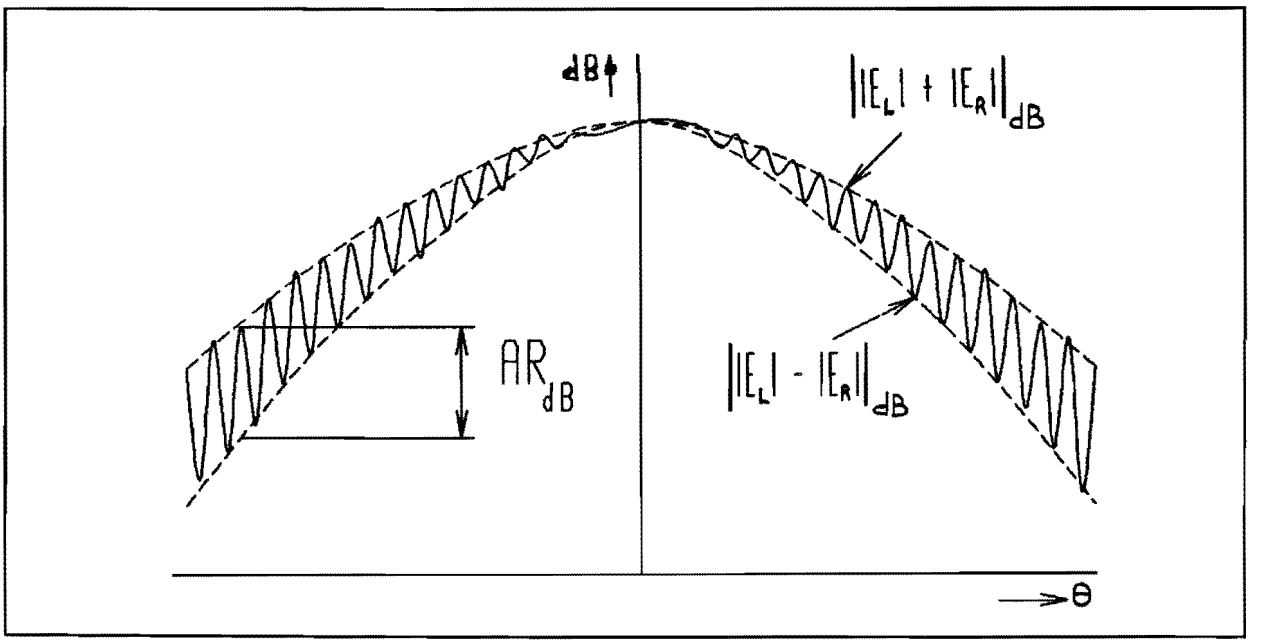

Fig 2.6 - Extraction of Axial Ratio from radiation pattern

§2.1.4 - Relationship Between Polarization Efficiency and Axial Ratio

If the axial ratio of transmitting and receiving antenna (formulas (2.16) and (2.17)) are indicated by r_{tr} and r_{re} and the ratio of E_R and E_L is indicated by ρ (as in formula (2.4)), formula (2.12) for the polarization loss can be used for an elliptically polarized wave that is split up in RHC and LHC components:

$$\Gamma = \frac{1 + |\rho_{tr}|^2 \cdot |\rho_{re}|^2 + 2 \cdot |\rho_{tr}| \cdot |\rho_{re}| \cdot \cos(\delta_{\rho_{re}} - \delta_{\rho_{tr}})}{(1 + |\rho_{tr}|^2) \cdot (1 + |\rho_{re}|^2)} \qquad (2.18)$$

Using equations (2.16) and (2.17), for $|\rho|$ can be written:

$$|\rho| = \frac{r + 1}{r - 1} \qquad \text{RHC} \tag{2.19a}$$

$$|\rho| = \frac{r - 1}{r + 1} \qquad \text{LHC} \tag{2.19b}$$

Substitution of one of the above relations in (2.18), thus polarization of transmitting antenna and receiving antenna having the same sense of rotation, gives:

$$\Gamma = \frac{(1+r_{tr}^2)\cdot(1+r_{re}^2) + 4\cdot r_{tr}\cdot re_{re} + (1-r_{tr}^2)\cdot(1-r_{re}^2)\cdot\cos\Delta}{2\cdot(1+r_{tr}^2)\cdot(1+r_{re}^2)} \tag{2.20a}$$

with:

$$\Delta = (\delta_{\rho_{tr}} - \delta_{\rho_{re}}) \tag{2.20b}$$

When the polarization of transmitting and receiving antenna have opposite senses of rotation, the relationship between polarization efficiency and axial ratio becomes:

$$\Gamma = \frac{(1+r_{tr}^2)\cdot(1+r_{re}^2) - 4\cdot r_{tr}\cdot re_{re} + (1-r_{tr}^2)\cdot(1-r_{re}^2)\cdot\cos\Delta}{2\cdot(1+r_{tr}^2)\cdot(1+r_{re}^2)} \tag{2.21}$$

Formulas (2.20) and (2.21) give the relationship between the polarization efficiency and the axial ratio for all kinds of polarization of transmitting and receiving antenas. A graphical representation of this relationship is given in figure 2.7 [2-7].

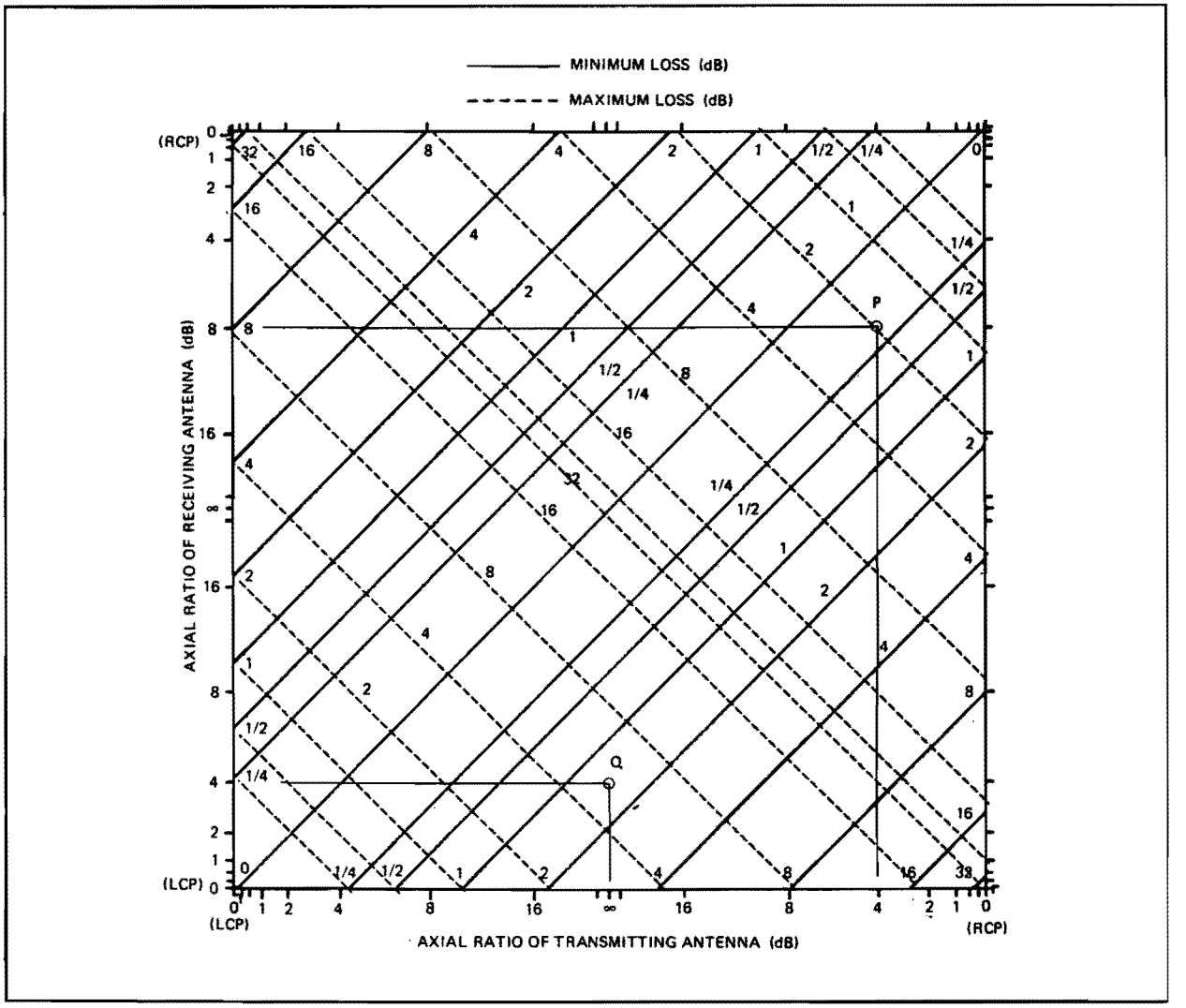

Fig.2.7 - Polarization efficiency

§2.1.5 - Antenna Gain, Efficiency and Directivity

The power density radiated by an isotropic antenna at a distance R and with input power P_0 is given by:

$$S = \frac{P_0}{4\pi R^2} \qquad (2.22)$$

An isotropic antenna radiates uniformly in all directions; the power density S is found by dividing the radiated power by the area of the sphere with radius R. The isotropic radiator is considered to be 100 percent efficient, which means that the radiator is lossless.
By directing the radiation of a real antenna, some parts of the

radiation sphere will have power less than the isotropic radiator, other parts of the radiation sphere will have power more than the isotropic radiator. The gain of the antenna increases the power density in the direction of the peak radiation:

$$S(\vartheta,\varphi) = \frac{P_0 \cdot g(\vartheta,\varphi)}{4\pi R^2} \tag{2.23}$$

So the antenna gain is:

$$g(\vartheta,\varphi) = \frac{S(\vartheta,\varphi)}{P_0/4\pi R^2} = \frac{S(\vartheta,\varphi)}{S_{iso}(\vartheta,\varphi)} \tag{2.24}$$

The antenna radiation intensity is defined by [2-2]:

$$U(\vartheta,\varphi) = \frac{P_0 \cdot g(\vartheta,\varphi)}{4\pi} \tag{2.25}$$

The surface integral of the radiation intensity over the radiation sphere divided by the input power P_0 is a measure of the relative power radiated by the antenna, or the antenna efficiency [2-2]. With P_r the radiated power, the antenna efficiency is:

$$\eta_e = \frac{P_r}{P_0} = \int_0^{2\pi} \int_0^{\pi} \frac{g(\vartheta,\varphi)}{4\pi} \cdot \sin\vartheta \cdot d\vartheta \cdot d\varphi \tag{2.26}$$

Directivity is a measure of the concentration of the radiation in the direction of the maximum [2-2]:

$$D = \frac{\text{maximum radiation intensity}}{\text{average radiation intensity}} = \frac{U_{max}}{U_0} \tag{2.27}$$

with:

$$U_0 = \frac{1}{4\pi} \cdot \int_0^{2\pi} \int_0^{\pi} U(\vartheta,\varphi) \cdot \sin\vartheta \cdot d\vartheta \cdot d\varphi \qquad (2.28)$$

By inspection of (2.25) to (2.28) it follows that the following is also true:

$$g(\vartheta,\varphi) = D(\vartheta,\varphi) \cdot \eta_e \qquad (2.29)$$

§2.1.6 - Voltage Standing Wave Ratio

When the antenne input is not connected to a matched transmission line, on the transmission line and at the antenna input there will be two traveling waves, an incident and a reflected one. These two waves will establish a standing wave. The relation between reflected and incidinent wave voltage is given by:

$$V_{refl} = |\rho| \cdot V_{inc} \qquad (2.30)$$

in which ρ is called the reflection factor.
With the above equation the maximum and minimum wave voltage can be determined:

$$V_{max} = (1 + |\rho|) \cdot V_{inc} \qquad (2.31a)$$

$$V_{min} = (1 - |\rho|) \cdot V_{inc} \qquad (2.31b)$$

The Voltage Standing Wave Ratio (VSWR) is defined as [2-2]:

$$VSWR = \frac{V_{max}}{V_{min}} = \frac{1 + |\rho|}{1 - |\rho|} \qquad (2.32)$$

This quantity is always greater than or equal to 1 and in the ideal case, that is in the case of a matched connetion, the equal sign holds true.

§2.2 - Specifications

Now that the antenna parameters are defined, the specifications for the antennas and for the communication link between vehicle and satellite, as asked for by INMARSAT and MSATX, can be discussed. In the following first the antenna parameters will be discussed and afterwards the desired specifications for the communication link, of which the antennas form part, will be stated by means of a so called link budget for the INMARSAT case.

§2.2.1 - Antenna specifications

The antenna parameters, as discussed in section §2.1, will be given here for a mobile communication system proposed by the International Maritime Satellite Organization (INMARSAT) [2-8] and for the Mobile Satellite Experiment (MSATX) [2-9].
INMARSAT proposes a system for satellite communications for aircraft (see figure 2.8 [2-10]). The antennas for the aircraft should be small sized and light weight and so it should be possible to use these antennas and the communication system for vehicles too.
Although the MSATX specifications are much lesser detailed than the INMARSAT specifications, they still are disussed because this project is specially aimed for mobile communications with vehicles and above all, as will turn out in the rest of the report, these asked specifications seem to be more realistic, that is: easier to realise, than the specifications asked for by INMARSAT.

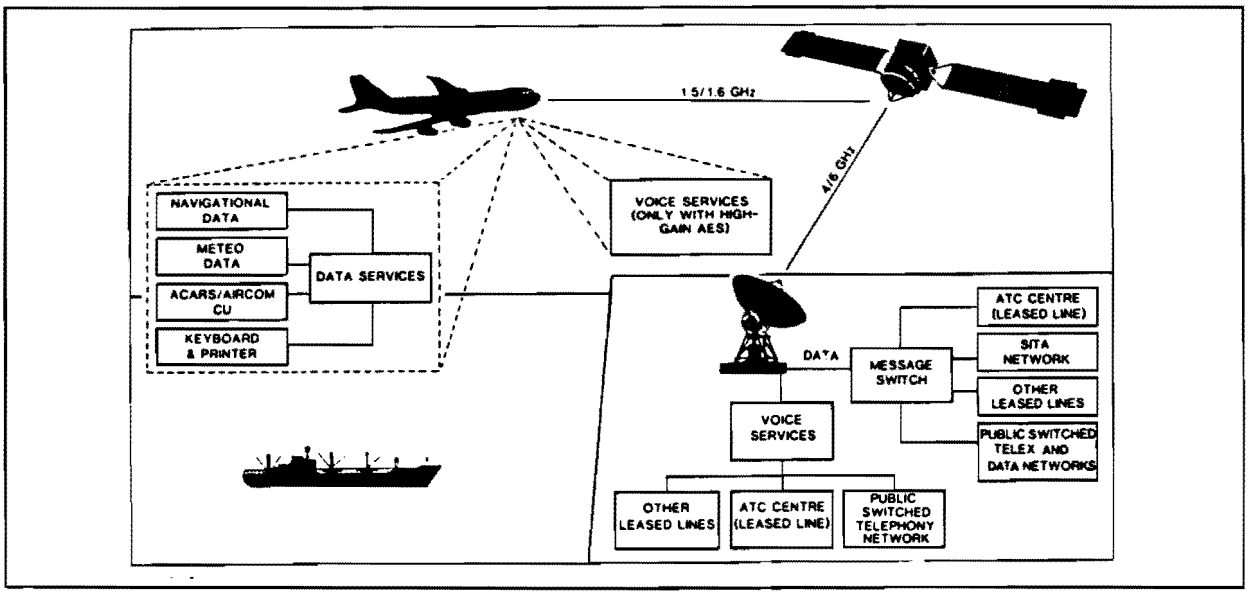

Fig.2.8 - INMARSAT aeronautical satellite communictions networks

In table 2.1 the antenna parameters for INMARSAT data, INMARSAT voice and for MSATX are given.

Table 2.1 - Antenna parameters

Parameter	INMARSAT data	INMARSAT voice	MSATX
Frequency	1.5 to 1.6GHz	1.5 to 1.6GHz	1.5 to 1.6GHz
Coverage: elevation	5^0 to 90^0	5^0 to 90^0	20^0 to 60^0
azimuth	360^0	360^0	360^0
Gain (vehicle)	1dB	12dB	10dB
Polarization	Right Hand Circular	Right Hand Circular	Circular
Max. Axial Ratio	2.5dB	1dB	4dB
Max. VSWR	1.4	1.4	-

§2.2.2 - Link Budget

In a link budget the losses that occur in a communication link are grouped together and so describe the quality of the link. The transmitting and receiving antenna only form part of the communication link. To give an impression the link budgets for INMARSAT data [2-8] and INMARSAT voice [2-8] are given below. A link budget for MSATX is not known, but it should be like the link budget for INMARSAT voice

with the MSATX characteristics of table 2.1 substituted in the corresponding places.
Terms of the link budget wil be explained after the link budget is given.

Forward Link Budget Data

Satellite EIRP	21dBW
Path loss 0^0 elevation	188.8dB
Atmospheric absorption	0.2dB
Polarization Loss (AR 2/5 dB)	0.7dB
Aircraft G/T	-26dB/K
Downlink C/N_0	33.9dBHz
E_s/N_0 for 600 symbols/s	6.1dB
Modem implementation loss	0.5dB
System margin	1.6dB
Average SER (C/M = 10dB, DECPSK)	5%
Equivalent E_s/N_0 for Gaussian Channel	1.6dB
BER after convolutional decoding	10^{-5}
Received signal level with 1dB antenna	-137.7dBm

Return Link Budget Data (MCS)

Aircraft net antenna gain	1dB
Output power	17dBW
Uplink EIRP	18dBW
Path loss 0^0 elevation	189.4dB
Atmospheric absorption	0.2dB
Polarization Loss (AR 5/2 dB)	0.7dB
Satellite G/T	-13dB/K
Uplink C/N_0	43.3dBHz
Satellite gain	148dB
Satellite EIRP	-24.3dBW
Path loss 5^0 elevation	197.2dB
Atmospheric absorption	0.4dB
Ground earth station G/T	32dB/K
Downlink C/N_0	38.7dBHz
Link C/N_0	37.4dBHz
E_s/N_0 for 1200 symbols/s	6.6dB
Modem implementation loss	0.5dB
System margin	2.1dB
Average SER (C/M = 10dB, DECPSK)	.5%
Equipment E_s/N_0 for Gaussian Channel	1.6dB
BER after convolutional decoding (K = 7)	10^{-5}

Forward Link Budget Voice

Satellite EIRP	21dBW
Path loss 0^0 elevation	188.8dB
Atmospheric absorption	0.2dB
Polarization Loss (AR 2/2 dB)	0.25dB
Aircraft G/T	-13dB/K
Downlink C/N_0	47.4dBHz
E_s/N_0 for 21000 symbols/s	4.2dB
Modem implementation loss	0.5dB
Average SER (C/M = 10dB, QPSK)	8%
Corresponding E_s/N_0 for Gaussian Channel	0dB
BER after convolutional decoding	10^{-3}
Received signal level with 12dB antenna	-126.3dBm

Return Link Budget Voice (MCS)

Aircraft net antenna gain	12dB
Output power/channel	15dBW
Uplink EIRP	27dBW
Path loss 0^0 elevation	189.4dB
Atmospheric absorption	0.2dB
Polarization Loss (AR 2/2 dB)	0.25dB
Satellite G/T	-13dB/K
Uplink C/N_0	52.57dBHz
Satellite gain (MCS)	148dB
Satellite EIRP	-15.9dBW
Path loss 5^0 elevation	197.2dB
Atmospheric absorption	0.4dB
Ground earth station G/T	32.0dB/K
Downlink C/N_0	48.1dBHz
Overall link C/N_0	46.8dBHz
E_s/N_0 for 21000 symbols/s	3.6dB
Modem implementation loss	0.5dB
System margin	1.6dB
Average CER (C/M = 10dB, QPSK)	8%
Equivalent E_s/N_0 (CER = 8%) for Gaussian Channel	0dB
BER after convolutional decoding (K = 7)	10^{-3}

Now there are some terms from the above link budgets that need some explanation. To start with EIRP stands for Equivalent Isotropic Radiated Power and is defined by [2-11]:

$$EIRP = G_T(dB) + P_T(dB) \tag{2.33a}$$

with:

P_T = transmitted power (2.33b)

G_T = antenna gain (2.33c)

G/T (dBK^{-1}), the ratio of antenna power gain to the total noise temperature at the reeiver input, is called the figure of merit with the total noise temperature at the receiver input given by [2-11]:

$$T = T_A/L + \vartheta_L \cdot (1 - 1/L) + T_R \tag{2.34a}$$

with:

T_A = antenna noise temperature (2.34b)

L = circuit attenuation (2.34c)

ϑ_L = physical temperature (2.34d)

T_R = receiver effective input noise temperature (2.34e)

C/N_0 (dBHz) is called the carrier to noise power ratio at the receiver input and is given by [2-11]:

$$\left(\frac{C}{N_0}\right)_{dBHz} = \underset{\substack{\text{EIRP}\\(dBW)}}{10\cdot\log(P_T G_T)} - \underset{\substack{\text{Free space loss}\\(dB)}}{20\cdot\log\left(\frac{4\pi R}{\lambda}\right)} + \underset{\substack{\text{Figure of merit of}\\\text{receiving station}\\(dBK^{-1})}}{10\cdot\log\left(\frac{G\cdot R}{T}\right)} +$$

$$- \underset{\substack{\text{Additional}\\\text{losses}\\(dB)}}{10\cdot\log(L_A)} - \underset{-228.6dBWK^{-1}Hz^{-1}}{10\cdot\log(k)} \qquad (2.35a)$$

with:

$N_0 = N/B_{IF}$ (WHz): noise power spectral density (2.35b)

B_{IF} = noise equivalent bandwidth (2.35c)

The last term to be explained is E_s/N_0:

$$\frac{E_s}{N_0} = \text{energy per symbol/noise power} \qquad (2.36)$$

This quantity is commnly used in relation with the Bit Error Rate (BER) as a measure of performance for digital communication techniques.

§2.3 - References

[2-1] Jeuken, M.E.J., *'Elektromagnetische Golven en Antennes '*, Professional Group Elektromagnetism and Circuit Theory, Department of Electrical Engineering, Eindhoven University of Technology, Netherlands, 1983, (in Dutch).

[2-2] Milligan, T.A., *' Modern Antenna Design '*, McGraw-Hill Book Company, 1985.

[2-3] -, ' *Standards on Wave Propagation: Definitions of Terms* ',
Proc. IRE, Vol.38, No.11, November 1950, p.1267.

[2-4] Murakami, G., Wickizer, G.S., '*Ionosphere Phase Distortion and Faraday Rotation and Radio Waves* ',
RCA Review, Vol.30, 1969, pp.488-491.

[2-5] Balanis, C.A., ' *Antenna Theory: Analysis and Design* ',
Harper & Row, 1982.

[2-6] Vrinten, M.L.A., ' *A Wideband Circularly Polarized Microstrip Antenna Array* ',
Graduate Report, Professional Group Elektromagnetism and Circuit Theory, Department of Electrical Engineering, Eindhoven University of Technology, Netherlands, 1988.

[2-7] Ludwig, A.C., ' *A Simple Graph for Determining Polarization Loss* ,
Microwave Journal, Vol.19, No.9, September 1976, p.63.

[2-8] INMARSAT, ' *Request For Proposals Number 085, Aircraft Earth Stations* ',
9 May 1986.

[2-9] Huang J., ' *L-band Phased Array Antennas for Mobile Satellite Communications* ',
IEEE 37th Vehicular Technology Conference, Tampa, Florida, June 1987.

[2-10] Da Silva Curiel A., ' *INMARSAT's Present and Future Maritime Communications Systems* ',
Tijdschrift van het Nederlands Elektronica- en Radiogenoodschap, Deel 51, Nr.4, 1986, p.128.

[2-11] Maral G., Bousquet M., ' *Satellite Communications Systems* ',
John Wiley & Sons, 1986, pp.49-75.

3. Circular Polarization with Microstrip Array Antennas

This part of the report describes methods to realize a circularly polarized microstrip antenna. First of all ways to generate a circular polarized field with a single microstrip patch are discussed. It will turn out that the most agreeable way to reach this goal is the use of multiple feed connections to the patch.
When looking at the antenna gain requirements (chapter 2) it will be obvious that a single microstrip patch will not do for voice transmission and so an array of microstrip patches has to be formed. After general array properties are described, a microstrip array antenna consisting of circularly polarized patches will be discussed. Arising from the practical drawbacks of the above mentioned array, new arrays will be discussed, based on the concept of sequential rotation. In this chapter electronic beam steering will not be treated; this subject is postponed to chapter 4, in which scanning properties will come up for discussion. So the array antennas developed in this chapter are only valid for keeping track of the satellite signal by mechanical steering. A detailed treatment of tracking properties will be given in chapter 6.

§3.1 - Methods to create a circularly polarized element

There are two methods for creating circular polarization with a single patch: use of perturbation techniques and use of multiple (coaxial) feeds.
Circular polarization can also be obtained by microstrip elements different from the patch, like the annular dipole [3-1], the cross antenna [3-2] and the stacked disk [3-3, 3-4]. The disadvantage of the annular dipole and the cross antenna, when used in an array, is the size, which is in the order of one and a half wavelength, which is too much as will be shown in chapter 4. The disadvantage of the stacked disk is that there is no simple model available, like the cavity model for microstrip patches and one has to resort to numerical methods to analyse this microstrip antenna type.
Instead of patch or stripline like antennas, also use can be made of slotline type antennas like the crossed slot radiator [3-5, 3-6].

The choise has been made in favor of the patch antenna beause of the experience with this type [3-7, 3-8, 3-9].

§3.1.1 - Perturbation techniques

Circular polarization with a single microstrip patch is obtained when two orthogonal modes with equal amplitude and in-phase quadrature are excited within the cavity region

In the pertubation approach a single feed is used. To excite the two orthogonal modes, the patch has to be perturbated [3-10, 3-11, 3-12]. Examples of geometrical arrangements for circularly polarization with one feed are shown in figure 3.2 [3-10, 3-11].

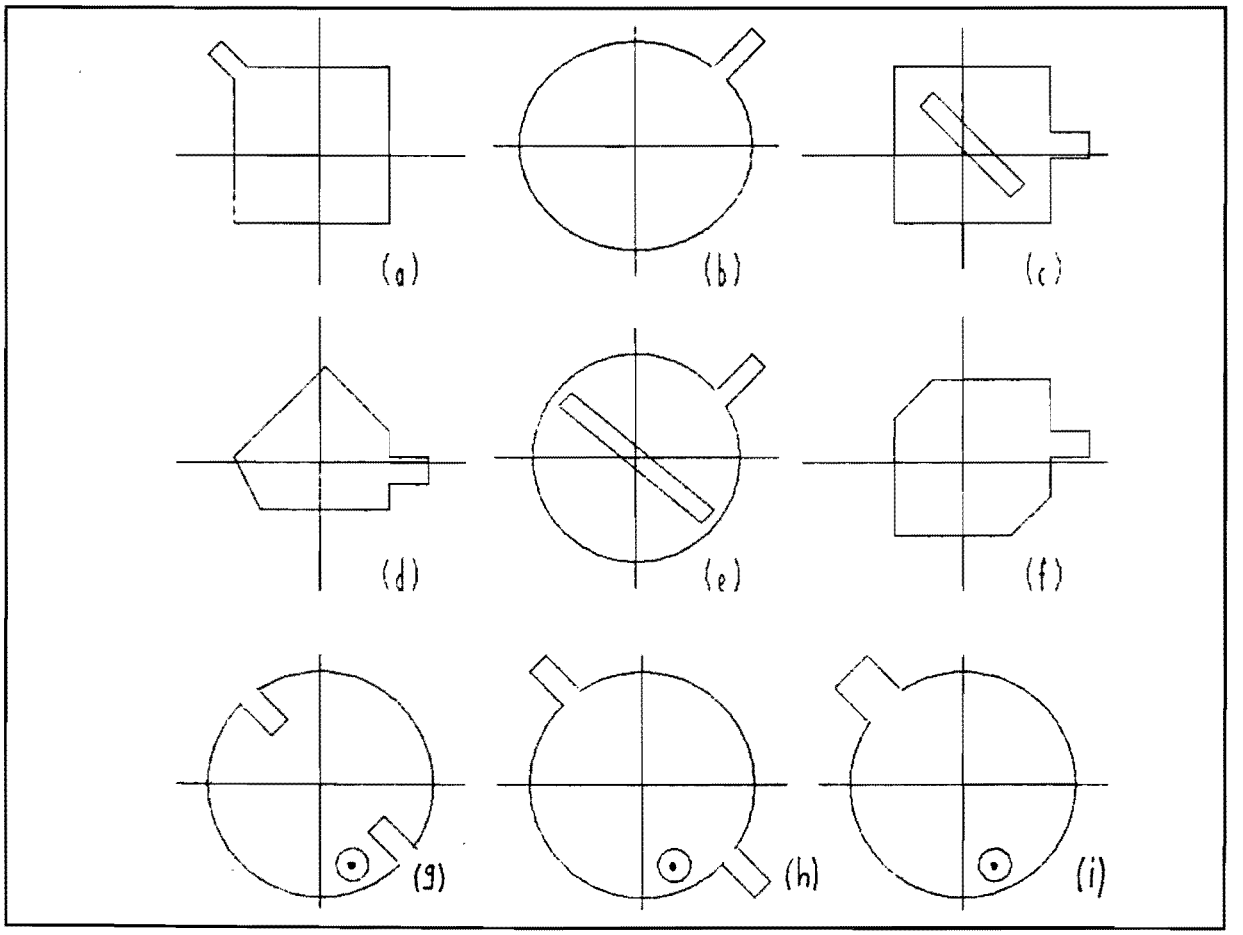

Fig 3.1 - Single feed circularly polarized asymmetrical patches

(a) Almost square, corner fed
(b) Elliptical
(c) Square with 45^{0} slot
(d) Pentagon
(e) Circle with slot
(f) Square with cut corners
(g) Circle with notches
(h) Circle with stubs
(i) Circle with stub

Although the perturbated patch has the advantage of only one feed, a great disadvantage is the lack of a proper model for most of them and the very small bandwidth of the patch. Calculation methods to give an indication of the sizes of the perturbation segments do excist [3-11, 3-12], but the right dimensions will be obtained by cut and trial or cut, etch and trial.

§3.1.2 - Multiple Feeds

The most direct approach to obtain circular polarization with a single patch is to use two separate and spatially orthogonal feeds, excited with a relative phase shift of 90^0. This configuration then provides two orthogonal linearly polarized waves which are in time phase quadrature (see figure 3.3).

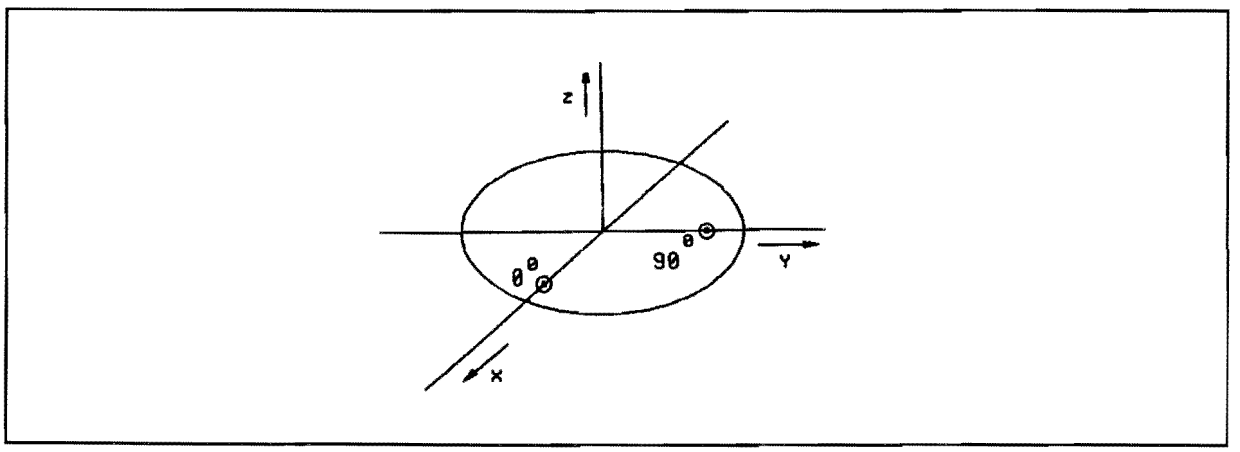

Fig. 3.2 - Circularly polarized circular microstrip patch

Using equations (1.2a) and (1.2b) with $n = 1$, the field components of the above antenna for the TM_{11}-mode can be written as:

$$E_\vartheta = e^{j0^0} \cdot E_\vartheta(\vartheta,\varphi) + e^{j90^0} \cdot E_\vartheta(\vartheta,\varphi - 90^0)$$

$$= A(r) \cdot F_1(\vartheta) \cdot \left\{ \cos(\varphi) + j \cdot \cos(\varphi - 90^0) \right\} \qquad (3.1a)$$

$$E_\varphi = e^{j0^0}\cdot E_\varphi(\vartheta,\varphi) + e^{j90^0}\cdot E_\varphi(\vartheta,\varphi - 90^0)$$

$$= A(r)\cdot F_2(\vartheta)\cdot\cos(\vartheta)\cdot\left\{\sin(\varphi) + j\cdot\sin(\varphi - 90^0)\right\} \qquad (3.1b)$$

with:

$$A(r) = j\cdot\frac{Vak_0}{2}\cdot\frac{e^{-jk_0r}}{r} \qquad (3.1c)$$

$$F_1(\vartheta) = J_0(\, k_0a\cdot\sin(\vartheta)\,) - J_2(\, k_0a\cdot\sin(\vartheta)\,) \qquad (3.1d)$$

$$F_2(\vartheta) = J_0(\, k_0a\cdot\sin(\vartheta)\,) + J_2(\, k_0a\cdot\sin(\vartheta)\,) \qquad (3.1e)$$

The left and right hand components of the electric field can now be calculated with (2.15) and the above equations:

$$E_L = \frac{1}{\sqrt{2}}\cdot(E_\vartheta - j\cdot E_\varphi)$$

$$= -\frac{A(r)}{\sqrt{2}}\cdot e^{j\varphi}\cdot\left[F_1(\vartheta) + F_2(\vartheta)\cdot\cos(\vartheta)\right] \qquad (3.2a)$$

$$E_R = \frac{1}{\sqrt{2}}\cdot(E_\vartheta + j\cdot E_\varphi)$$

$$= -\frac{A(r)}{\sqrt{2}}\cdot e^{j\varphi}\cdot\left[F_1(\vartheta) - F_2(\vartheta)\cdot\cos(\vartheta)\right] \qquad (3.2b)$$

With (2.17) for the axial ratio is found:

$$AR = \left| \frac{|E_L| + |E_R|}{|E_L| - |E_R|} \right|$$

$$= \left| \frac{|F_1(\vartheta) + F_2(\vartheta)\cdot\cos(\vartheta)| + |F_1(\vartheta) - F_2(\vartheta)\cdot\cos(\vartheta)|}{|F_1(\vartheta) + F_2(\vartheta)\cdot\cos(\vartheta)| - |F_1(\vartheta) - F_2(\vartheta)\cdot\cos(\vartheta)|} \right| \qquad (3.3)$$

This formula, the axial ratio of one circularly polarized patch antenna, is of great importance when considering the quality of a circularly polarized microstrip phased array antenna, as will turn out in the following part of this chapter and in chapter 4.
With program FREQSCAN (see appendix G) the the radiation pattern (on power basis) and the axial ratio, both as function of the frequency, are calculated for a dielectric substrate with $\varepsilon_r = 2.33$ (see figure 3.3), a dielectric substrate with $\varepsilon_r = 6$ (see figure 3.4) and for a dielectric substrate with $\varepsilon_r = 10.5$ (see figure 3.5).

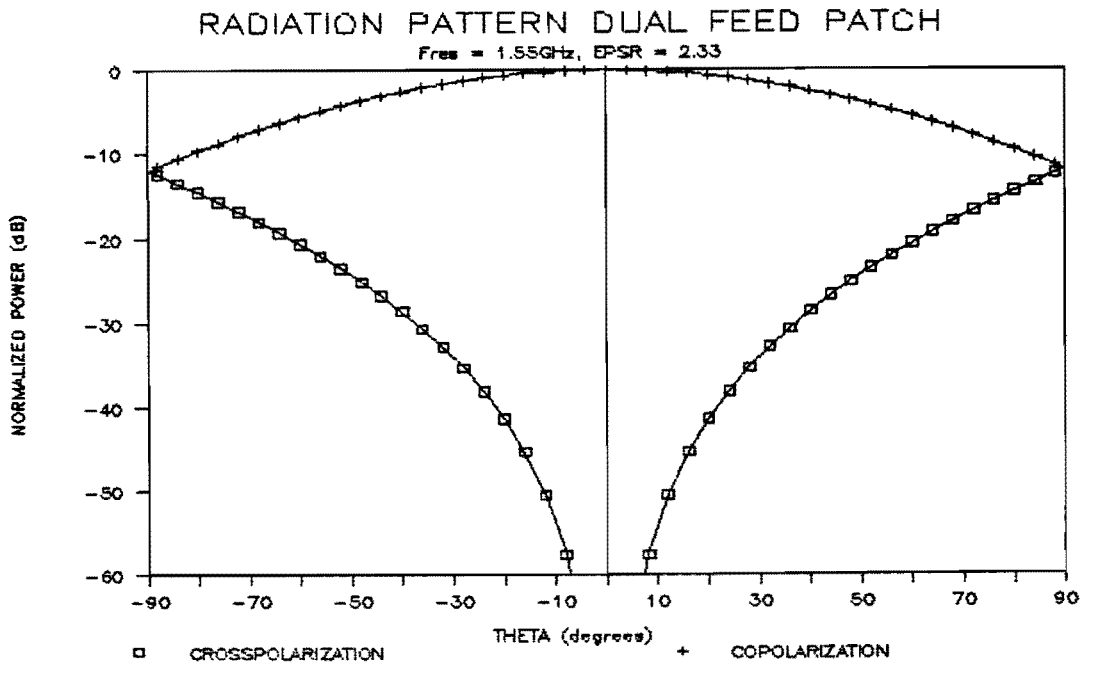

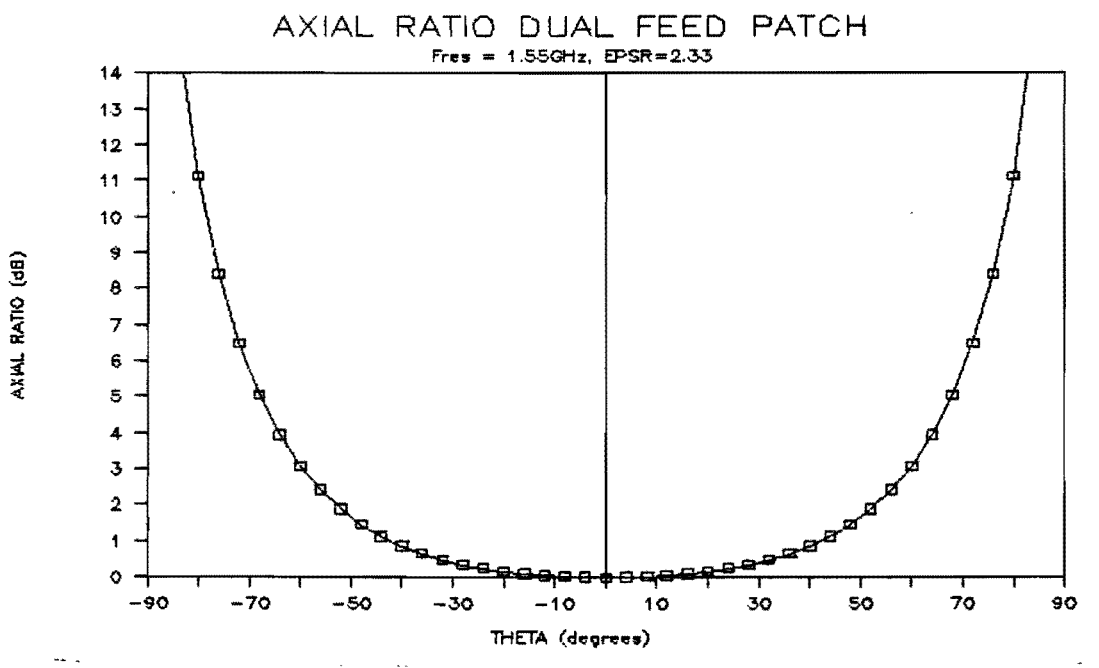

Fig.3.3 - Calculated CP characteristics (ε_r = 2.33)

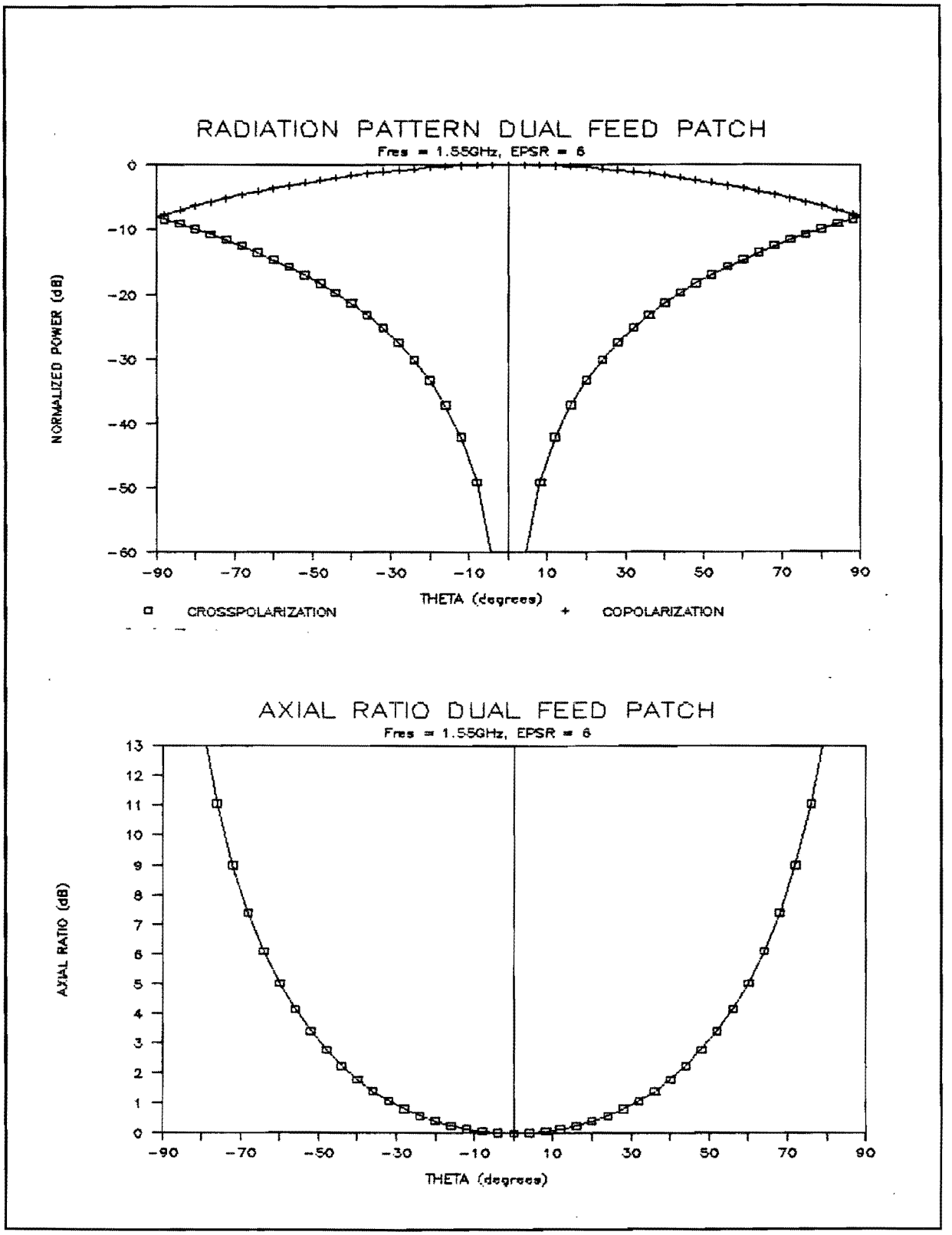

Fig.3.4 - Calculated CP characteristics (ε_r = 6)

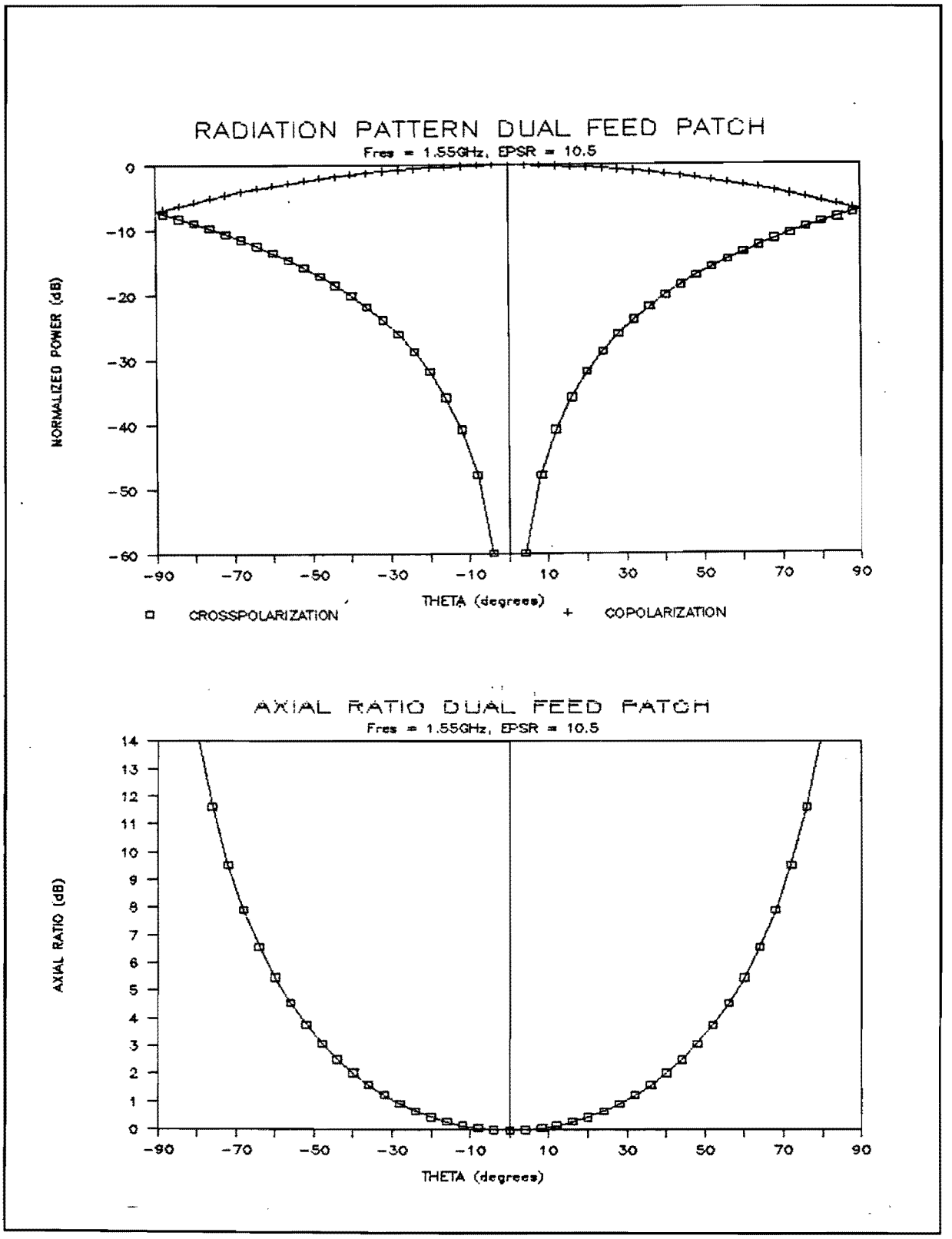

Fig.3.5 - Calculated CP characteristics (ε_r = 10.5)

§3.2 - Array Properties

To satisfy the gain requirements for voice transmission, it is necessary to use more than one microstrip patch antenna. The radiating elements can be placed in several array configurations. The most important is the two dimensional planar array configuration, because with this one it will be possible to steer the beam away from broadside in any desired direction. This will be discussed in the next chapter; in the following the attention is focussed on ' fixed-beam ' arrays.

To simplify the discussion of two dimensional planar arrays, first the properties of linear arrays will be treated. A linear array is a group of antenna elements in a straight line.

§3.2.1 - Linear Array

Figure 3.6 [3-13] shows a linear array consisting of M elements. The elements are considered point sources and are equally spaced by distance d along the x axis.

ϑ is the angle an arriving plane wave makes with the array normal. The wavefront of a plane wave is perpendicular to its direction of arrival, thus making an angle ϑ with the x axis. Since all the points on the wavefront have the same amplitude and phase, the signal arriving at the m^{th} element leads that arriving at the $(m-1)^{th}$ element by a phase shift ϕ given by:

$$\phi = 2\pi \cdot \frac{d}{\lambda} \cdot \sin(\vartheta) \quad = 2\pi \cdot \frac{d}{\lambda} \cdot T \tag{3.4}$$

with λ the free space wavelength.

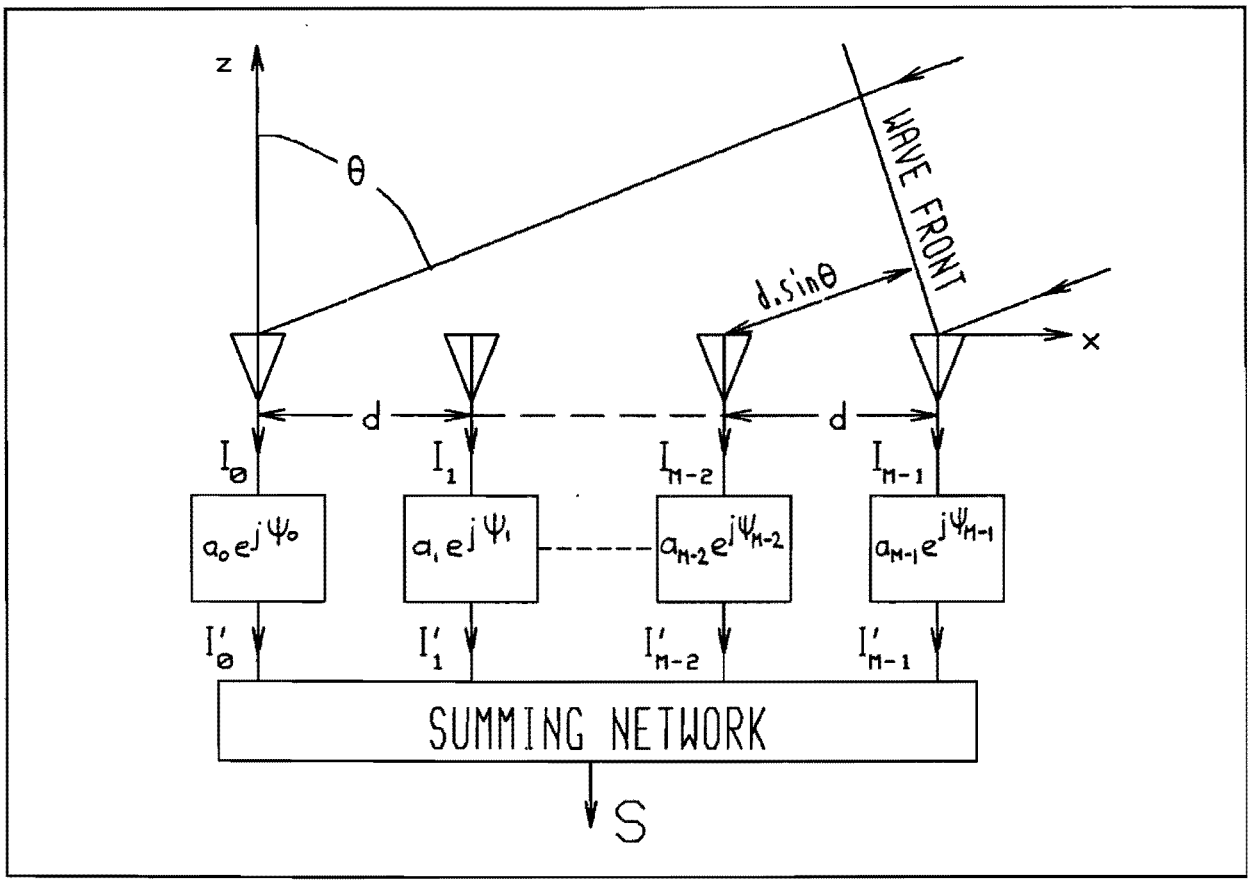

Fig. 3.6 - Linear array geometry

If the phase of the current flowing from element 0 is zero, the current flowing from element m can be written as:

$$I_m = S_m(\vartheta) \cdot e^{jm2\pi \cdot \frac{d}{\lambda} \cdot T} \qquad (3.5)$$

where $S_m(\vartheta)$ is proportional to the radiation pattern of an individual antenna element and is called the element factor. The time variation $e^{j\omega t}$ is omitted for the sake of convenience

If, as figure 3.6 depicts, a network is placed in the transmission line behind each element which, for the m^{th} network has the transfer function [3-13]:

$$\frac{I'_m}{I_m} = a_m \cdot e^{j\psi_m} \qquad (3.6)$$

where a_m and ψ_m are the current gain and phase shift of the network, then the summing network produces the signal:

$$S(\vartheta) = \sum_{m=0}^{M-1} S_m(\vartheta) \cdot a_m \cdot e^{j\psi_m} \cdot e^{jm2\pi \cdot \frac{d}{\lambda} \cdot T} \qquad (3.7)$$

The same expression is valid for the radiation pattern of the array [3-13].
A grating lobe occurs whenever the argument of $S(\vartheta)$ is a multiple of 2π. To avoid grating lobes for all possible angles ϑ, it is necessary that:

$$\frac{d}{\lambda} \leq 1 \qquad (3.8)$$

§3.2.2 - Planar Array

Figure 3.7 shows a two dimensional expansion of the antenna array of figure 3.6 [3-13].

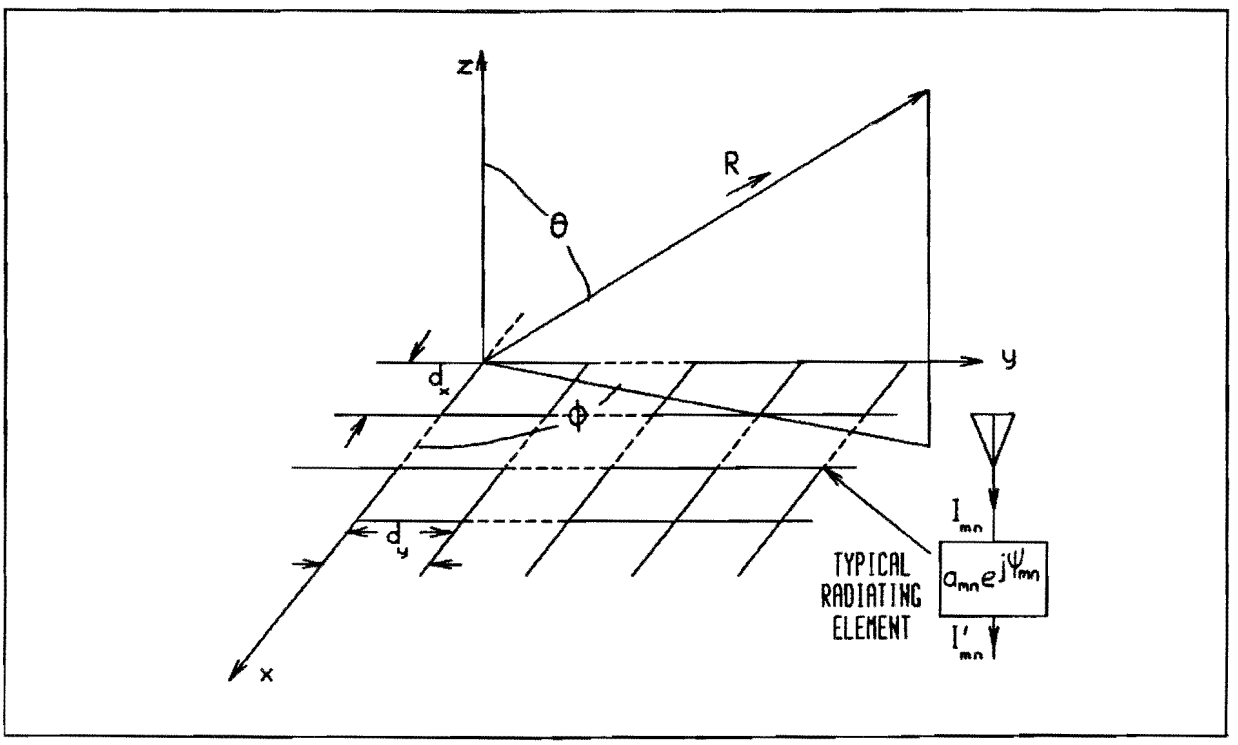

Fig. 3.7 - Planar array of radiating elements

The mn^{th} element of the array is located by a vector $\bar{\rho}_{mn}$, given by:

$$\bar{\rho}_{mn} = x_m \cdot \bar{a}_x + y_n \cdot \bar{a}_y \tag{3.9}$$

The phase shift, arising from the electrical path difference between the mn^{th} element and the 00^{th} element is:

$$\phi_{mn} = (\frac{2\pi}{\lambda}) \cdot \bar{\rho}_{mn} \cdot \bar{a}_r \tag{3.10}$$

with $\bar{a}_r$ given by (2.2a):

$$\bar{a}_r = \sin\vartheta \cdot \cos\varphi \cdot \bar{a}_x + \sin\vartheta \cdot \sin\varphi \cdot \bar{a}_y + \cos\vartheta \cdot \bar{a}_z =$$

$$= T_x \cdot \bar{a}_x + T_y \cdot \bar{a}_y + T_z \cdot \bar{a}_z \tag{3.11}$$

(3.8) and (3.10) substituted in (3.9) gives:

$$\phi_{mn} = \frac{2\pi}{\lambda} \cdot (x_m \cdot T_x + y_n \cdot T_y) \tag{3.12}$$

For a planar array with M×N elements in which the mn^{th} element is located at $x_m = m \cdot d_x$ and $y_n = n \cdot d_y$ the array radiation pattern similar to the linear array case can be written as:

$$S(\vartheta,\varphi) = \sum_{m=0}^{M-1} \sum_{n=0}^{N-1} S_{mn}(\vartheta,\varphi) \cdot a_{mn} \cdot e^{j\psi_{mn}} \cdot e^{j\frac{2\pi}{\lambda} \cdot (md_x T_x + nd_y T_y)} \tag{3.13}$$

The permitted element spacings in x and y directions to avoid the occurence of grating lobes are given by:

$$\frac{d_x}{\lambda} \leq 1 \qquad (3.14a)$$

$$\frac{d_y}{\lambda} \leq 1 \qquad (3.14b)$$

for fixed beams.

§3.2.3 - Rectangular Array of Circularly Polarized Patches

Considered is a rectangular MxN array of two-feed circularly polarized patches. The patch will be considered a point source and the two orthogonal linear polarizations (horizontal and vertical) will be indicated by a horizontal and vertical arrow (see figure 3.8), arising from a magnetic dipole approximation. This approximation will be explained in appendix B. Assumed is a 90^0 phase shift between the polarization directions.

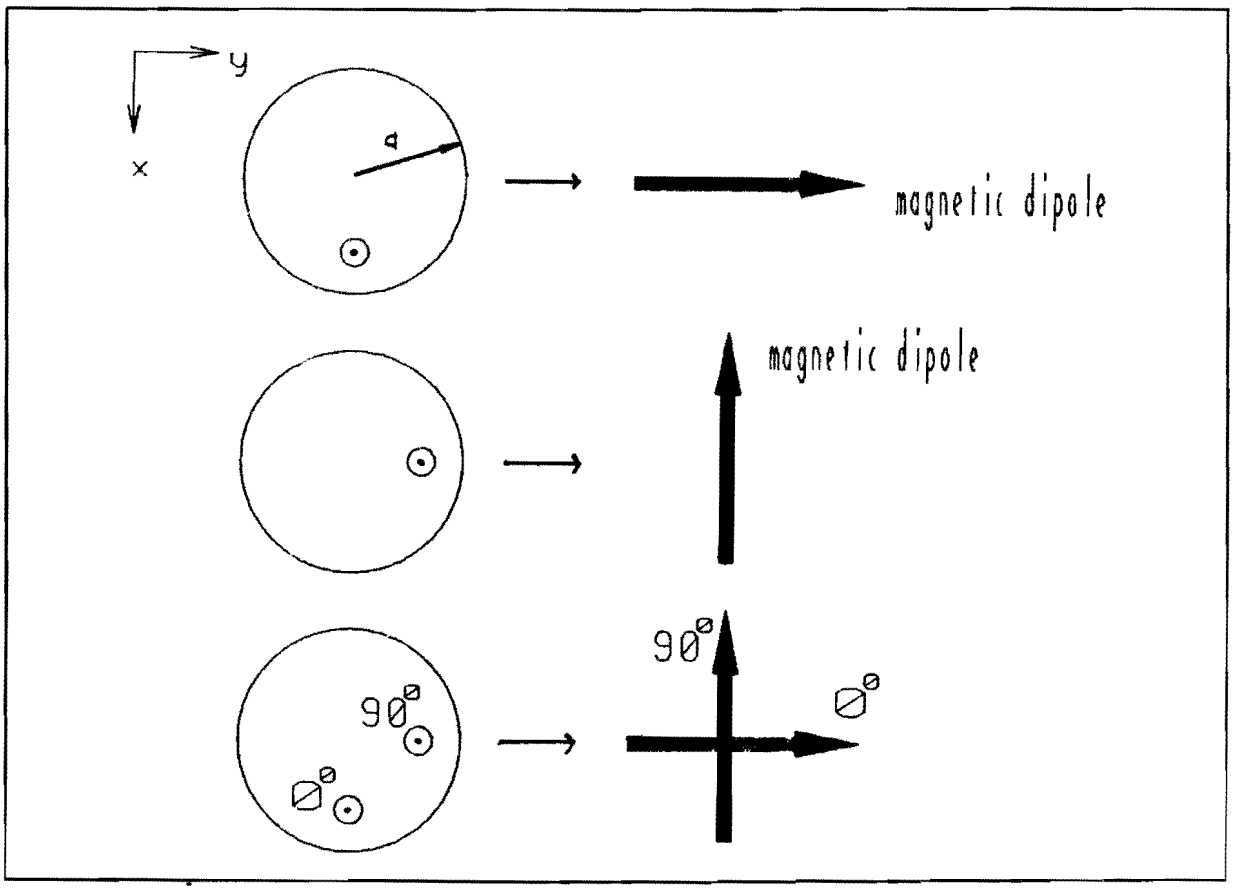

Fig. 3.8 - Indication of polarization directions

A MxN array with equal spacing in x-direction and y direction between the circularly polarized elements is shown in figure 3.9.

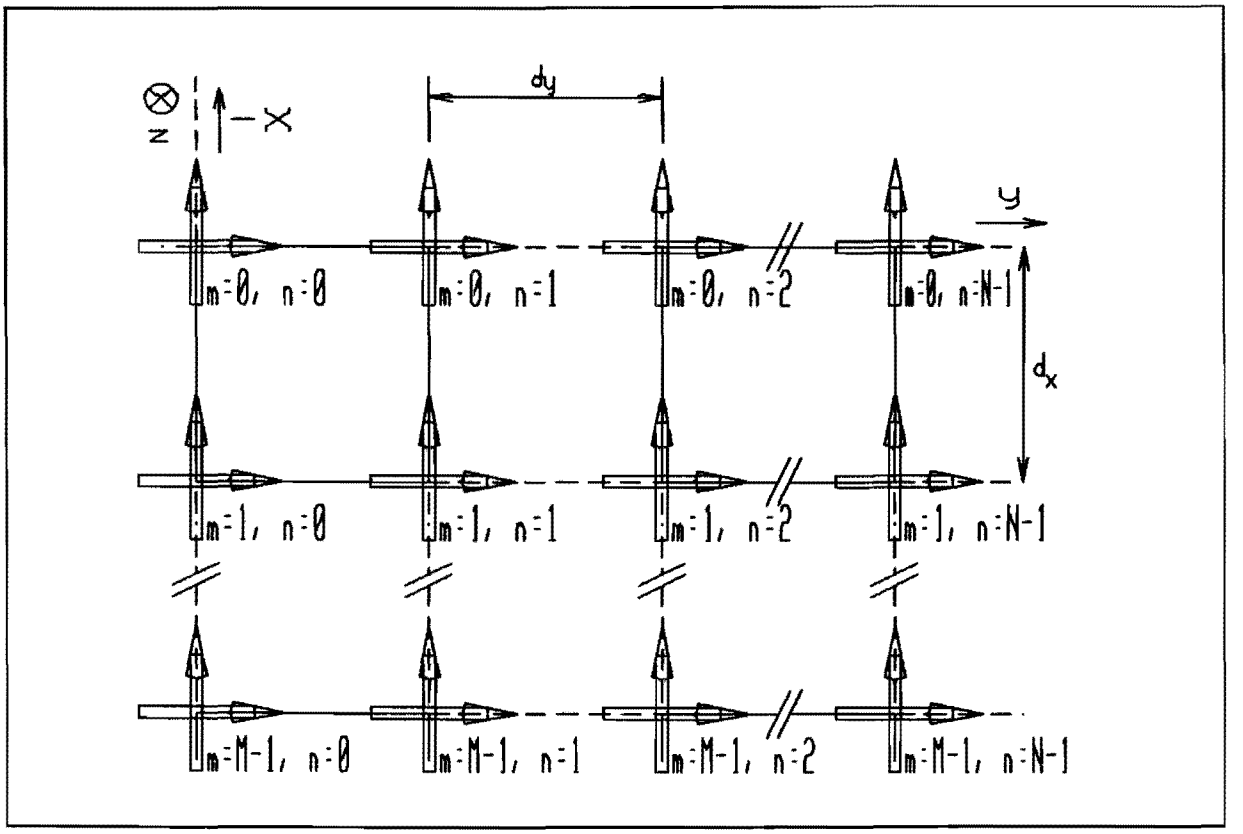

Fig. 3.9 - MxN array of equaly spaced circularly polarized elements

When calculating the radiation pattern of the array using equation (3.13), the term $S_{mn}(\vartheta,\varphi)\cdot a_{mn}\cdot e^{j\psi_{mn}}$ can be replaced by a term $E_{mn}(\vartheta,\varphi)$. This term follows from formula (3.1), leaving the distance-dependent part out of it. So for the case $S(\vartheta,\varphi) = E_{\vartheta}(\vartheta,\varphi)$ with (3.1a):

$$E_{mn}(\vartheta,\varphi) = -e^{j\varphi}\cdot F_1(\vartheta) \qquad (3.15a)$$

and

$$E_{\vartheta}(\vartheta,\varphi) = -e^{j\varphi}\cdot F_1(\vartheta)\cdot\sum_{m=0}^{M-1}\sum_{n=0}^{N-1} e^{j\frac{2\pi}{\lambda}\cdot(md_xT_x + nd_yT_y)} \tag{3.15b}$$

For the case $S(\vartheta,\varphi) = E_{\varphi}(\vartheta,\varphi)$ with (3.1b):

$$E_{mn}(\vartheta,\varphi) = -j\cdot e^{j\varphi}\cdot\cos(\vartheta)\cdot F_2(\vartheta) \tag{3.16a}$$

and

$$E_{\varphi}(\vartheta,\varphi) = -j\cdot e^{j\varphi}\cdot\cos(\vartheta)\cdot F_2(\vartheta)\cdot\sum_{m=0}^{M-1}\sum_{n=0}^{N-1} e^{j\frac{2\pi}{\lambda}\cdot(md_xT_x + nd_yT_y)} \tag{3.16b}$$

Calculating the radiation pattern of the left and right hand polarized electric field, gives with (2.15), only looking at the angle-dependent part, and the above formulas:

$$E_L(\vartheta,\varphi) = E_{\vartheta}(\vartheta,\varphi) - j\cdot E_{\varphi}(\vartheta,\varphi) =$$

$$= -e^{j\varphi}\left(F_1(\vartheta) + \cos(\vartheta)\cdot F_2(\vartheta)\right)\sum_{m=0}^{M-1}\sum_{n=0}^{N-1} e^{j\frac{2\pi}{\lambda}\cdot(md_xT_x + nd_yT_y)} \tag{3.17}$$

$$E_R(\vartheta,\varphi) = E_{\vartheta}(\vartheta,\varphi) + j\cdot E_{\varphi}(\vartheta,\varphi) =$$

$$= -e^{j\varphi}\left(F_1(\vartheta) - \cos(\vartheta)\cdot F_2(\vartheta)\right)\sum_{m=0}^{M-1}\sum_{n=0}^{N-1} e^{j\frac{2\pi}{\lambda}\cdot(md_xT_x + nd_yT_y)} \tag{3.18}$$

The axial ratio can be calculated with (2.17) and gives:

$$AR = \left| \frac{|F_1(\vartheta) + \cos(\vartheta)\cdot F_2(\vartheta)| + |F_1(\vartheta) - \cos(\vartheta)\cdot F_2(\vartheta)|}{|F_1(\vartheta) + \cos(\vartheta)\cdot F_2(\vartheta)| - |F_1(\vartheta) - \cos(\vartheta)\cdot F_2(\vartheta)|} \right| \qquad (3.19)$$

This formula is the same as that found for the single circularly polarized patch (formula (3.3)).
So, in every plane φ, the axial ratio of a rectangular MxN array of circularly polarized patches is the same as the axial ratio of a single circularly polarized patch and is given by the above formula. Note that the axial ratio is φ- and d-independent.

To decide what number of microstrip patches is necessary to meet the gain requirements of INMARSAT and MSATX (12dB), the directivity as function of the elementspacing is calculated for 6 square arrays ($d_x = d_y$). The directivity can be calculated with the formulas in paragraph 2.1.5:

$$D = 4\pi\cdot\frac{|\bar{E}(\vartheta,\varphi)|^2_{max}}{\int_0^{\frac{\pi}{2}}\int_0^{2\pi}|\bar{E}(\vartheta,\varphi)|^2\cdot\sin(\vartheta)\cdot d\vartheta\cdot d\varphi} =$$

$$\frac{4\pi\cdot\left(F_1^2(0) + F_2^2(0)\right)\cdot M^2\cdot N^2}{\int_0^{\frac{\pi}{2}}\int_0^{2\pi}\left(F_1^2(\vartheta)+\cos^2(\vartheta)F_2^2(\vartheta)\right)\cdot\frac{\sin^2(\frac{\pi}{\lambda}Md_xT_x)}{\sin^2(\frac{\pi}{\lambda}d_xT_x)}\cdot\frac{\sin^2(\frac{\pi}{\lambda}Nd_yT_y)}{\sin^2(\frac{\pi}{\lambda}d_yT_y)}\cdot\sin(\vartheta)\,d\vartheta d\varphi}$$

(3.20a)

Used in the above expression is:

$$\left| \sum_{m=0}^{M-1} \sum_{n=0}^{N-1} e^{j\frac{2\pi}{\lambda}\cdot(md_xT_x + nd_yT_y)} \right| =$$

$$= \left| \frac{1 - (e^{j\frac{2\pi}{\lambda}\cdot d_xT_x})^M}{1 - e^{j\frac{2\pi}{\lambda}\cdot d_xT_x}} \right| \cdot \left| \frac{1 - (e^{j\frac{2\pi}{\lambda}\cdot d_yT_y})^N}{1 - e^{j\frac{2\pi}{\lambda}\cdot d_yT_y}} \right| =$$

$$= \left| \frac{\sin(\frac{\pi}{\lambda}\cdot M\cdot d_xT_x)}{\sin(\frac{\pi}{\lambda}\cdot d_xT_x)} \right| \cdot \left| \frac{\sin(\frac{\pi}{\lambda}\cdot N\cdot d_yT_y)}{\sin(\frac{\pi}{\lambda}\cdot d_yT_y)} \right| \qquad (3.20b)$$

The computer program with which formula (3.20a) is calculated is given in appendix G. The double integral is calculated using the Monte Carlo Integration Method [3-14].
The results are given in table 3.1 and figure 3.10. Figure 3.11 [3-15] gives the antenna efficiency as function of the frequency. For a frequency of 1.55GHz, the antenna efficiency can be as bad as 0.1 or -10dB for a high dielectric constant. Since the antenna gain is given by $g = \eta_e \cdot D$, the antenna gain is obtained from the directivity by adding the efficiency (dB).

Table 3.1 - Antenna element characteristics

ε_r \ Property	Directivity (dB)	Radius (cm)
2.33	6.9	3.72
6	5.5	2.32
10.5	5.1	1.75

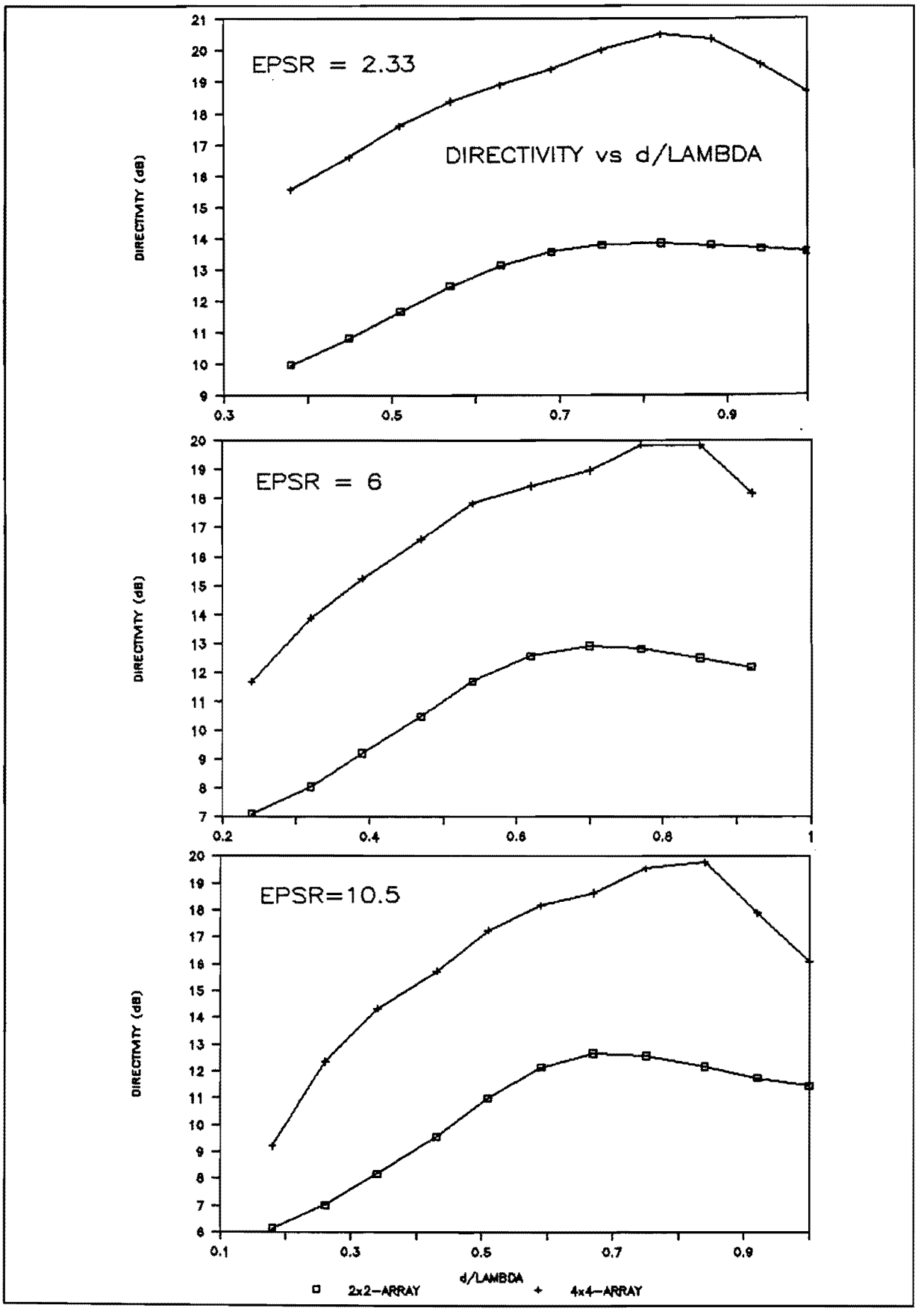

Fig. 3.10 - Directivity vs element spacing for different square arrays ($d_x = d_y$)

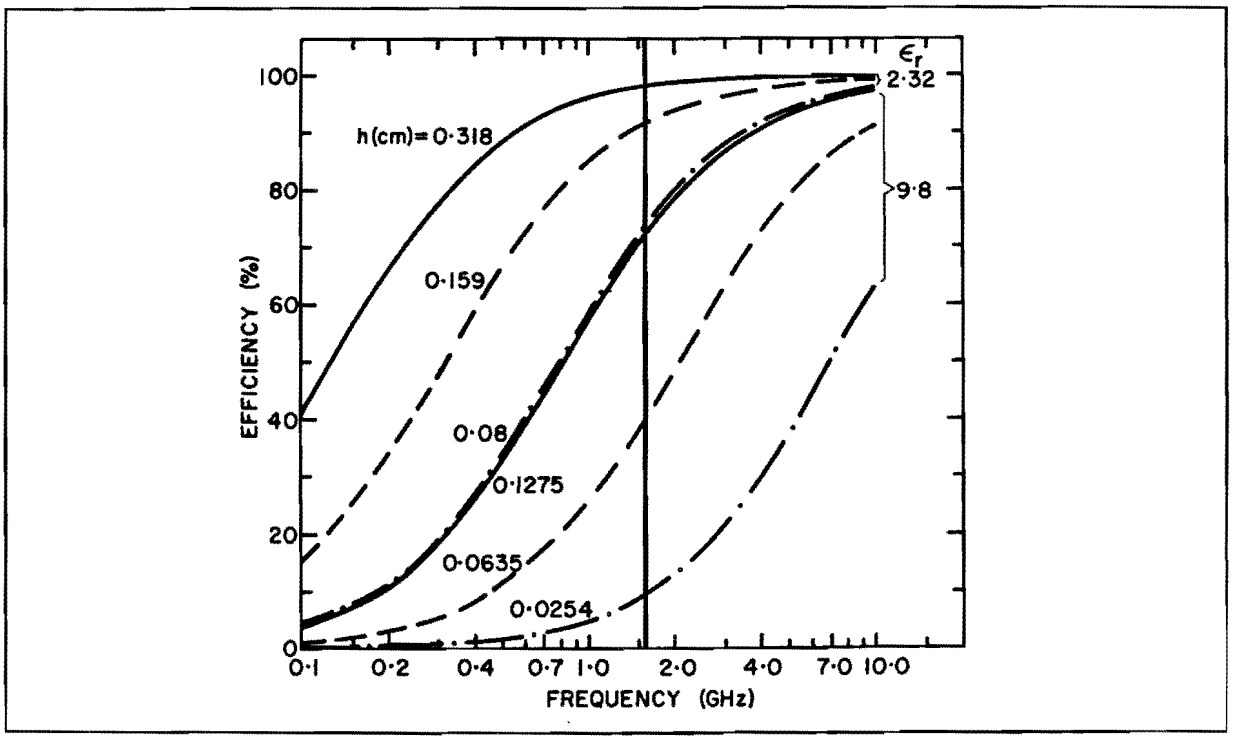

Fig. 3.11 - Efficiency vs frequency for different dielectric substrates

From the above figures can be concluded that for a substrate with a low dielectric constant the gain requirement can be met with a 2x2-array with element spacing approximately 0.75 Lambda. Use of substrates with a higher dielectric constant will make it necessary to use more radiating elements (16 will do in those cases).

A disadvantage of the above discussed array is the great number of coaxial-to-patch connections (2MN) and in phase quadrature power splitters (MN). By using the technique of sequential rotation to obtain a circularly polarized array,employing linearly polarized elements, both numbers can be halved.

§3.3 - Sequential Rotation

In the sequential rotation technique, circular polarization is obtained with linearly polarized antenna elements. This part of the report will deal with two kinds of sequential rotation techniques. First a 'limited' sequential rotation technique will be discussed and after that a 'complete' sequential rotation technique. The meaning of

the terms limited and complete will become apparent in the discussion of complete sequential rotation.

§3.3.1 - Limited Sequential Rotation Technique

It is well known that circular polarization can be achieved in the broadside direction of an array composed of two linearly polarized elements with angle and phase arranged in a 0^0, 90^0 fashion [3-16] (see figure 3.12).

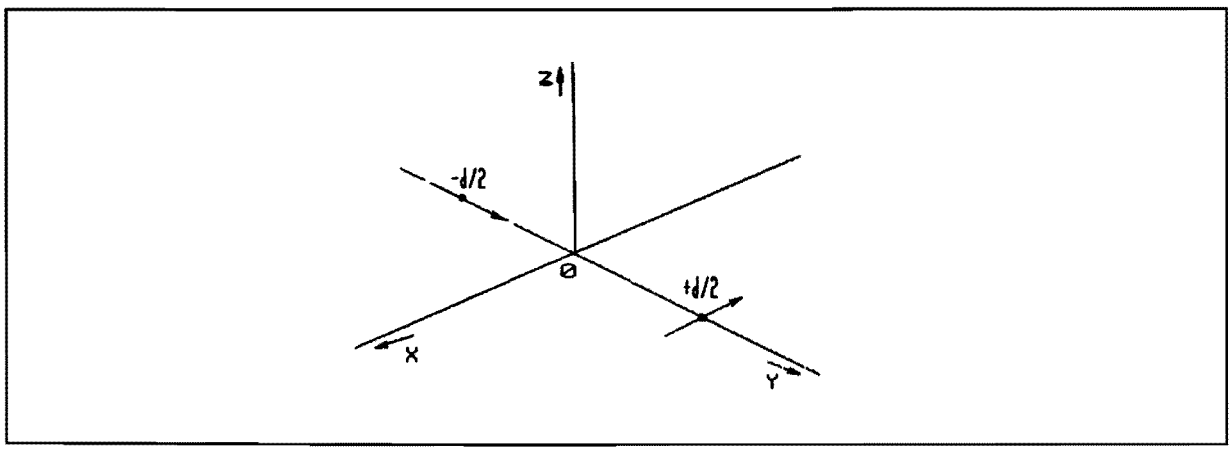

Fig. 3.12 - Array of two linearly polarized elements

For very small angles ϑ however, the axial ratio already becomes poor, because of the spatial phase delay ($\Delta\psi = k_0 d\sin(\vartheta)$), that disturbs the 90^0 phase delay between the two elements (figure 3.13).

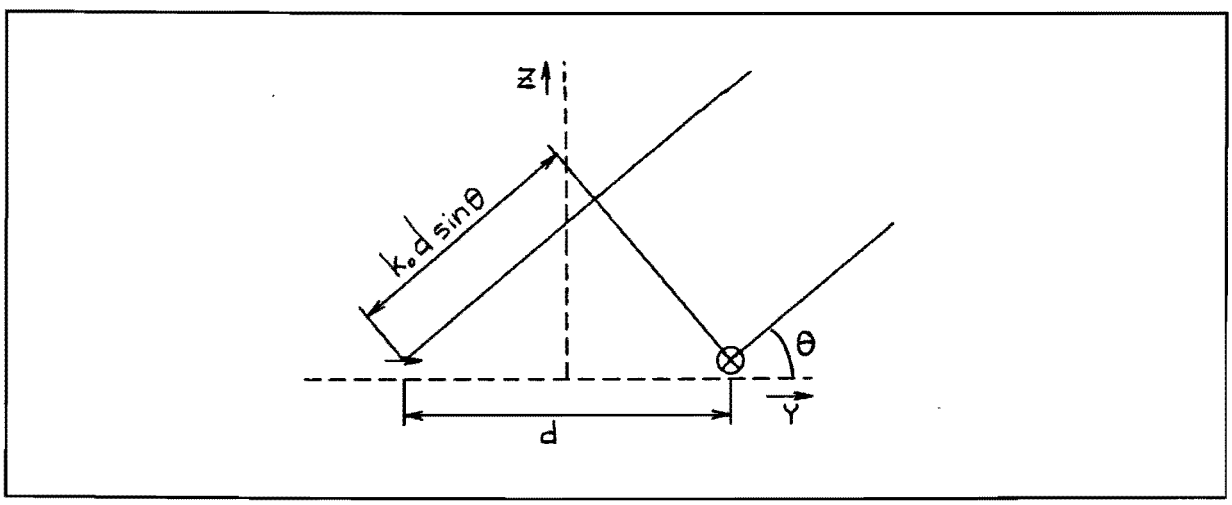

Fig. 3.13 - Spatial phase delay

The CP (Circular Polarization) degradation off broadside can be eliminated by placing two more elements in the fashion shown in figure 3.14.

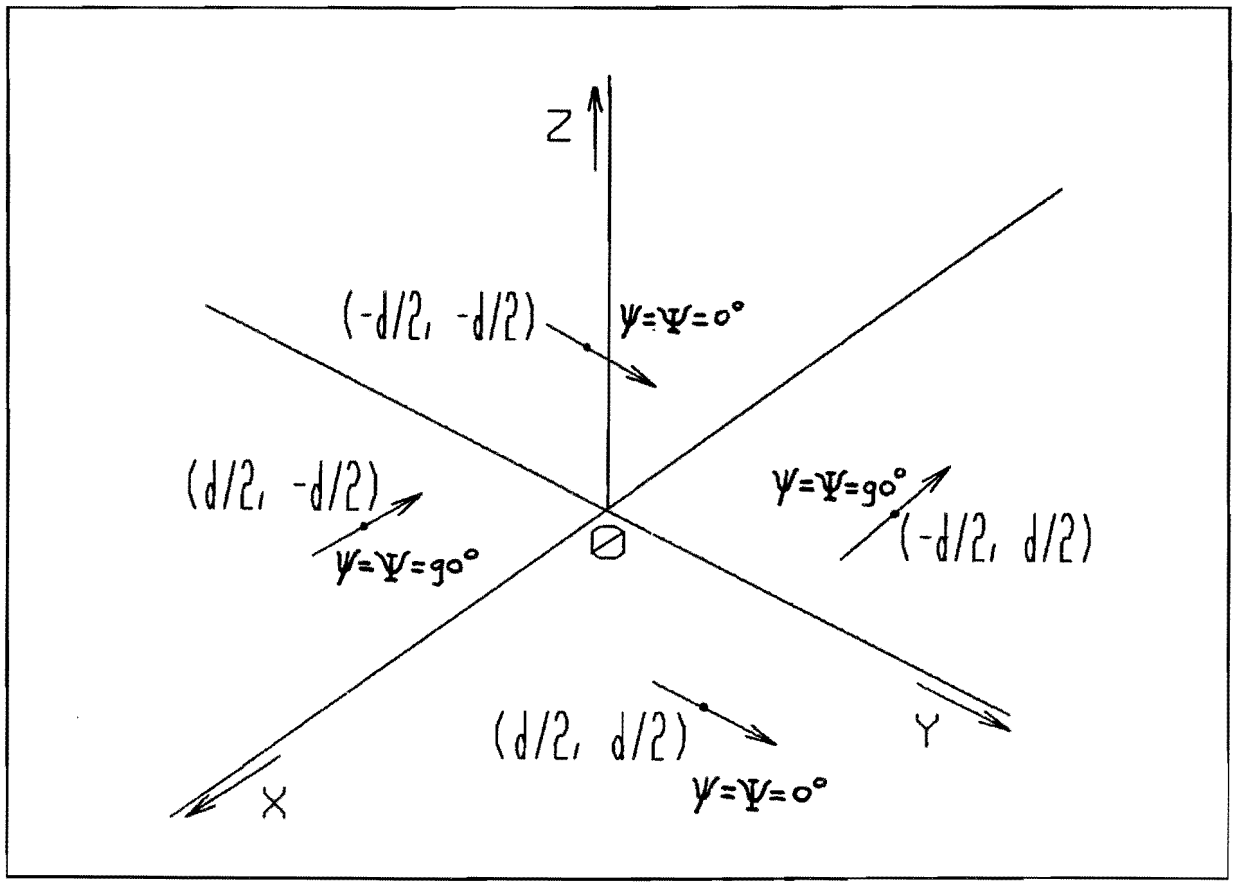

Fig. 3.14 - Spatial phase delay eliminating configuration

Within the two principal planes ($\varphi = 0^0$, $\varphi = 90^0$) the spatial phase delay in one row or column is opposite to that of the other row or column and, consequently, they cancel each other [3-16]. This is only true for the principal planes; in other planes the CP quality will worsen compared to the CP quality in the principal planes. To illustrate the above figure 3.15 gives a two element array with the radiation pattern and axial ratio as function of ϑ for the planes $\varphi = 0^0$ and $\varphi = 90^0$ and figure 3.16 gives a four element array with the radiation pattern and axial ratio as function of ϑ for the two principal planes (program FREQSCAN). In figure 3.17 the axial ratio as function of φ for one angle ϑ is depicted for the 2x2-array (program POLARAX, see appendix G).

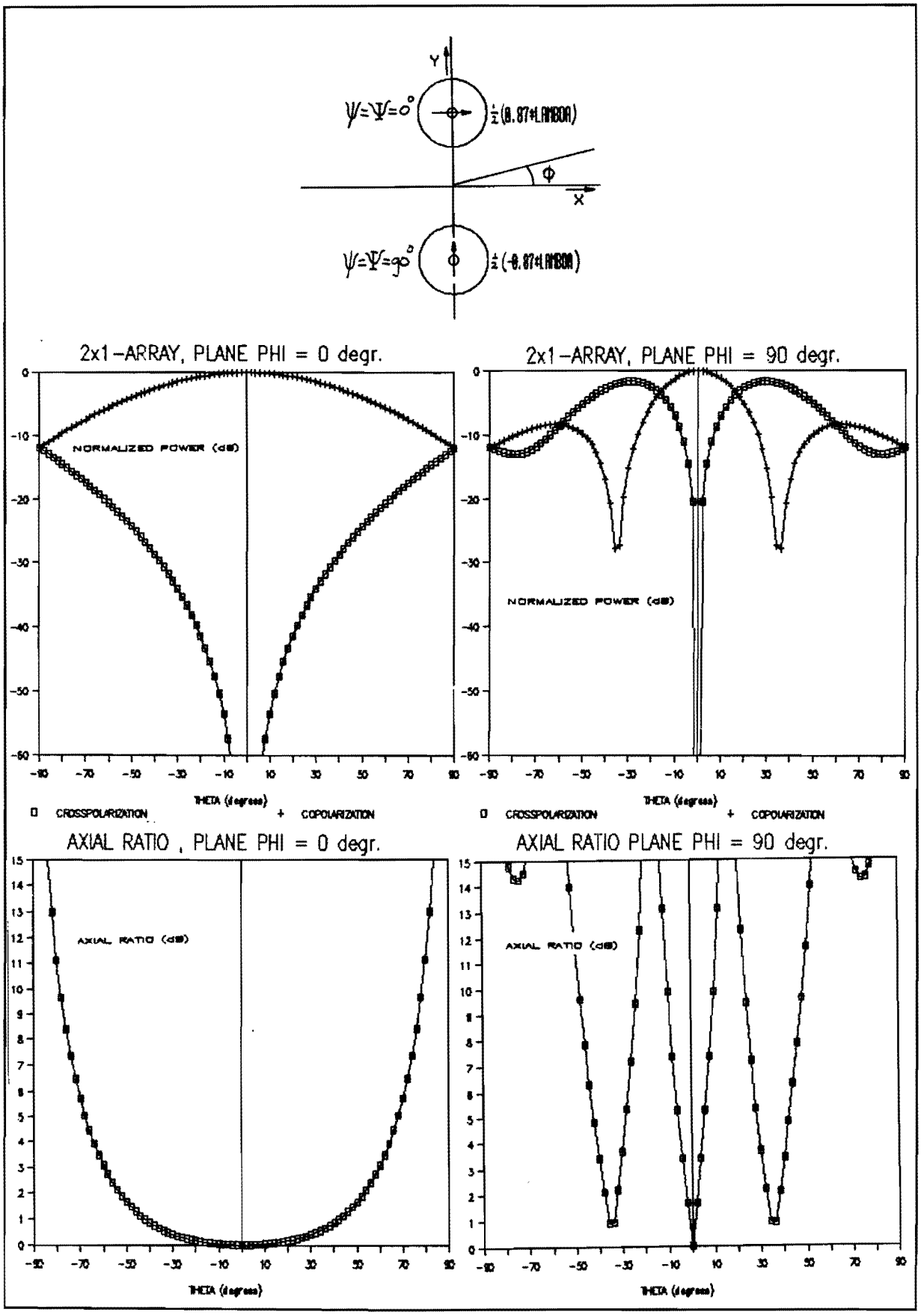

Fig. 3.15 - Radiation characteristics of two element array

f_{res} = 1.55GHz, ε_r = 2.33, elementspacing = 0.87*λ

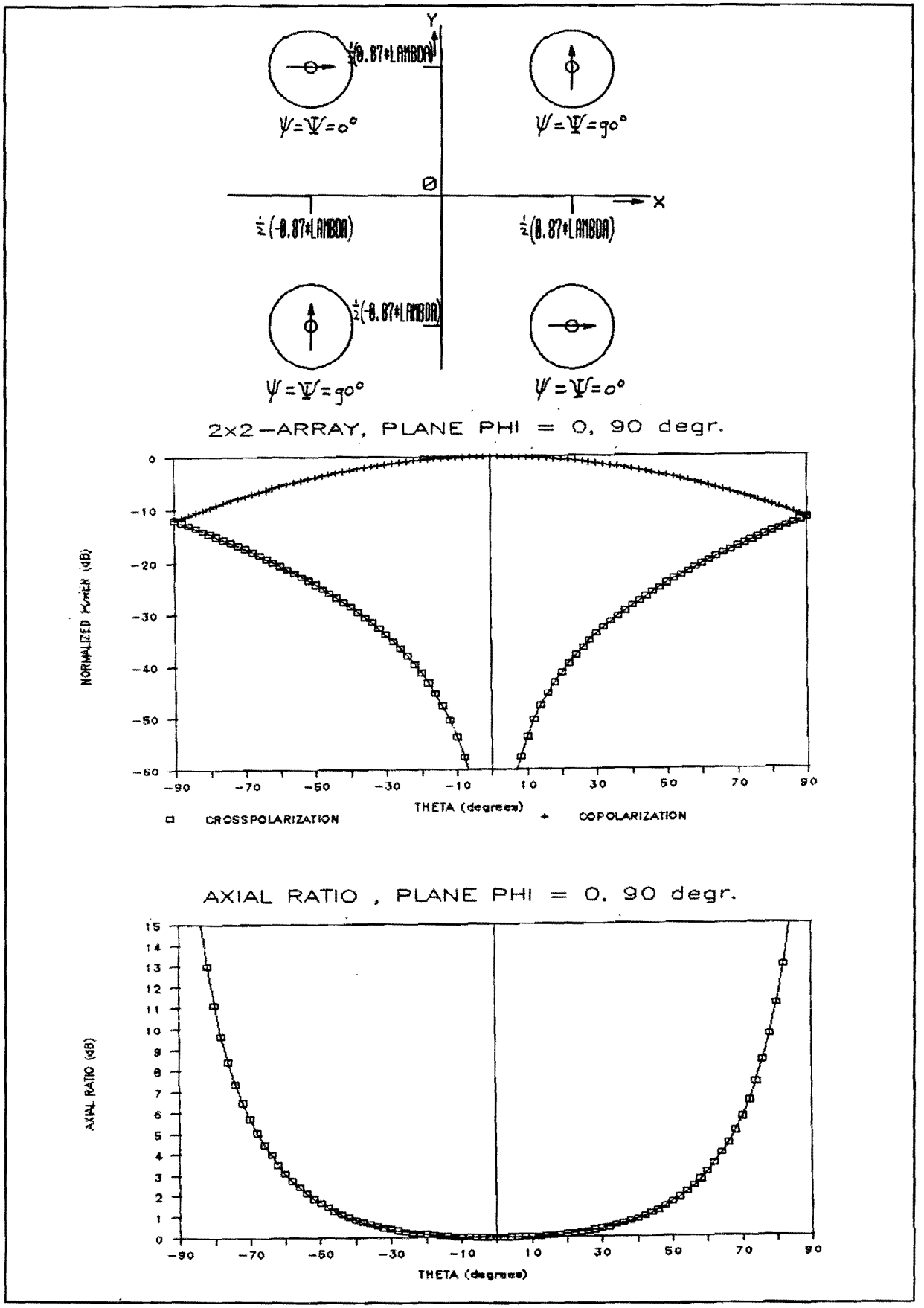

Fig. 3.16 - Radiation characteristics of four element array

f_{res} = 1.55GHz, ε_r = 2.33, elementspacing = 0.87*λ

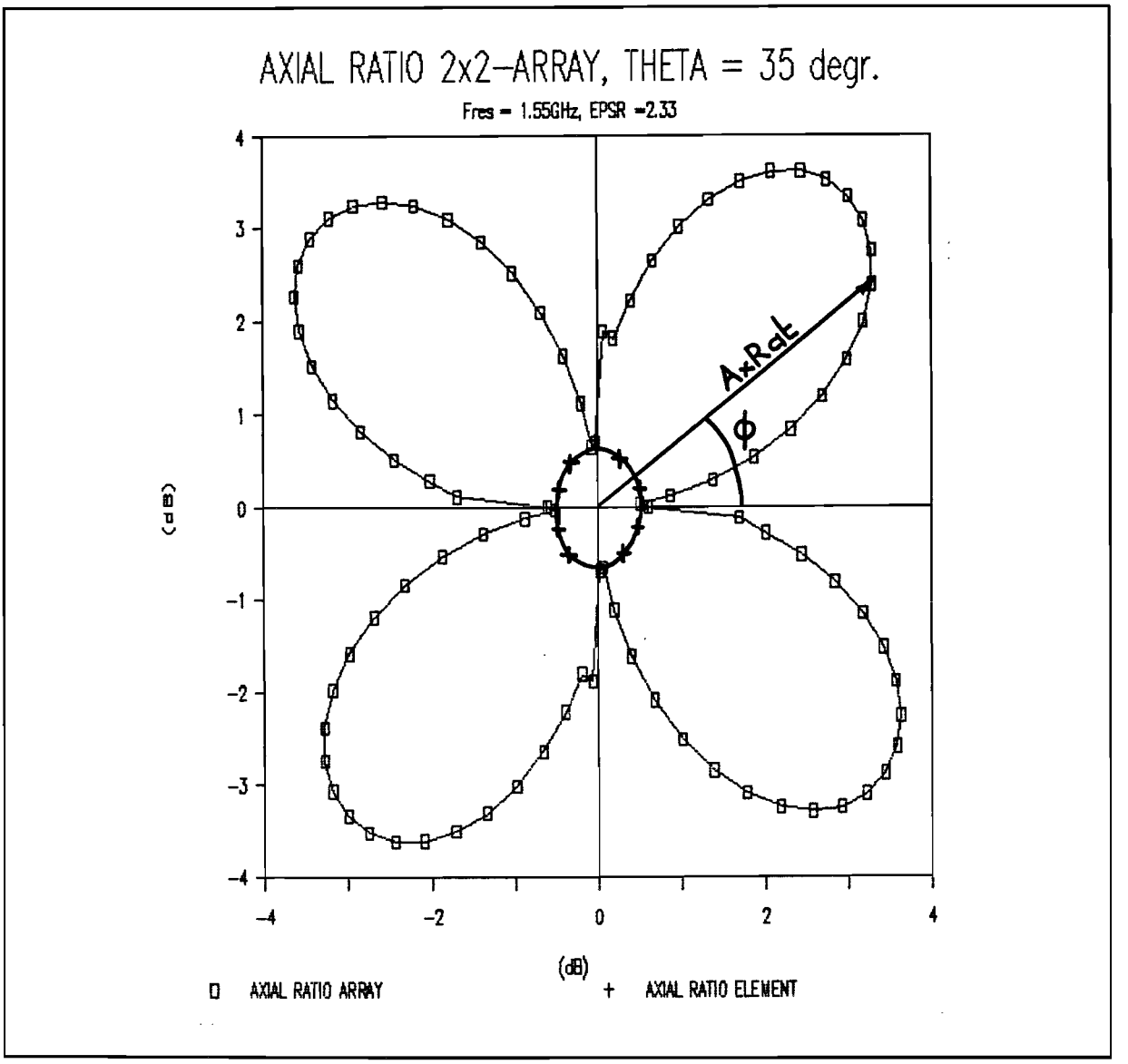

Fig. 3.17 - Axial ratio of 2x2-array as function of φ, polar plot, d/λ = 0.87

The last figure shows that for the array as shown in figure 3.14 and 3.15, in the principal planes the axial ratio is the same as the axial ratio of a single circularly polarized element. This will be proven in the following.

§3.3.2 - Rectangular Array of Linearly Polarized Patches

A MxN array with equaly spacing in x- and y-direction, composed of subarrays as shown in figure 3.14, is depicted in figure 3.18.

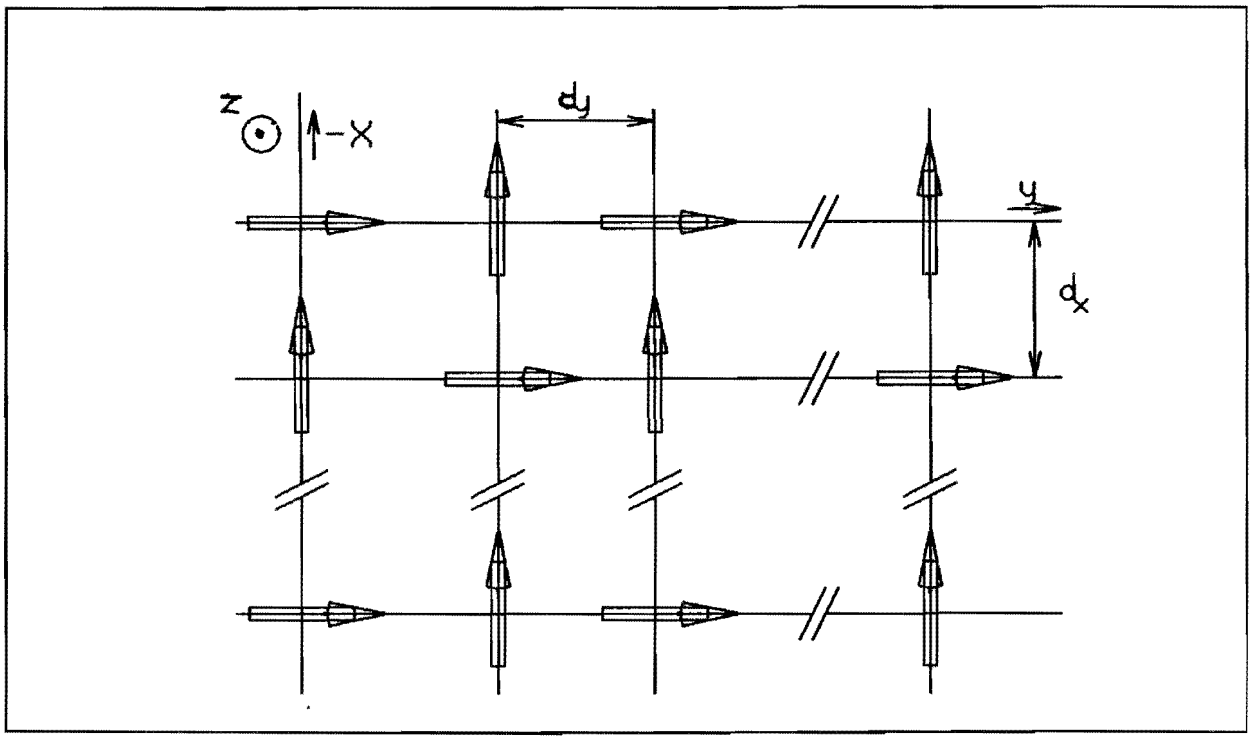

Fig. 3.18 - Rectangular array of sequentially rotated and fed linearly polarized patches

The electric field of the above array can be calculated by first calculating the electric field of one 2x2 subarray and then adding the subarray-fields with taking in account the position of each subarray to get the total electric field.
The position of an element in the subarray is described by the numbers p and q ($0 \le p \le 1$, $0 \le q \le 1$). The position of a subarray in the array is indicated by the numbers m and n ($0 \le m \le \frac{M-2}{2}$, $0 \le n \le \frac{N-2}{2}$). The element distances in the subarray are d_x and d_y; the subarray distances are $2d_x$ and $2d_y$. This is depicted in figure 3.19.

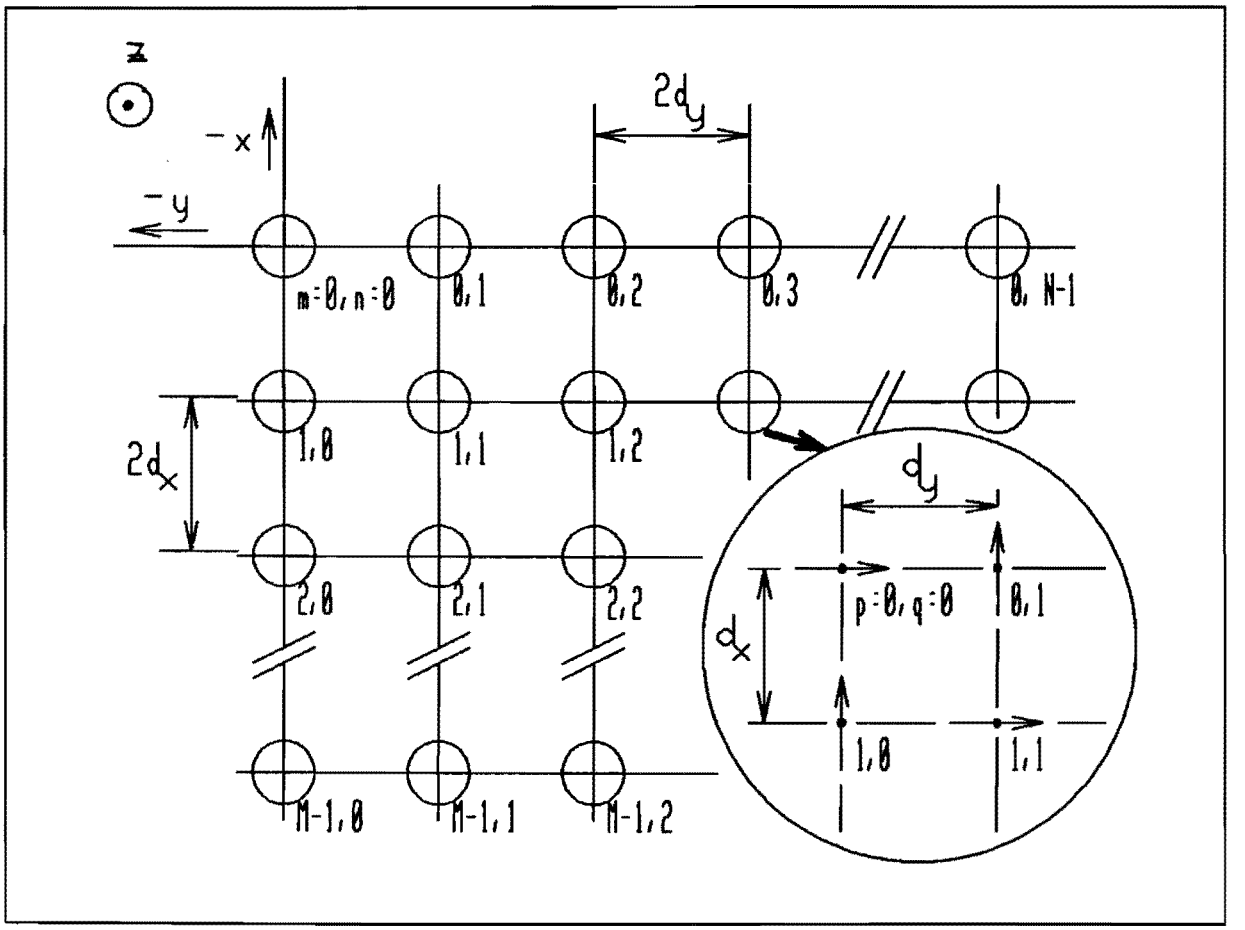

Fig. 3.19 - Array and subarrays

With (3.13) the electric field components of a subarray can be calculated:

$$E_{\vartheta_{sub}}(\vartheta,\varphi) = \sum_{p=0}^{1}\sum_{q=0}^{1} E_{\vartheta_{mn}} \cdot e^{j\cdot\frac{2\pi}{\lambda}\cdot(pd_xT_x + qd_yT_y)} \qquad (3.21a)$$

$$E_{\varphi_{sub}}(\vartheta,\varphi) = \sum_{p=0}^{1}\sum_{q=0}^{1} E_{\varphi_{mn}} \cdot e^{j\cdot\frac{2\pi}{\lambda}\cdot(pd_xT_x + qd_yT_y)} \qquad (3.21b)$$

with:

$$E_{\vartheta_{00}} = E_{\vartheta_{11}} = -\cos(\varphi)\cdot F_1(\vartheta) \tag{3.21c}$$

$$E_{\varphi_{00}} = E_{\varphi_{11}} = \cos(\vartheta)\sin(\varphi)\cdot F_2(\vartheta) \tag{3.21d}$$

$$E_{\vartheta_{01}} = E_{\vartheta_{10}} = -j\cdot\sin(\varphi)\cdot F_1(\vartheta) \tag{3.21e}$$

$$E_{\varphi_{01}} = E_{\varphi_{10}} = -j\cdot\cos(\vartheta)\cos(\varphi)\cdot F_2(\vartheta) \tag{3.21f}$$

When the field contributions of the subarrays are added to get the total electric field,

$$E_{\vartheta}(\vartheta,\varphi) = E_{\vartheta_{sub}}(\vartheta,\varphi)\cdot\sum_{m=0}^{\frac{M-2}{2}}\sum_{n=0}^{\frac{N-2}{2}} e^{j\cdot\frac{4\pi}{\lambda}\cdot(md_xT_x + nd_yT_y)} \tag{3.22a}$$

$$E_{\varphi}(\vartheta,\varphi) = E_{\varphi_{sub}}(\vartheta,\varphi)\cdot\sum_{m=0}^{\frac{M-2}{2}}\sum_{n=0}^{\frac{N-2}{2}} e^{j\cdot\frac{4\pi}{\lambda}\cdot(md_xT_x + nd_yT_y)} \tag{3.22b}$$

The radiation pattern of the left and right hand polarized electric field can be calculated with (2.15) and (3.20):

$$E_L(\vartheta,\varphi) = E_{\vartheta}(\vartheta,\varphi) - j\cdot E_{\varphi}(\vartheta,\varphi) =$$

$$= \left(E_{\vartheta_{sub}}(\vartheta,\varphi) - j\cdot E_{\varphi_{sub}}(\vartheta,\varphi) \right)\cdot\sum_{m=0}^{\frac{M-2}{2}}\sum_{n=0}^{\frac{N-2}{2}} e^{j\cdot\frac{4\pi}{\lambda}\cdot(md_xT_x + nd_yT_y)} \tag{3.23a}$$

$$E_R(\vartheta,\varphi) = E_\vartheta(\vartheta,\varphi) + j\cdot E_\varphi(\vartheta,\varphi) =$$

$$= \left(E_{\vartheta_{sub}}(\vartheta,\varphi) + j\cdot E_{\varphi_{sub}}(\vartheta,\varphi) \right) \cdot \sum_{m=0}^{\frac{M-2}{2}} \sum_{n=0}^{\frac{N-2}{2}} e^{j\cdot\frac{4\pi}{\lambda}\cdot(md_xT_x + nd_yT_y)} \qquad (3.23b)$$

The axial ratio can be calculated with (2.17) and gives:

$$AR = \left| \frac{\left|E_{\vartheta_{sub}}(\vartheta,\varphi) - j\cdot E_{\varphi_{sub}}(\vartheta,\varphi)\right| + \left|E_{\vartheta_{sub}}(\vartheta,\varphi) + j\cdot E_{\varphi_{sub}}(\vartheta,\varphi)\right|}{\left|E_{\vartheta_{sub}}(\vartheta,\varphi) - j\cdot E_{\varphi_{sub}}(\vartheta,\varphi)\right| - \left|E_{\vartheta_{sub}}(\vartheta,\varphi) + j\cdot E_{\varphi_{sub}}(\vartheta,\varphi)\right|} \right| \qquad (3.24)$$

For the planes $\varphi = 0^0$ and $\varphi = 90^0$ the axial ratio is the same as the axial ratio of a single circularly polarized patch. This was already mentioned in paragraph 3.3.1 in connection with figure 3.17. The validity of the above statement follows from the substitution of the formulas below in the expression for the axial ratio.
With (3.19):

$$E_{\vartheta_{sub}}(\vartheta,\varphi) \pm j\cdot E_{\varphi_{sub}}(\vartheta,\varphi) =$$

$$= -\left[\cos(\varphi)F_1(\vartheta) \mp j\cdot\cos(\vartheta)\sin(\varphi)F_2(\vartheta)\right]\cdot\left[1 + e^{j\frac{2\pi}{\lambda}(d_xT_x + d_yT_y)}\right] +$$

$$- j\cdot\left[\sin(\varphi)F_1(\vartheta) \pm j\cdot\cos(\vartheta)\cos(\varphi)F_2(\vartheta)\right]\cdot\left[e^{j\frac{2\pi}{\lambda}d_xT_x} + e^{j\frac{2\pi}{\lambda}d_yT_y}\right] \qquad (3.25a)$$

with:

$$T_x = \sin(\vartheta)\cdot\cos(\varphi) \tag{3.25b}$$

$$T_y = \sin(\vartheta)\cdot\sin(\varphi) \tag{3.25c}$$

To decide what number of microstrip patches is necessary to reach the 12dB gain requirement, the directivity has to be calculated. With the formulas in paragraph 2.1.5:

$$D = 4\pi\cdot\frac{|\bar{E}(\vartheta,\varphi)|^2_{max}}{\int_0^{\frac{\pi}{2}}\int_0^{2\pi}|\bar{E}(\vartheta,\varphi)|^2\cdot\sin(\vartheta)\cdot d\vartheta\cdot d\varphi} \tag{3.26}$$

The term $|\bar{E}(\vartheta,\varphi)|^2$ is calculated as follows with (3.22):

$$|\bar{E}(\vartheta,\varphi)|^2 = |E_\vartheta(\vartheta,\varphi)|^2 + |E_\varphi(\vartheta,\varphi)|^2 =$$

$$= \left(|E_{\vartheta_{sub}}(\vartheta,\varphi)|^2 + |E_{\varphi_{sub}}(\vartheta,\varphi)|^2\right)\cdot$$

$$\cdot\frac{\sin^2(\frac{\pi}{\lambda}\cdot M\cdot d_x T_x)}{\sin^2(2\cdot\frac{\pi}{\lambda}\cdot d_x T_x)}\cdot\frac{\sin^2(\frac{\pi}{\lambda}\cdot N\cdot d_y T_y)}{\sin^2(2\cdot\frac{\pi}{\lambda}\cdot d_y T_y)} \tag{3.27a}$$

Used in the above expression is:

$$\left|\sum_{m=0}^{\frac{M-2}{2}}\sum_{n=0}^{\frac{N-2}{2}} e^{j\frac{4\pi}{\lambda}\cdot(md_xT_x + nd_yT_y)}\right| =$$

$$= \left|\frac{1-(e^{j\frac{4\pi}{\lambda}\cdot d_xT_x})^{\frac{M}{2}}}{1-e^{j\frac{4\pi}{\lambda}\cdot d_xT_x}}\right|\cdot\left|\frac{1-(e^{j\frac{4\pi}{\lambda}\cdot d_yT_y})^{\frac{N}{2}}}{1-e^{j\frac{4\pi}{\lambda}\cdot d_yT_y}}\right| =$$

$$= \left| \frac{\sin(\frac{\pi}{\lambda}\cdot M\cdot d_x T_x)}{\sin(2\frac{\pi}{\lambda}\cdot d_x T_x)} \right| \cdot \left| \frac{\sin(\frac{\pi}{\lambda}\cdot N\cdot d_y T_y)}{\sin(2\frac{\pi}{\lambda}\cdot d_y T_y)} \right| \qquad (3.27b)$$

With formulas (3.21) worked out:

$$E_{\vartheta_{sub}}(\vartheta,\varphi) = -F_1(\vartheta)\cdot$$

$$\cdot\left(\cos(\varphi)\left[1 + e^{j\frac{2\pi}{\lambda}(d_x T_x + d_y T_y)}\right] + j\cdot\sin(\varphi)\left[e^{j\frac{2\pi}{\lambda}d_x T_x} + e^{j\frac{2\pi}{\lambda}d_y T_y}\right]\right) =$$

$$= -F_1(\vartheta)\cdot\left(\cos(\varphi)\cdot P + j\cdot\sin(\varphi)\cdot Q\right) \qquad (3.28a)$$

$$E_{\varphi_{sub}}(\vartheta,\varphi) = \cos(\vartheta)\cdot F_2(\vartheta)\cdot$$

$$\cdot\left(\sin(\varphi)\left[1 + e^{j\frac{2\pi}{\lambda}(d_x T_x + d_y T_y)}\right] - j\cdot\cos(\varphi)\left[e^{j\frac{2\pi}{\lambda}d_x T_x} + e^{j\frac{2\pi}{\lambda}d_y T_y}\right]\right) =$$

$$= \cos(\vartheta)\cdot F_2(\vartheta)\cdot\left(\sin(\varphi)\cdot P - j\cdot\cos(\varphi)\cdot Q\right) \qquad (3.28b)$$

and:

$$\left|E_{\vartheta_{sub}}(\vartheta,\varphi)\right|^2 =$$

$$= F_1^2(\vartheta)\cdot\left(\cos(\varphi)\cdot P + j\cdot\sin(\varphi)\cdot Q\right)\cdot\left(\cos(\varphi)\cdot P^* - j\cdot\sin(\varphi)\cdot Q^*\right) =$$

$$= 2\cdot F_1^2(\vartheta)\cdot\left[\cos^2(\varphi)\cdot\left\{1+\cos\left[\frac{2\pi}{\lambda}(d_xT_x+d_yT_y)\right]\right\}+\right.$$

$$\left.+\sin^2(\varphi)\cdot\left\{1+\cos\left[\frac{2\pi}{\lambda}(d_xT_x-d_yT_y)\right]\right\}\right] \quad (3.28c)$$

$$|E_{\varphi_{sub}}(\vartheta,\varphi)|^2 =$$

$$= \cos^2(\vartheta)\cdot F_2^2(\vartheta)\cdot\left(\sin(\varphi)\cdot P - j\cdot\cos(\varphi)\cdot Q\right)\cdot\left(\sin(\varphi)\cdot P^* + j\cdot\cos(\varphi)\cdot Q^*\right) =$$

$$= 2\cdot\cos^2(\vartheta)\cdot F_2^2(\vartheta)\cdot\left[\sin^2(\varphi)\cdot\left\{1+\cos\left[\frac{2\pi}{\lambda}(d_xT_x+d_yT_y)\right]\right\}+\right.$$

$$\left.+\cos^2(\varphi)\cdot\left\{1+\cos\left[\frac{2\pi}{\lambda}(d_xT_x-d_yT_y)\right]\right\}\right] \quad (3.28d)$$

because:

$$P\cdot P^* = 2\cdot\left\{1+\cos\left[\frac{2\pi}{\lambda}\cdot(d_xT_x+d_yT_y)\right]\right\} \quad (3.28e)$$

$$Q\cdot Q^* = 2\cdot\left\{1+\cos\left[\frac{2\pi}{\lambda}\cdot(d_xT_x-d_yT_y)\right]\right\} \quad (3.28f)$$

$$P\cdot Q^* - P^*\cdot Q = 2\cdot\mathrm{Im}\{P\cdot Q^*\} = 0 \quad (3.28g)$$

The directivity finaly becomes:

$$D = \frac{4\pi \cdot \left(F_1^2(0) + F_2^2(0) \right) \cdot \frac{1}{8} \cdot M^2 \cdot N^2}{\int_0^{\frac{\pi}{2}} \int_0^{2\pi} \left[\left\{ \cos^2(\varphi) F_1^2(\theta) + \cos^2(\theta) \sin^2(\varphi) F_2^2(\theta) \right\} \cdot \left\{ 1 + \cos\left[\frac{2\pi}{\lambda} \cdot (d_x T_x + d_y T_y) \right] \right\} + \left\{ \sin^2(\varphi) F_1^2(\theta) + \cos^2(\theta) \cos^2(\varphi) F_2^2(\theta) \right\} \cdot \left\{ 1 + \cos\left[\frac{2\pi}{\lambda} \cdot (d_x T_x - d_y T_y) \right] \right\} \right] \cdot \frac{\sin^2\left(\frac{\pi}{\lambda} \cdot M \cdot d_x T_x \right)}{\sin^2\left(2 \cdot \frac{\pi}{\lambda} \cdot d_x T_x \right)} \cdot \frac{\sin^2\left(\frac{\pi}{\lambda} \cdot N \cdot d_y T_y \right)}{\sin^2\left(2 \cdot \frac{\pi}{\lambda} \cdot d_y T_y \right)} \cdot \sin(\theta) d\theta d\varphi}$$

(3.29)

This directivity is calculated for 6 different square arrays ($d_x = d_y$) with program DIRECTI2 (appendix G). The results are given in the figures 3.20, 3.21 and 3.22. For reasons of comparison the results of the directivity calculations for the arrays composed of circularly polarized elements are given too in these figures.

The curves show that the directivity of an array composed of sequentially rotated linearly polarized elements compared with the directivity of an array composed of circularly polarized elements, can be much less for relatively large element distances. This gain loss phenomenon has beeen reported in [3-6] too.
For relatively small element distances, both directivities are almost identical. This effect increases with increasing dielectric constant.

To reach the 12dB requirement in the limited sequential rotation technique, a 16-element array will be necessary. The element distance should be kept as small as possible, to limit the axial ratio in planes other than the principal ones. To illustrate this, in figure 3.23 the axial ratio of a 2x2-array is given as function of φ and the element distance, for one angle theta. Also given in this figure is the axial ratio of a single circularly polarized patch.

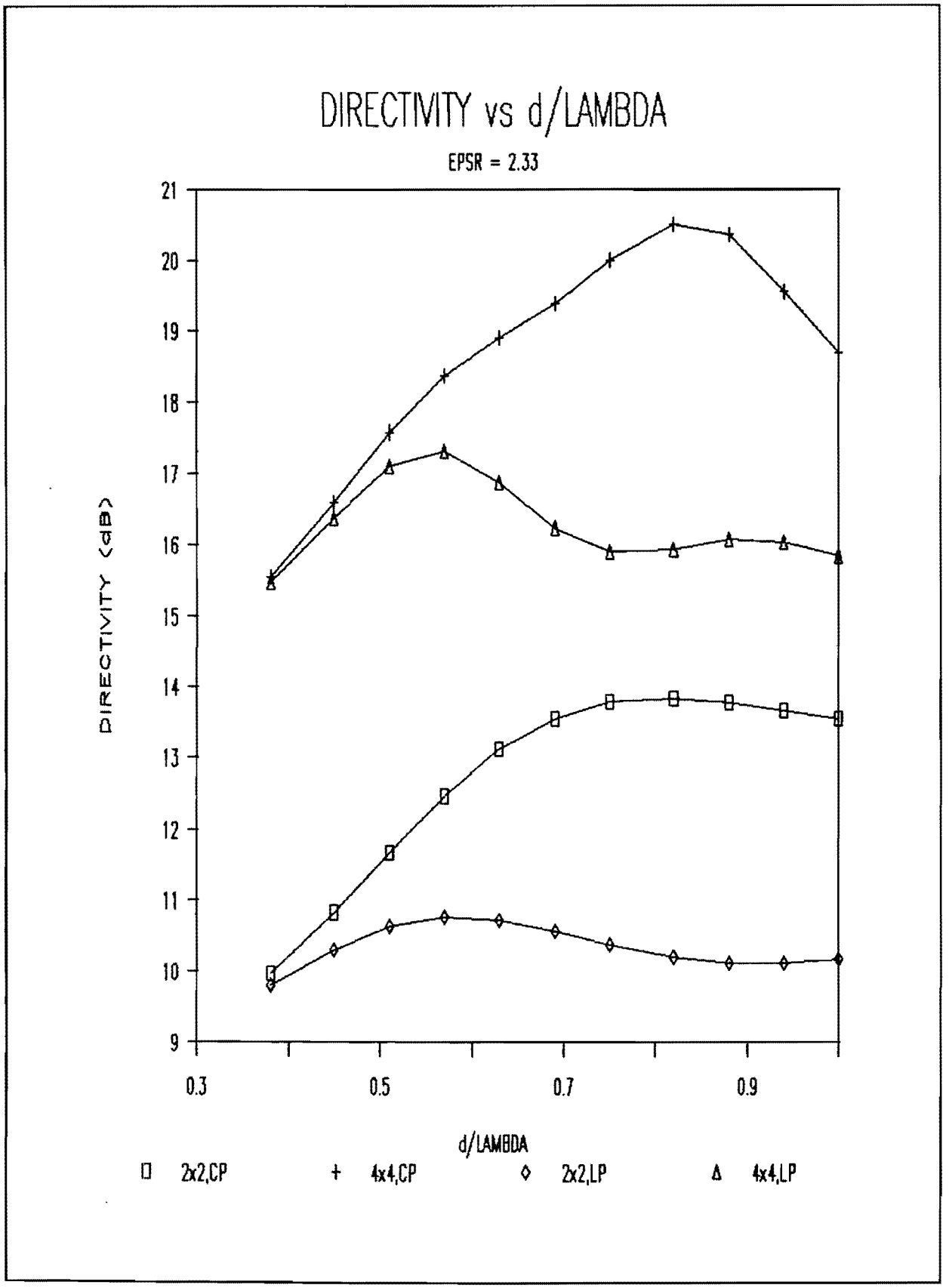

Fig. 3.20 - Directivity as function of elementspacing, ε_r = 2.33

CP = Circularly Polarized elements

LP = Linearly Polarized elements

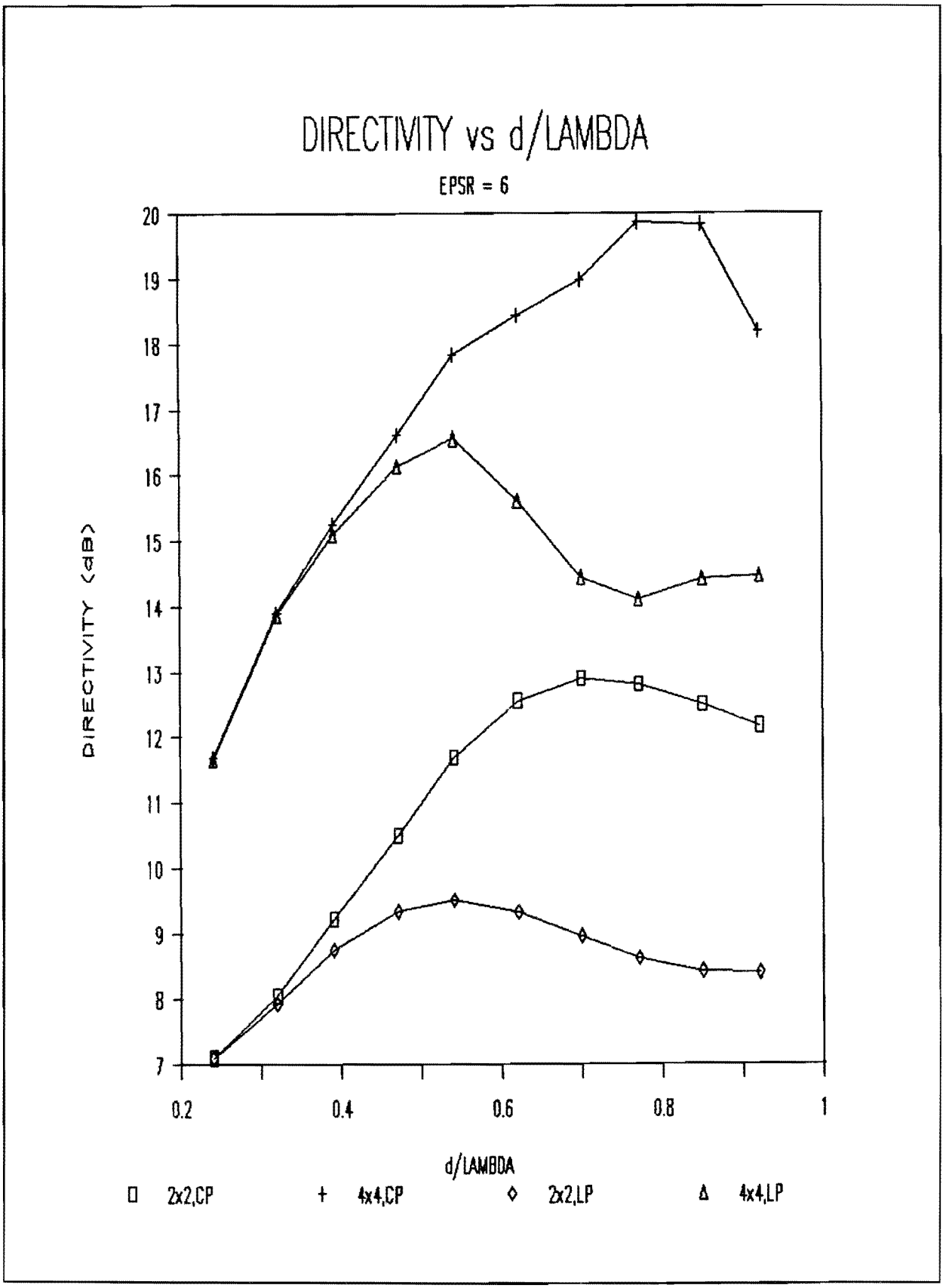

Fig. 3.21 - Directivity as function of elementspacing, $\varepsilon_r = 6$

CP = Circularly Polarized elements

LP = Linearly Polarized elements

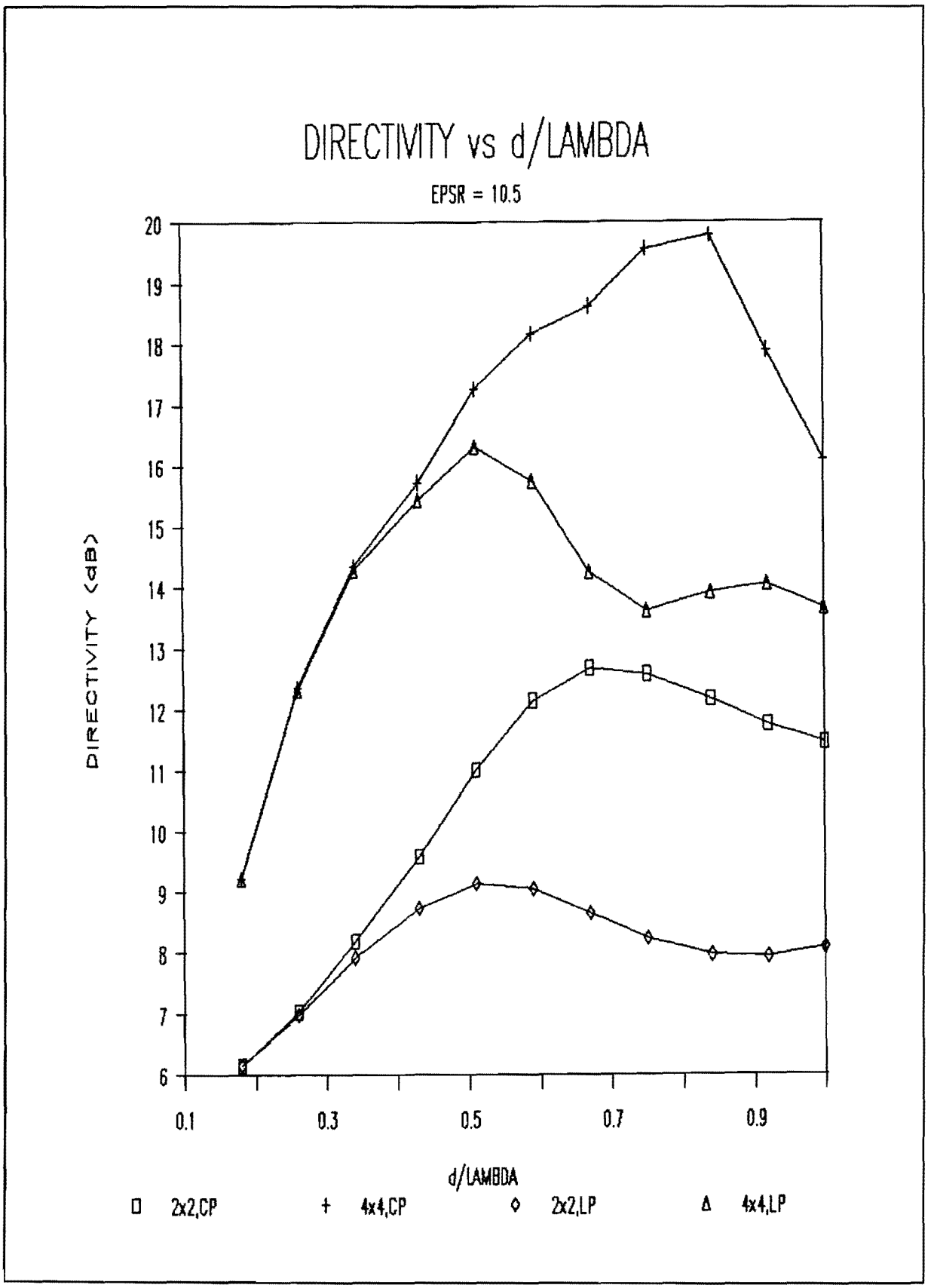

Fig. 3.22 - Directivity as function of elementspacing, ε_r = 10.5

CP = Circularly Polarized elements

LP = Linearly Polarized elements

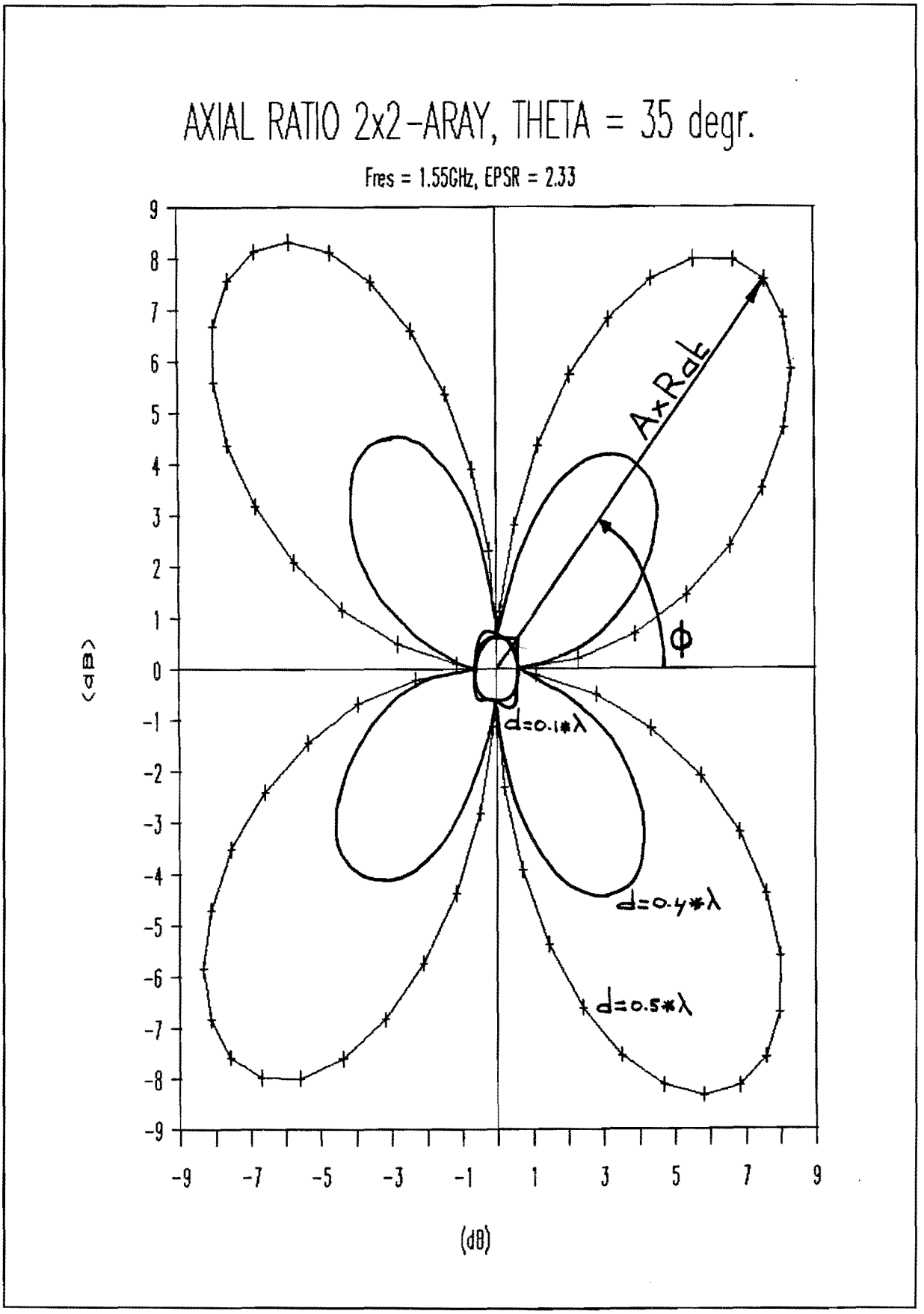

Fig. 3.23 - Axial ratio of 2x2-array as function of φ and elementspacing, polar plot

The foregoing calculations were based on the subarray as given in figure 3.14 and figure 3.24a. These calculations also hold true for the subarray as depicted in figure 3.24b [3-16]. Actually this array can be called sequentially rotated. The idea behind this 0^0, 90^0, 180^0, 270^0 rotation configuration is that radiation impurity (due to higher order modes) from the 0^0 element cancels that from the 180^0 element and likewise for the 90^0 and 270^0 elements.

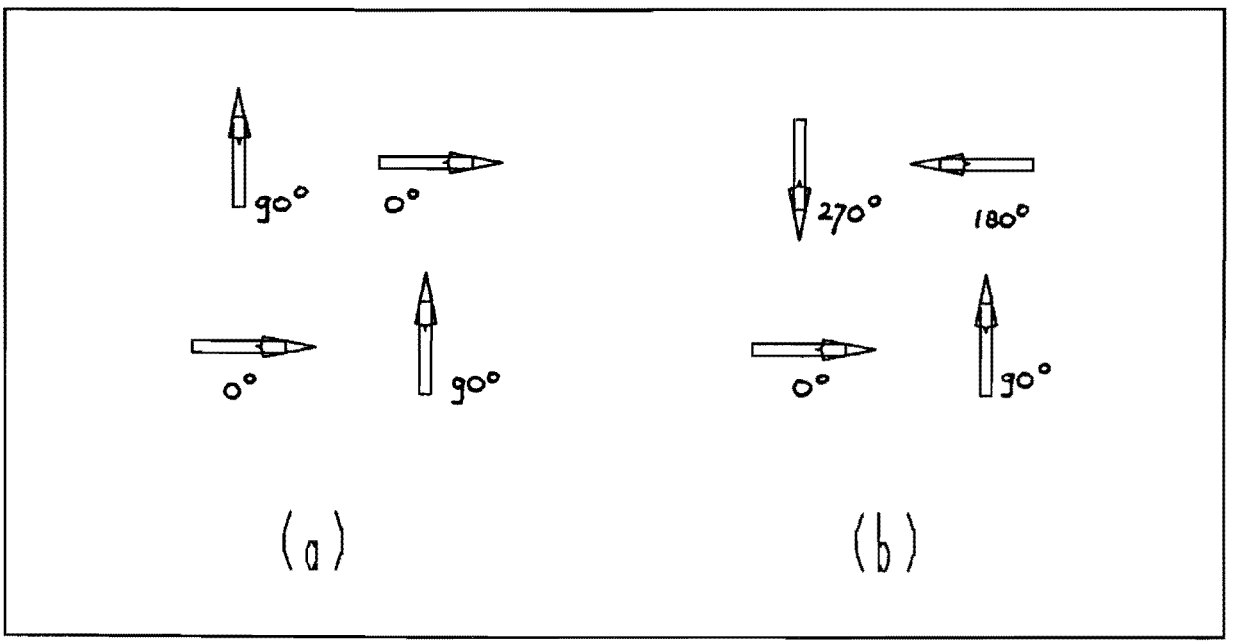

Fig 3.24 - 2x2-subarrays
(a) 0^0, 90^0, 0^0, 90^0 configuration
(b) 0^0, 90^0, 180^0, 270^0 configuration

§3.3.3 - Complete Sequential Rotation Technique

In the complete sequential rotation technique each radiating patch has a unique orientation angle and phase shift [3-17]. For the n^{th} element of an array, located at an arbitrary position:

$$\psi_n = \Psi_n = \frac{n \cdot 2\pi}{N} \qquad (3.30)$$

$$0 \leq n \leq N-1$$

with ψ_n the element rotation angle and Ψ_n the element phase shift.

Note that for N = 4 the situation is the same, as far as rotation and phase shift are concerned, as for a 2x2-subarray in the limited sequential rotation technique.

It is easy to prove that circular polarization in the boresight direction is obtained, independent of the polarization of the element [3-17].
The element position was assumed to be arbitrary. If, however, a low axial ratio off boresight is desired, attention must be paid to the element position. From the discussion of the limited sequential rotation technique it has become clear that a low axial ratio off boresight is obtained in a given direction, if pairs of elements with a mutual 90^0 rotation and phase shift are located perpendicular to this direction (broadside direction). This is depicted in figure 3.25.

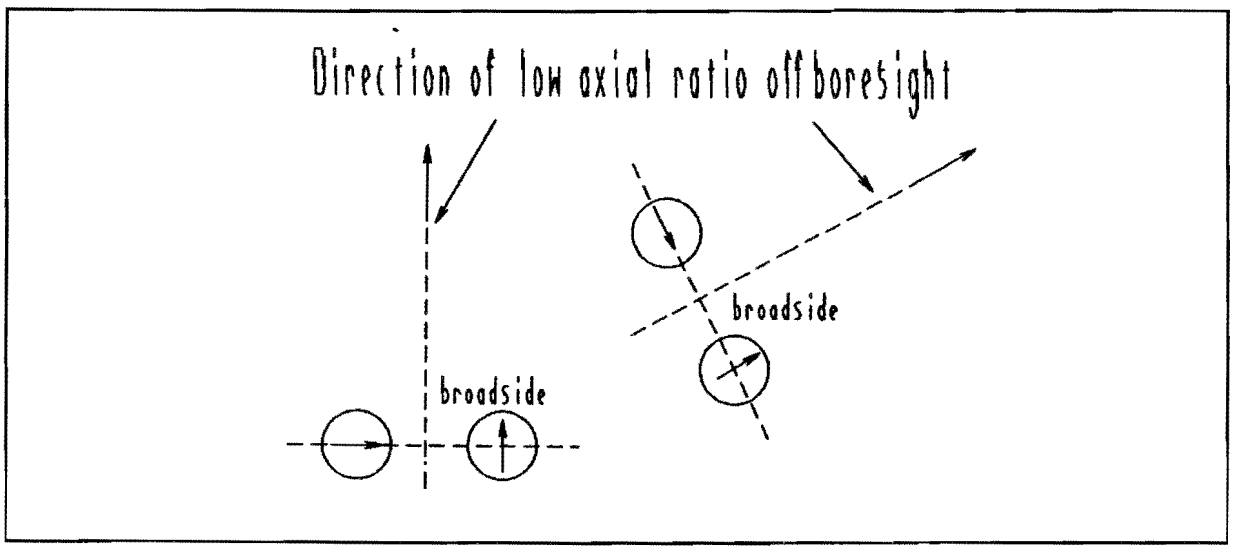

Fig. 3.25 - Element positions in relation with low axial ratio directions

To construct a MxN-array with low axial ratio off boresight in the principal planes is relatively easy using the limited sequential rotation technique. To obtain the same characteristics using the complete sequential rotation technique is quite cumbersome. First it will take some effort to find the correct element positions and second the positioning of the elements will be more difficult, due to their unique rotation angle. To illustrate this, figure 3.26 gives two 4x2-arrays designed with both techniques.

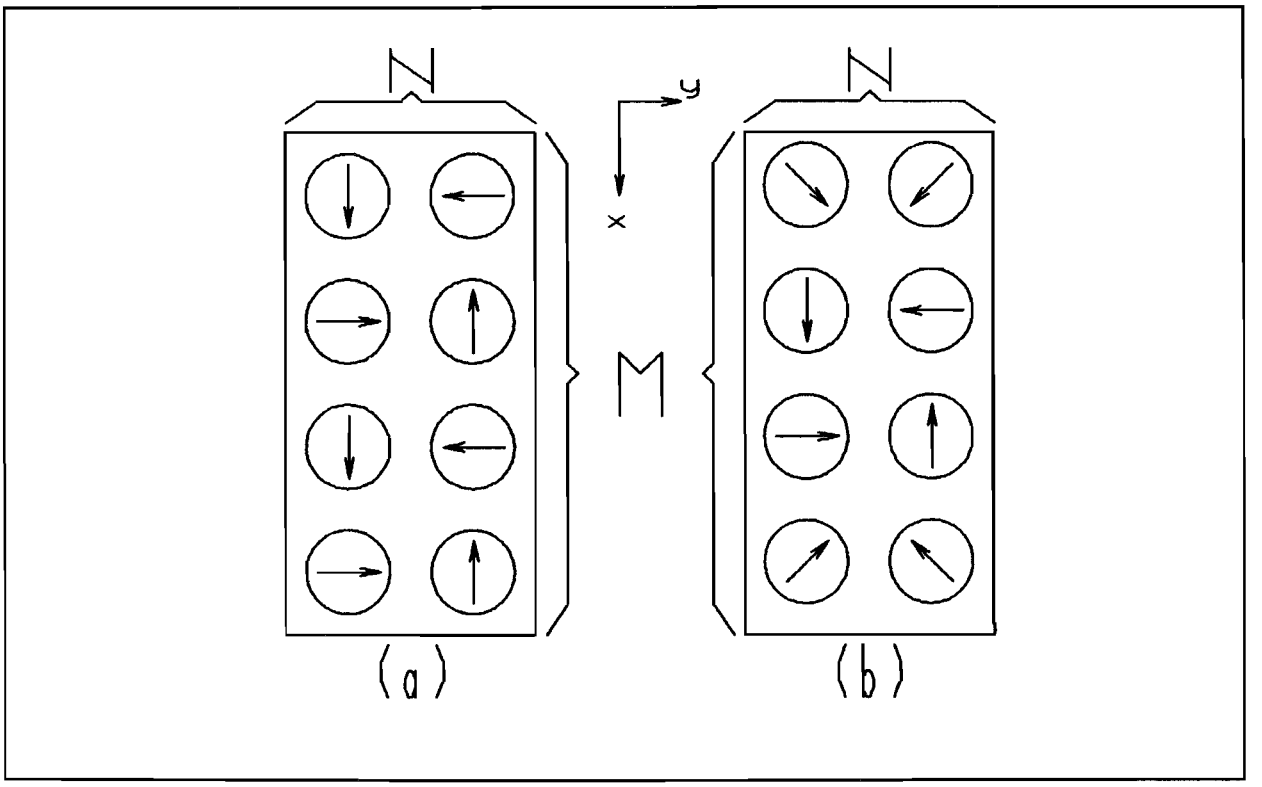

Fig. 3.26 - Arrays of sequentially rotated and fed linearly polarized elements

(a) limited sequential rotation technique

(b) complete sequential rotation technique, $\psi_1 = \Psi_1 = 45^0$

A third drawback of the complete sequential rotation technique follows from inspection of figure 3.26: it is obvious that the array of figure 3.26(b) will be more sensitive to mutual coupling than the one of figure 3.26(a).

§3.3.4 - Circular Array of Linearly Polarized Patches

The rectangular array discussed in paragraph 3.3.2 has a low axial ratio off boresight in the planes $\varphi = 0^0$ and $\varphi = 90^0$. If a low axial ratio off boresight is desired in more planes φ, then from inspection of figure 3.25 it follows that the elements should be positioned on a circle. Figure 3.27 gives an example of an 8-elements-array, meant for a low axial ratio off boresight in the halfplanes $\varphi = 0^0$, 45^0, 90^0, 135^0, 180^0, 225^0, 270^0 and 315^0.

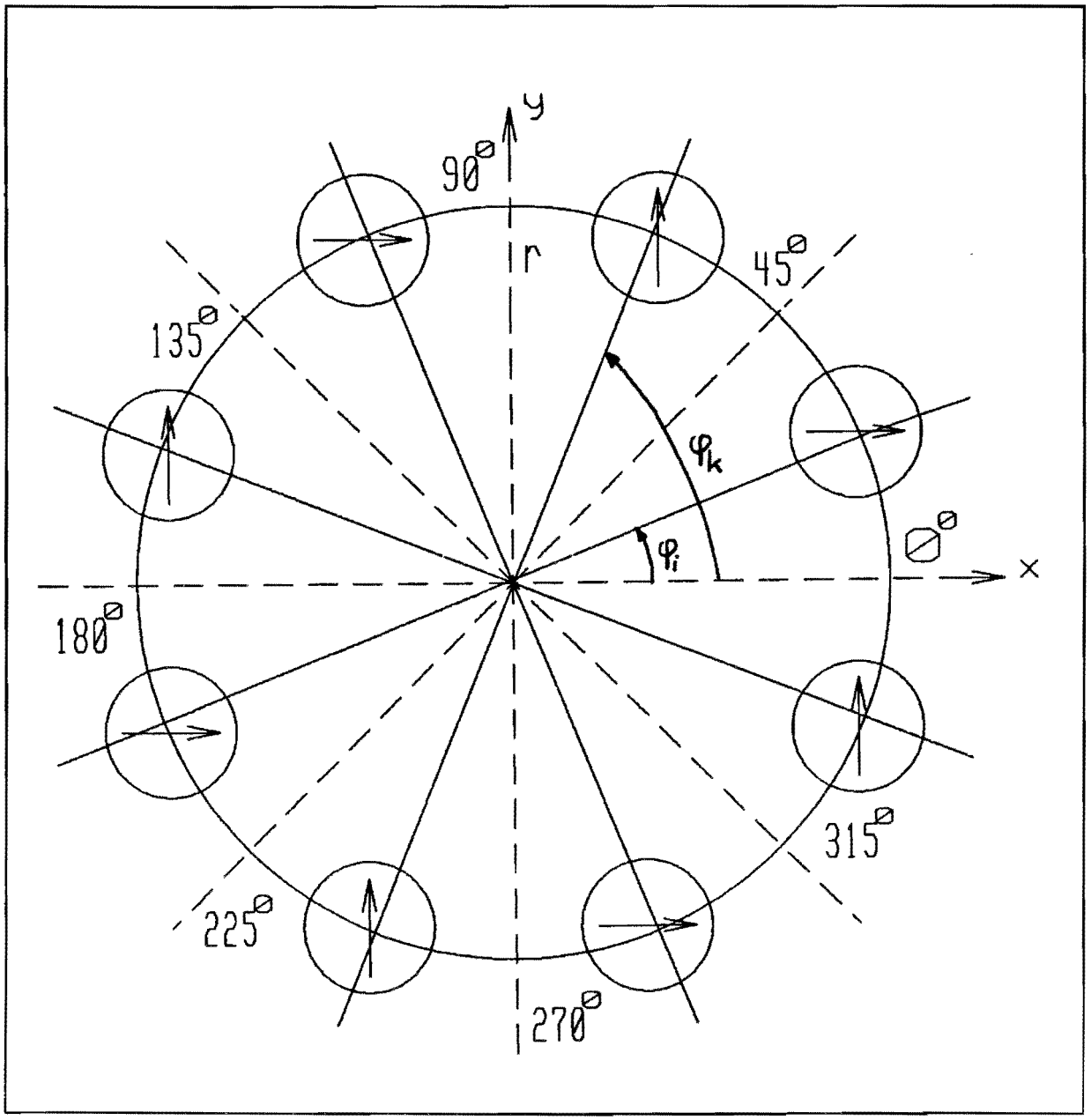

Fig. 3.27 - 8 elements circular array of sequentially rotated and fed linearly polarized patches

The analysis of a circular array goes as follows:

The number of elements N is equal to the number of halfplanes in which a low axial ratio off boresight is desired. N is a multiple of 4. The electric field components of the n^{th} element in the array are given by:

$$E_{\vartheta_n}(\vartheta,\varphi) = -\cos(\varphi - \psi_n)\cdot F_1(\vartheta)\cdot e^{j\Psi_n} \tag{3.31a}$$

$$E_{\varphi_n}(\vartheta,\varphi) = \sin(\varphi - \psi_n)\cos(\vartheta)\cdot F_2(\vartheta)\cdot e^{j\Psi_n} \tag{3.31b}$$

with ψ_n the element rotation angle and Ψ_n the element phase shift. The electric field components of all the elements with $\psi_n = \Psi_n = 0^0$ are given by:

$$E_{\vartheta_0}(\vartheta,\varphi) = -\cos(\varphi)F_1(\vartheta)\sum_{i=0}^{\frac{N-2}{2}} e^{j\frac{2\pi}{\lambda}\sin(\vartheta)\left[x_i\cos(\varphi) + y_i\sin(\varphi)\right]} \tag{3.32a}$$

$$E_{\varphi_0}(\vartheta,\varphi) = \sin(\varphi)\cos(\vartheta)F_2(\vartheta)\sum_{i=0}^{\frac{N-2}{2}} e^{j\frac{2\pi}{\lambda}\sin(\vartheta)\left[x_i\cos(\varphi) + y_i\sin(\varphi)\right]} \tag{3.32b}$$

with:

$$x_i = r\cdot\cos(\varphi_i) \tag{3.32c}$$

$$y_i = r\cdot\sin(\varphi_i) \tag{3.32d}$$

$$\varphi_i = (1 + 4i)\cdot\frac{360}{2N} \tag{3.32e}$$

The electric field components of all the elements with $\psi_n = \Psi_n = 90^0$ are given by:

$$E_{\vartheta_{90}}(\vartheta,\varphi) = -j\sin(\varphi)F_1(\vartheta)\sum_{k=0}^{\frac{N-2}{2}} e^{j\frac{2\pi}{\lambda}\sin(\vartheta)\left[x_k\cos(\varphi) + y_k\sin(\varphi)\right]} \tag{3.33a}$$

$$E_{\varphi_{90}}(\vartheta,\varphi) = -j\cos(\varphi)\cos(\vartheta)F_2(\vartheta)\sum_{k=0}^{\frac{N-2}{2}} e^{j\frac{2\pi}{\lambda}\sin(\vartheta)\left[x_k\cos(\varphi) + y_k\sin(\varphi)\right]} \tag{3.33b}$$

with:

$$x_k = r\cdot\cos(\varphi_k) \tag{3.33c}$$

$$y_k = r\cdot\sin(\varphi_k) \tag{3.33d}$$

$$\varphi_k = (3 + 4k)\cdot\frac{360}{2N} \tag{3.33e}$$

The Left Hand Circular and Right Hand Circular polarized parts of the electric field can be calculated with (3.33):

$$E_{\substack{R\\L}}(\vartheta,\varphi) \quad \left(E_{\vartheta_0}(\vartheta,\varphi) + E_{\vartheta_{90}}(\vartheta,\varphi)\right) \pm j\cdot\left(E_{\varphi_0}(\vartheta,\varphi) + E_{\varphi_{90}}(\vartheta,\varphi)\right) =$$

$$= -\cos(\varphi)\cdot\left[F_1(\vartheta)\cdot\sum\nolimits_1 \mp \cos(\vartheta)\cdot F_2(\vartheta)\cdot\sum\nolimits_2\right] +$$

$$- j\cdot\sin(\varphi)\cdot\left[F_1(\vartheta)\cdot\sum\nolimits_2 \mp \cos(\vartheta)\cdot F_2(\vartheta)\cdot\sum\nolimits_1\right] \tag{3.34a}$$

with:

$$\sum\nolimits_1 = \sum_{i=0}^{\frac{N-2}{2}} e^{j\cdot r\cdot\frac{2\pi}{\lambda}\cdot\sin(\vartheta)\cdot\cos(\varphi - \varphi_i)} \tag{3.34b}$$

$$\sum_2 = \sum_{i=0}^{\frac{N-2}{2}} e^{j\cdot r\cdot\frac{2\pi}{\lambda}\cdot\sin(\vartheta)\cdot\cos(\varphi - \varphi_i - \frac{360}{N})} \qquad (3.34c)$$

$$\varphi_i = (1 + 4i)\cdot\frac{360}{N} \qquad (3.34d)$$

Used in the above is:

$$\varphi_k = \varphi_i + \frac{360}{N} \qquad (3.35)$$

It appears that for the halfplanes $\varphi = n\cdot\frac{360}{N}$ $(0 \le n \le N-1)$ the two summations $\sum_1$ and $\sum_2$ are equal, as is proven in appendix C, and consequently in those halfplanes:

$$AR = \left| \frac{|F_1(\vartheta) + \cos(\vartheta)\cdot F_2(\vartheta)| + |F_1(\vartheta) - \cos(\vartheta)\cdot F_2(\vartheta)|}{|F_1(\vartheta) + \cos(\vartheta)\cdot F_2(\vartheta)| - |F_1(\vartheta) - \cos(\vartheta)\cdot F_2(\vartheta)|} \right| \qquad (3.36)$$

the axial ratio of a single circularly polarized patch.

Interesting is to compare the axial ratio off boresight in planes in between the low axial ratio planes. This is done both for a 16 element circular array and for a 4x4-element array of sequentially rotated linearly polarized patches. The results are given in figure 3.29.
In both arrays the distance between adjacent elements is chosen to be minimal (see figure 3.28).

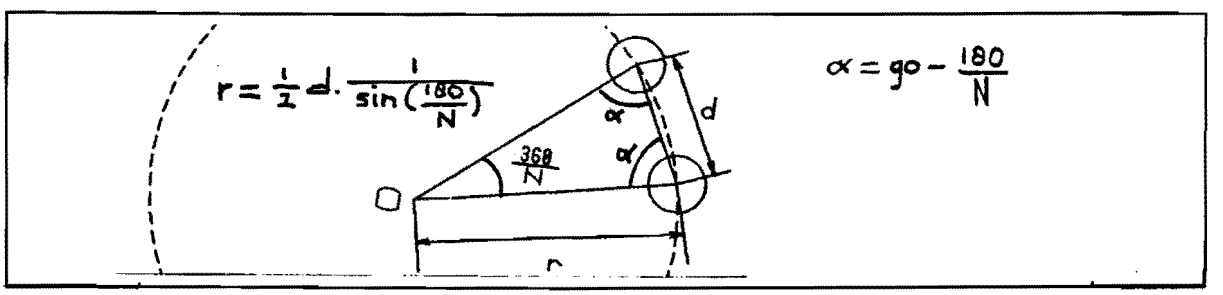

Fig. 3.28 - Elementspacing in circular array

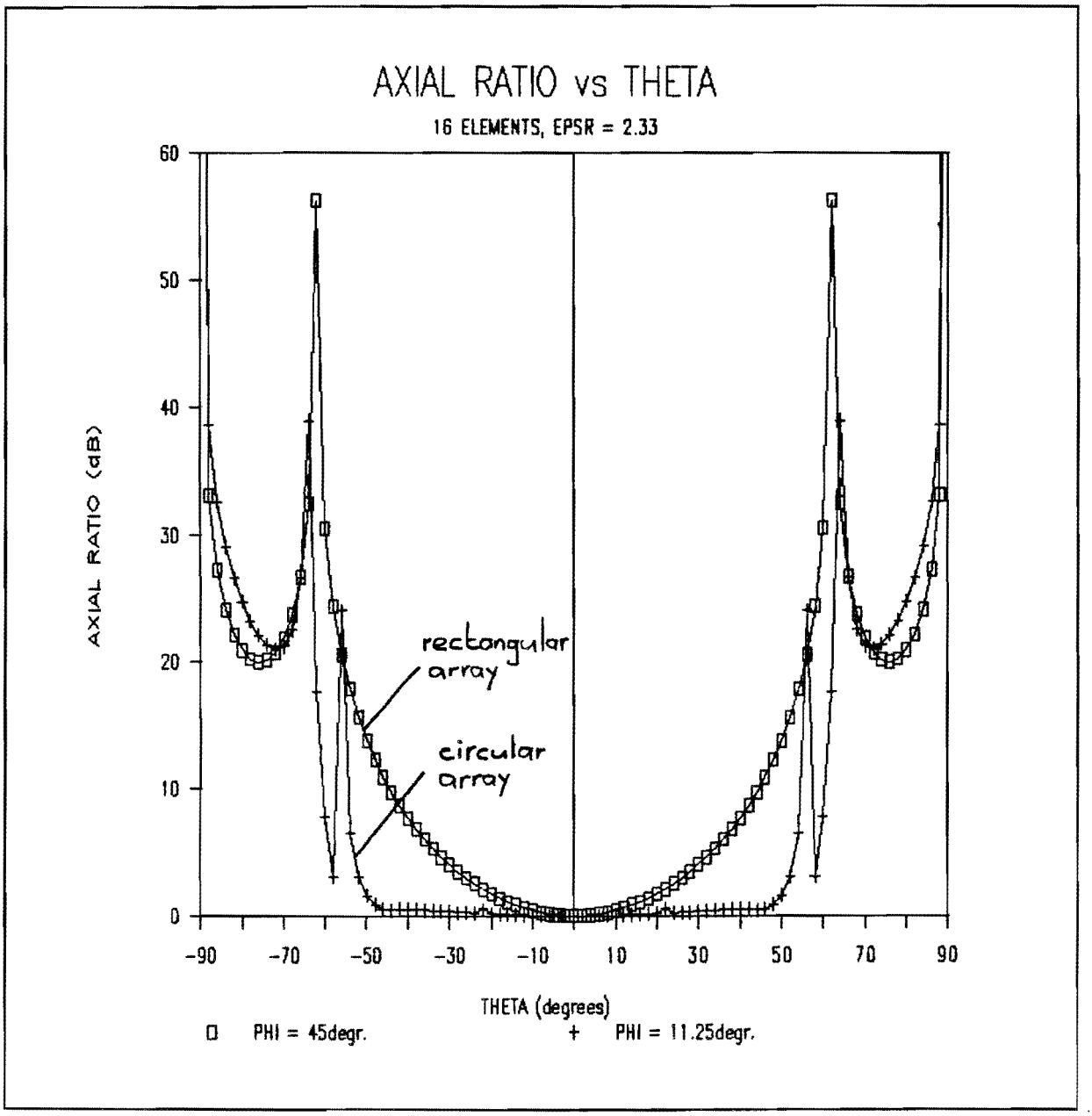

Fig. 3.29 - Axial ratio in between low axial ratio planes

The above figure reveals that the axial ratio performance of the circular array is better than that of the rectangular one. This at the expense of a larger surface.

To decide what number of microstrip patches is necessary to meat the 12dB gain requirement, the directivity of a number of circular arrays is calculated:

With (3.32) and (3.33):

$$E_{\vartheta}(\vartheta,\varphi) = E_{\vartheta_0}(\vartheta,\varphi) + E_{\vartheta_{90}}(\vartheta,\varphi) =$$

$$= - F_1(\vartheta)\cdot\left(\cos(\varphi)\cdot\sum\nolimits_{1} + j\cdot\sin(\varphi)\cdot\sum\nolimits_{2} \right) \qquad (3.37a)$$

$$E_{\varphi}(\vartheta,\varphi) = E_{\varphi_0}(\vartheta,\varphi) + E_{\varphi_{90}}(\vartheta,\varphi) =$$

$$= \cos(\vartheta)\cdot F_2(\vartheta)\cdot\left(\sin(\varphi)\cdot\sum\nolimits_{1} - j\cdot\cos(\varphi)\cdot\sum\nolimits_{2} \right) \qquad (3.37b)$$

With (3.34):

$$\sum\nolimits_{1} = \sum_{i=0}^{\frac{N-2}{2}} \cos\left[\frac{2\pi}{\lambda}\cdot r\cdot\sin(\vartheta)\cdot\cos(\varphi - \varphi_i)\right] +$$

$$+ j\cdot\sum_{i=0}^{\frac{N-2}{2}} \sin\left[\frac{2\pi}{\lambda}\cdot r\cdot\sin(\vartheta)\cdot\cos(\varphi - \varphi_i)\right] =$$

$$= \sum\nolimits_{A} + j\cdot\sum\nolimits_{B} \qquad (3.38a)$$

$$\sum_2 = \sum_{i=0}^{\frac{N-2}{2}} \cos\left[\frac{2\pi}{\lambda}\cdot r\cdot\sin(\vartheta)\cdot\cos(\varphi - \varphi_i - \frac{360}{N})\right] +$$

$$+ j\cdot\sum_{i=0}^{\frac{N-2}{2}} \sin\left[\frac{2\pi}{\lambda}\cdot r\cdot\sin(\vartheta)\cdot\cos(\varphi - \varphi_i - \frac{360}{N})\right] =$$

$$= \sum_C + j\cdot\sum_D \qquad (3.38b)$$

$$|E_\vartheta(\vartheta,\varphi)|^2 = F_1^2(\vartheta)\cdot$$

$$\cdot\left(\cos(\varphi)\cdot\sum_1 + j\cdot\sin(\varphi)\cdot\sum_2\right)\cdot\left(\cos(\varphi)\cdot\sum_1^* - j\cdot\sin(\varphi)\cdot\sum_2^*\right) =$$

$$= F_1^2(\vartheta)\cdot\left(\cos^2(\varphi)\cdot\left[\sum_A^2 + \sum_B^2\right] + \sin^2(\varphi)\cdot\left[\sum_C^2 + \sum_D^2\right] +\right.$$

$$\left. + 2\cdot\sin(\varphi)\cdot\cos(\varphi)\cdot\left[\sum_B\cdot\sum_C - \sum_A\cdot\sum_D\right]\right) \qquad (3.39a)$$

$$|E_\varphi(\vartheta,\varphi)|^2 = \cos^2(\vartheta)\cdot F_2^2(\vartheta)\cdot$$

$$\cdot\left(\sin(\varphi)\cdot\sum_1 - j\cdot\cos(\varphi)\cdot\sum_2\right)\cdot\left(\sin(\varphi)\cdot\sum_1^* + j\cdot\cos(\varphi)\cdot\sum_2^*\right) =$$

$$= \cos^2(\vartheta)F_2^2(\vartheta)\left(\sin^2(\varphi)\left[\sum_A^2 + \sum_B^2\right] + \cos^2(\varphi)\left[\sum_C^2 + \sum_D^2\right] +\right.$$

$$\left. - 2\cdot\sin(\varphi)\cdot\cos(\varphi)\cdot\left[\sum_B\cdot\sum_C - \sum_A\cdot\sum_D\right]\right) \qquad (3.39b)$$

With $|E_\vartheta(\vartheta,\varphi)|^2 = |E_\vartheta(\vartheta,\varphi)|^2 + |E_\varphi(\vartheta,\varphi)|^2$ for the directivity is finally found:

$$D = \frac{\pi \cdot N^2 \cdot \langle F_1^2(0) + F_2^2(0) \rangle}{\int_0^{2\pi} \int_0^{\frac{\pi}{2}} \left[\left(\cos^2(\varphi) \cdot F_1^2(\theta) + \sin^2(\varphi) \cdot \cos^2(\theta) \cdot F_2^2(\theta) \right) \cdot \left(\sum_A^2 + \sum_B^2 \right) + \left(\sin^2(\varphi) \cdot F_1^2(\theta) + \cos^2(\varphi) \cdot \cos^2(\theta) \cdot F_2^2(\theta) \right) \cdot \left(\sum_C^2 + \sum_D^2 \right) + 2 \cdot \sin(\varphi) \cdot \cos(\varphi) \cdot \left(F_1^2(\theta) - \cos^2(\theta) \cdot F_2^2(\theta) \right) \cdot \left(\sum_B \cdot \sum_C - \sum_A \cdot \sum_D \right) \right] \cdot \sin(\theta) \cdot d\theta \cdot d\varphi}$$

(3.40a)

with:

$$r = \frac{1}{2} \cdot d \cdot \frac{1}{\sin(\frac{180}{N})} \qquad (3.40b)$$

$$\varphi_i = (1 + 4i) \cdot \frac{180}{N} \qquad (3.40c)$$

with d the distance between adjacent elements.
The results of the directivity calculations are shown in figures 3.30, 3.31 and 3.32.
To reach the 12dB gain requirement the use of a relatively small dielectric constant is recommended, because of the patch efficiency (see figure 3.11). When designing a circular array, careful attention should be given to the element spacing, because of the gain-reducing effect of side lobes (see figures 3.30, 3.31 and 3.32). This gain reducing effect becomes more important with increasing N.
When carefully designed however, an increase in N can improve both the gain and the overall axial ratio performance of the array.

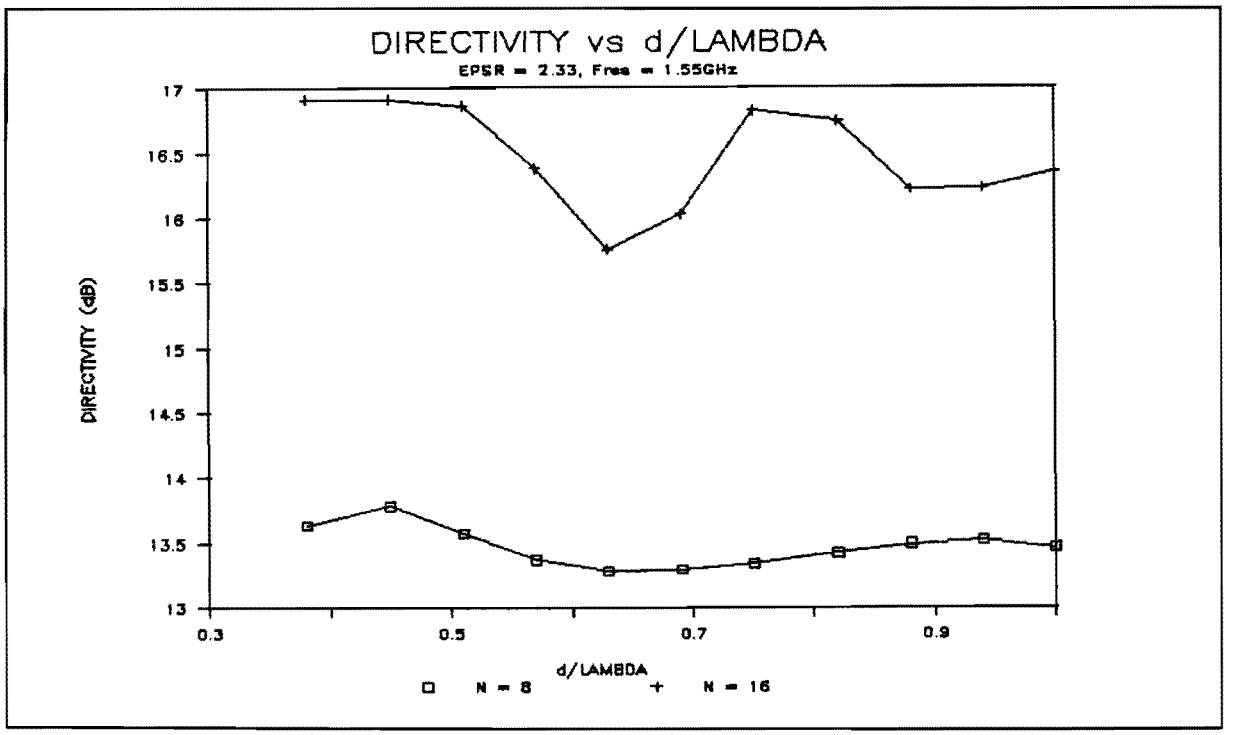

Fig. 3.30 - Directivity as function of element spacing

EPSR = 2.33

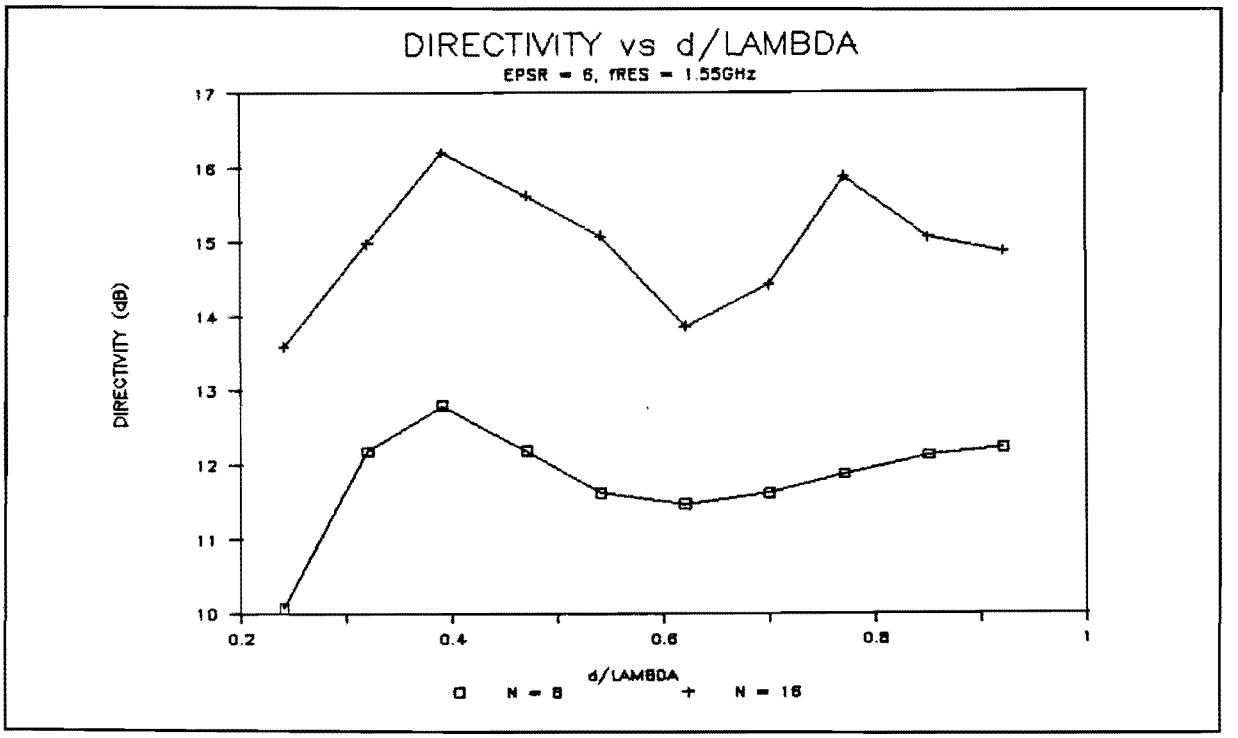

Fig. 3.31 - Directivity as function of element spacing

EPSR = 6

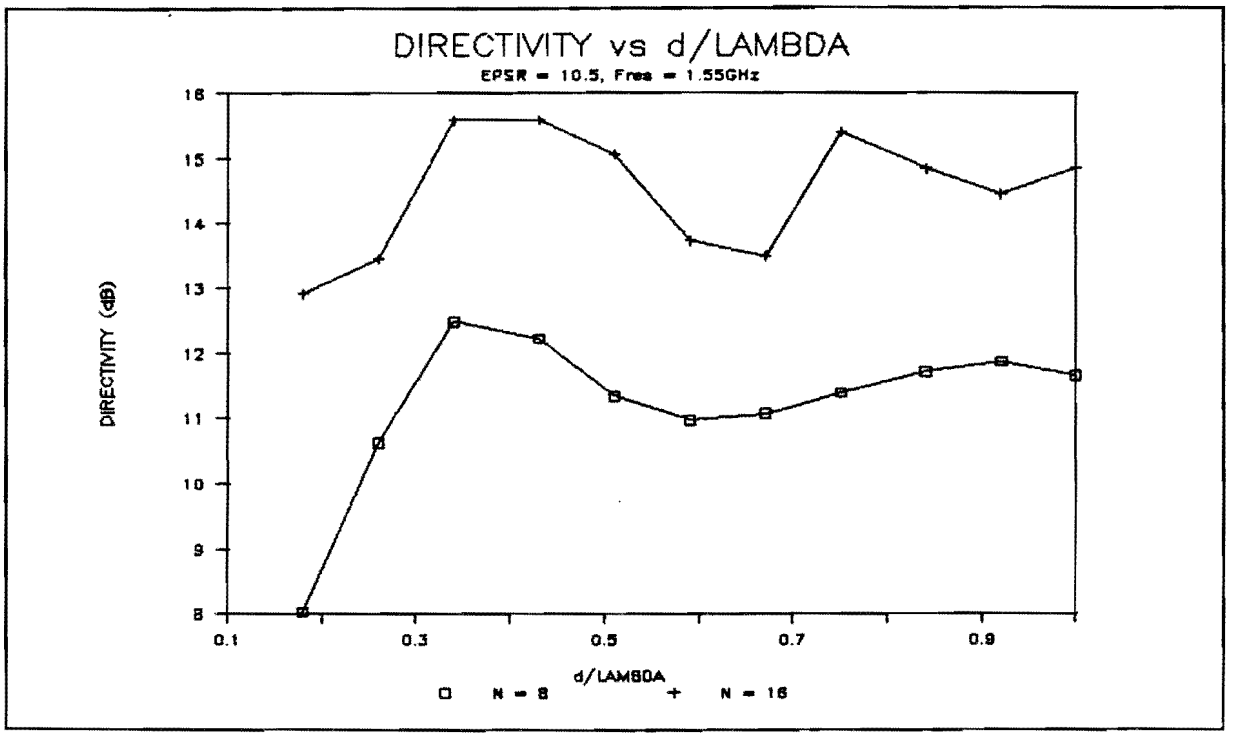

Fig. 3.32 - Directivity as function of element spacing

EPSR = 10.5

In the remainder of this report only rectangular arrays will be considered, because of the ease in applying a phase taper to electronically stear the beam away from boresight.

§3.4 - References

[3-1] Brunner A., ' *Printed Antenna Elements for Special Phased Array Applications* ',
Proceedings of the COST213/KUL Phased Array Workshop, Leuven Belgium, October 1988, pp.85-92.

[3-2] Roederer A.G., Molker A., Griffin J., Martin Pascual C., ' *Recent European Array Antenna Developments For Mobile Communications* ',
Proceedings of the COST213/KUL Phased Array Workshop, Leuven Belgium, October 1988, p.154.

[3-3] Ando M., *'Recent Array Works in Japan '*,
Proceedings of the COST213/KUL Phased Array Workshop, Leuven Belgium, October 1988, p.222

[3-4] Mosig J.R., Barlatey L., Gardiol F.E., *' Stacked Microstrip Patches '*,
Proceedings of the COST213/KUL Phased Array Workshop, Leuven Belgium, October 1988, pp.37-43.

[3-5] Chung H.H., Wong F., Peng S.Y., *'MSAT-X Phased Array Crosssed-Slot Element Design '*,
IEEE 1987 International Symposium Digest Antennas & Propagations, Vol.1, pp.356-359, June 1987.

[3-6] Huang J, Rahmat-Samii Y., *' Recent Array Antenna Developments at JPL '*,
Proceedings of the COST213/KUL Phased Array Workshop, Leuven Belgium, October 1988, p.53-61.

[3-7] Visser H.J., *' Microstripantennes, Het Trilholtemodel '*,
Research Report, Eindhoven University of Technology, Department of Electrical Engineering, Professional Group Electromagnetism and Circuit Theory, Report No.ET.7-87, 1987 (in Dutch).

[3-8] Vrinten M.L.A., *' A Wideband Circularly Polarized Microstrip Antenna Array '*,
Graduate Report, Eindhoven University of Technology, Department of Electrical Engineering, Professional Group Electromagnetism and Circuit Theory, Report No.ET.6-88, 1988.

[3-9] Smolders A.B., *' Microstriparray Geschikt voor Ontvangst van Satelliet-TV Signalen '*,
Research Report, Eindhoven University of Technology, Department of Electrical Engineering, Professional Group Electromagnetism and Circuit Theory, Report No.ET.20-88, 1988 (in Dutch).

[3-10] Karver K.R., Mink J.W., ' *Microstrip Antenna Technology* ', IEEE Trans. on Antennas & Propagat., Vol.AP-29, No.1, January 1981, pp.16-18.

[3-11] Haneishi M., Yoshida S., Goto N., ' *A Broadband Microstrip Array Composed of Single-Feed Type Circularly Polarized Microstrip Antennas* ', AP-S International Symposium 1982, 1982 International Symposium Digest Antennas & Propagation, Vol.1, pp.160-163.

[3-12] Richards W.F., Lo Y.T., Simon P., ' *Design and Theory of Circularly Polarized Microstrip Antennas* ', AP-S International Symposium 1979, 1979 International Symposium Digest Antennas & Propagation, Vol.1, pp.117-120.

[3-13] Amitay N., Pecina R.G., Wu C.P., ' *Radiation Properties of Large Planar Arrays* ', Bell Telephone Laboratories, Incorporated, Whippany, New Jersey, February 18, 1965.

[3-14] Press W.H., Flannery B.P., Teukolsky S.A., Vetterling W.T., ' *Numerical Recipes, The Art of Scientific Computing* ', Cambridge University Press, 1986, pp.221-225.

[3-15] Bahl I.J., Bhartia P., ' *Microstrip Antennas* ', Artech House, 1980, p.123.

[3-16] Huang J., ' *A Technique For An Array To Generate Circular Polarization With Linearly Polarized Elements* ', IEEE Transactions on Antennas & Propagation, Vol. AP-34, No.9, September 1986, pp.1113-1124.

[3-17] Teshirogi T., Tanaka M., Chujo W., ' *Wideband Circularly Polarized Array Antenna With Sequential Rotations and Phase Shift of Elements* ', Proceedings of ISAP '85, 1985, pp.117-120.

4. Scanning Properties of Microstrip Array Antennas

The array antennas discussed in the preceding chapter are fixed beam antennas. For use in mobile satellite communications these antennas must be supplied with a steering device to keep track of the satellite. It is preferable, however, to give the antenna a fixed position (conform a vehicle surface like the roof of a car) and to use electronic beamsteering.
In this chapter such phased arrays will be discussed. Only rectangular arrays will be considered, because of the ease in describing the phased array operation for this class of arrays. After a general discussion of phased array operation, the theory will be applied to a rectangular array of circularly polarized patches and an array of sequentially rotated linearly polarized patches.
After that a phaseshifter reducing technique, called subarray-level-scanning will be discussed for both above mentioned arrays.

§4.1 Theory of Phased Array Antennas

Making use of the theory of paragraph 3.2.2, phased array principles are easily explained. The rectangular array of figure 3.7 is shown again in figure 4.1.

Assumed is that each element is provided with a tuneable phaseshifter and a fixed phaseshifter (0^0 or 90^0 phaseshift), in such a way that the transfer function of the mn^{th} network is given by [4-1]:

$$\frac{I'_{mn}}{I_{mn}} = a_{mn} \cdot e^{j\psi_{mn}} \cdot e^{-j\frac{2\pi}{\lambda} \cdot (md_x T_{xs} + nd_y T_{ys})} \qquad (4.1a)$$

with:

$$T_{xs} = \sin(\vartheta_s) \cdot \cos(\varphi_s) \qquad (4.1b)$$

$$T_{ys} = \sin(\vartheta_s)\cdot\sin(\varphi_s) \tag{4.1c}$$

with ϑ_s and φ_s defining the desired beam direction as will be explained.

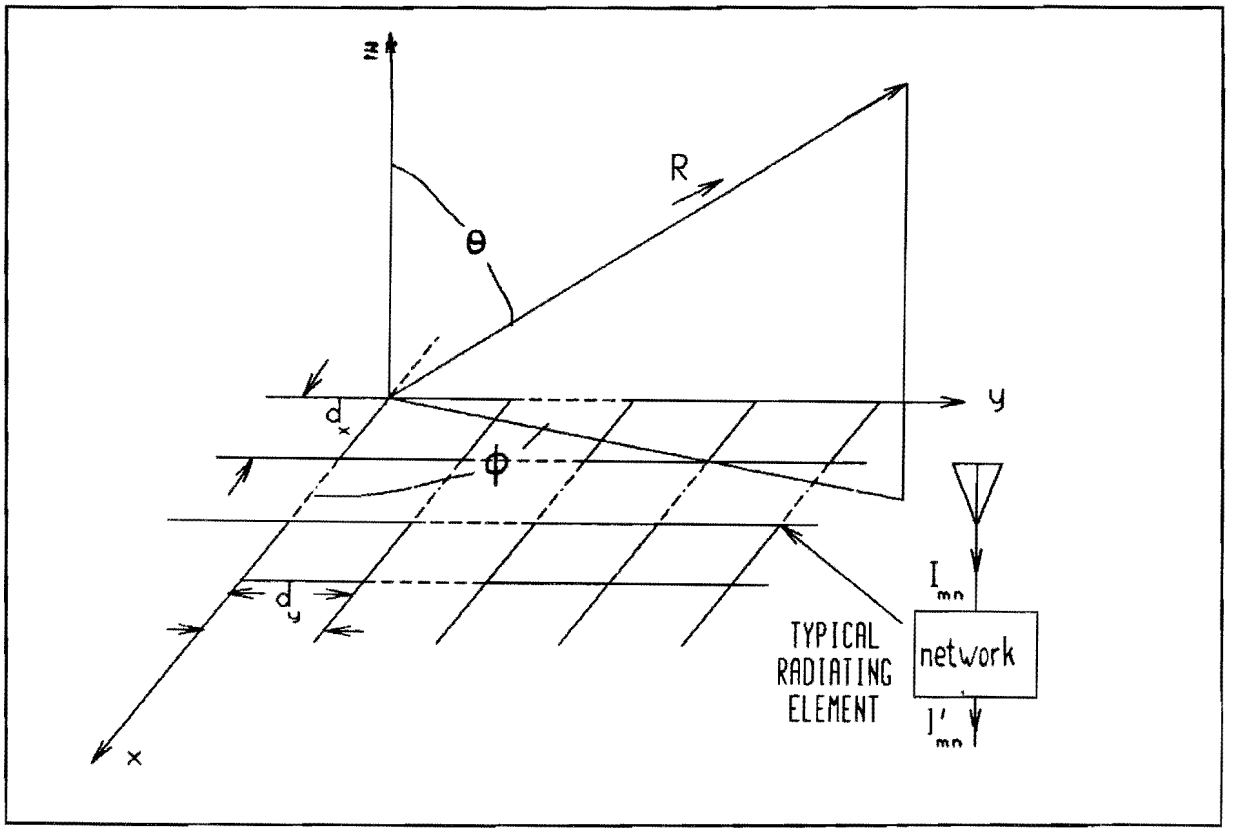

Fig. 4.1 - Rectangular array of radiating elements

From inspection of formula (3.13) it follows that the array radiation pattern can be written as:

$$S(\vartheta,\varphi) = \sum_{m=0}^{M-1}\sum_{n=0}^{N-1} S_{mn}(\vartheta,\varphi)\, a_{mn} e^{j\psi_{mn}} e^{j\frac{2\pi}{\lambda}\left[md_x(T_x - T_{xs}) + nd_y(T_y - T_{ys})\right]} \tag{4.2}$$

When the radiation pattern of formula (3.13) is regarded as a function of T_x and T_y, then the new radiation pattern (4.2) is mereley the original one translated by (T_{xs}, T_{ys}). Since the original array was

designed for maximum radiation at boresight, the application of the phase taper moves the maximum to a new position that is calculated as follows, assuming that grating lobes do not occur:

For maximum radiation:

$$\left(T_x - T_{xs}\right) = \left(\sin(\vartheta)\cos(\varphi) - \sin(\vartheta_s)\cos(\varphi_s)\right) = 0 \qquad (4.3a)$$

$$\left(T_y - T_{ys}\right) = \left(\sin(\vartheta)\sin(\varphi) - \sin(\vartheta_s)\sin(\varphi_s)\right) = 0 \qquad (4.3b)$$

Since $-90^0 \leq \vartheta \leq 90^0$ the solution of (4.3) is:

$$\vartheta = \vartheta_s \qquad (4.4a)$$

$$\varphi = \varphi_s \qquad (4.4b)$$

A grating lobe will occur when

$$\frac{2\pi}{\lambda}\cdot d_i\cdot(T_i - T_{is}) = k\cdot 2\pi \ , \quad i = x, y \quad k = \pm 1, \pm 2, \text{ etc} \qquad (4.5)$$

So to avoid grating lobes the element spacing should satisfy:

$$\frac{d_i}{\lambda} \leq \frac{1}{|T_i| + |T_{is}|} = \frac{1}{1 + |\sin(\vartheta_{max})|} \ , \quad i = x, y \qquad (4.6)$$

with ϑ_{max} the maximum angle to wich the beam can be scanned off boresight without causing a greating lobe to appear.
From (4.6) it follows that for scanning the whole hemisphere the element distances in x- and y-directions should be less than half a wavelength. Formula (4.6) only holds true for the principal planes; for scanning in other planes the maximum d will be less.

§4.2 - A Phased Array With Circularly Polarized Microstrip Patches

In this section the radiation pattern of a rectangular array of circularly polarized patches will be calculated with the beam electronically steared away from boresight. The directivity will be calculated as well and will be compared with the directivity of an unscanned array.

§4.2.1 - Radiation Pattern

A rectangular array of circularly polarized patches is depicted in figure 3.9. When calculating the radiation pattern of the array using equation (4.2), the term $S_{mn}(\vartheta,\varphi)\cdot a_{mn}\cdot e^{j\cdot\psi_{mn}}$ can be replaced by a term $E_{mn}(\vartheta,\varphi)$. This term differs for the calculation of the field component $E_{\vartheta}(\vartheta,\varphi)$ and the component $E_{\varphi}(\vartheta,\varphi)$.
Since these calculations are already carried out for an unscanned array with formula (3.13), that differs only slightly from (4.2), the results can be obtained from inspection of formulas (3.15b) and (3.16b):

$$E_{\vartheta}(\vartheta,\varphi) = -\,e^{j\varphi}\cdot F_1(\vartheta)\cdot \cdot\sum_{m=0}^{M-1}\sum_{n=0}^{N-1} e^{j\frac{2\pi}{\lambda}\left[md_x(T_x-T_{xs})+nd_y(T_y-T_{ys})\right]} \qquad (4.7a)$$

$$E_{\varphi}(\vartheta,\varphi) = -j\cdot e^{j\varphi}\cdot\cos(\vartheta)\cdot F_2(\vartheta)\cdot \cdot\sum_{m=0}^{M-1}\sum_{n=0}^{N-1} e^{j\frac{2\pi}{\lambda}\left[md_x(T_x-T_{xs})+nd_y(T_y-T_{ys})\right]} \qquad (4.7b)$$

The Left and Right Hand Polarized components of the electric field can be calculated with the formulas above:

$$E_L(\vartheta,\varphi) = E_\vartheta(\vartheta,\varphi) - j\cdot E_\varphi(\vartheta,\varphi) =$$

$$= - e^{j\varphi}\cdot\Big(F_1(\vartheta) + \cos(\vartheta)\cdot F_2(\vartheta) \Big)\cdot$$

$$\cdot\sum_{m=0}^{M-1}\sum_{n=0}^{N-1} e^{j\frac{2\pi}{\lambda}\left[md_x(T_x - T_{xs}) + nd_y(T_y - T_{ys})\right]} \qquad (4.8a)$$

$$E_R(\vartheta,\varphi) = E_\vartheta(\vartheta,\varphi) + j\cdot E_\varphi(\vartheta,\varphi) =$$

$$= - e^{j\varphi}\cdot\Big(F_1(\vartheta) - \cos(\vartheta)\cdot F_2(\vartheta) \Big)\cdot$$

$$\cdot\sum_{m=0}^{M-1}\sum_{n=0}^{N-1} e^{j\frac{2\pi}{\lambda}\left[md_x(T_x - T_{xs}) + nd_y(T_y - T_{ys})\right]} \qquad (4.8b)$$

The axial ratio can be calculated with (2.17) and gives:

$$AR = \left| \frac{|F_1(\vartheta) + \cos(\vartheta)\cdot F_2(\vartheta)| + |F_1(\vartheta) - \cos(\vartheta)\cdot F_2(\vartheta)|}{|F_1(\vartheta) + \cos(\vartheta)\cdot F_2(\vartheta)| - |F_1(\vartheta) - \cos(\vartheta)\cdot F_2(\vartheta)|} \right| \qquad (4.9)$$

This again is the axial ratio of a single circularly polarized patch. Thus the axial ratio of a rectangular phased array of circularly polarized patches is φ-, d- and scanning-independent; scanning will not affect the axial ratio.
To show this, the radiation pattern and axial ratio as function of theta are calculated (program FREQSCAN) for two 4x4-arrays (figure 4.2 to figure 4.5).

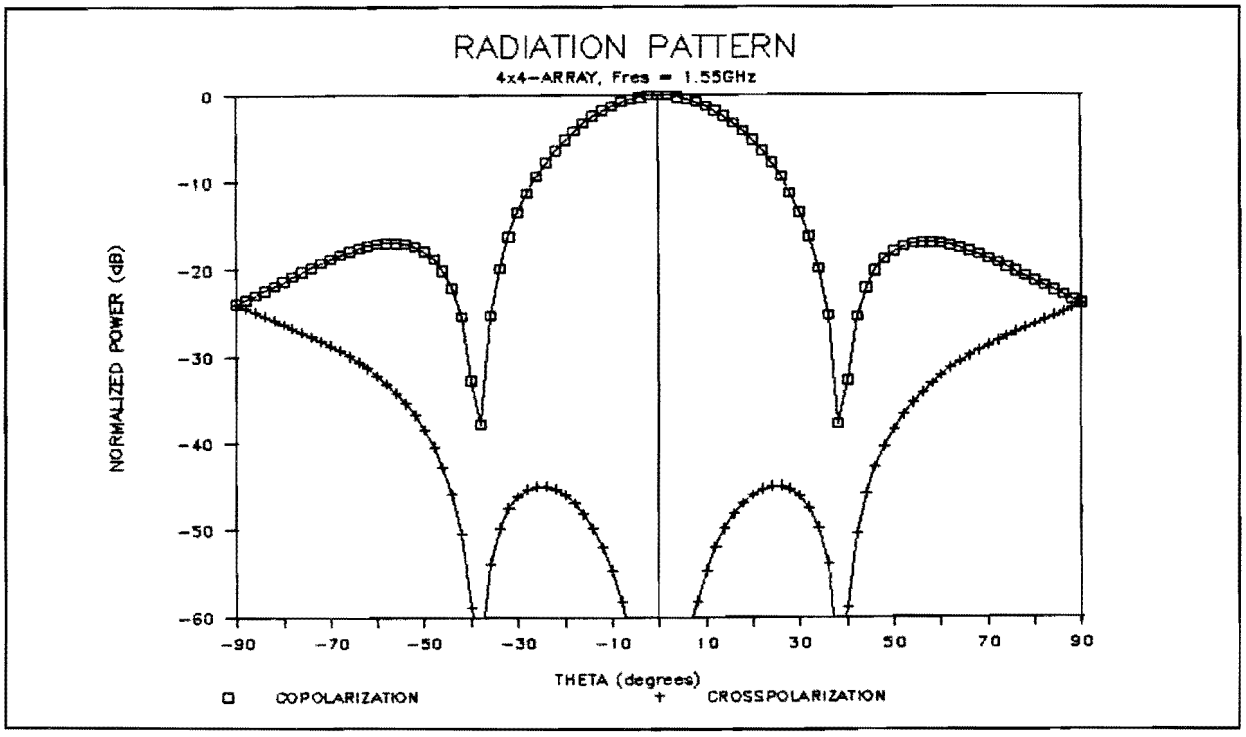

Fig. 4.2 - Radiation pattern 4x4-array, $\varepsilon_r = 2.33$, $d = 0.4*\lambda$

$\varphi = \varphi_s = 0^0$, $\vartheta_s = 0^0$

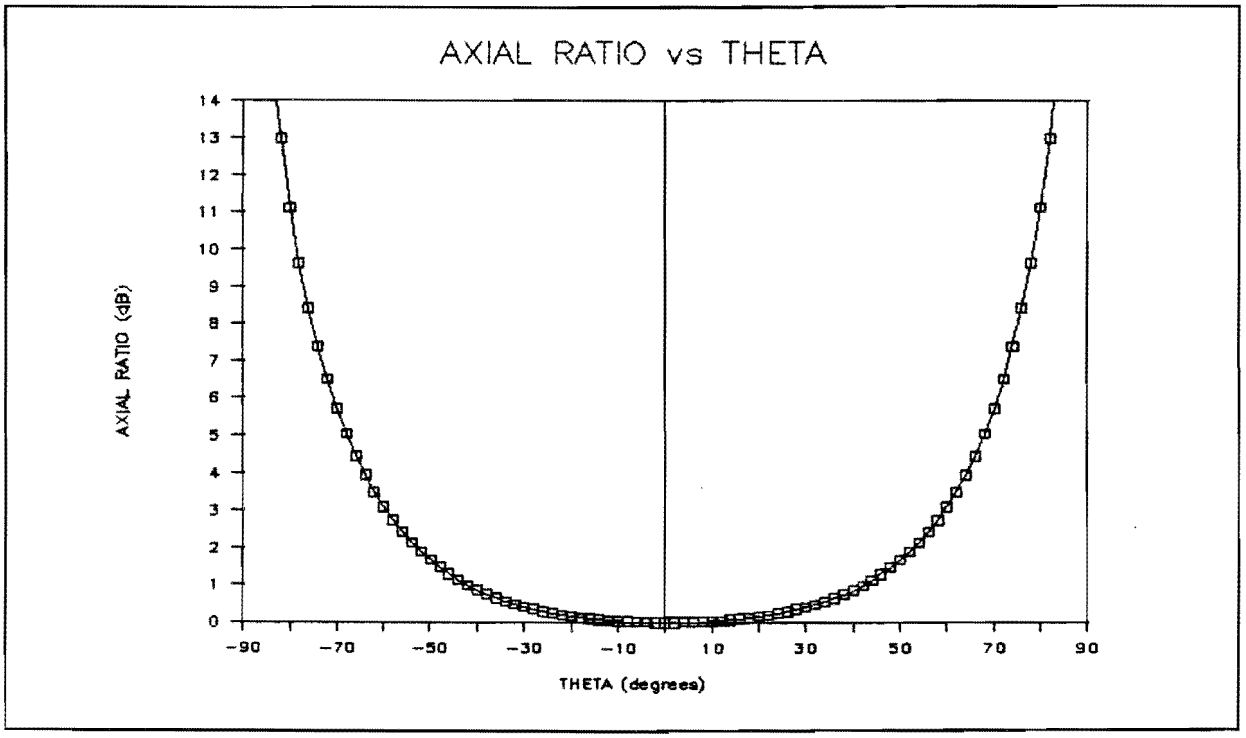

Fig. 4.3 - Axial ratio, $\varepsilon_r = 2.33$, $d = 0.4*\lambda$

$\varphi = \varphi_s = 0^0$, $\vartheta_s = 0^0$

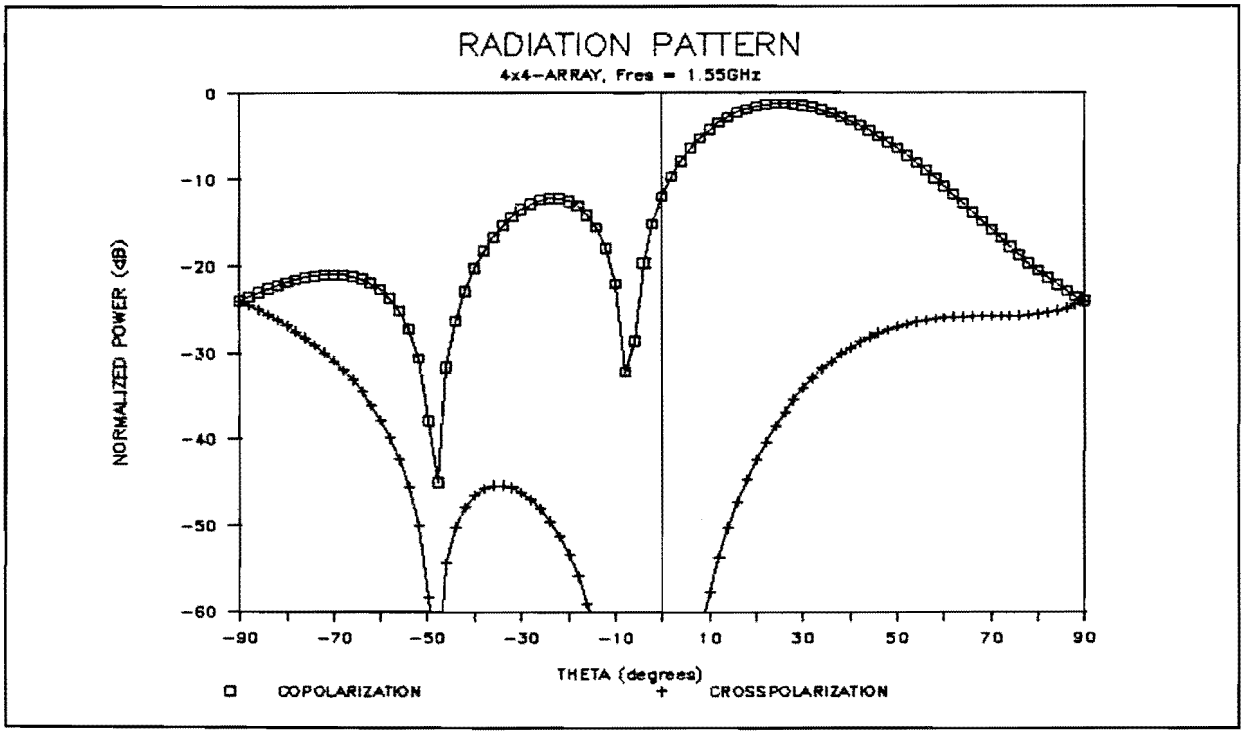

Fig. 4.4 - Radiation pattern 4x4-array, $\varepsilon_{r_0} = 2.33$, $d = 0.4*\lambda$

$\varphi = \varphi_s = 0^0$, $\vartheta_s = 30^0$

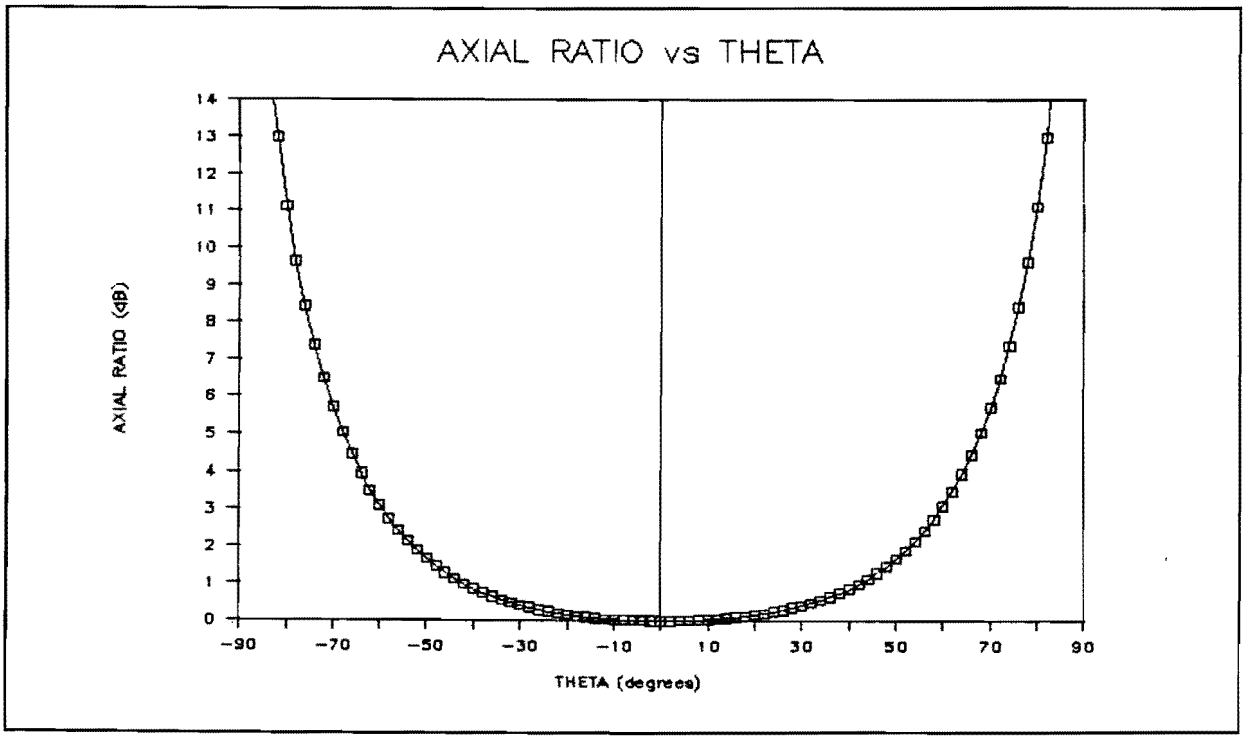

Fig. 4.5 - Axial ratio, $\varepsilon_r = 2.33$, $d = 0.4*\lambda$

$\varphi = \varphi_s = 0^0$, $\vartheta_s = 30^0$

The figures on the previous pages reveal that scanning will result in a degradation of the directivity. This effect and the fact that the angle of maximum radiation differs a little from ϑ_s are caused by beam distortion, introduced by the element radiation pattern [4-2]. Both effects will be discussed in the next paragraph.

§4.2.2 - Directivity

The directivity of the array can be calculated with the formulas in paragraph 2.1.5 and formulas (4.7a) and (4.7b):

$$D = 4\pi \cdot \frac{|\bar{E}(\vartheta,\varphi)|^2_{max}}{\int_0^{\frac{\pi}{2}} \int_0^{2\pi} |\bar{E}(\vartheta,\varphi)|^2 \cdot \sin(\vartheta) \cdot d\vartheta \cdot d\varphi} =$$

$$\frac{4\pi \cdot \{\, F_1^2(\vartheta_s) + \cos^2(\vartheta_s) \cdot F_2^2(\vartheta_s) \,\} \cdot M^2 \cdot N^2}{\int_0^{\frac{\pi}{2}} \int_0^{2\pi} \{F_1^2(\vartheta) + \cos^2(\vartheta) F_2^2(\vartheta)\} \left[\frac{\sin\left[\frac{\pi}{\lambda} M d_x (T_x - T_{xs})\right] \sin\left[\frac{\pi}{\lambda} N d_y (T_y - T_{ys})\right]}{\sin\left[\frac{\pi}{\lambda} d_x (T_x - T_{xs})\right] \sin\left[\frac{\pi}{\lambda} d_y (T_y - T_{ys})\right]} \right]^2 \sin(\vartheta)\, d\vartheta d\varphi} \qquad (4.10)$$

Used in the above expression is:

$$\left| \sum_{m=0}^{M-1} \sum_{n=0}^{N-1} e^{j\frac{2\pi}{\lambda} \cdot \left[m \cdot d_x \cdot (T_x - T_{xs}) + n \cdot d_y \cdot (T_y - T_{ys}) \right]} \right| =$$

$$= \left| \frac{1 - \left[e^{j\frac{2\pi}{\lambda} d_x (T_x - T_{xs})} \right]^M}{1 - e^{j\frac{2\pi}{\lambda} d_x (T_x - T_{xs})}} \right| \cdot \left| \frac{1 - \left[e^{j\frac{2\pi}{\lambda} d_y (T_y - T_{ys})} \right]^N}{1 - e^{j\frac{2\pi}{\lambda} d_y (T_y - T_{ys})}} \right| =$$

$$= \left| \frac{\sin\left[\frac{\pi}{\lambda} \cdot M \cdot d_x \cdot (T_x - T_{xs}) \right]}{\sin\left[\frac{\pi}{\lambda} \cdot d_x \cdot (T_x - T_{xs}) \right]} \right| \cdot \left| \frac{\sin\left[\frac{\pi}{\lambda} \cdot N \cdot d_y \cdot (T_y - T_{ys}) \right]}{\sin\left[\frac{\pi}{\lambda} \cdot d_y \cdot (T_y - T_{ys}) \right]} \right| \qquad (4.11)$$

This directivity as function of ϑ_s is calculated for some arrays with an element spacing of 0.4*λ, following from figures 3.20, 3.21 and 3.22 that indicate that the directivity increases with increasing element spacing. The element spacing is chosen to be less than half a wavelength, to avoid grating lobes. The results are given in figures 4.6, 4.7 and 4.8.

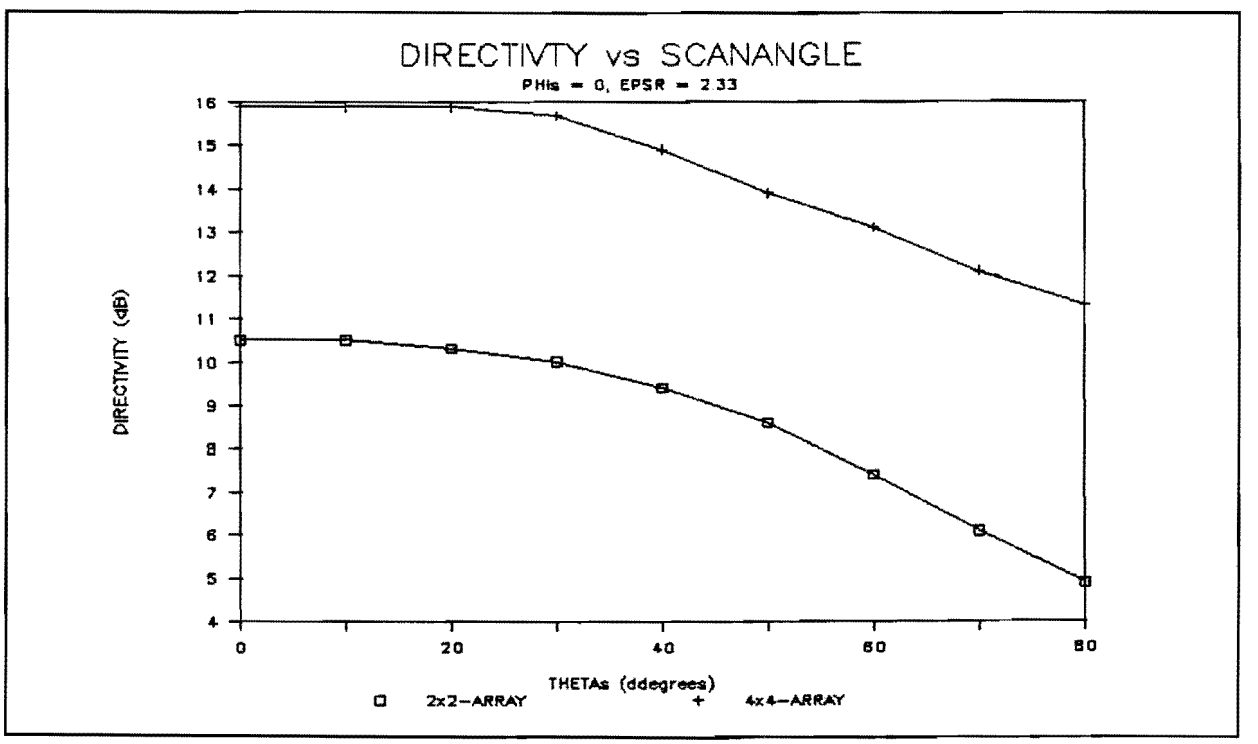

Fig. 4.6 - Directivity as function of ϑ_s

ε_r = 2.33, Fres = 1.55GHz, d = 0.4*λ

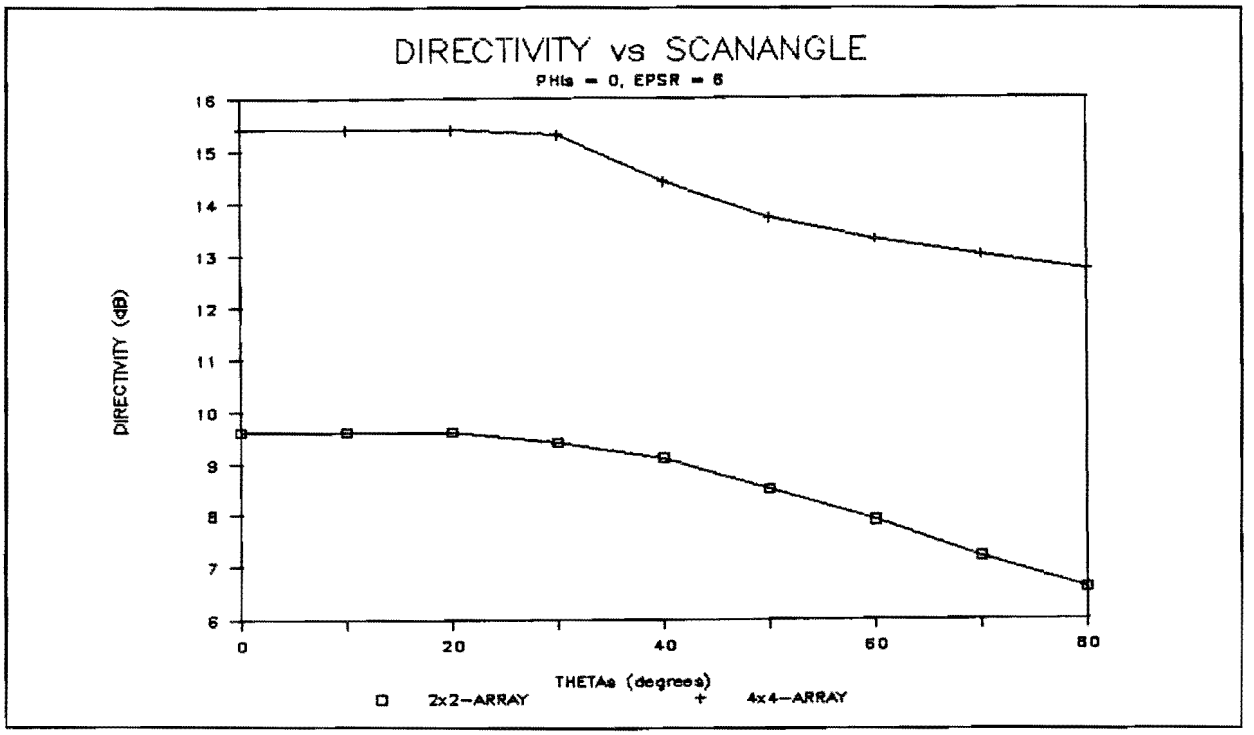

Fig. 4.7 - Directivity as function of ϑ_s

ε_r = 6, Fres = 1.55GHz, d = 0.4*λ

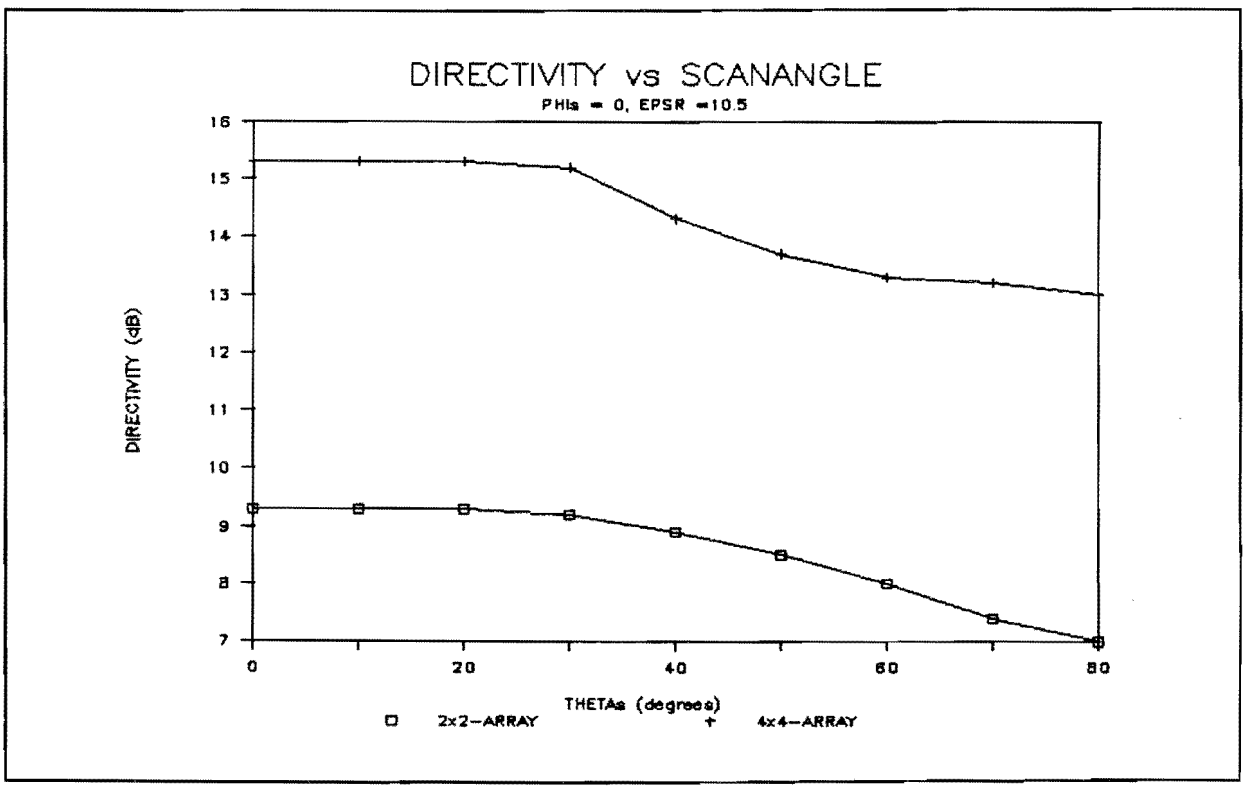

Fig. 4.8 - Directivity as function of ϑ_s

ε_r = 10.5, Fres = 1.55GHz, d = 0.4*λ

The directivity calculations of the 4x4-arrays are less accurate than those of the 2x2-arrays, because calculating the 4x4-array-directivities (program DIRECTI5, appendix G) with the same accuracy as the 2x2-array-directivities would be too time consuming.
The figures as a whole however, are accurate enough to conclude that a 4x4-array is necessary to satisfy the 12dB gain requirement. The figures also reveal that use of a substrate with a relatively high dielectric constant makes the directivity less scanning-dependent although the axial ratio will worsen in comparison with low dielectric constant arrays (see figures 3.3 to 3.5).

The above described phenomenon can be explained as follows:
Since the array radiation pattern arises from the multiplication of element radiation pattern with arrayfactor radiation pattern, use of a small- beamwidth element will result in an array main beam peak that is lower than one originating from use of a large-beamwidth element. This is shown in figure 4.9, that also shows the influence of the element radiation pattern on the distortion of the angle of maximum radiation ($\Delta\vartheta_s$).

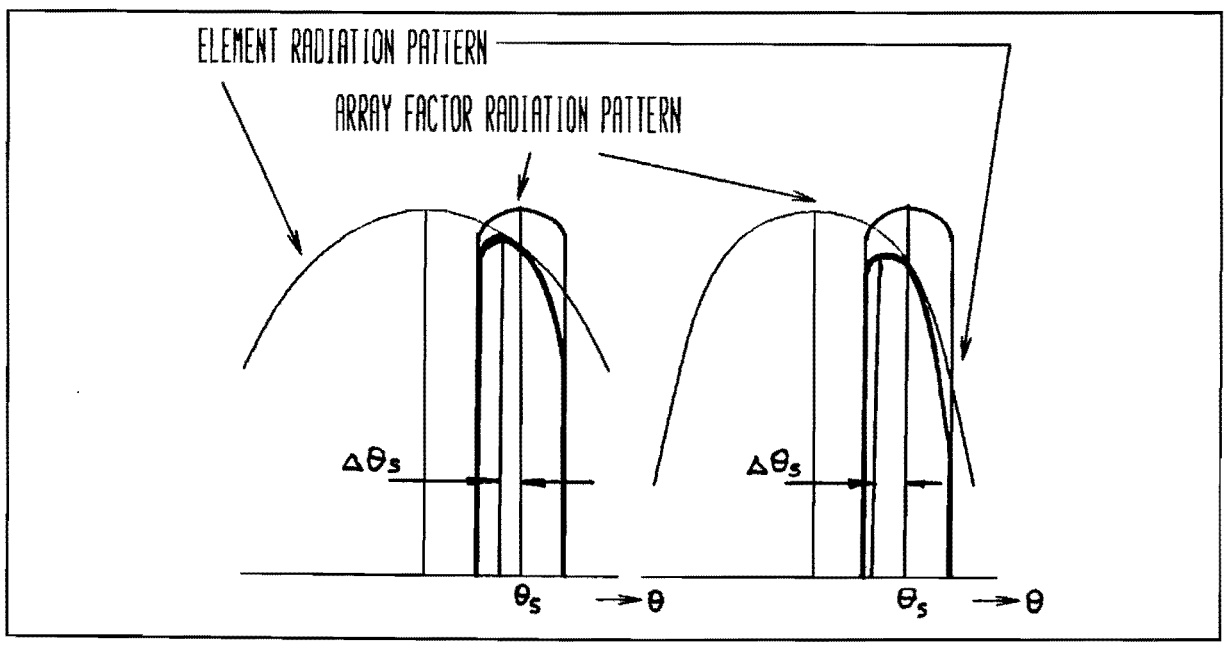

Fig. 4.9 - Influence of element radiation pattern on directivity and angle of maximum radiation

Figures 3.3 to 3.5 show that the element beamwidth broadens with increasing ε_r.

§4.3 - A Phased Array With Sequentially Rotated Linearly Polarized Patches

In this section the theory derived in paragraph 3.3.2 wil be used as a start to calculate the properties of a phased array composed of sequentially rotated linearly polarized elements.

§4.3.1 - Radiation Pattern

The array of which the radiation pattern will be calculated with use of formula (4.2) is depicted in figure 3.18. The calculations will be carried out along the same ways as done in paragraph 3.3.2: first the electric field of one 2x2-subarray will be calculated and then the subarray-fields are added to get the total electric field (see figure 3.19). Because of the similarity of formulas (3.13) and (4.2), the electric field components can be obtained from those derived in paragaph 3.3.2 by replacing T_x by (T_x-T_{xs}) and T_y by (T_y-T_{ys}). So the electric field components of a subarray are given by (from inspection of (3.21a) and (3.21b)):

$$E_{\vartheta_{sub}}(\vartheta,\varphi) = \sum_{p=0}^{1}\sum_{q=0}^{1} E_{\vartheta_{mn}} \cdot e^{j\frac{2\pi}{\lambda}\left[pd_x(T_x-T_{xs}) + qd_y(T_y-T_{ys})\right]} \qquad (4.12a)$$

$$E_{\varphi_{sub}}(\vartheta,\varphi) = \sum_{p=0}^{1}\sum_{q=0}^{1} E_{\varphi_{mn}} \cdot e^{j\frac{2\pi}{\lambda}\left[pd_x(T_x-T_{xs}) + qd_y(T_y-T_{ys})\right]} \qquad (4.12b)$$

and the total electric field components are found to be (from inspection of (3.22a) and (3.22b)):

$$E_{\vartheta}(\vartheta,\varphi) = E_{\vartheta_{sub}}(\vartheta,\varphi) \cdot \sum_{m=0}^{\frac{M-2}{2}}\sum_{n=0}^{\frac{N-2}{2}} e^{j\frac{4\pi}{\lambda}\left[md_x(T_x-T_{xs}) + nd_y(T_y-T_{ys})\right]} \qquad (4.13a)$$

$$E_{\varphi}(\vartheta,\varphi) = E_{\varphi_{sub}}(\vartheta,\varphi) \cdot \sum_{m=0}^{\frac{M-2}{2}}\sum_{n=0}^{\frac{N-2}{2}} e^{j\frac{4\pi}{\lambda}\left[md_x(T_x-T_{xs}) + nd_y(T_y-T_{ys})\right]} \qquad (4.13b)$$

The radiation patterns of the left and right hand polarized electric field are:

$$E_{L,R}(\vartheta,\varphi) = E_{\vartheta}(\vartheta,\varphi) \mp j\cdot E_{\varphi}(\vartheta,\varphi) =$$

$$= \left(E_{\vartheta_{sub}}(\vartheta,\varphi) \mp j\cdot E_{\varphi_{sub}}(\vartheta,\varphi)\right)\cdot\sum_{m=0}^{\frac{M-2}{2}}\sum_{n=0}^{\frac{N-2}{2}} e^{j\frac{4\pi}{\lambda}\left[md_x(T_x-T_{xs}) + nd_y(T_y-T_{ys})\right]} \tag{4.14}$$

and the axial ratio is with (2.17):

$$AR = \left|\frac{\left|E_{\vartheta_{sub}}(\vartheta,\varphi) - j\cdot E_{\varphi_{sub}}(\vartheta,\varphi)\right| + \left|E_{\vartheta_{sub}}(\vartheta,\varphi) + j\cdot E_{\varphi_{sub}}(\vartheta,\varphi)\right|}{\left|E_{\vartheta_{sub}}(\vartheta,\varphi) - j\cdot E_{\varphi_{sub}}(\vartheta,\varphi)\right| - \left|E_{\vartheta_{sub}}(\vartheta,\varphi) + j\cdot E_{\varphi_{sub}}(\vartheta,\varphi)\right|}\right| \tag{4.15}$$

The components of the axial ratio can be written as:

$$E_{\vartheta_{sub}}(\vartheta,\varphi) \pm j\cdot E_{\varphi_{sub}}(\vartheta,\varphi) =$$

$$= -\left[\cos(\varphi)F_1(\vartheta) \mp j\cdot\cos(\vartheta)\sin(\varphi)F_2(\vartheta)\right]\cdot$$

$$\cdot\left[1 + e^{j\frac{2\pi}{\lambda}\left[d_x(T_x-T_{xs}) + d_y(T_y-T_{ys})\right]}\right] +$$

$$-j\cdot\left[\sin(\varphi)F_1(\vartheta) \pm j\cdot\cos(\vartheta)\cos(\varphi)F_2(\vartheta)\right]\cdot$$

$$\cdot\left[e^{j\frac{2\pi}{\lambda}d_x(T_x-T_{xs})} + e^{j\frac{2\pi}{\lambda}d_y(T_y-T_{ys})}\right] \tag{4.16a}$$

with:

$$T_x = \sin(\vartheta)\cdot\cos(\varphi) \quad , \quad T_{xs} = \sin(\vartheta_s)\cdot\cos(\varphi_s) \tag{4.16b}$$

$$T_y = \sin(\vartheta)\cdot\sin(\varphi) \quad , \quad T_{ys} = \sin(\vartheta_s)\cdot\sin(\varphi_s) \tag{4.16c}$$

With formulas (4.15) and (4.16) some typical characteristics of this phased array can be found.

First it appears that for the two situations $\varphi = \varphi_s = 0^0$ and $\varphi = \varphi_s = 90^0$ the axial ratio is the same as the axial ratio of a single circularly polarized element and consequently distance- and scanning-independent.

Second for the situation $\varphi = \varphi_s$, $\vartheta = \vartheta_s$, that is for the main beam position, the axial ratio turns out to be:

$$AR(\varphi_s,\vartheta_s) = \left| \frac{|F_1(\vartheta_s) + \cos(\vartheta_s)\cdot F_2(\vartheta_s)| + |F_1(\vartheta_s) - \cos(\vartheta_s)\cdot F_2(\vartheta_s)|}{|F_1(\vartheta_s) + \cos(\vartheta_s)\cdot F_2(\vartheta_s)| - |F_1(\vartheta_s) - \cos(\vartheta_s)\cdot F_2(\vartheta_s)|} \right| \tag{4.17}$$

the axial ratio of a single circularly polarized element for $\vartheta = \vartheta_s$.

This means that the axial ratio of the array with the beam scanned away from boresight can be evaluated from the axial ratio as function of theta of a single circularly polarized element. Figure 4.10 gives this function for 3 values of ε_r. In these figures are indicated the maximum scanangles ϑ, arising from the INMARSAT- and MSATX-requirements (2.5dB for INMARSAT and 4dB for MSATX). These limits, being independent of the elementspacing, also hold true for the array discussed in paragraph 4.2.

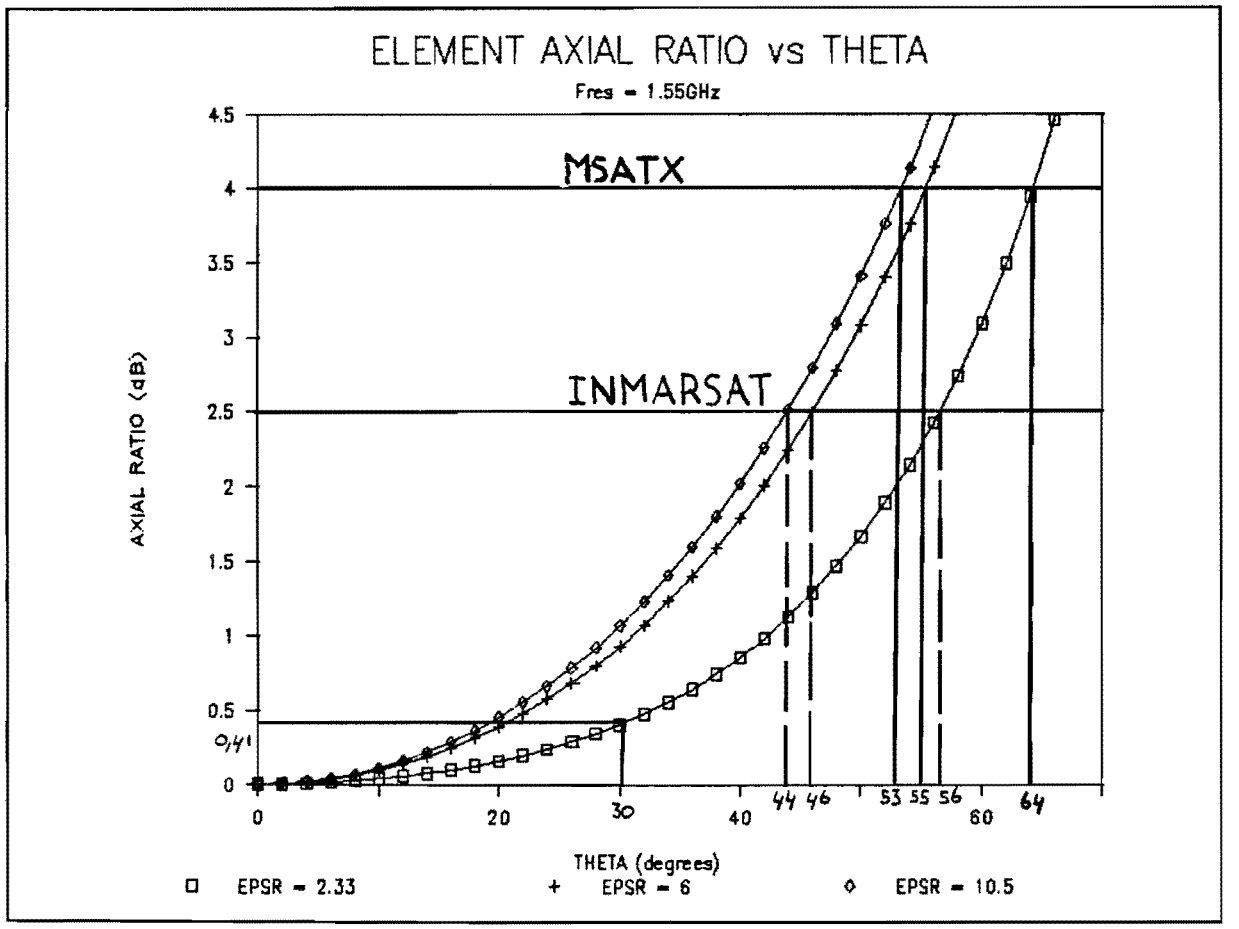

Fig. 4.10 - Axial ratio and scanlimits

In the above figure is also indicated the axial ratio for $\vartheta = 30^0$ and $\varepsilon_r = 2.33$. To illustrate the validity of formula (4.17), the radiation pattern and the axial ratio for a 4x4-array with $\varepsilon_r = 2.33$ are calculated (program FREQSCAN), with the main beam scanned to the position $\varphi_s = 45^0$, $\vartheta_s = 30^0$ (figures 4.11 and 4.12). Figure 4.12 reveals that the axial ratio for $\vartheta = 30^0$ is the same as indicated in figure 4.10.

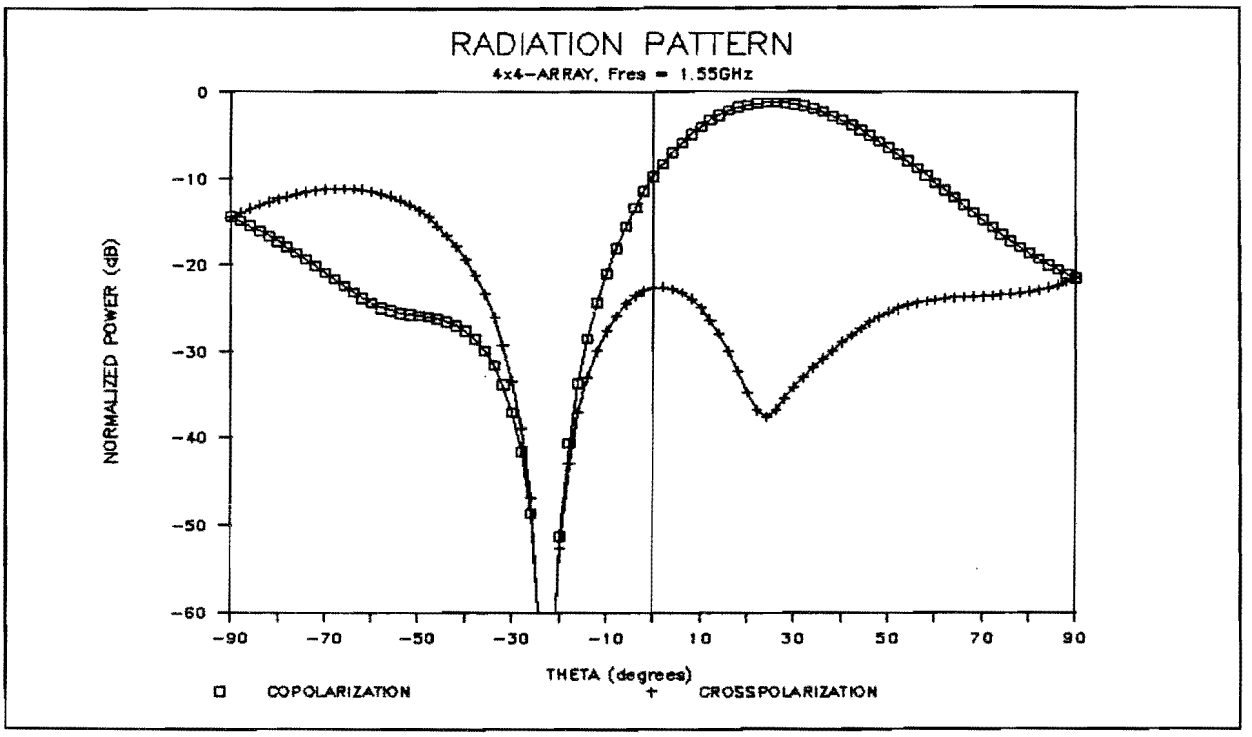

Fig. 4.11 - Radiation pattern 4x4-array, $\varepsilon_r = 2.33$, $d = 0.4*\lambda$

$\varphi = \varphi_s = 45^0$, $\vartheta_s = 30^0$

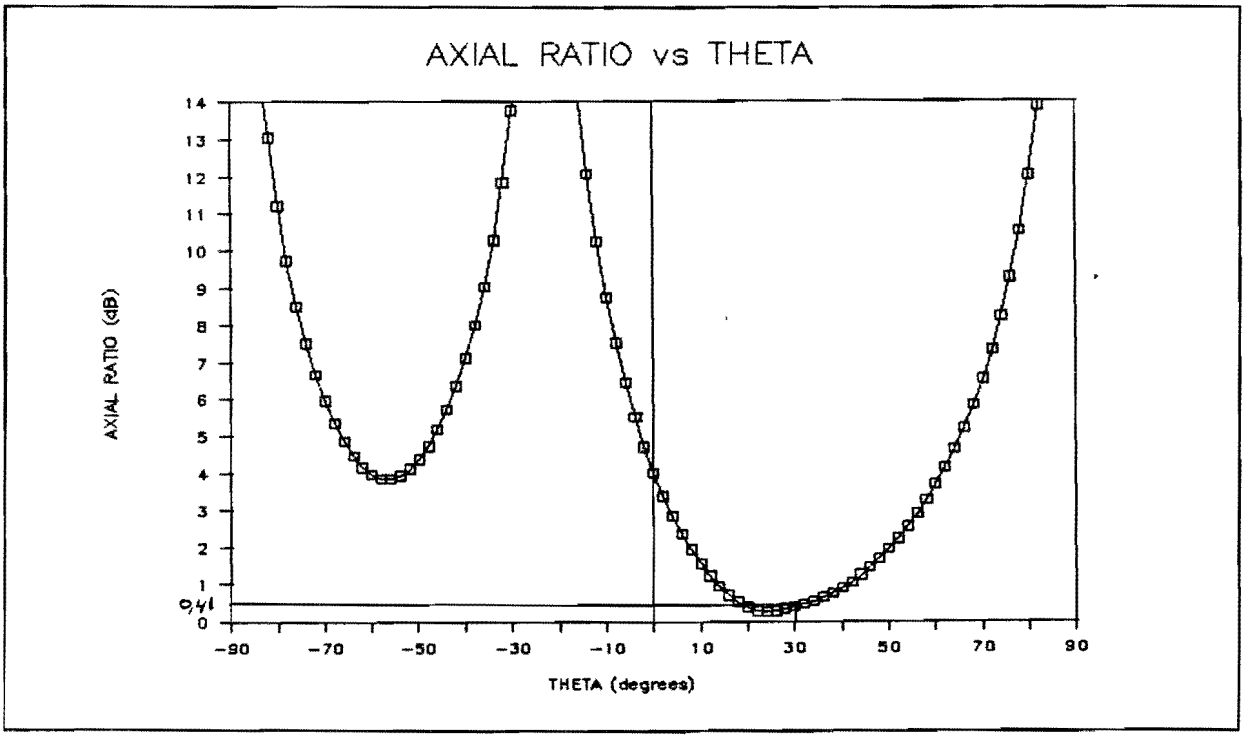

Fig. 4.12 - Axial ratio, $\varepsilon_r = 2.33$, $d = 0.4*\lambda$

$\varphi = \varphi_s = 45^0$, $\vartheta_s = 30^0$

§4.3.2 - Directivity

The directivity of the array can be found by inspection of formula (3.29), replacing T_x by $(T_x - T_{xs})$ and T_y by $(T_y - T_{ys})$:

$$D = \frac{4\pi \cdot \left(F_1^2(\theta_s) + \cos^2(\theta_s) \cdot F_2^2(\theta_s) \right) \cdot \frac{1}{8} \cdot M^2 \cdot N^2}{\int_0^{\frac{\pi}{2}} \int_0^{2\pi} \left[\left\{ \cos^2(\varphi) F_1^2(\theta) + \cos^2(\theta) \sin^2(\varphi) F_2^2(\theta) \right\} \cdot \left\{ 1 + \cos\left[\frac{2\pi}{\lambda} \cdot \left[d_x(T_x - T_{xs}) + d_y(T_y - T_{ys}) \right] \right] \right\} + \right.$$

$$\left. + \left\{ \sin^2(\varphi) F_1^2(\theta) + \cos^2(\theta) \cos^2(\varphi) F_2^2(\theta) \right\} \cdot \left\{ 1 + \cos\left[\frac{2\pi}{\lambda} \cdot \left[d_x(T_x - T_{xs}) - d_y(T_y - T_{ys}) \right] \right] \right\} \right] \cdot$$

$$\cdot \frac{\sin^2\left[\frac{\pi}{\lambda} \cdot M \cdot d_x(T_x - T_{xs}) \right]}{\sin^2\left[2 \cdot \frac{\pi}{\lambda} \cdot d_x(T_x - T_{xc}) \right]} \cdot \frac{\sin^2\left[\frac{\pi}{\lambda} \cdot N \cdot d_y(T_y - T_{ys}) \right]}{\sin^2\left[2 \cdot \frac{\pi}{\lambda} \cdot d_y(T_y - T_{yc}) \right]} \cdot \sin(\theta) d\theta d\varphi \qquad (4.18)$$

This directivity has been calculated for 3 different 4x4-arrays with

This directivity has been calculated for 3 different 4x4-arrays with the beam scanned to the maximum ϑ in the plane $\varphi = 45^0$, to check if the maximum scanangle is restricted by the directivity. The results of the calculations are given in table 4.1:

Table 4.1 - 4x4-array directivity for maximum scanangle

ε_r	d/λ	ϑ_s(degr.)	φ_s(degr.)	D(dB)
2.33	0.40	64	45	13.7
6	0.40	55	45	14.3
10.5	0.40	53	45	14.4

The table above indicates that the maximum scanangle for a 4x4-array of sequentially rotated linearly polarized patches is defined by the patch-axial-ratio and not by the array-directivity.

§4.4 - A Phased Array With Circularly Polarized Patches, Scanned on Subarraylevel

A drawback of the phased arrays discussed before is the number of tuneable phaseshifters (MxN) used to steer the beam away from boresight. Since it is likely that these tuneable phaseshifters will define the costs of the array, it is useful to look for methods to reduce the number of tuneable phaseshifters needed.
A way to reduce the number of tuneable phaseshifters is to use one phaseshifter for a 2x2-subarray, instead of one phaseshifter for one patch. In the following the radiation pattern and directivity for a rectangular array of circularly polarized patches, scanned on subarraylevel, will be discussed.

§4.4.1 - Radiation Pattern

The electric field components of the array are calculated by first calculating the electric field components of one 2x2-subarray. These field components are added, taking into account the phaseshifts between the subarrays, to get the total electric field of the array.

The array configuration is depicted in figure 3.9. Phaseshifts are applied between 2x2-subarrays; no tuneable phaseshifters are used inside a subarray. So the electric field components of a subarray can be calculated with formulas (3.15b) and (3.16b) and give:

$$E_{\vartheta_{sub}}(\vartheta,\varphi) = -e^{j\varphi}\cdot F_1(\vartheta)\cdot \sum_{p=0}^{1}\sum_{q=0}^{1} e^{j\frac{2\pi}{\lambda}\cdot(pd_xT_x + qd_yT_y)} \tag{4.19a}$$

$$E_{\varphi_{sub}}(\vartheta,\varphi) = -j\cdot e^{j\varphi}\cdot\cos(\vartheta)\cdot F_2(\vartheta)\cdot \sum_{p=0}^{1}\sum_{q=0}^{1} e^{j\frac{2\pi}{\lambda}\cdot(pd_xT_x + qd_yT_y)} \tag{4.19b}$$

The subarray-spacings in x- and y-direction are $2*d_x$ and $2*d_y$, with d_x and d_y the elementspacings in x- and y-direction. The positions of the subarrays in the array are described by the numbers m and n ($0 \le m \le \frac{M-2}{2}$, $0 \le n \le \frac{N-2}{2}$) as in paragraph 3.3.2.
If each subarray is provided with a phaseshift:

$$\psi_{mn} = -\frac{2\pi}{\lambda}\cdot(m\cdot 2d_xT_{xs} + n\cdot 2d_yT_{ys}) \tag{4.20}$$

the total electric field components are given by:

$$E_{\vartheta}(\vartheta,\varphi) = E_{\vartheta_{sub}}(\vartheta,\varphi)\cdot \sum_{m=0}^{\frac{M-2}{2}}\sum_{n=0}^{\frac{N-2}{2}} e^{j\frac{4\pi}{\lambda}\left[md_x(T_x-T_{xs}) + nd_y(T_y-T_{ys})\right]} \tag{4.21a}$$

$$E_{\varphi}(\vartheta,\varphi) = E_{\varphi_{sub}}(\vartheta,\varphi)\cdot \sum_{m=0}^{\frac{M-2}{2}}\sum_{n=0}^{\frac{N-2}{2}} e^{j\frac{4\pi}{\lambda}\left[md_x(T_x-T_{xs}) + nd_y(T_y-T_{ys})\right]} \tag{4.21b}$$

The left and right hand polarized parts of the electric field are:

$$E_{L_R}(\vartheta,\varphi) = E_\vartheta(\vartheta,\varphi) \mp j\cdot E_\varphi(\vartheta,\varphi) =$$

$$= \left(E_{\vartheta_{sub}}(\vartheta,\varphi) \mp j\cdot E_{\varphi_{sub}}(\vartheta,\varphi)\right)\cdot \sum_{m=0}^{\frac{M-2}{2}} \sum_{n=0}^{\frac{N-2}{2}} e^{j\frac{4\pi}{\lambda}\left[md_x(T_x-T_{xs}) + nd_y(T_y-T_{ys})\right]}$$

$$= -e^{j\varphi}\cdot\left(F_1(\vartheta) \pm \cos(\vartheta)\cdot F_2(\vartheta)\right)\cdot \sum_{p=0}^{1} \sum_{q=0}^{1} e^{j\frac{2\pi}{\lambda}\cdot(pd_xT_x + qd_yT_y)}\cdot$$

$$\cdot \sum_{m=0}^{\frac{M-2}{2}} \sum_{n=0}^{\frac{N-2}{2}} e^{j\frac{4\pi}{\lambda}\left[md_x(T_x-T_{xs}) + nd_y(T_y-T_{ys})\right]} \qquad (4.22)$$

With (2.17) and (4.22) the axial ratio becomes:

$$AR = \left| \frac{|F_1(\vartheta) + \cos(\vartheta)\cdot F_2(\vartheta)| + |F_1(\vartheta) - \cos(\vartheta)\cdot F_2(\vartheta)|}{|F_1(\vartheta) + \cos(\vartheta)\cdot F_2(\vartheta)| - |F_1(\vartheta) - \cos(\vartheta)\cdot F_2(\vartheta)|} \right| \qquad (4.23)$$

Again the axial ratio of a single circularly polarized patch is found for an array composed of these patches. This axial ratio is φ-, d- and scanning-independent.

§4.4.2 - Directivity

The directivity is found to be, with the theory of paragraph 2.1.5:

$$D = 4\pi\cdot \frac{|\bar{E}(\vartheta,\varphi)|^2_{max}}{\int_0^{\frac{\pi}{2}} \int_0^{2\pi} |\bar{E}(\vartheta,\varphi)|^2\cdot\sin(\vartheta)\cdot d\vartheta\cdot d\varphi} \qquad (4.24)$$

The term $|\bar{E}(\vartheta,\varphi)|^2$ is calculated as follows with (4.21):

$$|\bar{E}(\vartheta,\varphi)|^2 = |E_\vartheta(\vartheta,\varphi)|^2 + |E_\varphi(\vartheta,\varphi)|^2 =$$

$$= \left(|E_{\vartheta_{sub}}(\vartheta,\varphi)|^2 + |E_{\varphi_{sub}}(\vartheta,\varphi)|^2\right) \cdot$$

$$\cdot \frac{\sin^2\left[\frac{\pi}{\lambda}\cdot M\cdot d_x(T_x-T_{xs})\right]}{\sin^2\left[2\cdot\frac{\pi}{\lambda}\cdot d_x(T_x-T_{xs})\right]} \cdot \frac{\sin^2\left[\frac{\pi}{\lambda}\cdot N\cdot d_y(T_y-T_{ys})\right]}{\sin^2\left[2\cdot\frac{\pi}{\lambda}\cdot d_y(T_y-T_{ys})\right]}$$

(4.25a)

Used in the above expression is formula (3.27b) with T_x replaced by (T_x-T_{xs}) and T_y replaced by (T_y-T_{ys}).

Formula (4.25) can be worked out further with (4.19) to give:

$$|\bar{E}(\vartheta,\varphi)|^2 = 4\cdot\left[F_1^2(\vartheta) + \cos^2(\vartheta)\cdot F_2^2(\vartheta)\right]\cdot\cos^2\left(\frac{\pi}{\lambda}d_xT_x\right)\cdot\cos^2\left(\frac{\pi}{\lambda}d_yT_y\right)\cdot$$

$$\cdot \frac{\sin^2\left[\frac{\pi}{\lambda}\cdot M\cdot d_x(T_x-T_{xs})\right]}{\sin^2\left[2\cdot\frac{\pi}{\lambda}\cdot d_x(T_x-T_{xs})\right]} \cdot \frac{\sin^2\left[\frac{\pi}{\lambda}\cdot N\cdot d_y(T_y-T_{ys})\right]}{\sin^2\left[2\cdot\frac{\pi}{\lambda}\cdot d_y(T_y-T_{ys})\right]}$$

(4.25b)

Used in the above expression is:

$$\left|\sum_{p=0}^{1}\sum_{q=0}^{1} e^{j\frac{2\pi}{\lambda}\cdot(pd_xT_x + qd_yT_y)}\right| =$$

$$= \left|\frac{1-\left(e^{j\frac{2\pi}{\lambda}\cdot d_xT_x}\right)^2}{1-e^{j\frac{2\pi}{\lambda}d_xT_x}}\right| \cdot \left|\frac{1-\left(e^{j\frac{2\pi}{\lambda}\cdot d_yT_y}\right)^2}{1-e^{j\frac{2\pi}{\lambda}d_yT_y}}\right| =$$

$$= \left| \frac{\sin(\frac{2\pi}{\lambda} \cdot d_x T_x)}{\sin(\frac{\pi}{\lambda} \cdot d_x T_x)} \right| \cdot \left| \frac{\sin(\frac{2\pi}{\lambda} \cdot d_y T_y)}{\sin(\frac{\pi}{\lambda} \cdot d_y T_y)} \right| =$$

$$= 4 \cdot \left| \cos(\frac{\pi}{\lambda} \cdot d_x T_x) \right| \cdot \left| \cos(\frac{\pi}{\lambda} \cdot d_y T_y) \right| \qquad (4.26)$$

The directivity finaly becomes:

$$D = \frac{\frac{1}{4} \cdot \pi \cdot \langle F_1^2(\theta_s) + \cos^2(\theta_s) \cdot F_2^2(\theta_s) \rangle \cdot \cos^2(\frac{\pi}{\lambda} \cdot d_x T_{xs}) \cdot \cos^2(\frac{\pi}{\lambda} \cdot d_y T_{ys}) \cdot M^2 \cdot N^2}{\int_0^{\frac{\pi}{2}} \int_0^{2\pi} \langle F_1^2(\theta) + \cos^2(\theta) \cdot F_2^2(\theta) \rangle \cdot \cos^2(\frac{\pi}{\lambda} d_x T_x) \cdot \cos^2(\frac{\pi}{\lambda} d_y T_y) \cdot \frac{\sin^2[\frac{\pi}{\lambda} \cdot M \cdot d_x (T_x - T_{xs})]}{\sin^2[2 \cdot \frac{\pi}{\lambda} \cdot d_x (T_x - T_{xs})]} \cdot \frac{\sin^2[\frac{\pi}{\lambda} \cdot N \cdot d_y (T_y - T_{ys})]}{\sin^2[2 \cdot \frac{\pi}{\lambda} \cdot d_y (T_y - T_{ys})]} \cdot \sin(\theta) \cdot d\theta \cdot d\varphi} \qquad (4.27)$$

The relationship between elementspacing and ϑ_{max} as stated in formula (4.6) should be applied now not to the elementspacing but to the subarrayspacing.
The directivity of a 4x4-array is calculated for 3 situations:

- minimal elementspacing (two times patch radius, see table 3.1);
- $\vartheta_{max} = 90^0$;
- $\vartheta_{max} = 64^0$.

All the calcuations are performed for $\varphi_s = 45^0$ and ϑ_s the angle corresponding with a 4dB axial ratio (see table 4.1). The arrays are not calculated for $\varepsilon_r = 2.33$ because the radius of the patch for this ε_r is 3.72cm = 0.20*λ, which is to much for use in subarraylevel-scanning. The results are given in table 4.2.

Table 4.2 - directivities 4x4-array

MINIMAL ELEMENTSPACING		
ε_r \ Property	d/λ	D (dB)
6	0.23	10.2
10.5	0.18	8.8
$\vartheta_{max} = 90^0$		
ε_r \ Property	d/λ	D (dB)
6	0.25	10.5
10.5	0.25	10.7
$\vartheta_{max} = 64^0$		
ε_r \ Property	d/λ	D (dB)
6	0.27	10.7
10.5	0.27	10.9

Table 4.2 reveals that a rectangular 4x4-array with circularly polarized patches, scanned on subarray-level does satisfy the MSATX gain requirement (10dB), if a proper elementspacing is applied. Since the directivity difference for ε_r =6 and ε_r = 10.5 is minimal, the

lower dielectric constant should be used, to gain axial ratio performance and to lower costs.
The directivity for the situation that ϑ_s corresponds with a 2.5dB axial ratio, is not calculated but is expected to satisfy the INMARSAT gain requirement (12dB), since the elementspacing can be enlarged due to the lower ϑ_s (see figure 4.10).
Compared with scanning on elementlevel, scanning on subarraylevel reduces the number of tuneable phaseshifters with a factor 4. This at the price of a lower directivity.

§4.5 - A Phased Array With Sequentially Rotated Linearly Polarized Patches, Scanned on Subarraylevel

The theory derived in the preceding paragraph will be used as a basis for calculating the radiation pattern and directivity of a rectangular array composed of sequentially rotated and fed linearly polarized patches, scanned on subarraylevel.

§4.5.1 - Radiation Pattern

The array configuration is depicted in figure 3.19. Phaseshifts between 2x2-subarrays are inserted in the same way as discussed in the preceding paragraph. Tuneable phaseshifters are not used inside a subarray.
The components of the electric field are given by eqs.(21a,b) of the preceding paragraph, but now with different expressions for the subarray field components:

$$E_\vartheta(\vartheta,\varphi) = E_{\vartheta_{sub}}(\vartheta,\varphi)\cdot\sum_{m=0}^{\frac{M-2}{2}}\sum_{n=0}^{\frac{N-2}{2}} e^{j\frac{4\pi}{\lambda}\left[md_x(T_x-T_{xs}) + nd_y(T_y-T_{ys})\right]} \tag{4.28a}$$

$$E_\varphi(\vartheta,\varphi) = E_{\varphi_{sub}}(\vartheta,\varphi)\cdot\sum_{m=0}^{\frac{M-2}{2}}\sum_{n=0}^{\frac{N-2}{2}} e^{j\frac{4\pi}{\lambda}\left[md_x(T_x-T_{xs}) + nd_y(T_y-T_{ys})\right]} \tag{4.28b}$$

and the left and right hand polarized parts of the electric field are:

$$E_{\substack{L\\R}}(\vartheta,\varphi) = E_{\vartheta}(\vartheta,\varphi) \mp j\cdot E_{\varphi}(\vartheta,\varphi) =$$

$$= \left(E_{\vartheta_{sub}}(\vartheta,\varphi) \mp j\cdot E_{\varphi_{sub}}(\vartheta,\varphi)\right)\cdot \sum_{m=0}^{\frac{M-2}{2}} \sum_{n=0}^{\frac{N-2}{2}} e^{j\frac{4\pi}{\lambda}\left[md_x(T_x-T_{xs}) + nd_y(T_y-T_{ys})\right]} \tag{4.29}$$

With (2.17) and (4.29) for the axial ratio is found:

$$AR = \left| \frac{\left|E_{\vartheta_{sub}}(\vartheta,\varphi) - j\cdot E_{\varphi_{sub}}(\vartheta,\varphi)\right| + \left|E_{\vartheta_{sub}}(\vartheta,\varphi) + j\cdot E_{\varphi_{sub}}(\vartheta,\varphi)\right|}{\left|E_{\vartheta_{sub}}(\vartheta,\varphi) - j\cdot E_{\varphi_{sub}}(\vartheta,\varphi)\right| - \left|E_{\vartheta_{sub}}(\vartheta,\varphi) + j\cdot E_{\varphi_{sub}}(\vartheta,\varphi)\right|} \right| \tag{4.30}$$

The subarray field components are calculated already in paragraph 3.3.2 and are given by (formulas (3.28a) and (3.28b)):

$$E_{\vartheta_{sub}}(\vartheta,\varphi) = -F_1(\vartheta)\cdot$$

$$\cdot\left(\cos(\varphi)\left[1 + e^{j\frac{2\pi}{\lambda}(d_xT_x + d_yT_y)}\right] + j\cdot\sin(\varphi)\left[e^{j\frac{2\pi}{\lambda}d_xT_x} + e^{j\frac{2\pi}{\lambda}d_yT_y}\right]\right) \tag{4.31a}$$

$$E_{\varphi_{sub}}(\vartheta,\varphi) = \cos(\vartheta)\cdot F_2(\vartheta)\cdot$$

$$\cdot\left(\sin(\varphi)\left[1 + e^{j\frac{2\pi}{\lambda}(d_xT_x + d_yT_y)}\right] - j\cdot\cos(\varphi)\left[e^{j\frac{2\pi}{\lambda}d_xT_x} + e^{j\frac{2\pi}{\lambda}d_yT_y}\right]\right) \tag{4.31b}$$

Formulas (4.30) and (4.31) reveal that for the situations $\varphi = 0^0$ and $\varphi = 90^0$ the axial ratio of the array is the same as the axial ratio of a single circularly polarized element.
For the situation $\varphi = \varphi_s$, $\vartheta = \vartheta_s$ however, the axial ratio is not the same as the axial ratio of a single circularly polarized element for $\vartheta = \vartheta_s$, as was the case for the array scanned on elementlevel.
The axial ratio behaviour of the array can be evaluated from the axial ratio as function of ϑ of a 2x2-subarray. Figure 4.13 gives this axial ratio for $\varepsilon_r = 6$ for the planes $\varphi = 0^0$ and $\varphi = 45^0$ and an elementspacing of $0.27*\lambda$ (see table 4.2). Figure 4.14 gives the same characteristics for $\varepsilon_r = 10.5$.

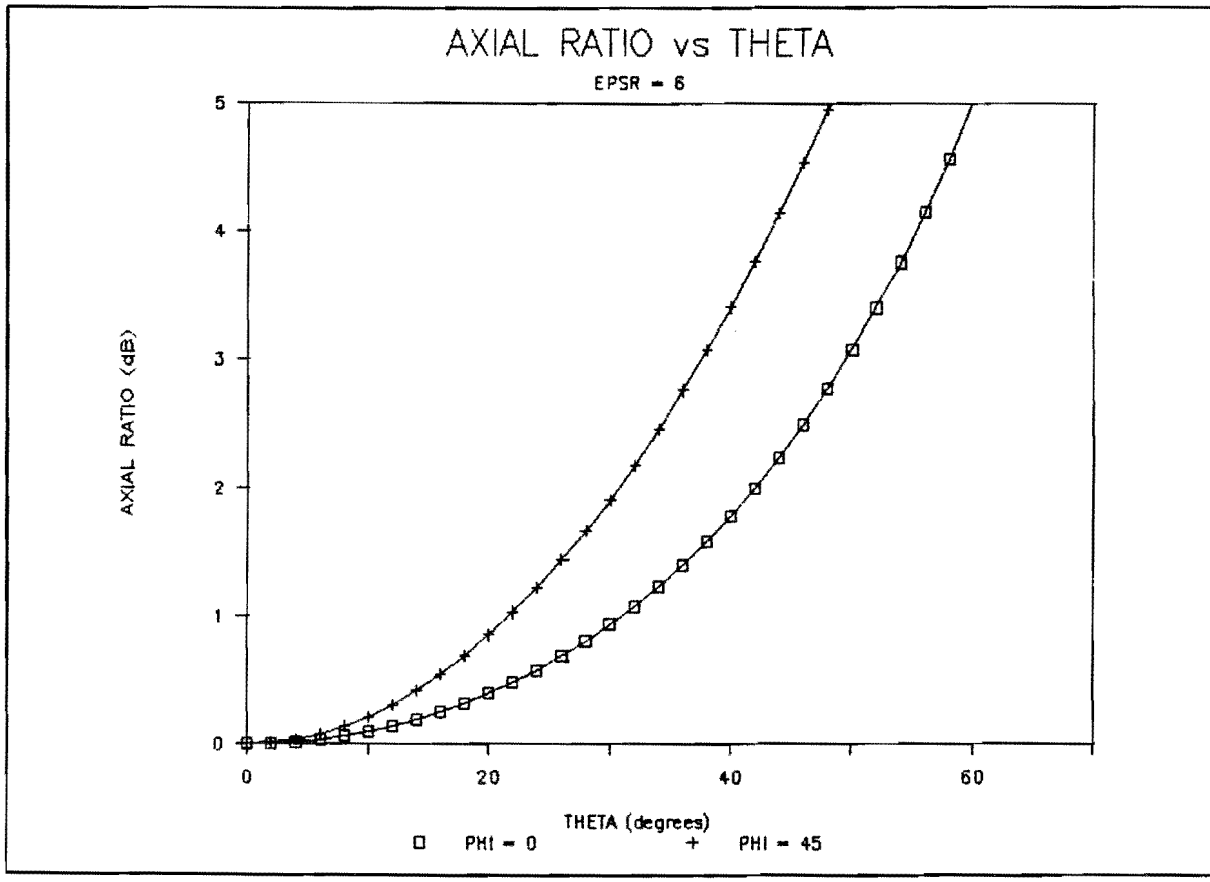

Fig. 4.13 - Axial ratio 2x2-array, $\varepsilon_r = 6$, Fres = 1.55GHz
d = $0.27*\lambda$

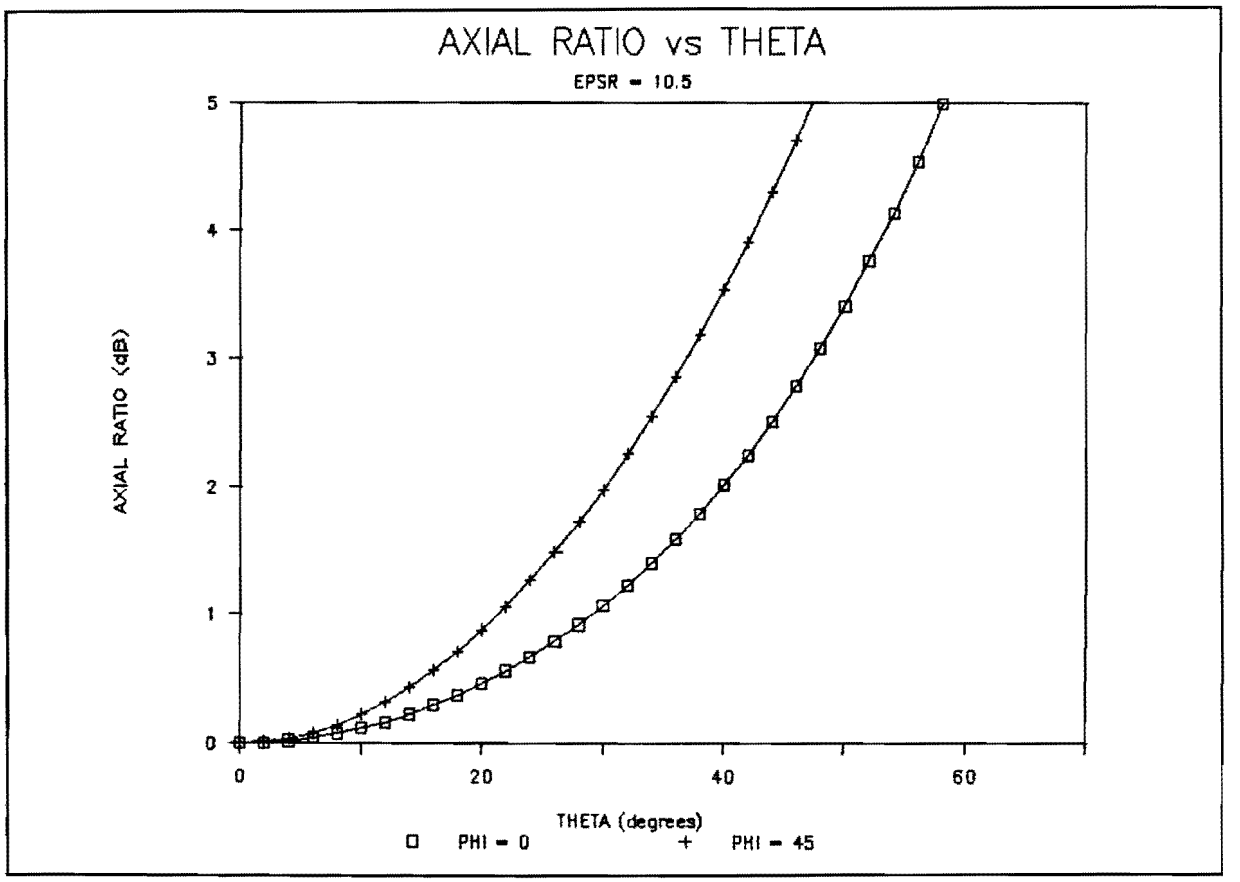

Fig. 4.14 - Axial ratio 2x2-array, ε_r = 10.5, Fres = 1.55GHz

d = 0.27*λ

For both arays the axial ratio in the diagonalplane is approximately 2dB worse compared with the principal planes.

§4.5.2 - Directivity

To find the formula for the directivity, $|\bar{E}(\vartheta,\varphi)|^2$ has to be calculated. With (4.25a), for different subarray field components as in the paragraph before:

$$|\bar{E}(\vartheta,\varphi)|^2 = |E_\vartheta(\vartheta,\varphi)|^2 + |E_\varphi(\vartheta,\varphi)|^2 =$$

$$= \left(|E_{\vartheta_{sub}}(\vartheta,\varphi)|^2 + |E_{\varphi_{sub}}(\vartheta,\varphi)|^2\right) \cdot$$

$$\cdot \frac{\sin^2\left[\frac{\pi}{\lambda}\cdot M\cdot d_x(T_x-T_{xs})\right]}{\sin^2\left[2\cdot\frac{\pi}{\lambda}\cdot d_x(T_x-T_{xs})\right]} \cdot \frac{\sin^2\left[\frac{\pi}{\lambda}\cdot N\cdot d_y(T_y-T_{ys})\right]}{\sin^2\left[2\cdot\frac{\pi}{\lambda}\cdot d_y(T_y-T_{ys})\right]} \qquad (4.32a)$$

Worked out with formulas (3.28c) and (3.28d):

$$|\bar{E}(\vartheta,\varphi)|^2 =$$

$$= 2\left\{\left[\cos^2(\varphi)F^2(\vartheta) + \sin^2(\varphi)\cos^2(\vartheta)F_2^2(\vartheta)\right]\left[1 + \cos\left\{\frac{2\pi}{\lambda}(d_x T_x + d_y T_y)\right\}\right] +\right.$$

$$\left. + \left[\sin^2(\varphi)F_1^2(\vartheta) + \cos^2(\varphi)\cos^2(\vartheta)F_2^2(\vartheta)\right]\cdot\left[1 + \cos\left\{\frac{2\pi}{\lambda}(d_x T_x - d_y T_y)\right\}\right]\right\}\cdot$$

$$\cdot\frac{\sin^2\left[\frac{\pi}{\lambda}\cdot M\cdot d_x(T_x - T_{xs})\right]}{\sin^2\left[2\cdot\frac{\pi}{\lambda}\cdot d_x(T_x - T_{xs})\right]}\cdot\frac{\sin^2\left[\frac{\pi}{\lambda}\cdot N\cdot d_y(T_y - T_{ys})\right]}{\sin^2\left[2\cdot\frac{\pi}{\lambda}\cdot d_y(T_y - T_{ys})\right]} \qquad (4.32b)$$

and the directivity becomes:

$$D = \frac{\pi \cdot \frac{1}{4} \cdot \left\{ \left[\cos^2(\varphi_s) F_1^2(\theta_s) + \sin^2(\varphi_s)\cos^2(\theta_s) F_2^2(\theta_s)\right] \cdot \left[1 + \cos\left\{\frac{2\pi}{\lambda}(d_x T_{xs} + d_y T_{ys})\right\}\right] + \left[\sin^2(\varphi_s) F_1^2(\theta_s) + \cos^2(\varphi_s)\cos^2(\theta_s) F_2^2(\theta_s)\right] \cdot \left[1 + \cos\left\{\frac{2\pi}{\lambda}(d_x T_{xs} - d_y T_{ys})\right\}\right]\right\} \cdot M^2 \cdot N^2}{\int_0^{\frac{\pi}{2}} \int_0^{2\pi} \left\{\left[\cos^2(\varphi) F_1^2(\theta) + \sin^2(\varphi)\cos^2(\theta) F_2^2(\theta)\right] \cdot \left[1 + \cos\left\{\frac{2\pi}{\lambda}(d_x T_x + d_y T_y)\right\}\right] + \left[\sin^2(\varphi) F_1^2(\theta) + \cos^2(\varphi)\cos^2(\theta) F_2^2(\theta)\right] \cdot \left[1 + \cos\left\{\frac{2\pi}{\lambda}(d_x T_x - d_y T_y)\right\}\right]\right\} \cdot \frac{\sin^2\left[\frac{\pi}{\lambda} \cdot M \cdot d_x \cdot (T_x - T_{xs})\right]}{\sin^2\left[\frac{\pi}{\lambda} \cdot 2 \cdot d_x \cdot (T_x - T_{xs})\right]} \cdot \frac{\sin^2\left[\frac{\pi}{\lambda} \cdot N \cdot d_y \cdot (T_y - T_{ys})\right]}{\sin^2\left[\frac{\pi}{\lambda} \cdot 2 \cdot d_y \cdot (T_y - T_{ys})\right]} \cdot \sin(\theta) \cdot d\theta \cdot d\varphi}$$

(4.33)

The directivity has not been calculated, but comparison of table 4.1 with figures 4.6 to 4.8 and inspection of figures 3.21 to 3.23 give the expectation that the directivities will be approximately the same as those calculated in the preceding paragraph.

Concluding, scanning on subarraylevel with circularly polarized patches reduces the number of tuneable phaseshifters with a factor 4, at the expense of a degradation of the directivity.
Scanning on subarraylevel with sequentially rotated linearly polarized patches reduces the number of coaxial-to-patch-connections with a factor 2 at the extra expense of a degradation in the axial ratio performance.

§4.6 - References

[4-1] Amitay N., Pecina R.G., Wu C.P., *'Radiation Properties of Large Planar Arrays '*, Bell Telephone Laboratories, Incorporated, Whippany, New Jersey, February 18, 1965, pp.25-36.

[4-2] Aulock W.von, *' Properties of Phased Arrays '*, Proceedings of the IRE, pp.1715-1727, 1960.

5. The Array Antenna Feeding Network

This chapter discusses the elements of which the array feeding network consists. In the foregoing chapters the arrays were assumed being uniformly excited. To obtain a uniform excitation, power splitters with an equal output power distribution are needed. To maintain the specific advantage of microstrip antennas: flatness, these power splitters have to be performed in microstrip technology. Discussed are the T Power Splitter and the Wilkinson Power Splitter. For the 90^0-phaseshifters, also needed in the feeding network, quarter lambda (microstrip) transmissionlines are used.
Before these components are treated, the microstrip antenna patch has to be discussed, especially the antenna input impedance, since the feeding network should be matched to the patches.

§5.1 - Characteristics of the Circular Patch

In the following first a choise will be made for the model with which the circular patch will be analysed. After this model is treated, the feed location corresponding with a 50Ω impedance and the patch-VSWR will be discussed.

§5.1.1 - Choise of Model

Of the different models of the circular microstrip antenna, the cavity model is the less complex and, as far as resonance frequency is concerned, expected to be accurate enough when fringe fields along the edge of the patch are included in the model [5-1].
The input impedance of the patch is modeled as a parallel RLC-circuit [5-1] with a series inductance that is associated with the microstrip antenna feed [5-2]. The series inductance is especially important for microstrip antennas with more than one feed [5-2, 5-3]. For a one-feed patch the series inductance is dominated by the parallel RLC-circuit and may be omitted. For the one-feed patch an analysis according to Derneryd [5-4] is advised [5-2]. In [5-4] the input impedance of a circular patch at resonance is calculated. A more general analysis is given in [5-1] and will be briefly summarized in the next paragraph.

§5.1.2 - The Cavity Model

Figure 5.1 shows a circualar microstrip antenna element. The feed position is indicated by ρ and φ.

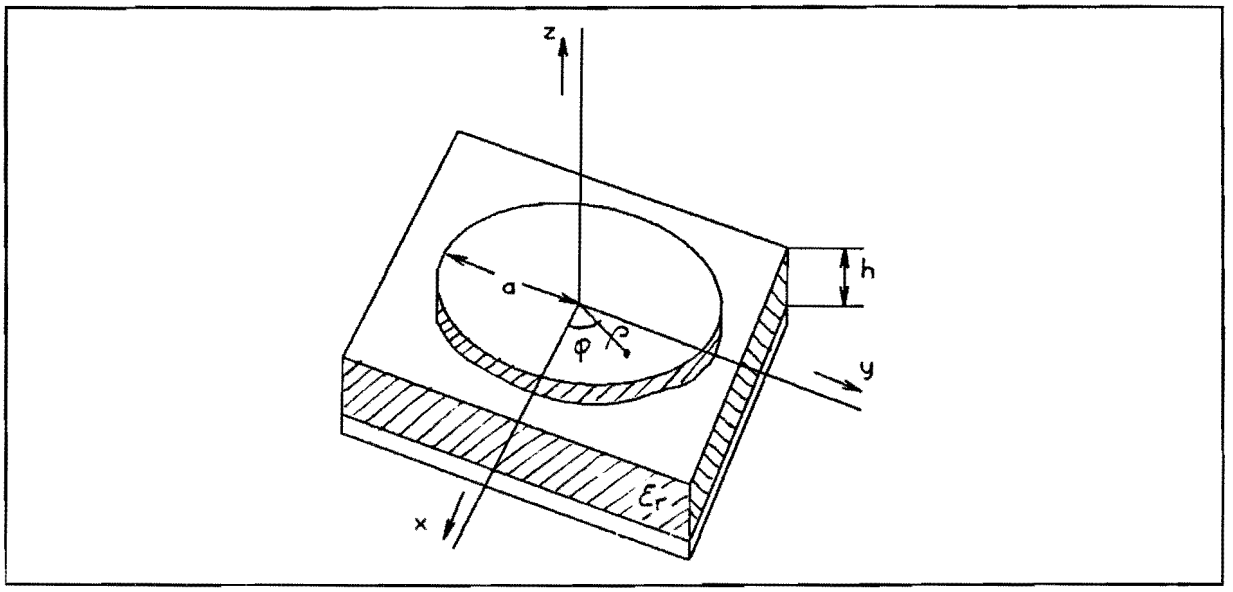

Fig. 5.1 - Circular microstrip antenna element

The resonance frequency of the patch for the TM_{mn}-mode is given by:

$$f_r = \frac{K_{nm} \cdot c_0}{2\pi \cdot a_e \cdot \sqrt{\varepsilon_r}} \tag{5.1}$$

with c_0 the velocity of light in free space and K_{nm} (= ka) the m^{th} zero of the derivative of the Bessel function of order n.
An effective radius a_e is used to account for the fringe fields along the edge of the patch:

$$a_e = a \cdot \left[1 + \frac{2h}{\pi a \varepsilon_r} \cdot \left(\ln\frac{\pi a}{2h} + 1.7726\right)\right]^{\frac{1}{2}} \tag{5.2}$$

At resonance the input impedance of the patch is real and given by:

$$R = \frac{V^2}{2P_T} \tag{5.3a}$$

with:

$$V = h \cdot E_0 \cdot J_n(ka) \tag{5.3b}$$

the edge voltage for $\varphi = 0$ and P_T the total dissipated power. With the feed located at $(\rho,\varphi) = (\rho_0,0)$, (5.3) becomes:

$$R = \frac{h^2 \cdot E_0^2 \cdot J_n^2(k\rho_0)}{2 \cdot P_T} \tag{5.4}$$

The total dissipated power P_T consists of 3 parts: Radiated power P_r, power dissipated in the conductors P_c and power dissipated in the dielectric substrate P_d.

$$P_r = \frac{\left(h \cdot E_0 \cdot J_n(ka) \cdot a \cdot k_0\right)^2}{16 \cdot Z_0} \cdot \pi \cdot I_1 \tag{5.5a}$$

with:

$$I_1 = \int_0^{\pi} \left[\left\{ J_{n+1}(k_0 a \cdot \sin\vartheta) - J_{n-1}(k_0 a \cdot \sin\vartheta) \right\}^2 + \right.$$

$$\left. + \cos^2(\vartheta) \cdot \left\{ J_{n+1}(k_0 a \cdot \sin\vartheta) + J_{n-1}(k_0 a \cdot \sin\vartheta) \right\}^2 \right] \cdot \sin(\vartheta) \cdot d\vartheta \tag{5.5b}$$

$$k_0 = \frac{2\pi}{\lambda_0} \quad , \qquad k = \frac{2\pi}{\lambda_g} = \sqrt{\varepsilon_r}\cdot k_0 \tag{5.5c}$$

$$Z_0 = 120\cdot\pi\Omega \tag{5.5d}$$

$$P_c = \left[\frac{\pi f \mu}{\sigma} \right]^{\frac{1}{2}} \cdot \frac{E_0^2}{(\omega\cdot\mu)^2} \cdot \pi \cdot \left[\frac{1}{2} \cdot J_n^2(ka) \cdot \left\{ (ka)^2 - n^2 \right\} \right] \tag{5.6}$$

with σ the conductivity of the metal.

$$P_d = \frac{h\cdot\tan\delta\cdot E_0^2}{8\mu f} \cdot J_n^2(ka) \cdot \left\{ (ka)^2 - n^2 \right\} \tag{5.7}$$

with $\tan\delta$ the loss tangent of the dielectric substrate.

As mentioned before the input impedance of the patch can be modeled as a parallel RLC-circuit.The resonance frequency of this circuit is:

$$f_r = \frac{1}{2\pi\cdot\sqrt{LC}} \tag{5.8}$$

The quality factor is given by:

$$Q_T = R\cdot\sqrt{LC} \tag{5.9}$$

So L and C are found to be:

$$L = \frac{R}{2\pi \cdot f_r \cdot Q_T} \tag{5.10}$$

$$C = \frac{Q_T}{2\pi \cdot f_r \cdot R} \tag{5.11}$$

The input impedance is:

$$Z_{in} = R_{in} + j \cdot X_{in} = \frac{1}{\frac{1}{R} + j\omega C + \frac{1}{j\omega L}} \tag{5.12a}$$

and at resonance:

$$Z_{in} = R_{in} = R \tag{5.12b}$$

The quality factor of the patch is defined as:

$$Q_T = \frac{\omega \cdot W_T}{P_T} \tag{5.13a}$$

with:

$$W_T = \frac{h \cdot E_0^2}{8\omega f \mu} \cdot J_n^2(ka) \cdot \left\{ (ka)^2 - n^2 \right\} \tag{5.13b}$$

Now all the information is available to calculate the input impedance and Voltage Standing Wave Ratio of the patch.

§5.1.3 - Input Impedance at Resonance

The input impedance at resonance in the (principal) TM_{11}-mode (n = 1, K_{11} = 1.84118) can be calculated with (5.4), (5.5a), (5.6) and (5.7):

$$R = \frac{h^2 J_1^2(k\rho_0)}{2J_1^2(1.84118)\cdot\{1.84118^2 - 1\}} \cdot \left[\frac{(hk_0a)^2 \cdot I_1}{1920\cdot\{1.84118^2 - 1\}} + \frac{1}{8\cdot\sqrt{\pi\sigma f^3\mu^3}} + \frac{h\tan\delta}{8\mu f}\right]^{-1} \qquad (5.14a)$$

with:

$$I_1\Big|_{n=1} = \int_0^{\pi} \left[\left\{J_2(k_0a\cdot\sin\vartheta) - J_0(k_0a\cdot\sin\vartheta)\right\}^2 + \cos^2(\vartheta)\cdot\left\{J_2(k_0a\cdot\sin\vartheta) + J_0(k_0a\cdot\sin\vartheta)\right\}^2 \right]\cdot\sin(\vartheta)\cdot d\vartheta \qquad (5.14b)$$

and with (5.1) and (5.2):

$$a_e = \frac{c_0\cdot 1.84118}{2\pi\cdot f_r\cdot\sqrt{\varepsilon_r}} = a\cdot\left[1 + \frac{2h}{\pi a\varepsilon_r}\cdot\left(\ln\frac{\pi a}{2h} + 1.7720\right)\right]^{\frac{1}{2}} \qquad (5.14c)$$

To calculate R as function of ρ_0, first equation (5.14c) has to be solved for a. Then (5.14b) has to be solved and finaly with a and I_1 substituted in (5.14a), R can be calculated for different ρ_0.

Program FEEDLOC that performs these calculations is given in appendix G. Since (5.14c) is a smoothly varying function and $0 < a < a_e$,

(5.14) is solved for a using the Secant method [5-5]. I_1 is solved with Gauss- Legendre integration [5-5], a fast reliable integration method [5-6], with coefficients according to [5-7]. The reliability of the integration method has been tested with testfunctions according to [5-6]

Figure 5.2 shows R as function of ρ_0/a for different dielectric substrates and thicknesses.

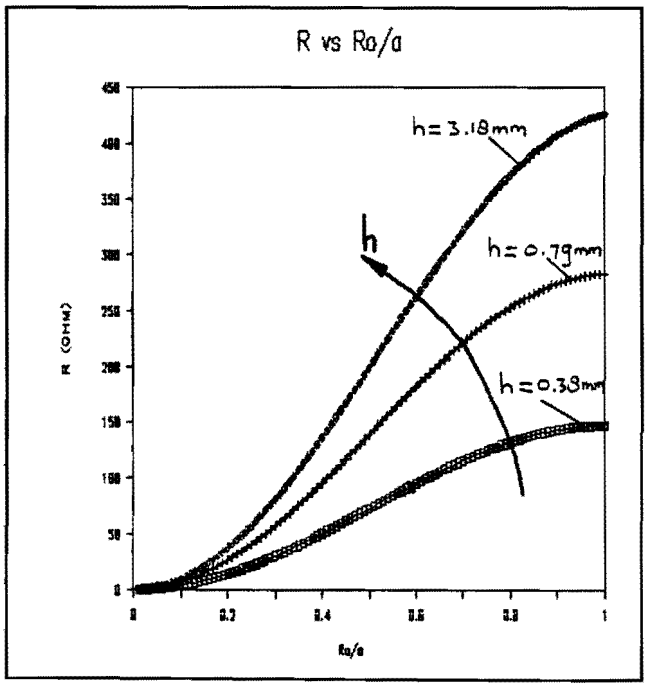

Fig 5.2a - R vs ρ_0/a for $\varepsilon_r = 2.33$

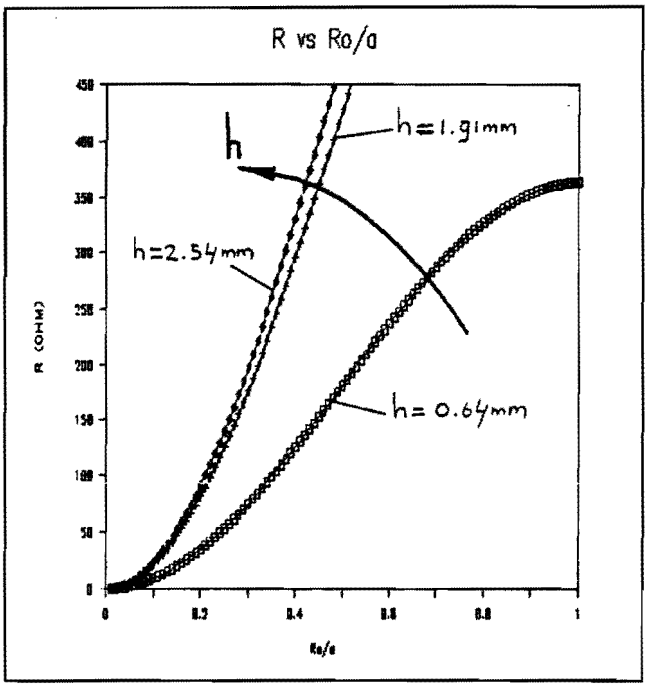

Fig. 5.2b - R vs ρ_0/a for $\varepsilon_r = 10.5$

The above figures show that it will be more difficult to position the feed when a substrate with a relatively high dielectric constant is used; a small construction error will result in a larger mismatch. For the same reason it is desirable to use a relatively thin substrate. The feed locations corresponding with R = 50Ω for different dielectric substrates and thicknesses are listed in table 5.1. The substrate characteristics (DUROID RT/D 5870, RT/D 6006 and RT/D 6010.5) are given in appendix D.

Table 5.1 - Feed locations, f_r = 1.55GHz

DUROID RT/D 5870, ε_r = 2.33		
h (mm)	a (cm)	ρ_o/a (R=50Ω)
0.13	3.70	-----
0.25	3.69	0.565
0.38	3.68	0.398
0.51	3.67	0.332
0.79	3.65	0.280
1.57	3.60	0.245
3.18	3.52	0.233
DUROID RT/D 6006, ε_r = 6		
h (mm)	a (cm)	ρ_0/a (R=50Ω)
0.25	2.31	0.590
0.64	2.30	0.289
1.27	2.28	0.217
1.91	2.27	0.195
2.54	2.26	0.187
DUROID RT/D 6010.5, ε_r = 10.5		
h (mm)	a (cm)	ρ_0/a (R=50Ω)
0.64	1.74	0.241
1.27	1.73	0.175
1.91	1.73	0.155
2.54	1.72	0.147

§5.1.4 - Patch VSWR

To calculate the input impedance (equation (5.12a)) of the patch in the TM_{11}-mode, an expression for Q_T is needed to calculate L and C. With (5.5), (5.6). (5.7) and (5.13) Q_T becomes:

$$Q_T = \left[\frac{1}{h \cdot \sqrt{\pi f \mu \sigma}} + \tan\delta + \frac{h \cdot \mu \cdot f \cdot (k_0 a)^2 \cdot I_1}{240 \cdot (1.84118^2 - 1)} \right]^{-1} \qquad (5.15)$$

The input impedance becomes:

$$Z = \frac{1}{\frac{1}{R} + j\omega C + \frac{1}{j\omega C}} = \frac{\omega^2 L^2 R + j\omega LR \cdot (R - \omega^2 LRC)}{(R - \omega^2 LRC)^2 + (\omega L)^2} = A + j \cdot B \qquad (5.16a)$$

with:

$$A = \frac{\omega^2 L^2 R}{(R - \omega^2 LRC)^2 + (\omega L)^2} \qquad (5.16b)$$

$$B = \frac{\omega LR \cdot (R - \omega^2 LRC)}{(R - \omega^2 LRC)^2 + (\omega L)^2} \qquad (5.16c)$$

With (5.16) the reflection coefficient can be calculated [5-8]:

$$|\Gamma| = \left| \frac{Z - Z_{tr}}{Z + Z_{tr}} \right| \qquad (5.17)$$

with Z_{tr} (=50Ω) the characteristic impedance of the transmission lines used in the feeding network. With (5.16) the reflection coefficient can be written as:

$$|\Gamma| = \left| \frac{A + j \cdot B - Z_{tr}}{A + j \cdot B + Z_{tr}} \right| = \frac{\sqrt{(A - Z_{tr})^2 + B^2}}{\sqrt{(A + Z_{tr})^2 + B^2}} \qquad (5.18)$$

With (2.32) the Voltage Standing Wave Ratio becomes:

$$S = \frac{1 + |\rho|}{1 - |\rho|} \tag{5.19}$$

With program STANWAVE (appendix G) the VSWR is calculated for different patches as function of the frequency with use of the information stated in table 5.1. The results are shown in figures 5.3 to 5.5. Indicated in these figures as well is the 1.4 VSWR-limit following from the INMARSAT- and MSATX-requirements (see table 2.1)

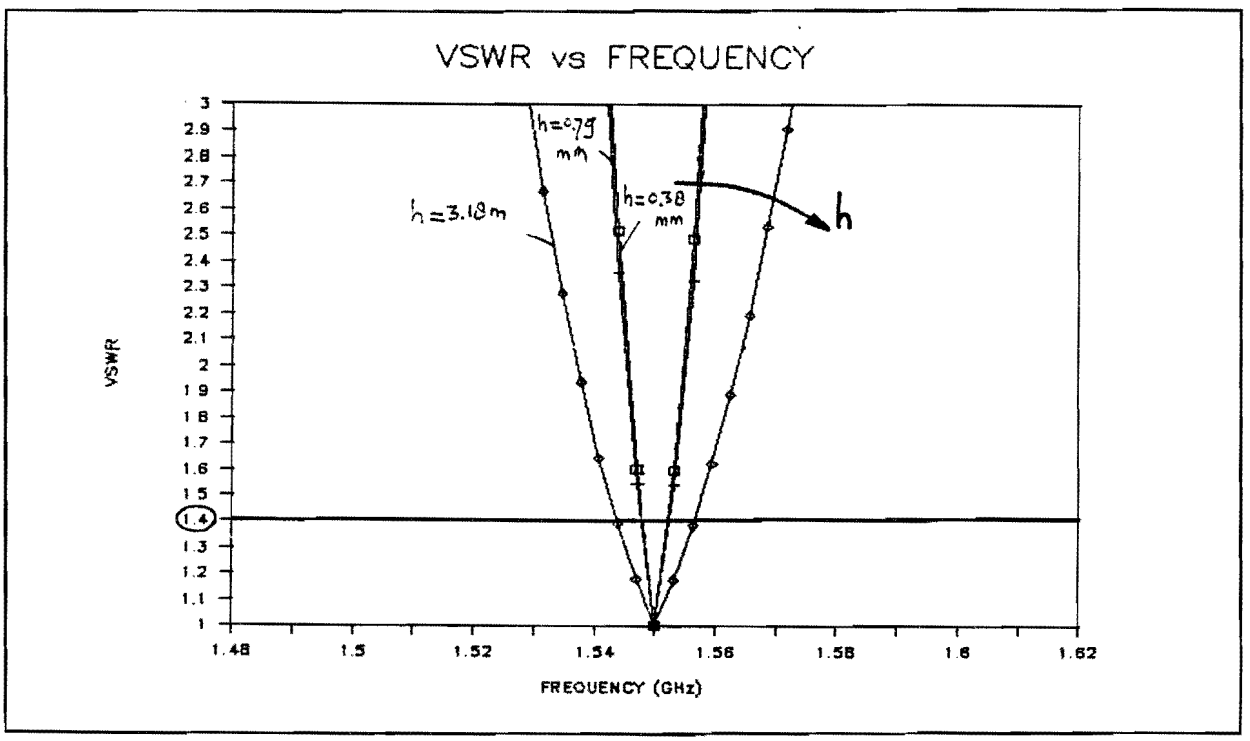

Fig. 5.3 - VSWR as function of f, ε_r = 2.33, f_r = 1.55GHz

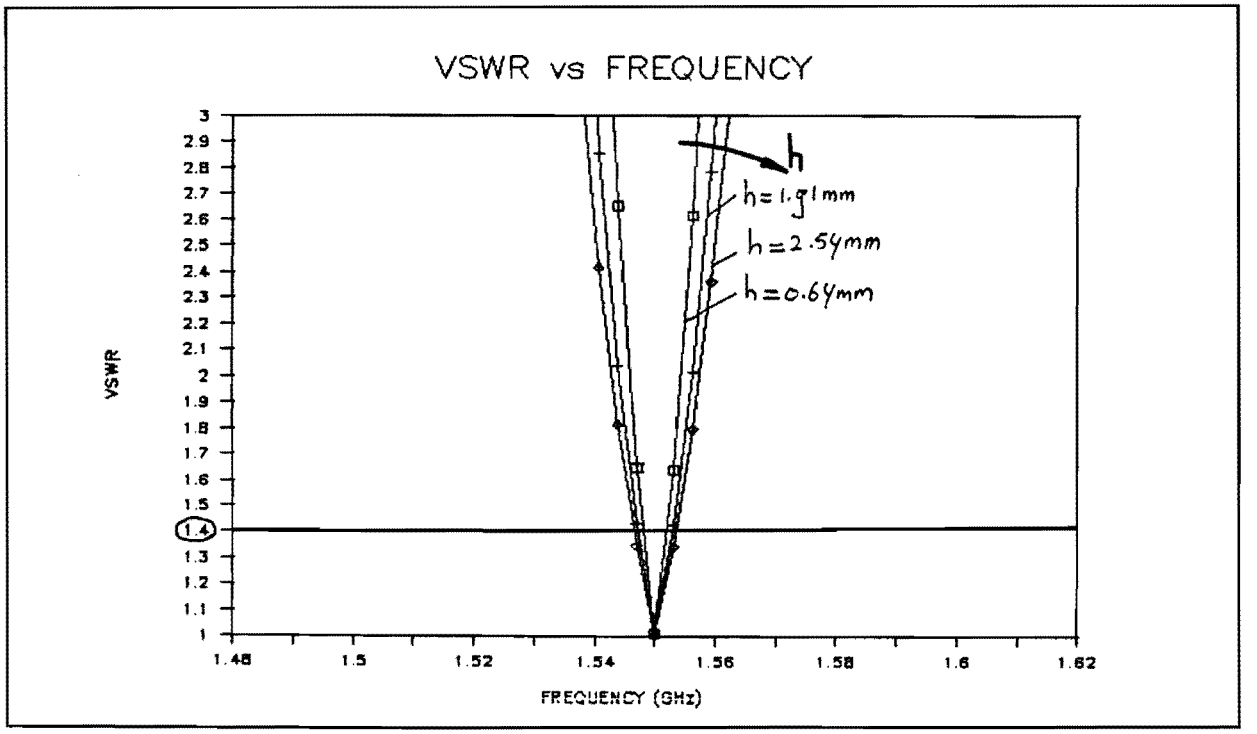

Fig. 5.4 - VSWR as function of f, ε_r = 6, f_r = 1.55GHz

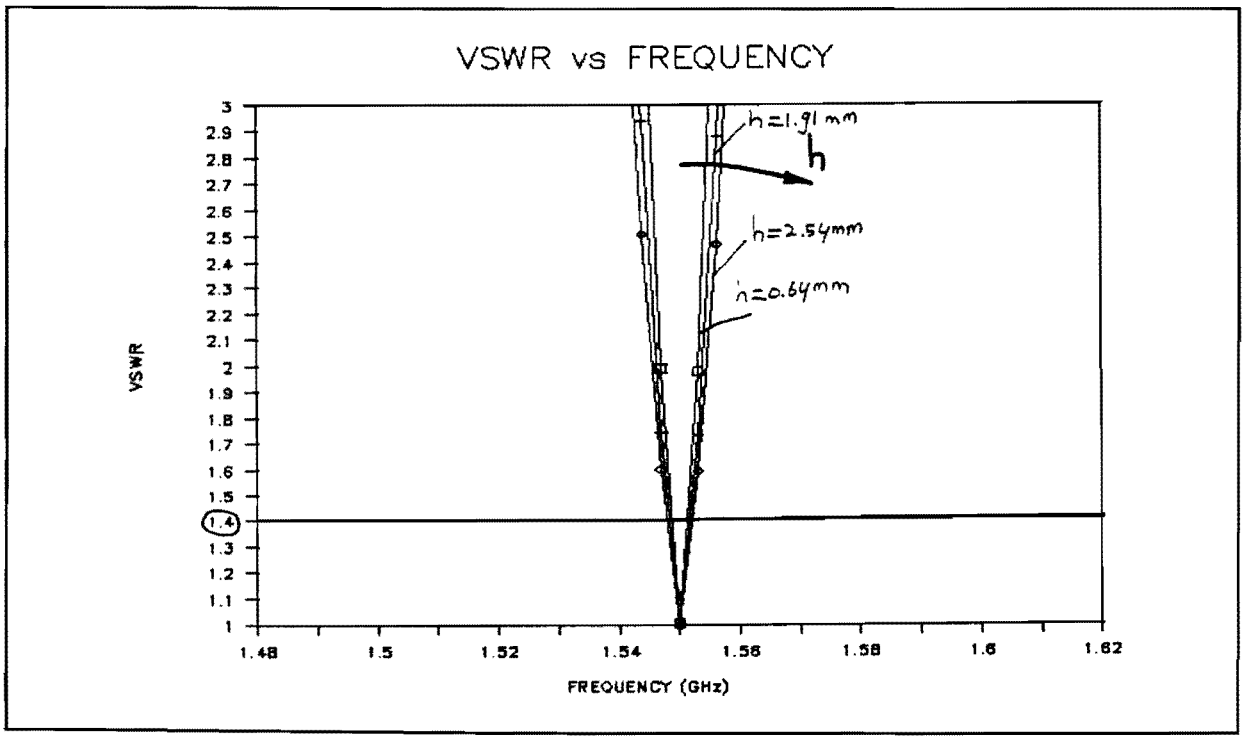

Fig. 5.5 - VSWR as function of f, ε_r = 10.5, f_r = 1.55GHz

The impedance- and VSWR-calculations agree well with measurements [5-9], which proves the validity of the used model.
The foregoing calculations show:

- An increase of ε_r decreases the VSWR-bandwidth;
- an increase of h increases the VSWR-bandwidth;
- The h-dependence of the VSWR-bandwidth decreases with increasing ε_r.

Some of these effects are reported too in [5-10].

Figures 5.3 to 5.5 show that is not possible to use one (array-) antenna for both transmitting and receiving. Without techniques to broaden the bandwidth it even wil not be possible to use the antenna for transmitting or receiving only: The figures show that the bandwidth is less than 30MHz. This bandwidth is needed for operation (receiving: 1530-1559MHz, transmitting: 1626.5-1660.5MHz) [5-11].

§5.2 - Wilkinson Power Splitter

Figure 5.6 shows a stripline Wilkinson power splitter for an arbitrary power division. Assume that the cross-sectional dimensions of the strip line are very small compared to a wavelength.Hence discontinuities caused by corners and junctions are negligible.

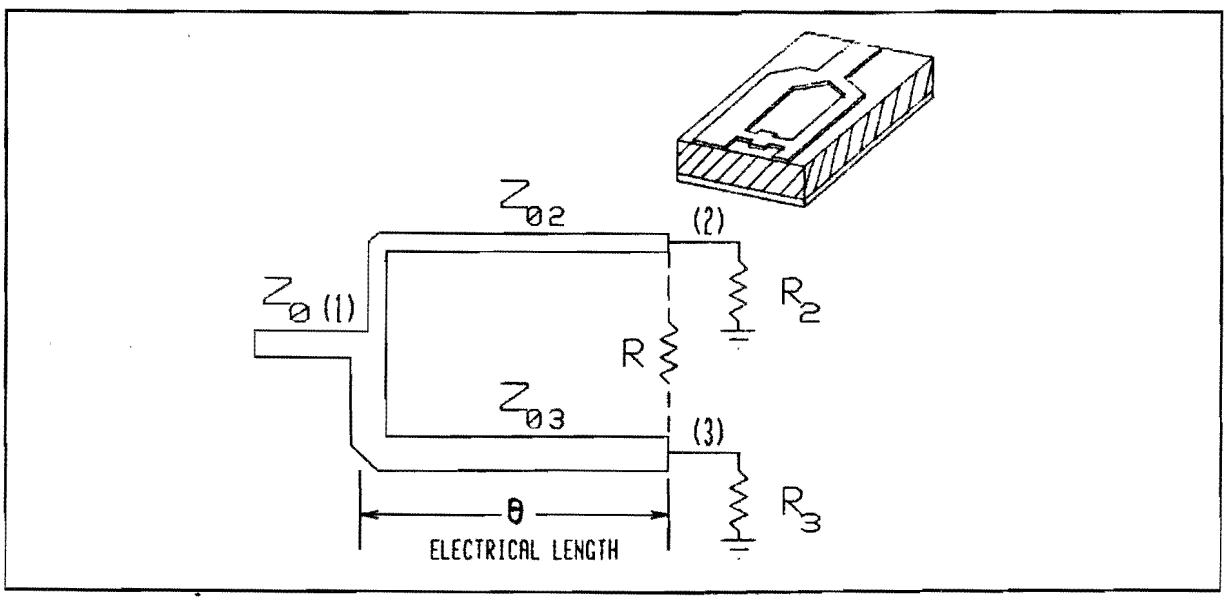

Fig. 5.6 - Power splitter with unequal output impedances

The power splitter is designed so that when fed from port 1, a match is seen; the power out of port 3 is K^2 times that out of port 2; and the voltage between arm 2 and ground is equal to that between arm 3 and ground when measured at equal distances from port 1 [5-12]. With ground is meant the lower conducting surface in the stripline structure (see figure 5.6). To satisfy the last two conditions, all impedances in arm 2 must be K^2 times the corresponding impedances in arm 3. To see a match at port 1, it follows that:

$$\frac{Z_{i2} \cdot Z_{i3}}{Z_{i2}+Z_{i3}} = \frac{K^2 \cdot Z_{i3}}{1+K^2} = Z_0 \qquad (5.20a)$$

$$Z_{i3} = \frac{1+K^2}{K^2} \cdot Z_0 \qquad (5.20b)$$

where Z_{i2} and Z_{i3} are the input impedances looking into arms 2 and 3 from port 1. The output impedances R_2 and R_3 are chosen to be [5-12]:

$$R_2 = K \cdot Z_0 \qquad R_3 = \frac{Z_0}{K} \qquad (5.21)$$

With (5.20) and (5.21) and $\vartheta = 90^0$ the characteristic impedances of the two arms can be calculated:

$$Z_{02} = Z_0 \cdot \sqrt{K \cdot (1 + K^2)} \qquad (5.22a)$$

$$Z_{03} = Z_0 \cdot \sqrt{\frac{1 + K^2}{K^3}} \qquad (5.22b)$$

Since the voltages at port 2 and port 3 are equal, a resistor may be placed between these ports (see figure 5.6). If the power splitter is fed from port 2 or port 3, energy will be dissipated in the resistor. Isolation between output ports and a good match seen looking in at any port is obtainable because of this resistor. The value of the

isolation resistor is given by [5-12]:

$$R = Z_0 \cdot \frac{1+K^2}{K} \tag{5.23}$$

§5.2.1 - Unnormalized Voltage Scattering Matrix

Since the splitter network has unequal impedance levels, the characteristics are described by the *unnormalized* voltage scattering matrix:

$$\begin{pmatrix} d_1 \\ d_2 \\ d_3 \end{pmatrix} = \begin{pmatrix} T_{11} & T_{12} & T_{13} \\ T_{21} & T_{22} & T_{23} \\ T_{31} & T_{32} & T_{33} \end{pmatrix} \cdot \begin{pmatrix} c_1 \\ c_2 \\ c_3 \end{pmatrix} \tag{5.24}$$

where d_j (j = 1, 2, 3) is the amplitude and phase of the voltage wave leaving the j^{th} port and c_k (k = 1, 2, 3) is the amplitude and phase of the voltage wave incident upon the k^{th} port. The relationship between T- and S-matrix is given in appendix E.

To determine the transfer coefficients T_{11}, T_{21}, T_{12}, T_{31} and T_{13}, the network is driven at port 1 and ports 2 and 3 are terminated with matched impedances ($R_2 = K \cdot Z_0$, $R_3 = Z_0/K$). The voltage from arm 2 to ground is the same as that from arm 3 to ground at any distance from port 1, so a short-circuiting line may be used to connect arms 2 and 3 together. The resulting network is shown in figure 5.7 where arms 2 and 3 have been connected in parallel as have the load resistor R_2 and R_3.

Before the equations that govern the network of figure 5.7 are given, some remarks have to be made about reflection coefficient (Γ) and transmitting coefficient (T). When two transmission lines a and b with characteristic impedances Z_a and Z_b are connected, the reflection coefficient looking from line a into line b is given by [5-8]:

$$\Gamma_{a \Rightarrow b} = \frac{Z_b - Z_a}{Z_b + Z_a} \tag{5.25}$$

and consequently $\Gamma_{b\Rightarrow a} = -\Gamma_{a\Rightarrow b}$. The relationship between reflection coefficient and transmission coefficient is given by [5-13]:

$$1 + \Gamma = T \tag{5.26}$$

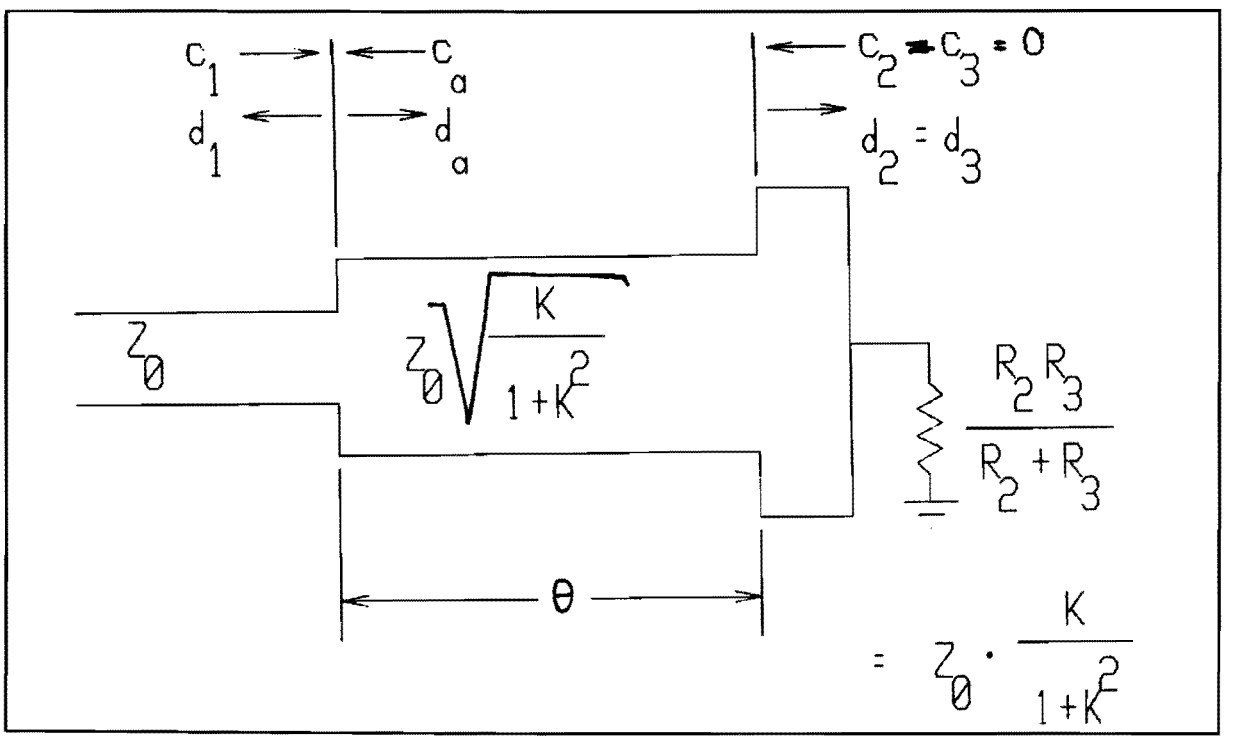

Fig. 5.7 - Equivalent circuit for determining T_{11}, T_{21}, T_{12}, T_{31} and T_{13}

The equations that govern the network are:

$$d_1 = \Gamma_1 \cdot c_1 + (1 - \Gamma_1) \cdot c_a \tag{5.27a}$$

$$d_a = (1 + \Gamma_1) \cdot c_1 - \Gamma_1 \cdot c_a \tag{5.27b}$$

$$c_a = \Gamma_1 \cdot e^{-j \cdot 2\vartheta} \cdot d_a \tag{5.27c}$$

$$d_2 = (1 + \Gamma_1) \cdot e^{j \cdot \vartheta} \cdot d_a \tag{5.27d}$$

with:

$$\Gamma_1 = \frac{\sqrt{K} - \sqrt{1 + K^2}}{\sqrt{K} + \sqrt{1 + K^2}} \qquad (5.27e)$$

Using the above equations gives [5-12]:

$$T_{11} = \left.\frac{d_1}{c_1}\right|_{c_2 = c_3 = 0} = \Gamma_1 \cdot \left[1 + \frac{(1 - \Gamma_1^2) \cdot e^{-j \cdot 2\vartheta}}{1 + \Gamma_1^2 \cdot e^{-j \cdot 2\vartheta}} \right] \qquad (5.28a)$$

$$T_{21} = T_{31} = \left.\frac{d_2}{c_1}\right|_{c_2 = c_3 = 0} = \frac{(1 + \Gamma_1)^2 \cdot e^{-j \cdot \vartheta}}{1 + \Gamma_1^2 \cdot e^{-j \cdot 2\vartheta}} \qquad (5.28b)$$

The values of T_{12} and T_{13} are obtained by using reciprocity (explained in appendix E) [5-12]:

$$T_{12} = \frac{T_{21}}{K} \quad , \qquad T_{13} = K \cdot T_{31} \qquad (5.28c)$$

The remaining coefficients (T_{23}, T_{32}, T_{22}, T_{33}) are determined by simultaneously exciting port 2 and port 3 in-phase (even excitation) and then exciting them out-of-phase (odd excitation) as depicted in figure 5.8 [5-12]. By superposition of odd and even exitations, the desired T-coefficients are obtained.

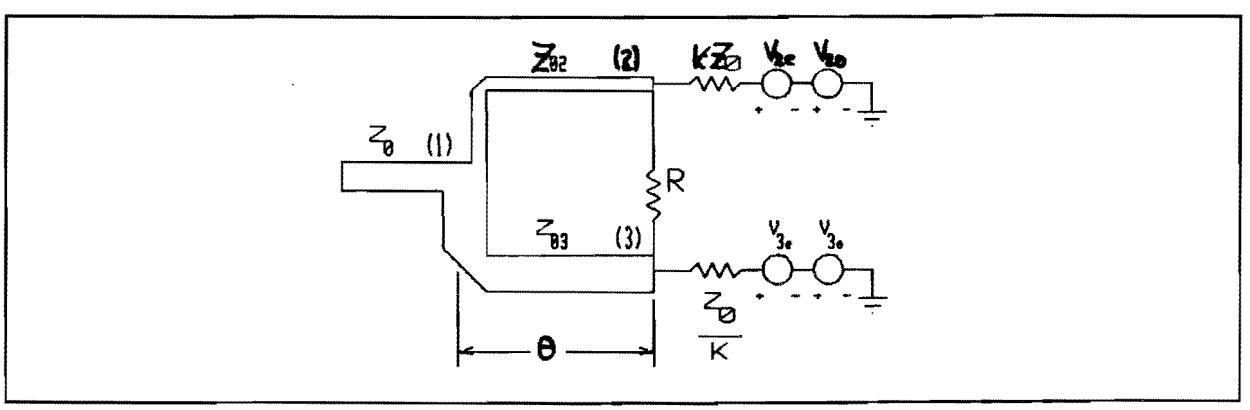

Fig. 5.8 - Even and odd excitations

With E_i (i = 2, 3) the voltage at port i, index e indicating the even excitation and index o indicating the odd excitation, the results of both excitations are (explained in appendix E) [5-12]:

$$E_{2e} = \frac{Z_{2e} \cdot V_{2e}}{K \cdot Z_0 + Z_{2e}} \tag{5.29a}$$

$$Z_{2e} = Z_{02} \cdot \frac{Z_0 \cdot (1 + K^2) + j \cdot Z_{02} \cdot \tan(\vartheta)}{Z_{02} + j \cdot Z_0 \cdot (1 + K^2) \cdot \tan(\vartheta)} \tag{5.29b}$$

$$E_{2o} = \frac{V_{2o}}{1 + K \cdot Y_{2o} \cdot Z_0} \tag{5.30a}$$

$$Y_{2o} = \frac{1}{K \cdot Z_0} + \frac{1}{j \cdot Z_0 \cdot \sqrt{K \cdot (1 + K^2)} \cdot \tan(\vartheta)} \tag{5.30b}$$

If $V_{2o} = -V_{2e}$, port 2 is not excited (see figure 5.8) and port 3 is excited with the voltage $V = V_{3e} + V_{3o} = V_{2e} - V_{2o}/K^2 = V_{2e}(1 + 1/K^2)$. If a short transmissionline of characteristic impedance Z_0/K is inserted between the generator resistance Z_0/K and port3 (see figure 5.8), the incident voltage wave will be $V_{2e} \cdot (1+K^2)/2K^2$ [5-12]. This will be explained in detail in appendix E.
T_{33} and T_{23} can be found from the total voltages across port 3 and 2:

$$V_{T3} = (1 + T_{33}) \cdot V_{inc} = (1 + T_{33}) \cdot \frac{V_{2e} \cdot (1 + K^2)}{2 \cdot K^2} \tag{5.31a}$$

$$V_{T3} = E_{3e} + E_{3o} = \frac{Z_{2e} \cdot V_{2e}}{K \cdot Z_0 + Z_{2e}} + \frac{V_{2e}}{K^2 \cdot (1 + K \cdot Y_{2o} \cdot Z_0)} \tag{5.31b}$$

$$T_{33} = \frac{2 \cdot K^2}{1 + K^2} \cdot \left[\frac{Z_{2e}}{K \cdot Z_0 + Z_{2e}} + \frac{1}{K^2 \cdot (1 + K \cdot Y_{2o} \cdot Z_0} \right] - 1 \tag{5.31c}$$

$$T_{23} = \frac{V_{T2}}{V_{inc}} = \frac{2\cdot K^2\cdot V_{T2}}{(1 + K^2)\cdot V_{2e}} = \frac{2\cdot K^2\cdot (E_{2e} + E_{2o})}{(1 + K^2)\cdot V_{2e}} =$$

$$= \frac{2\cdot K^2}{1 + K^2}\cdot\left[\frac{Z_{2e}}{K\cdot Z_0 + Z_{2e}} - \frac{1}{1 + K\cdot Y_{2o}\cdot Z_0}\right] \qquad (5.32)$$

If $V_{3o} = -V_{3e}$, port 3 is not excited and port 2 is excited with the voltage $V = V_{2e} + V_{2o} = V_{2e} - K^2\cdot V_{3o} = V_{2e}\cdot(1 + K^2)$. Inserting a short transmission line of characteristic impedance $K\cdot Z_0$ between the generator impedance $K\cdot Z_0$ and port 2, causes the incident voltage wave to be $\frac{1}{2}\cdot V_{2e}\cdot(1 + K^2)$ [5-12]. T_{22} and T_{32} can be found from the total voltages across port 2 and 3:

$$V_{T2} = (1 + T_{22})\cdot V_{inc} = \frac{1}{2}\cdot(1 + K^2)\cdot(1 + T_{22})\cdot V_{2e} \qquad (5.33a)$$

$$V_{T2} = E_{2e} + E_{2o} = \frac{Z_{2e}\cdot V_{2e}}{K\cdot Z_0 + Z_{2e}} + \frac{V_{2o}}{1 + K\cdot Y_{2o}\cdot Z_0} =$$

$$= \frac{Z_{2e}\cdot V_{2e}}{K\cdot Z_0 + Z_{2e}} + \frac{K^2\cdot V_{2e}}{1 + K\cdot Y_{2o}\cdot Z_0} \qquad (5.33b)$$

$$T_{22} = \frac{2}{1 + K^2}\cdot\left[\frac{Z_{2e}}{K\cdot Z_0 + Z_{2e}} + \frac{K^2}{1 + K\cdot Y_{2o}\cdot Z_0}\right] - 1 \qquad (5.33c)$$

$$T_{32} = \frac{V_{T3}}{V_{inc}} = \frac{2\cdot V_{T3}}{(1 + K^2)\cdot V_{2e}} = \frac{2\cdot (E_{3e} + E_{3o})}{(1 + K^2)\cdot V_{2e}} =$$

$$= \frac{2}{1 + K^2}\cdot\left[\frac{Z_{2e}}{K\cdot Z_0 + Z_{2e}} - \frac{1}{1 + K\cdot Y_{2o}\cdot Z_0}\right] \qquad (5.34)$$

§5.2.2 - Wilkinson Splitter Power Distribution

A general power splitter is depicted in figure 5.9.

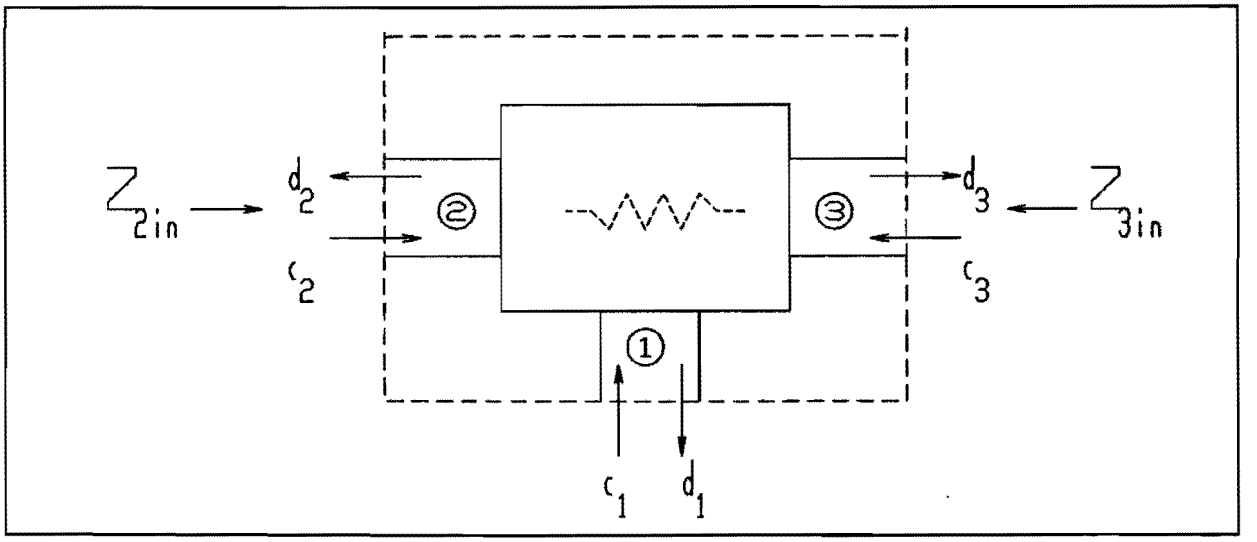

Fig. 5.9 - General power splitter

Needed in the feeding network are power splitters, that split the incoming power into two equal parts. So analyzed is the Wilkinson power splitter for the case K = 1. The relationships between d_i and c_i (i = 1, 2, 3) for this case are given by:

$$d_1 = T_{11}c_1 + T_{12}c_2 + T_{12}c_3 = T_{11}c_1 + T_{12}\rho_2 d_2 + T_{12}\rho_3 d_3 \qquad (5.35a)$$

$$d_2 = T_{12}c_1 + T_{22}c_2 + T_{23}c_3 = T_{12}c_1 + T_{22}\rho_2 d_2 + T_{23}\rho_3 d_3 \qquad (5.35b)$$

$$d_3 = T_{12}c_1 + T_{23}c_2 + T_{22}c_3 = T_{12}c_1 + T_{23}\rho_2 d_2 + T_{22}\rho_3 d_3 \qquad (5.35c)$$

with:

$$\rho_2 = \frac{Z_{L2} - Z_{2in}}{Z_{L2} + Z_{2in}} \quad , \qquad \rho_3 = \frac{Z_{L3} - Z_{3in}}{Z_{L3} + Z_{3in}} \qquad (5.35d)$$

where Z_{2in} and Z_{3in} are the input impedances looking ito ports 2 and 3 (see figure 5.9). Z_{L2} and Z_{L3} are the the impedances with which port 2 and port 3 are terminated.
With (5.35) follows:

$$d_1 = \left[T_{11} + T_{12}^2 \cdot \frac{\rho_2 + \rho_3 - 2\rho_2\rho_3 \cdot (T_{22} - T_{23})}{1 - T_{22} \cdot (\rho_2 + \rho_3) + \rho_2\rho_3 \cdot (T_{22}^2 - T_{23}^2)} \right] \cdot c_1 \qquad (5.36a)$$

$$d_2 = \left[\frac{1 - (T_{22} - T_{23}) \cdot \rho_3}{1 - T_{22} \cdot (\rho_2 + \rho_3) + \rho_2\rho_3 \cdot (T_{22}^2 - T_{23}^2)} \right] \cdot T_{12} c_1 \qquad (5.36b)$$

$$d_3 = \left[\frac{1 - (T_{22} - T_{23}) \cdot \rho_2}{1 - T_{22} \cdot (\rho_2 + \rho_3) + \rho_2\rho_3 \cdot (T_{22}^2 - T_{23}^2)} \right] \cdot T_{12} c_1 \qquad (5.36c)$$

The T-coefficients for the case $K = 1$, are given by:

$$T_{11} = - \frac{\sqrt{2}}{3\sqrt{2} + j \cdot 4 \cdot \tan(\vartheta)} \qquad (5.37a)$$

$$T_{12} = \frac{2}{3 \cdot \cos(\vartheta) + j \cdot 2\sqrt{2} \cdot \sin(\vartheta)} \qquad (5.37b)$$

$$T_{22} = - \frac{1}{3 - 8 \cdot \tan^2(\vartheta) + j \cdot 8\sqrt{2} \cdot \tan(\vartheta)} \qquad (5.37c)$$

$$T_{23} = \frac{2 \cdot (1 + j \cdot \sqrt{2} \cdot \tan(\vartheta))}{3 - 8 \cdot \tan^2(\vartheta) + j \cdot 8\sqrt{2} \cdot \tan(\vartheta)} \qquad (5.37d)$$

with:

$$\vartheta = \frac{2\pi}{\lambda} \cdot l = \frac{2\pi}{\lambda} \cdot \frac{\lambda_g}{\lambda} = \frac{\pi}{2} \cdot \frac{f}{f_r} \qquad (5.37e)$$

where λ_g is the wavelength in the dielectric substrate and f_r the

corresponding resonance frequency.

The power going into port 1 (P_{in}), the power returning at port 1 ($P1_{ret}$), the powers dissipated in the loads (P2 and P3) and the power dissipated in the isolation resistor (P_{diss}) are given by:

$$P_{in} = \frac{|c_1|^2}{2 \cdot Z_0} \tag{5.38a}$$

$$P1_{ret} = \frac{|d_1|^2}{2 \cdot Z_0} \tag{5.38b}$$

$$P2 = \frac{|d_2|^2}{2 \cdot Z_{2in}} \cdot \left(1 - |\rho_2|^2 \right) \quad 1) \tag{5.38c}$$

$$P3 = \frac{|d_3|^2}{2 \cdot Z_{3in}} \cdot \left(1 - |\rho_3|^2 \right) \tag{5.38d}$$

$$P_{diss} = \frac{|(c_2 + d_2) - (c_3 + d_3)|^2}{2 \cdot Re\{R\}} \tag{5.38e}$$

The input impedances can be calculated with [5-3]:

$$Z_{kin} = \frac{1}{2} \cdot (Z_{ke} + Z_{ko}), \quad k = 2, 3 \tag{5.39}$$

---

1) The power P dissipated in a load Z_L that is not matched to a transmission line with characteristic impedance Z_c, is given by [5-14]:

$$P = \frac{1}{2} \cdot Re(V_L I_L^*) = \frac{1}{2} \cdot Re\left[(V^+ + V^-) \cdot (I^+ - I^-)^* \right] =$$

$$= \frac{1}{2} \cdot Re\left[Y_c \cdot (V^+ + V^-) \cdot (V^+ - V^-)^* \right] =$$

$$= \frac{1}{2} \cdot Re\left[Y_c \cdot |V^+|^2 \cdot (1 + \Gamma) \cdot (1 - \Gamma)^* \right] =$$

$$= \frac{1}{2} \cdot Y_c \cdot |V^+|^2 \cdot (1 - |\Gamma|^2)$$

In general:

$$Z_{2in} = Z_{3in} = Z_0 \cdot \frac{1}{2} \cdot (1 + K^2) \cdot \frac{\sqrt{K \cdot (1 + K^2)} + j \cdot 2 \cdot K \cdot \tan(\vartheta)}{\sqrt{K \cdot (1 + K^2)} + j \cdot (1 + K^2) \cdot \tan(\vartheta)} \tag{5.40}$$

and for $K = 1$:

$$Z_{2in} = Z_{3in} = Z_0 \tag{5.41}$$

The power distribution as function of the frequency of a Wilkinson power splitter, designed for equal power splitting (K = 1), is shown in figure 5.10 (Calculated with program WILKPOW1). The splitter is terminated with microstrip patches that are matched for their resonance frequency. The powers are normalized to the ingoing power.

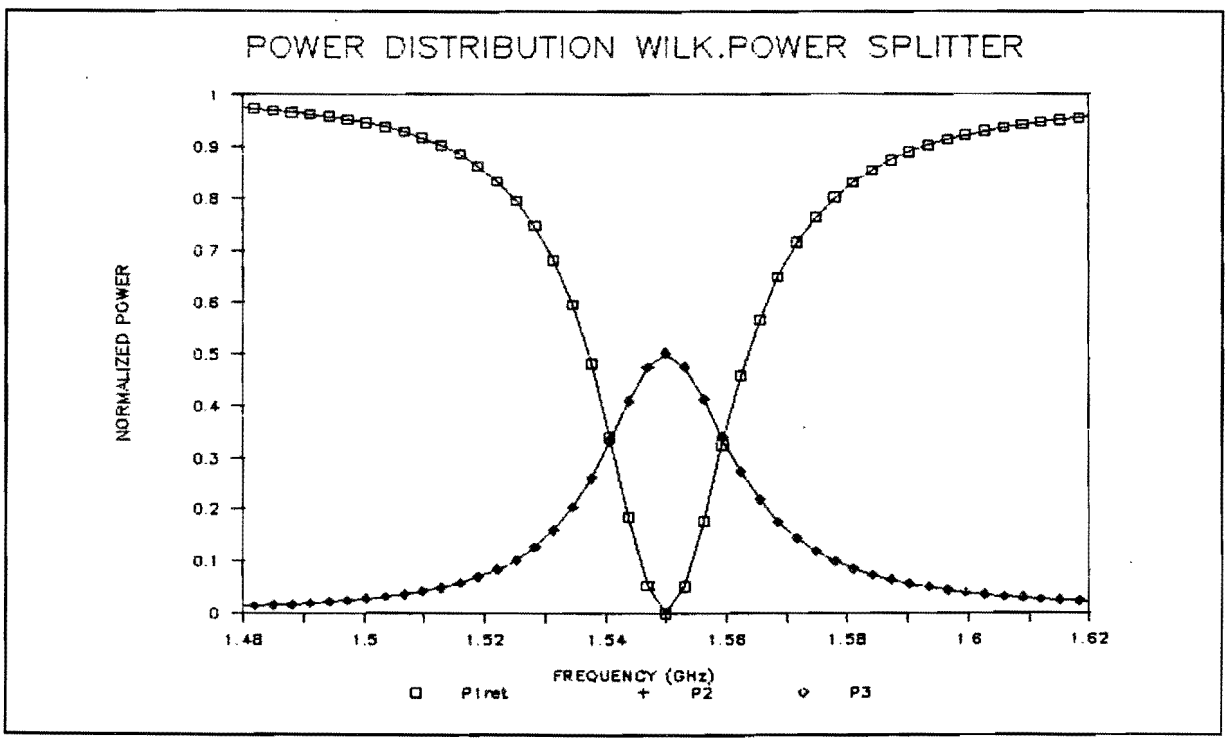

Fig. 5.10 - Power distribution Wilkinson power splitter

f_r = 1.55GHz, ε_r = 10.5, tanδ = 0.0015, h = 2.54mm, ρ_0/a = 0.147

The above figure shows that an equal amount of power is delivered to both output ports. Away from resonance most of the power returns at the input port. No power is dissipated in the isolation resistor. The situation in which one of output ports is provided with a quarter lambda transmission line (to create a 90^0 phaseshift) is shown in figure 5.11 (Calculated with program WILKPOW2).

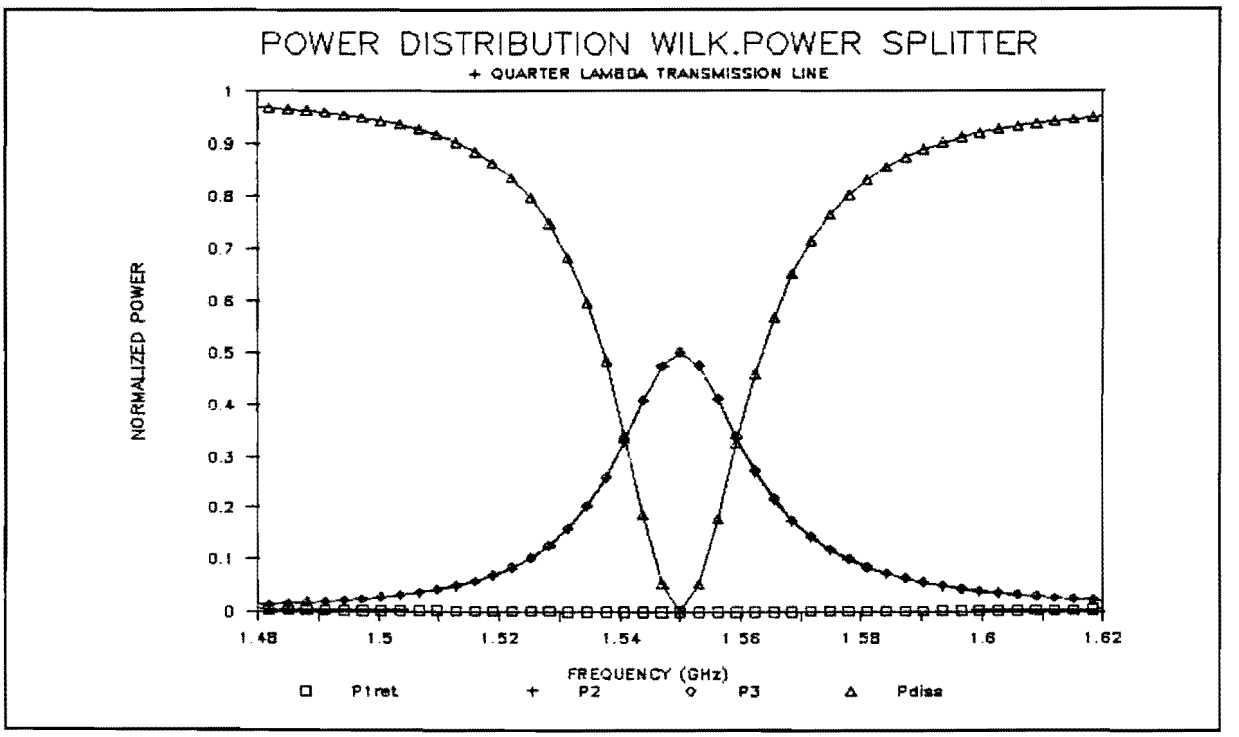

Fig. 5.11 - Power distribution Wilkinson power splitter

f_r = 1.55GHz, ε_r = 10.5, tanδ = 0.0015, h = 2.54mm, ρ_0/a = 0.147

Figure 5.11 shows that a small amount of power returns at the input port. The powers delivered at port 2 and port 3 are the same as in the situation without quarter lambda transmission line. Most of the power that returned at the input port in that situation is now dissipated in the isolation resistor.
To test the isolation between the two output ports, a mismatch at port 3 is created by multiplying the impedance value of the microstrip patch for every frequency with a factor 0.7. Such a mismatch could be caused by a construction error in one of the patches. The power distribution is shown in figure 5.12 (Calculated with program DISTURBW). A quarter lambda transmission line is not applied in this case.

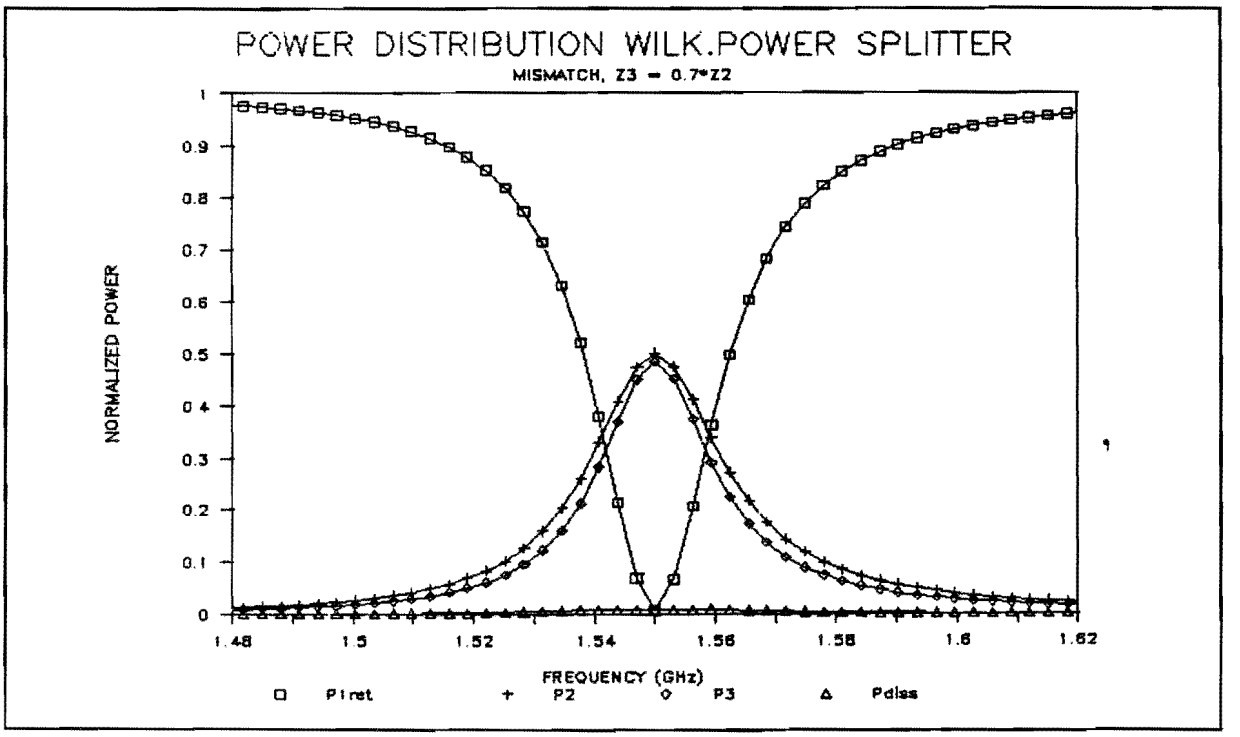

Fig. 5.12 - Power distribution Wilkinson power splitter

f_r = 1.55GHz, ε_r = 10.5, tanδ = 0.0015, h = 2.54mm, ρ_0/a = 0.147

Figure 5.12 shows a good isolation between the two output ports. This will become more obvious when the results are compared with those of a T power splitter that will be discussed in the next paragraph.

§5.3 - T Power Splitter

Figure 5.13 shows a T power splitter designed for splitting the incoming powers into two equal parts

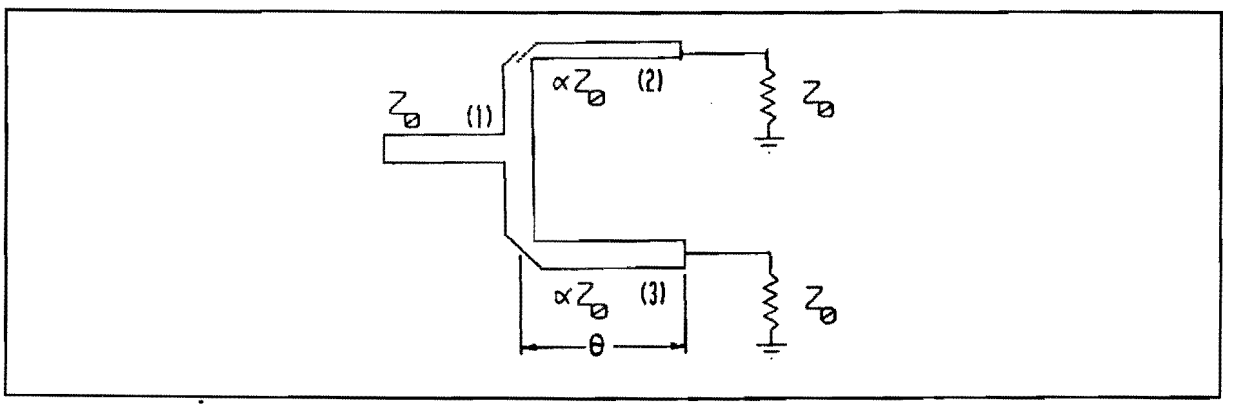

Fig. 5.13 - T power splitter for equal power splitting

The characteristic impedance αZ_0 has to be calculated. The calculation of the splitter characteristics will be carried out along the same ways as in the preceding paragraph.

§5.3.1 - Unnormalized Voltage Scattering Matrix

An equivalent circuit for determining the coefficients T_{11}, T_{21}, T_{12}, T_{31} and T_{13} is given in figure 5.14.

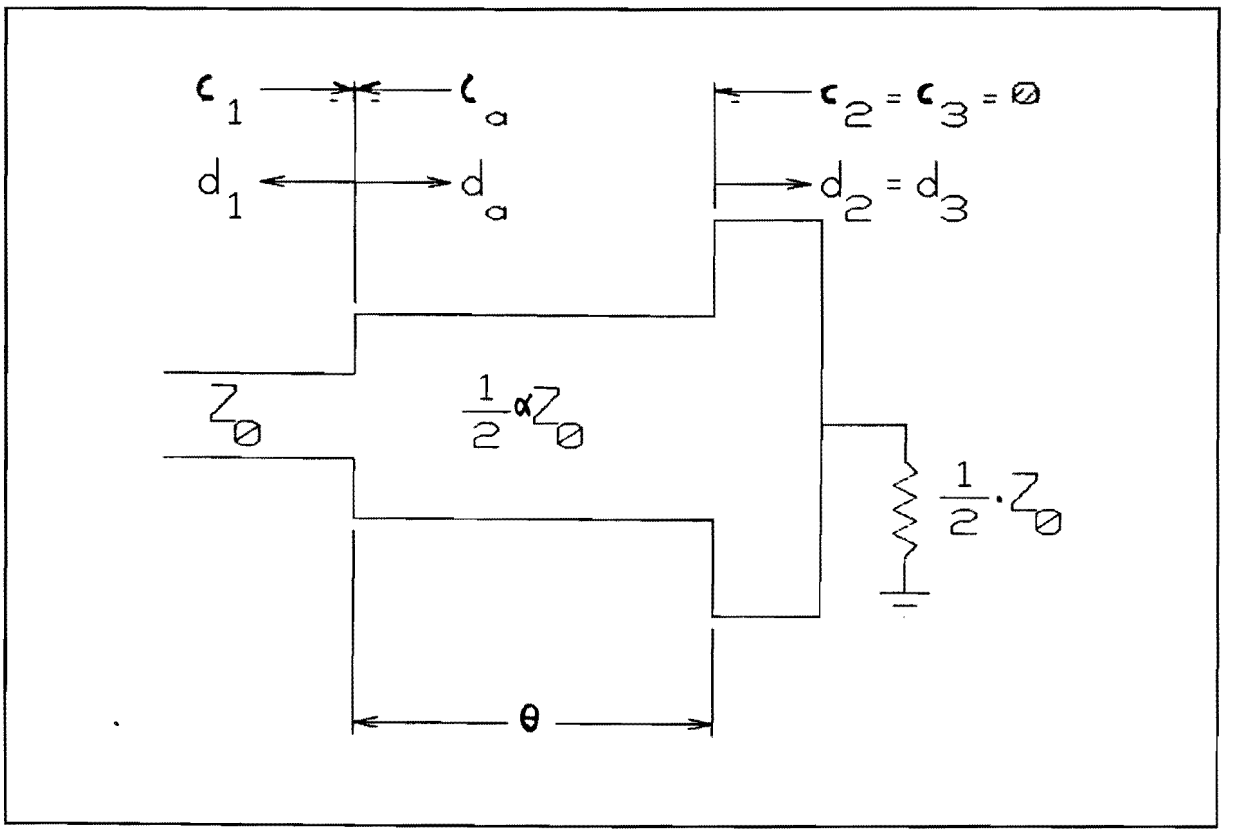

Fig. 5.14 - Equivalent circuit for determining T_{11}, T_{21}, T_{12}, T_{31} and T_{13}

The equations that govern the network are given by:

$$d_1 = \Gamma_1 \cdot c_1 + (1 - \Gamma_1) \cdot c_a \qquad (5.42a)$$

$$d_a = (1 + \Gamma_1) \cdot c_1 - \Gamma_1 \cdot c_a \qquad (5.42b)$$

$$c_a = d_a \cdot e^{-j\vartheta} \cdot \Gamma_2 \cdot e^{-j\vartheta} = \Gamma_2 \cdot e^{-j \cdot 2\vartheta} \cdot d_a \qquad (5.42c)$$

$$d_2 = (1 + \Gamma_2)\cdot e^{-j\vartheta}\cdot d_a \tag{5.42d}$$

with:

$$\Gamma_1 = \frac{1 - \dfrac{Z_0}{\frac{1}{2}\cdot\alpha\cdot Z_0}}{1 + \dfrac{Z_0}{\frac{1}{2}\cdot\alpha\cdot Z_0}} = \frac{\alpha - 2}{\alpha + 2} \tag{5.42e}$$

$$\Gamma_2 = \frac{\dfrac{\frac{1}{2}\cdot Z_0}{\frac{1}{2}\cdot\alpha\cdot Z_0} - 1}{\dfrac{\frac{1}{2}\cdot Z_0}{\frac{1}{2}\cdot\alpha\cdot Z_0} + 1} = \frac{1 - \alpha}{1 + \alpha} \tag{5.42f}$$

With (5.42) can be found:

$$T_{11} = \frac{d_1}{c_1}\bigg|_{c_2 = c_3 = 0} = \Gamma_1 + \frac{\Gamma_2\cdot(1 - \Gamma_1^2)\cdot e^{-j\cdot 2\vartheta}}{1 + \Gamma_1\cdot\Gamma_2\cdot e^{-j\cdot 2\vartheta}} \tag{5.43a}$$

$$T_{21} = T_{12} = T_{31} = T_{13} = \frac{d_2}{c_1}\bigg|_{c_2 = c_3 = 0} =$$

$$= \frac{(1 + \Gamma_1)\cdot(1 + \Gamma_2)\cdot e^{-j\vartheta}}{1 + \Gamma_1\cdot\Gamma_2\cdot e^{-j\cdot 2\vartheta}} \tag{5.43b}$$

The even and odd mode excitations are discussed in appendix F. The results are stated below:

$$E_{2e} = \frac{Z_{2e} \cdot V_{2e}}{Z_0 + Z_{2e}} \tag{5.44a}$$

$$Z_{2e} = \alpha \cdot Z_0 \cdot \frac{2 + j \cdot \alpha \cdot \tan(\vartheta)}{\alpha + j \cdot 2 \cdot \tan(\vartheta)} \tag{5.44b}$$

$$E_{2o} = \frac{V_{2o}}{1 + Y_{2o} \cdot Z_0} \tag{5.45a}$$

$$Y_{2o} = \frac{1}{j \cdot \alpha \cdot Z_0 \cdot \tan(\vartheta)} \tag{5.45b}$$

The input impedances looking into ports 2 and 3 are given by:

$$Z_{2in} = Z_{3in} = \frac{1}{2} \cdot (Z_{2e} + Z_{2o}) = \\ = \alpha \cdot Z_0 \cdot \left[\frac{(1 - \tan^2(\vartheta)) + j \cdot \alpha \cdot \tan(\vartheta)}{\alpha + j \cdot 2 \cdot \tan(\vartheta)} \right] \tag{5.46}$$

To be matched for the resonance frequency it follows that:

$$\vartheta = \pi \cdot \frac{f}{f_r} \tag{5.47}$$

The rest of the coefficients will be calculated when a choise has been made for α.

§5.3.2 - T Splitter Power Distribution

A general power splitter is given in figure 5.9. When there is no isolation resistor, as is the case for the T power splitter, the power distribution is given by:

$$P_{in} = \frac{|c_1|^2}{2 \cdot Z_0} \tag{5.48a}$$

$$P1_{ret} = \frac{|d_1|^2}{2 \cdot Z_0} \tag{5.48b}$$

$$P2 = \frac{|d_2|^2}{2 \cdot \mathrm{Re}\{Z_{2in}\}} \cdot \left(1 - |\rho_2|^2 \right) \tag{5.48c}$$

$$P3 = \frac{|d_3|^2}{2 \cdot \mathrm{Re}\{Z_{3in}\}} \cdot \left(1 - |\rho_3|^2 \right) \tag{5.48d}$$

with ρ_2 and ρ_3 according to (5.35d). d_1, d_2 and d_3 can be written as functions of c_1 with (5.36a,b,c).
In the above formulas $\mathrm{Re}\{Z_{kin}\}$, k = 2, 3 is used instead of Z_{kin}, that was used in the case of the Wilkinson power splitter. This is because of the fact that there is no α for which the impedance is real (see (5.46)).
For the resonance frequency the input impedances Z_{2in} and Z_{3in} are real and equal to Z_0. It is desirable to keep the real parts of the input impedances constant while ϑ varies, to achieve a maximum power dissipation in the patches (see (5.48c,d)):

$$\frac{\delta}{\delta \vartheta} \mathrm{Re}\{Z_{2in}\} = \frac{\delta}{\delta \vartheta} \left\{ \alpha^2 \cdot Z_0 \cdot \left[\frac{1 + \tan^2(\vartheta)}{\alpha^2 + 4 \cdot \tan^2(\vartheta)} \right] \right\} = 0 \tag{5.49a}$$

$$\Leftrightarrow 2 \cdot \alpha^2 \cdot Z_0 \cdot \frac{\tan(\vartheta)}{\cos^2(\vartheta)} \cdot \frac{\alpha^2 - 4}{\left[\alpha^2 + 4 \cdot \tan^2(\vartheta) \right]^2} = 0 \tag{5.49b}$$

Solving the last equation gives $\alpha = 2$. With this value of α, the remaining T-coefficients are calculated. T_{22}, T_{33}, T_{23} and T_{32} follow from (see appendix F):

$$T_{22} = T_{33} = \frac{Z_{2e}}{Z_0 + Z_{2e}} + \frac{1}{1 + Y_{2o} \cdot Z_0} - 1 =$$

$$= \frac{-1 + j \cdot 4 \cdot \tan(\vartheta)}{3 \cdot (1 + j \cdot 2 \cdot \tan(\vartheta))} \qquad (5.50a)$$

$$T_{23} = T_{32} = \frac{Z_{2e}}{Z_0 + Z_{2e}} - \frac{1}{1 + Y_{2o} \cdot Z_0} =$$

$$= \frac{2 \cdot (1 - j \cdot \tan(\vartheta))}{3 \cdot (1 + j \cdot 2 \cdot \tan(\vartheta))} \qquad (5.50b)$$

Equations (5.43a) and (5.43b) become, with $\alpha = 2$:

$$T_{11} = -\frac{1}{3} \cdot e^{-j \cdot 2\vartheta} \qquad (5.50c)$$

$$T_{21} = T_{12} = T_{31} = T_{13} = \frac{2}{3} \cdot e^{-j \cdot \vartheta} \qquad (5.50d)$$

The power distribution of the T power splitter is calculated for 3 situations. First the power distribution is calculated (program TEEPOW1) of a splitter terminated with microstrip patches that are matched for the resonance frequency. Then the power distribution is calculated (program TEEPOW2) of a splitter, terminated with microstrip patches, in which one of the output ports is provided with a quarter lambda transmission line. After that the power distribution is calculated (program DISTURBT) of a splitter, terminated with microstrip patches, with a mismatch introduced at one of the ports to test the isolation between the output ports. The results are shown in the figures 5.15, 5.16 and 5.17.

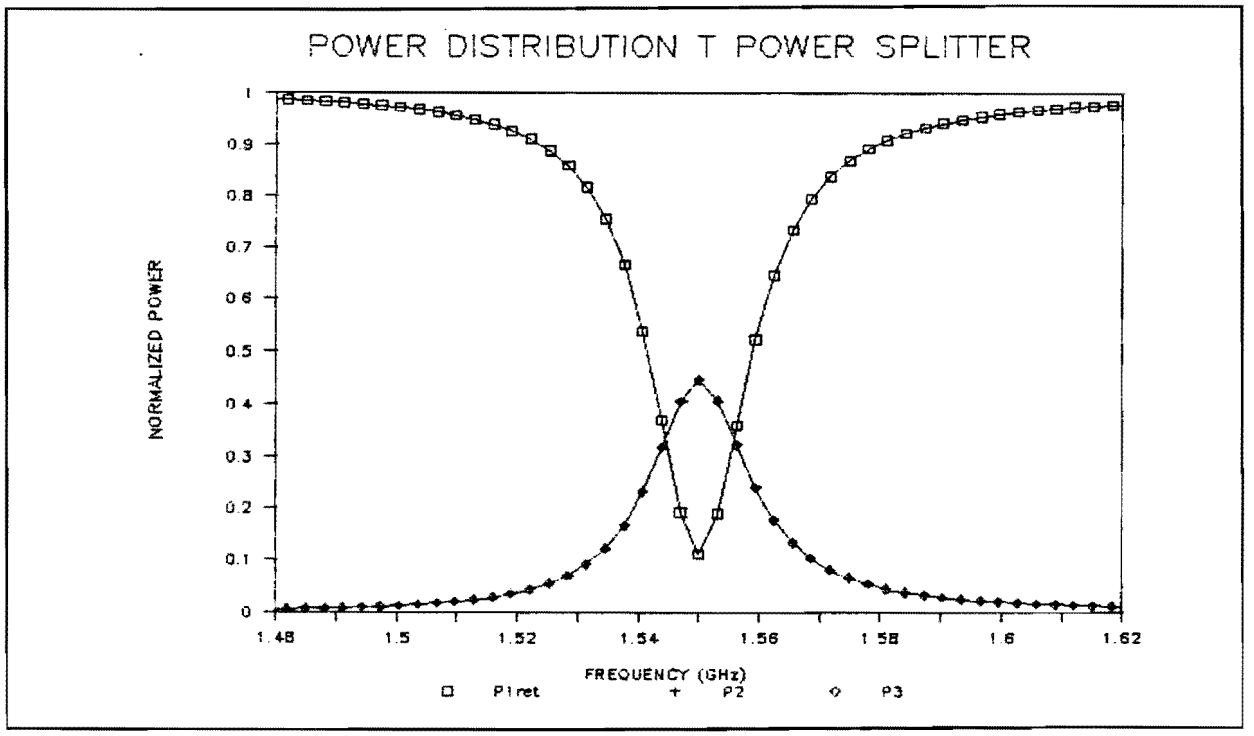

Fig 5.15 - Power distribution T power splitter

f_r = 1.55GHz, ε_r = 10.5, tanδ = 0.0015, h = 2.54mm, ρ_0/a = 0.147

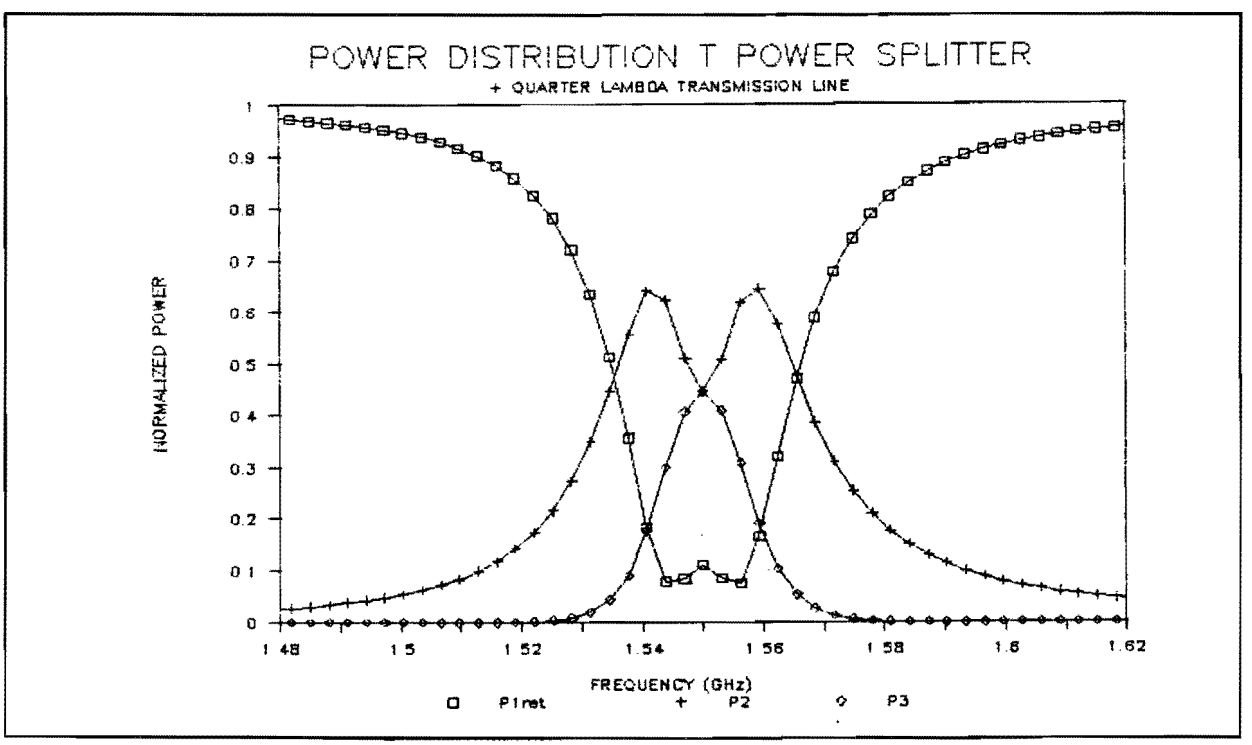

Fig 5.16 - Power distribution T power splitter

f_r = 1.55GHz, ε_r = 10.5, tanδ = 0.0015, h = 2.54mm, ρ_0/a = 0.147

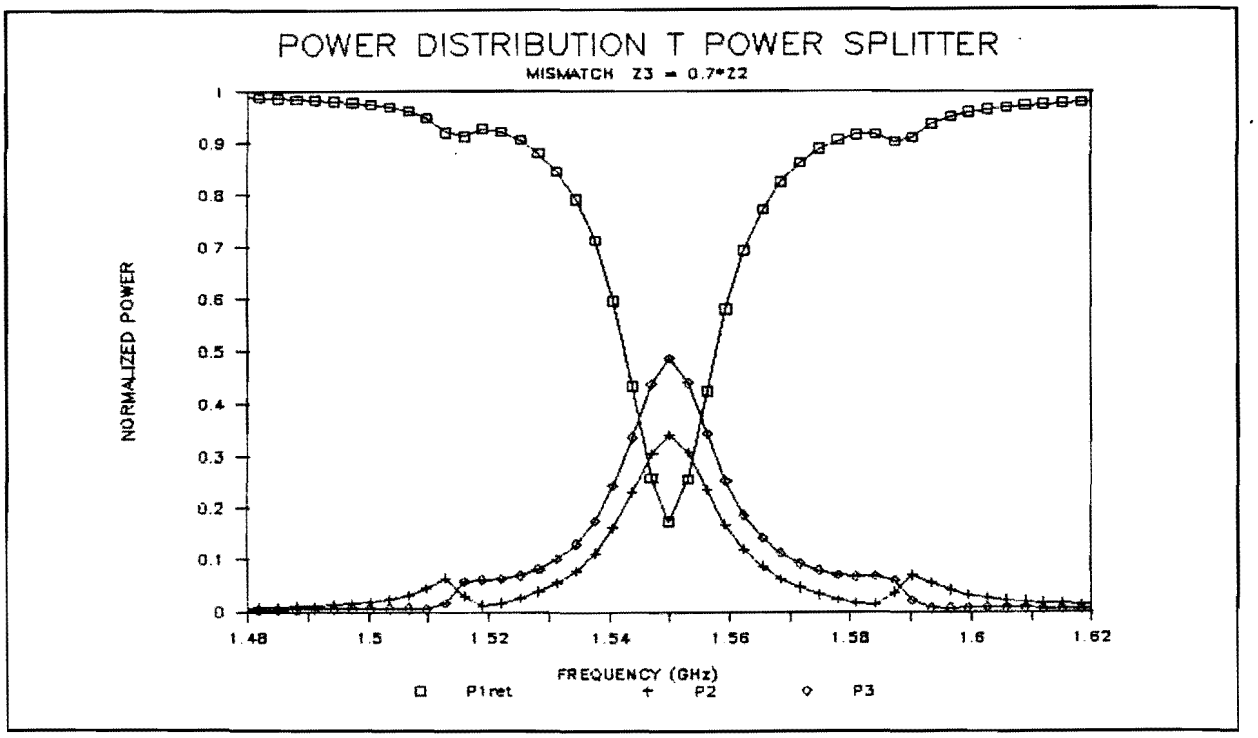

Fig 5.17 - Power distribution T power splitter

f_r = 1.55GHz, ε_r = 10.5, tanδ = 0.0015, h = 2.54mm, ρ_0/a = 0.147

The above figures reveal that the Wilkinson power splitter will do better than the T power splitter.
In the feeding network the Wilkinson power splitters will be cascaded. Because of the splitters that are provided with a quarter lambda transmission line, there will be only a small amount of power that returns at the input of the feeding network. This does not mean that the array antenna bandwidth has increased. Use of Wilkinson power splitters will make it easier to match transmitter or receiver and antenna.

§5.4 - Hybrid Branch Line Coupler

Figure 5.18 shows a hybrid branch line coupler [5-15] that can be used as a power splitter. For that purpose one of the outputs is terminated with a matched impedance. This power splitter is not analyzed, but since it is a three-port including a resistor, the performance is expected to be comparable with that of a Wilkinson power splitter.

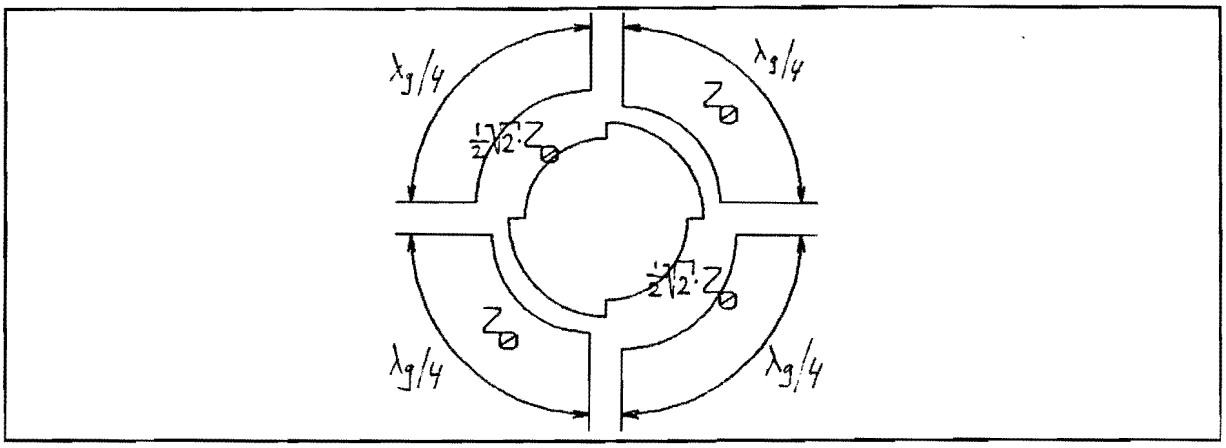

Fig. 5.18 - Hybrid branch line coupler

§5.5 - References

[5-1] Bahl I.J., Bhartia P., ' *Microstrip Antennas* ', Artech House Inc., 1980, pp.85-96.

[5-2] Richards W.F., Zinecker J.R., Clark R.D., ' *Experimental and Theoretical Investigation of the Inductance Associated with a Microstrip Antenna Feed* ', Electromagnetics, Vol.5, 1983, pp.327-346.

[5-3] Vrinten M.L.A., ' *A Wideband Circularly Polarized Microstrip Antenna Array* ', Graduation Report, Professional Group Electromagnetics & Circuit Theory, Department of Electrical Engineering, Eindhoven University of Technology, Netherlands, Report ET-6-88.

[5-4] Derneryd A.G., ' *Analysis of the Microstrip Disk Antenna Element* ', IEEE Trans. Ant. & Propagat., Vol.AP-27, No.5, Sept. 1979, pp.660-664.

[5-5] Press W.H., Flannery B.P., Teukolsky S.A., Vetterling W.T., ' *Numerical Recipes, the Art of Scientific Computing* ', Cambridge University Press, 1986.

[5-6] Engels H., ' *Numerical Quadrature and Cubature* ',
Academic Press, 1980.

[5-7] Abramowitz M., Stegun I.A., ' *Handbook of Mathematical Functions* ',
Dover Publications, 1968.

[5-8] Johnk C.T.A., ' *Engineering Electromagnetic Fields & Waves* ',
John Wiley & Sons Inc., 1975.

[5-9] Toom E.C. den, *Title unknown at the moment of publication*,
Graduation Report, Professional Group Electromagnetism & Circuit Theory, Department of Electrical Engineering, Eindhoven University of Technology, Netherlands.
To be published.

[5-10] Suzuki Y., iyano N., Chiba T., ' *Expanding the Frequency Bandwidth of a Microstrip Antenna* ',
IEEE Ant. & Propagat., Soc. Int. Symp. Dig., May 1982,
pp.366-369.

[5-11] INMARSAT, ' *Request for Proposals Number 085, Aircraft Earth Stations* ',
9 May 1986.

[5-12] Parad L.I., Moynihan R.L., ' *Split-Tee Power Divider* ',
IEEE Transactions on Microwave Theory and Techniques, January 1965, pp.91-95.

[5-13] Collin R.E., ' *Field Theory of Guided Waves* ',
McGraw-Hill Book Company, Inc., 1960, p.91.

[5-14] Collin R.E., ' *oundations of Microwave Engineering* ',
McGraw-Hill Book Company, Inc., 1966, p.91.

[5-15] Zinke O., Brunswig H., ' *Lehrbuch der Hochfrequenz-technik* ',
Springer-Verlag, 1986, p.180 (in German).

6. Keeping Track of the Satellite

Since the antennas discussed in the preceding chapters are meant for use on a vehicle, they have to be provided with a device that points the main antenna beam at the satellite while the vehicle moves. This means that the tuneable phaseshifters in the array antenna have to be tuned depending on the mutual position of vehicle and satellite.
The tuning information can be obtained from the signal received by the antenna with a technique called simultaneous lobe comparison (also called monopulse).
In the following a general discussion of this technique will be given, after which the technique will be applied to a subarraylevel-scanned array of circularly polarized patches and to a subarraylevel-scanned array of sequentially rotated linearly polarized patches.

§6.1 - Simultaneous Lobe Comparison Technique

To generate a tuning signal for pointing the antenna beam at the satelite, the antenna beam is successively and repeatedly pointed in the vicinity of the target (the satellite). Comparative measurements of the antennasignals indicate in which direction and how much the beam has to be readjusted. The principle is shown in figure 6.1 for pointing the antenna beam in elevation [6-1].

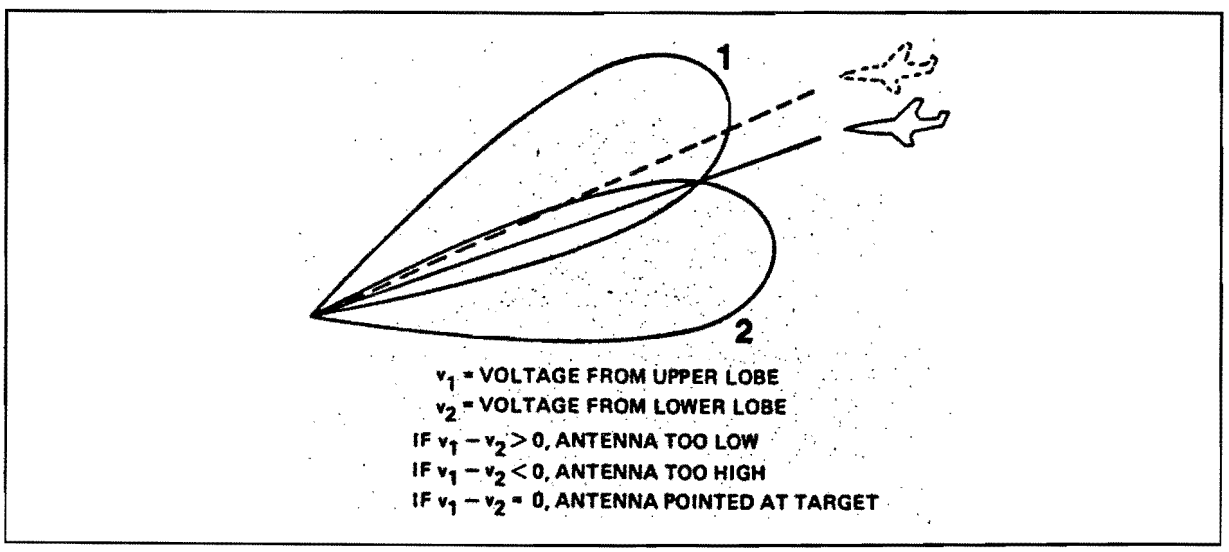

Fig. 6.1 - Aiming the antenna beam in elevation

For pointing the antenna beam in traverse, the same principle is used. Figure 6.2 shows the geometrical relations among the angles azimuth, elevation and traverse [6-1]. The line labeled "beam axis" refers to a mechanically steered antenna. A more general designation would be "normal to the antena aperture". Thus in the case of an electronically steered array that line represents the boresight direction.

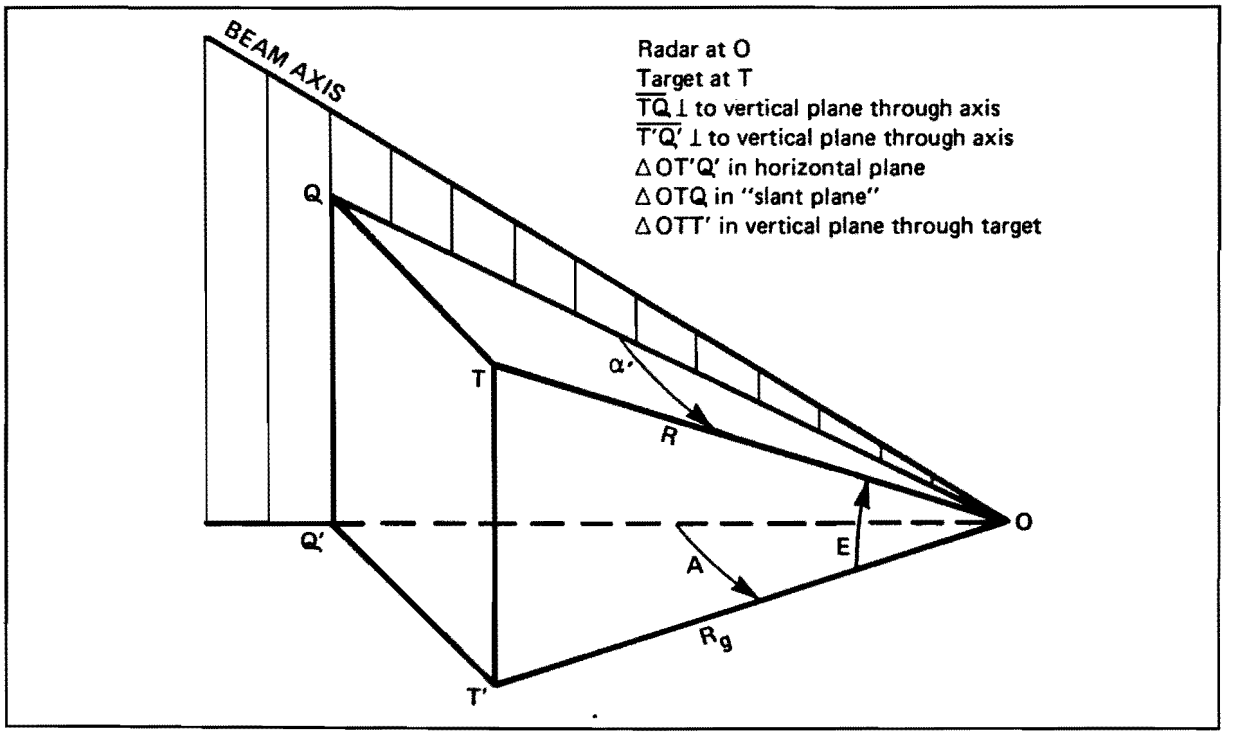

Fig. 6.2 - Geometric relations among angles: azimuth (A), elevation (E) and traverse (α')

Because of the sequential pointing of the antenna main lobe in the vicinity of the target, this technique is called sequential lobing. For keeping track of the satellite both in elevation and traverse, a sequence of 4 beam positions is necessary.
Instead of sequential pointing the antenna beam in the vicinity of the target, also use can be made of an antenna that produces 4 beams at the same time. This is depicted in figure 6.3 [6-1].
The technique in which such an antenna is used is called simultaneous lobing, simultaneous lobe comparison or monopulse.
The last term, originating from the RADAR technique (as all the tracking techniques discussed in this chapter do), arises from the fact that in contrast with sequential lobing the comparing operations

can be performed on the basis of one received (reflected) pulse.

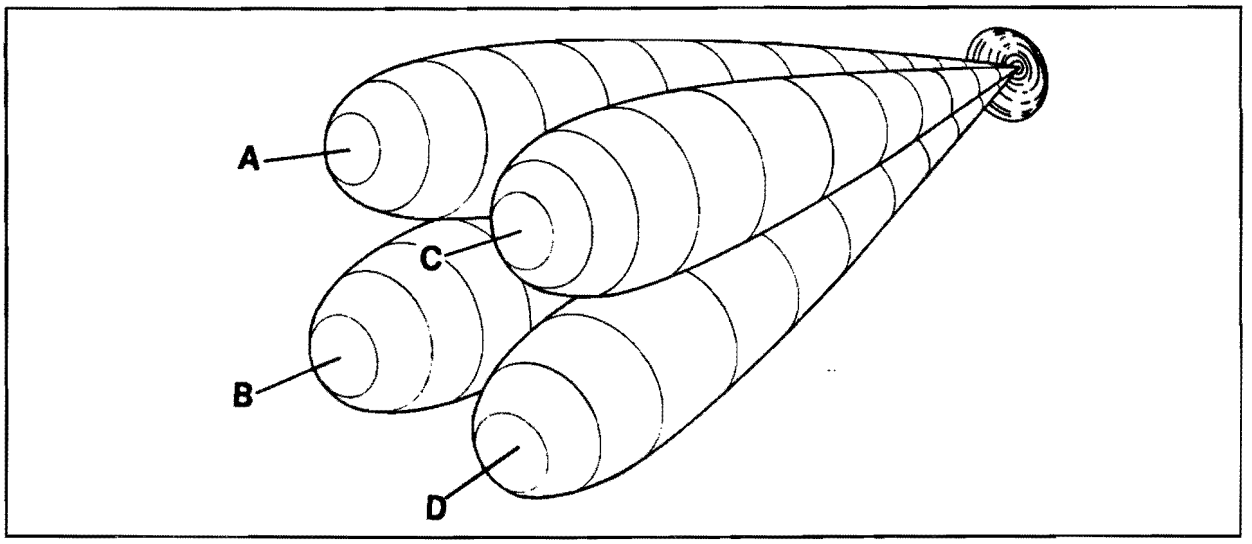

Fig. 6.3 - Four beam antenna for simultaneous lobe comparison

Figure 6.4 shows the beams in a plane perpendicular on the antenna scan direction.

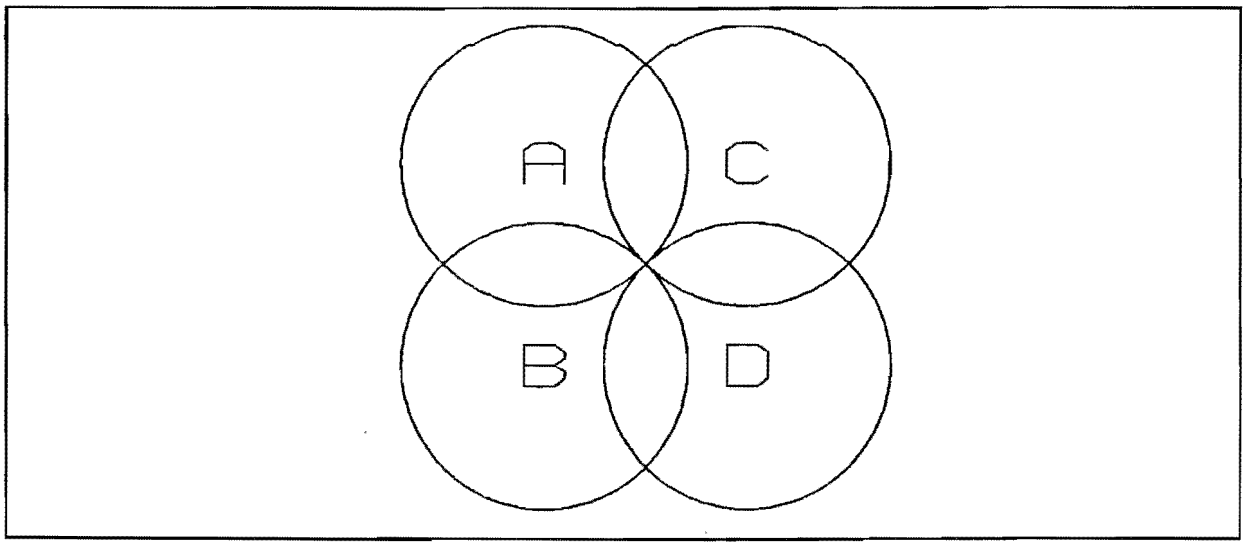

Fig. 6.4 - Antenna beams

With A, B, C and D the received antenna voltages, a traverse- and elevation-difference can be created that can be used to point the antenna at the satellite [6-1]:

$$\text{Sum} : \quad s = \frac{1}{2} \cdot (A + B + C + D) \tag{6.1a}$$

$$\text{Traverse difference} : \quad d_{tr} = \frac{1}{2} \cdot \left[(C + D) - (A + B) \right] \tag{6.1b}$$

$$\text{Elevation difference} : \quad d_{el} = \frac{1}{2} \cdot \left[(A + C) - (B + D) \right] \tag{6.1c}$$

A network to create sum- and difference-signals is depicted in figure 6.5.

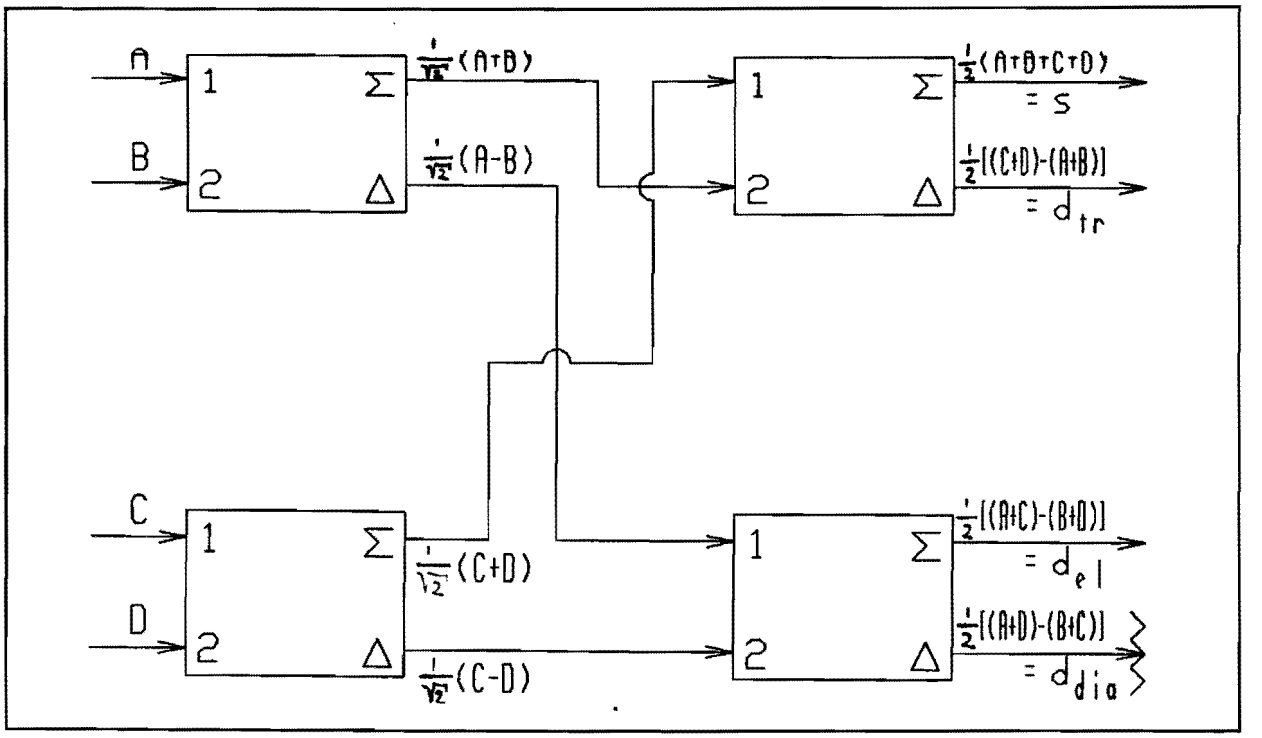

Fig. 6.5 - Sum and difference network

The factors $\frac{1}{2}$ follow from the law of conservation of energy:

$$A^2 + B^2 + C^2 + D^2 = s^2 + d_{tr}^2 + d_{el}^2 + d_{dia}^2 \tag{6.2}$$

The signal d_{dia} is the voltage difference between two diagonally pairs of beams. Since the information given by d_{dia} is redundant, its power may be dissipated in a matched impedance [6-2] (see figure 6.5).

Sum- and difference-signals are shown in figure 6.6 for one of the two angle coordinates (traverse, elevation) [6-1].

For traverse is $v_1 = (C + D)/\sqrt{2}$ and $v_2 = (A + B)/\sqrt{2}$. For elevation is $v_1 = (A + C)/\sqrt{2}$ and $v_2 = (B + D)/\sqrt{2}$.

$s = (v_1 + v_2)/\sqrt{2}$ and $d = (v_1 - v_2)/\sqrt{2}$.

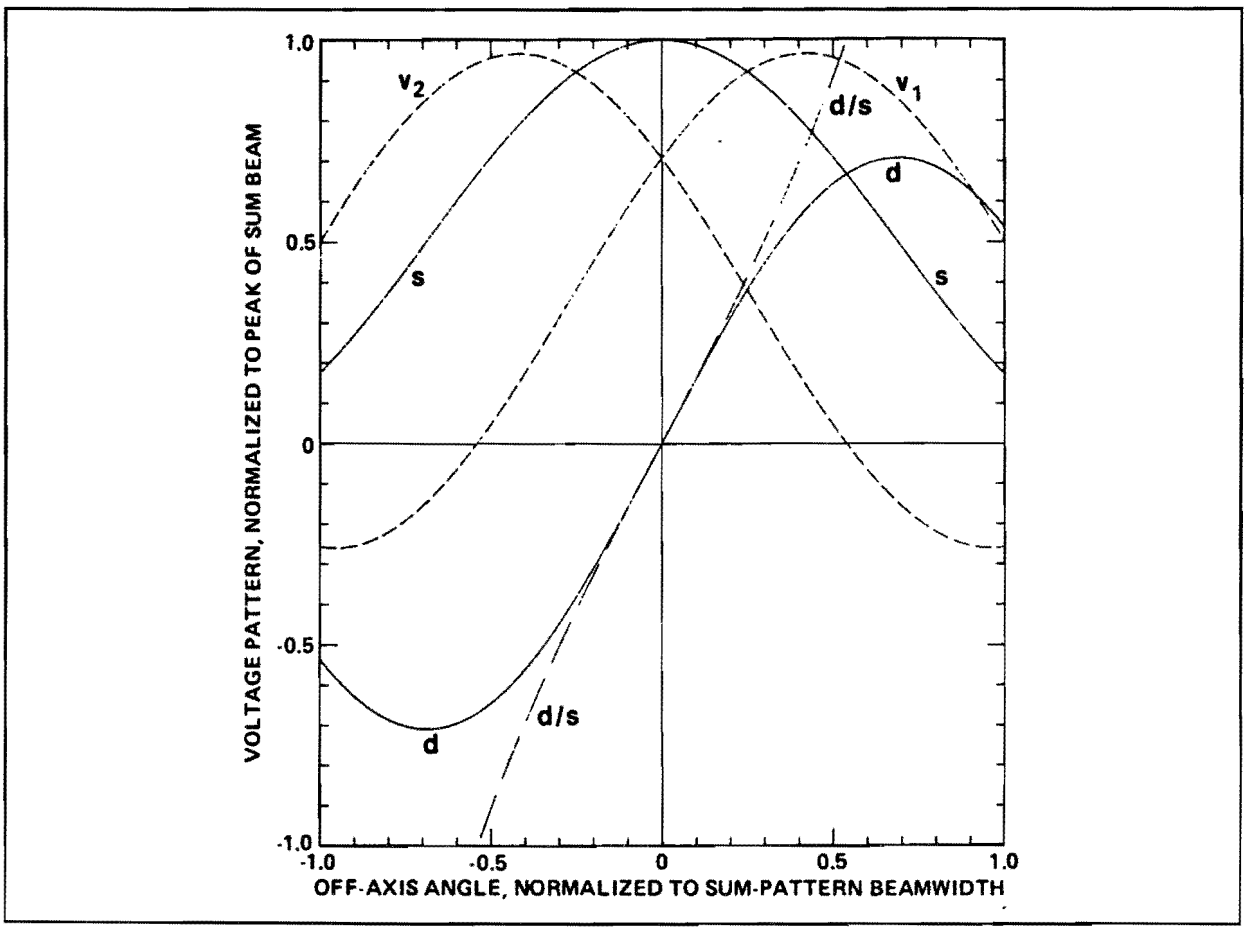

Fig. 6.6 - Sum- and difference-signals

The signal d/s is proportional to the angle deviation and can be used to point the antenna at the satellite. When d/s = 0, the beam axis of the antenna is pointed at the satellite.

Figure 6.7 depicts a tracking system with mechanically steered antenna for RADAR purposes [6-1]. For an electronically steered antenna, the section "antenna drive servos" has to be replaced by a section "phaseshifter drivers".

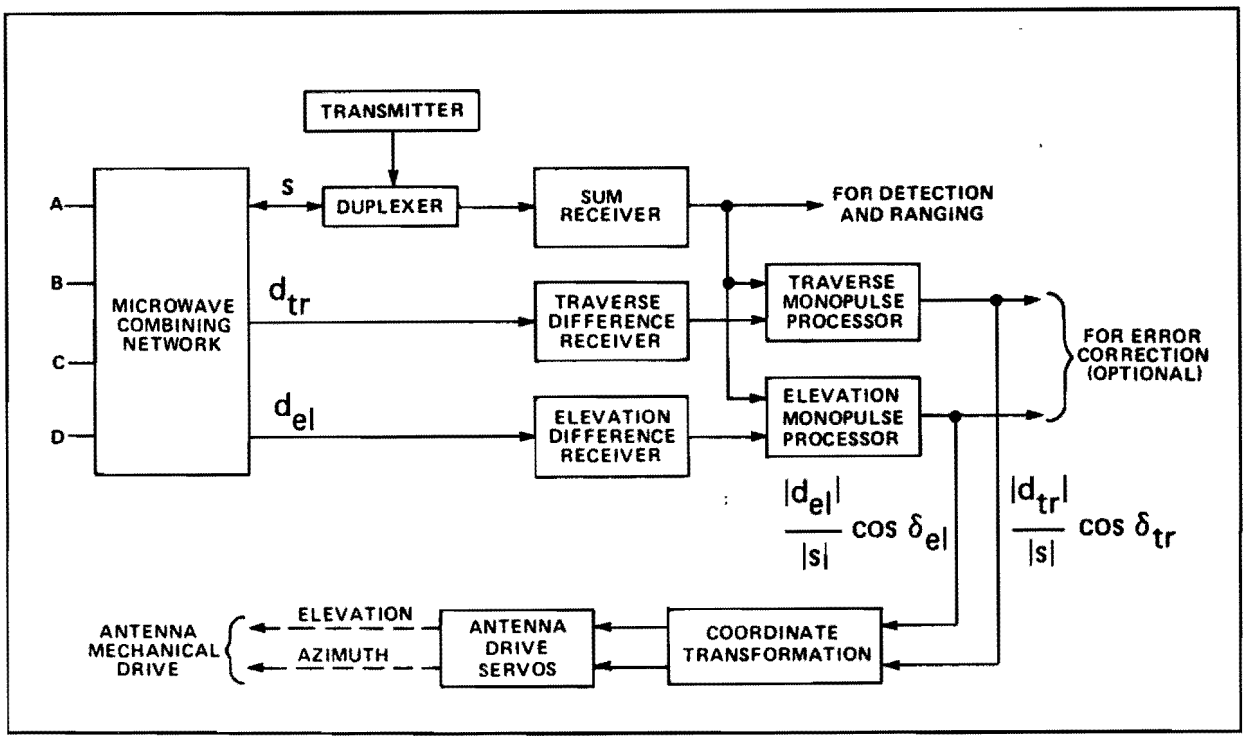

Fig. 6.7 - Antenna tracking system

§6.2 - Simultaneous Lobe Comparing with a Subarraylevel-scanned Array

A simple way to apply the simultaneous lobe comparison technique to an array is to split up the array in four equal symetric parts and summarize the element outputs in a quadrant to create four signals that can be combined to sum- and difference-signals [6-1]. Although only one antenna beam exists, the phased array can be treated mathematically as if it generates four separate beams. The most easily this technique can be applied to 4x4-arrays designed for scanning on subarray-level. In these arrays the four equal symetric parts with the element outputs summarized already exist because each quadrant (2x2-subarray) is connected with one tuneable phaseshifter.

§6.2.1 - A 4x4-subarraylevel-scanned Array of Circularly Polarized Patches

The 4x4-array, composed of 2x2-subarrays is depicted in figure 6.8.

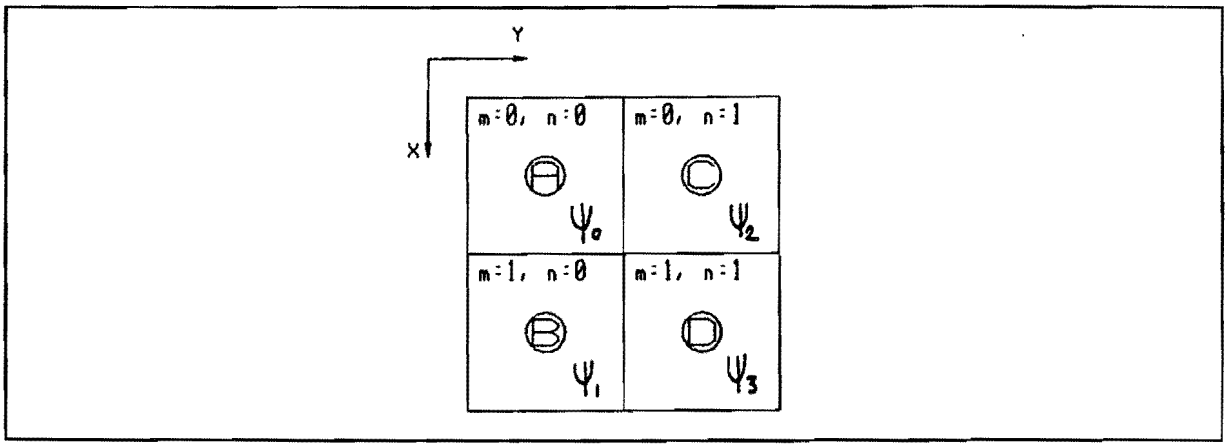

Fig. 6.8 - 4x4-array composed of 2x2-subarrays

The subarray field components are given in chapter 4 (formulas (4.19a) and (4.19b)):

$$E_{\vartheta_{sub}}(\vartheta,\varphi) = -e^{j\varphi}\cdot F_1(\vartheta)\cdot \sum_{p=0}^{1}\sum_{q=0}^{1} e^{j\frac{2\pi}{\lambda}\cdot(pd_xT_x + qd_yT_y)} \qquad (6.3a)$$

$$E_{\varphi_{sub}}(\vartheta,\varphi) = -j\cdot e^{j\varphi}\cdot\cos(\vartheta)\cdot F_2(\vartheta)\cdot \sum_{p=0}^{1}\sum_{q=0}^{1} e^{j\frac{2\pi}{\lambda}\cdot(pd_xT_x + qd_yT_y)} \qquad (6.3b)$$

With use of (4.21) the subarray field components with phaseshifts are found to be:

$$E_{\vartheta_i}(\vartheta,\varphi) = E_{\vartheta_{sub}}(\vartheta,\varphi)\cdot e^{j\psi_i}, \quad i = 0, 1, 2, 3 \qquad (6.4a)$$

$$E_{\varphi_i}(\vartheta,\varphi) = E_{\varphi_{sub}}(\vartheta,\varphi)\cdot e^{j\psi_i}, \quad i = 0, 1, 2, 3 \qquad (6.4b)$$

with:

$$\psi_0 = 0 \tag{6.4c}$$

$$\psi_1 = \frac{4\pi}{\lambda} \cdot d_x \cdot (T_x - T_{xs}) \tag{6.4d}$$

$$\psi_2 = \frac{4\pi}{\lambda} \cdot d_y \cdot (T_y - T_{ys}) \tag{6.4e}$$

$$\psi_3 = \psi_1 + \psi_2 \tag{6.4f}$$

It are the phaseshifts stated in (6.4c) to (6.4f) that deliver the signals with which the antenna beam can be pointed at the satellite as will be shown in the following.
With (6.4) sum- and difference-signals can be created:

$$\begin{aligned}\bar{\Sigma} &= \left[E_{\vartheta_{sub}}(\vartheta,\varphi)\cdot\bar{a}_\vartheta + E_{\varphi_{sub}}(\vartheta,\varphi)\cdot\bar{a}_\varphi\right]\cdot\left[e^{j\psi_0} + e^{j\psi_1} + e^{j\psi_2} + e^{j\psi_3}\right] = \\ &= \left[E_{\vartheta_{sub}}(\vartheta,\varphi)\cdot\bar{a}_\vartheta + E_{\varphi_{sub}}(\vartheta,\varphi)\cdot\bar{a}_\varphi\right]\cdot\left[1 + e^{j\psi_1}\right]\cdot\left[1 + e^{j\psi_2}\right] = \\ &= \left[E_{\vartheta_{sub}}(\vartheta,\varphi)\cdot\bar{a}_\vartheta + E_{\varphi_{sub}}(\vartheta,\varphi)\cdot\bar{a}_\varphi\right]\cdot e^{j\frac{\psi_1+\psi_2}{2}}\cdot 4\cdot\cos\left(\frac{\psi_1}{2}\right)\cdot\cos\left(\frac{\psi_2}{2}\right)\end{aligned} \tag{6.5a}$$

$$\begin{aligned}\bar{\Delta}_1 &= -\left[E_{\vartheta_{sub}}(\vartheta,\varphi)\cdot\bar{a}_\vartheta + E_{\varphi_{sub}}(\vartheta,\varphi)\cdot\bar{a}_\varphi\right]\cdot\left[e^{j\psi_0} + e^{j\psi_1} - e^{j\psi_2} - e^{j\psi_3}\right] = \\ &= -\left[E_{\vartheta_{sub}}(\vartheta,\varphi)\cdot\bar{a}_\vartheta + E_{\varphi_{sub}}(\vartheta,\varphi)\cdot\bar{a}_\varphi\right]\cdot\left[1 + e^{j\psi_1}\right]\cdot\left[1 - e^{j\psi_2}\right] = \\ &= j\cdot\left[E_{\vartheta_{sub}}(\vartheta,\varphi)\cdot\bar{a}_\vartheta + E_{\varphi_{sub}}(\vartheta,\varphi)\cdot\bar{a}_\varphi\right]e^{j\frac{\psi_1+\psi_2}{2}}\cdot 4\cdot\cos\left(\frac{\psi_1}{2}\right)\sin\left(\frac{\psi_2}{2}\right)\end{aligned} \tag{6.5b}$$

$$\bar{\Delta}_2 = \left[E_{\vartheta_{sub}}(\vartheta,\varphi)\cdot\bar{a}_\vartheta + E_{\varphi_{sub}}(\vartheta,\varphi)\cdot\bar{a}_\varphi\right]\cdot\left[e^{j\psi_0} + e^{j\psi_2} - e^{j\psi_1} - e^{j\psi_3}\right] =$$

$$= \left[E_{\vartheta_{sub}}(\vartheta,\varphi)\cdot\bar{a}_\vartheta + E_{\varphi_{sub}}(\vartheta,\varphi)\cdot\bar{a}_\varphi\right]\cdot\left[1 - e^{j\psi_1}\right]\cdot\left[1 + e^{j\psi_2}\right] =$$

$$= -j\cdot\left[E_{\vartheta_{sub}}(\vartheta,\varphi)\cdot\bar{a}_\vartheta + E_{\varphi_{sub}}(\vartheta,\varphi)\cdot\bar{a}_\varphi\right]e^{j\frac{\psi_1+\psi_2}{2}}\cdot 4\sin(\frac{\psi_1}{2})\cos(\frac{\psi_2}{2}) \qquad (6.5c)$$

With the above formulas:

$$s \quad \cos(\frac{\psi_1}{2})\cdot\cos(\frac{\psi_2}{2}) \qquad (6.6a)$$

$$d_{tr} \quad j\cdot\cos(\frac{\psi_1}{2})\sin(\frac{\psi_2}{2}) \qquad (6.6b)$$

$$d_{el} \quad -j\cdot\sin(\frac{\psi_1}{2})\cos(\frac{\psi_2}{2}) \qquad (6.6c)$$

When after the subtractions 90^0-phaseshifts are introduced, the normalized difference-voltages become:

$$\frac{d_{tr}}{s} = -\tan(\frac{\psi_2}{2}) = -\tan\left[\frac{2\pi}{\lambda}\cdot d_y\cdot(\sin\vartheta\sin\varphi - \sin\vartheta_s\sin\varphi_s)\right] \qquad (6.7a)$$

$$\frac{d_{el}}{s} = \tan(\frac{\psi_1}{2}) = \tan\left[\frac{2\pi}{\lambda}\cdot d_x\cdot(\sin\vartheta\cos\varphi - \sin\vartheta_s\cos\varphi_s)\right] \qquad (6.7b)$$

with ϑ_s and φ_s indicating the scan direction and ϑ and φ indicating the satellite direction. Since ϑ_s and φ_s are known, the satellite

direction can be found with (6.7a,b). Therefore these formulas are rewritten:

$$\sin(\vartheta)\cdot\sin(\varphi) = \sin(\vartheta_s)\cdot\sin(\varphi_s) - \frac{\lambda}{2\pi d_y}\cdot\arctan\left(\frac{d_{tr}}{s}\right) \qquad (6.8a)$$

$$\sin(\vartheta)\cdot\cos(\varphi) = \sin(\vartheta_s)\cdot\cos(\varphi_s) + \frac{\lambda}{2\pi d_x}\cdot\arctan\left(\frac{d_{el}}{s}\right) \qquad (6.8b)$$

Dividing the above equations gives:

$$\tan(\varphi) = \frac{\sin(\vartheta_s)\cdot\sin(\varphi_s) - \frac{\lambda}{2\pi d_y}\cdot\arctan\left(\frac{d_{tr}}{s}\right)}{\sin(\vartheta_s)\cdot\cos(\varphi_s) + \frac{\lambda}{2\pi d_x}\cdot\arctan\left(\frac{d_{el}}{s}\right)} \qquad (6.9)$$

and finaly the sattelite direction is found to be given by:

$$\varphi = \arctan\left[\frac{\sin(\vartheta_s)\cdot\sin(\varphi_s) - \frac{\lambda}{2\pi d_y}\cdot\arctan\left(\frac{d_{tr}}{s}\right)}{\sin(\vartheta_s)\cdot\cos(\varphi_s) + \frac{\lambda}{2\pi d_x}\cdot\arctan\left(\frac{d_{el}}{s}\right)}\right] \qquad (6.10a)$$

$$\vartheta = \arcsin\left[\frac{1}{\sin(\varphi)}\cdot\left\{\sin(\vartheta_s)\cdot\sin(\varphi_s) - \frac{\lambda}{2\pi d_y}\cdot\arctan\left(\frac{d_{tr}}{s}\right)\right\}\right] \qquad (6.10b)$$

To point the antenna beam at the satellite, the scanangles φ_s and ϑ_s should become equal to the satellite direction angles φ and ϑ.
If the scanangles and measured difference-signals are denoted by an index n, the new scanangles, denoted by the index n+1, are found with (6.10a,b):

$$\varphi_{s_{n+1}} = \arctan\left[\frac{\sin(\vartheta_{s_n})\cdot\sin(\varphi_{s_n}) - \frac{\lambda}{2\pi d_{y_n}}\cdot\arctan\left\{\left(\frac{d_{tr}}{s}\right)_n\right\}}{\sin(\vartheta_{s_n})\cdot\cos(\varphi_{s_n}) + \frac{\lambda}{2\pi d_x}\cdot\arctan\left\{\left(\frac{d_{el}}{s}\right)_n\right\}} \right] \tag{6.11a}$$

$$\vartheta_{s_{n+1}} = \arcsin\left[\frac{1}{\sin(\varphi_{s_{n+1}})}\cdot\left\{\sin(\vartheta_{s_n})\sin(\varphi_{s_n}) - \frac{\lambda}{2\pi d_{y_n}}\cdot\arctan\left\{\left(\frac{d_{tr}}{s}\right)_n\right\}\right\} \right] \tag{6.11b}$$

As mentioned before, the antenna beam has to be directed in the vicinity of the satellite for applying te above discussed tracking technique. So when the tracking operation starts, there has to be some knowledge of the satellite direction relative to the vehicle, or a search algorithm has to be used.

§6.2.2 - A 4x4-subarraylevel-scanned Array of Sequentially Rotated Linearly Polarized Patches

As the last paragraph shows, the phaseshifts between 2x2-subarrays dictate the tracking mechanism. As long as the subarrays are identical, this tracking mechanism is not affected by their internal structure. So the tracking operation for a 4x4-subarraylevel-scanned array of sequentially rotated linearly polarized patches is described by equations (6.11a) and (6.11b).

§6.2.3 - An Elementlevel-scanned Array of Circularly or Sequentially Rotated Linearly Polarized Patches

From the preceding paragraphs it has become clear that for applying the simultaneous lobe comparison technique to an electronically steered array, one needs four identical subarrays with phaseshifts in between.

If a 4x4-array is used, paragraph 4.3.1 shows that an array composed of sequentially rotated linearly polarized patches can be described as an array composed of four 2x2-subarrays with phaseshifts in between as stated in (6.4c) to (6.4f). An array composed of circularly polarized patches can be described in the same way, and so for both arrays the tracking operation is described by equations (6.11a) and (6.11b). Necessary is that subarray-outputs become available in the feeding network for summation- and subtrackting-purposes. Designing such a feeding network can be difficult.

§6.3 - Sum and Difference Network in Microstrip

Adding and subtracting can be performed with a "hybrid ring junction" or "rat race", the microstrip equivalent of the "magic T hybrid junction" that is used in waveguide circuits. A rat race is depicted in figure 6.9.

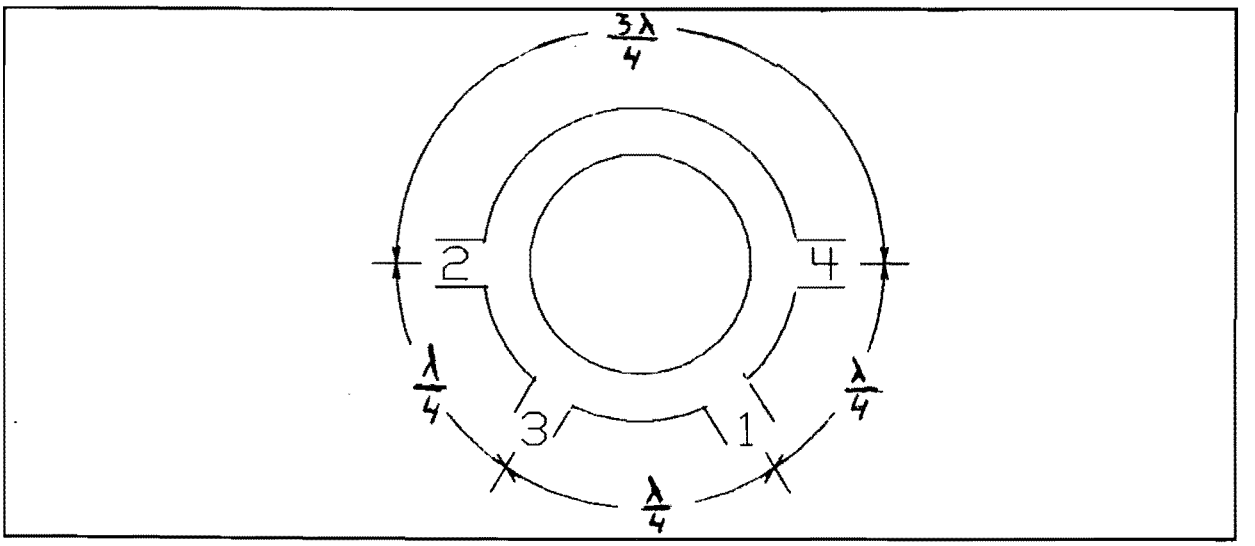

Fig. 6.9 - Rat race

The scatteringmatrix of the rat race is given by [6-3]:

$$S = -\frac{j}{\sqrt{2}} \cdot \begin{pmatrix} 0 & 0 & 1 & 1 \\ 0 & 0 & 1 & -1 \\ 1 & 1 & 0 & 0 \\ 1 & -1 & 0 & 0 \end{pmatrix} \qquad (6.12)$$

Thus with a_i the incoming normalized voltagewaves and b_i the outgoing normalized voltagewaves (i = 1, 2, 3, 4):

$$\begin{pmatrix} b_1 \\ b_2 \\ b_3 \\ b_4 \end{pmatrix} = -\frac{j}{\sqrt{2}} \cdot \begin{pmatrix} 0 & 0 & 1 & 1 \\ 0 & 0 & 1 & -1 \\ 1 & 1 & 0 & 0 \\ 1 & -1 & 0 & 0 \end{pmatrix} \cdot \begin{pmatrix} a_1 \\ a_2 \\ a_3 \\ a_4 \end{pmatrix} \qquad (6.13)$$

If ports 1 and 2 are provided with signals then at ports 3 and 4 appear:

$$b_3 = -\frac{j}{\sqrt{2}} \cdot (a_1 + a_2) \qquad (6.14a)$$

$$b_4 = -\frac{j}{\sqrt{2}} \cdot (a_1 - a_2) \qquad (6.14b)$$

At port 3 the sum-signal appears, at port 4 the difference-signal. If ports 3 and 4 are provided with signals then at ports 1 and 2 appear:

$$b_1 = -\frac{j}{\sqrt{2}} \cdot (a_3 + a_4) \qquad (6.15a)$$

$$b_2 = -\frac{j}{\sqrt{2}} \cdot (a_3 - a_4) \qquad (6.15$$

The sum and difference network, build up with rat races, is shown in figure 6.10.

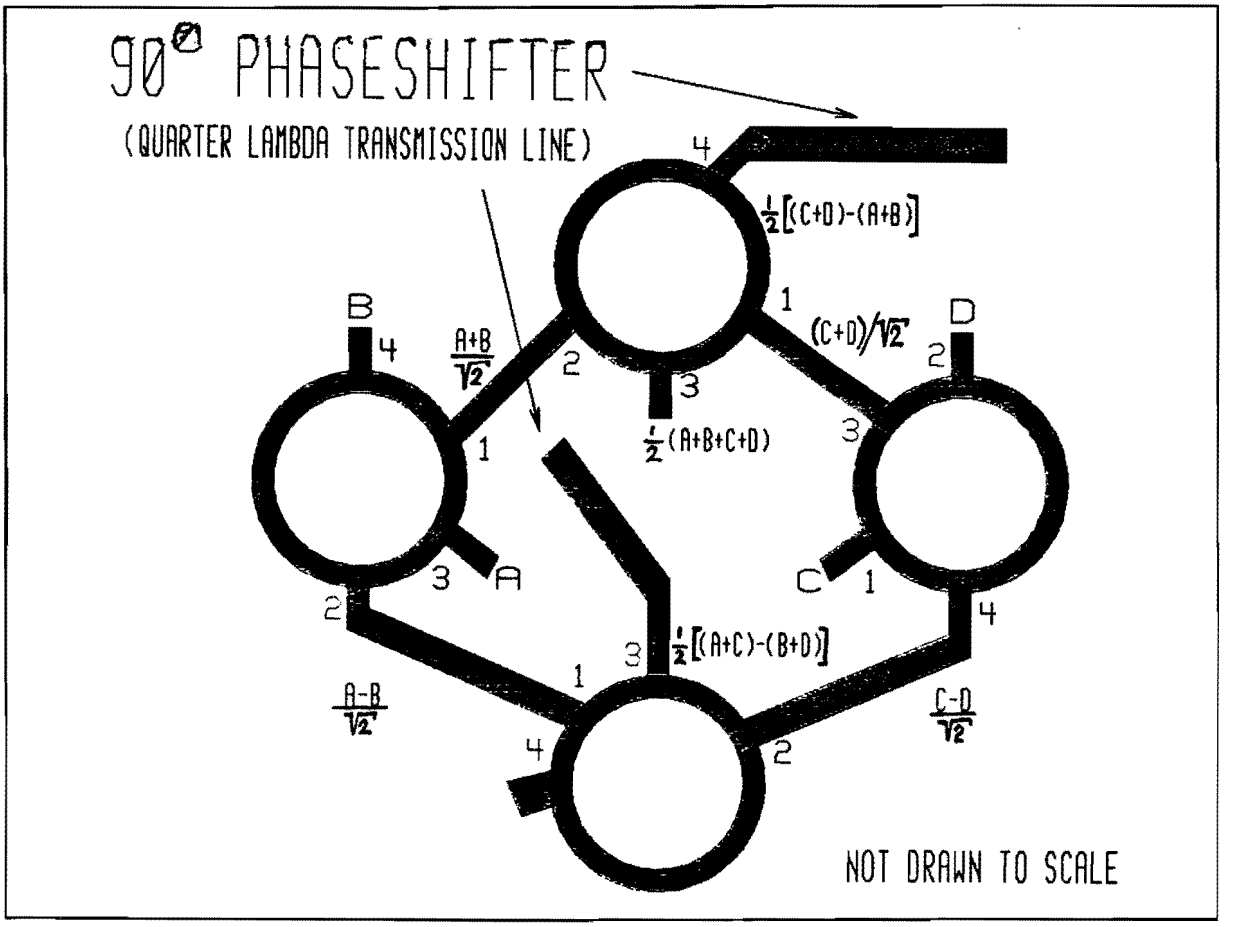

Fig. 6.10 - Sum and difference network

§6.4 - References

[6-1] Sherman S.M., ' *Monopulse Principles and Techniques* ', Artech House Inc., 1984.

[6-2] Rhodes D.R., ' *Introduction to Monopulse* ', McGraw Hill Inc., 1959.

[6-3] Altman J.L., '*Microwave Circuits* ', D. van Nostrand Company Inc., 1964, p.155.

7. Conclusions And Research Recommendations

The VSWR bandwidth and axial ratio performance of a phased array are limited by those of the used element. The greatest drawback of the circular microstrip patch as radiating element is its narrow bandwidth (< 10MHz for a centre frequency of 1.55GHz). For use in a phased array that meets the MSATX-requirements or even the INMARSAT-requirements, the patch will not do.
Recommended is therefore to look for methods to improve the impedance matching of the patch, or to look for microstrip radiators, other than the patch, that have a good impedance match over a larger frequency band. (Stacked microstrip structures seem to be good candidates [7-1]).

Supposed the VSWR bandwidth of the patch can be broadened, a suitable array can be found from comparison of the different antenna characteristics. For fixed beam antennas, these characteristics are stated in table 7.1. Only 16-element arrays are considered, because of the (12dB) gain requirement.

Table 7.1 - Characteristics fixed beam array antennas

16 element array / Characteristic	4x4, CP elements			4x4, LP elements seq. rotated			Circular array LP, seq. rotated		
ε_r	2.33	6	10.5	2.33	6	10.5	2.33	6	10.5
Directivity	++++	+++	+++	++	++	+	++	+	+
Axial Ratio	++++ ++	++++ +	++++ +	++	+	+	++++	+++	+++
VSWR bandw.	+++	++	+	+++	++	+	+++	++	+
# feeds	+	+	+	++	++	++	++	++	++
# splitters	+	+	+	++	++	++	++	++	++
Substr. costs	+++	++	+	+++	++	+	+++	++	+

In each row the quality is indicated by the number of +'s, relative to the worst quality in that row (indicated by one +). The best quality in each row is marked. The most suitable antennas are those with the

most marks in the column.
So for fixed beam antennas, recommended are a 4x4-array composed of circularly polarized patches on a substrate with dielectric constant $\varepsilon_r = 2.33$, a 4x4-array composed of sequentially rotated and fed linearly polarized patches on a substrate with dielectric constant $\varepsilon_r = 2.33$, or a 16-element circular array composed of sequentially rotated and fed linearly polarized patches on the same dielectric substrate.

The characteristics for scanning antennas are stated in table 7.2. The table is to be read in the same way as table 7.1. The maximum qualities are marked in grey. Special attention should be paid to the maximum scanangle and to the number of phaseshifters. One + in the row of the maximum scanangle indicates that the array is not suitable for scanning purposes (due to a too large minimum elementspacing). One + in the row of the number of phaseshifters indicates a too large number (16), that is not desirable because of the costs. These qualities are marked with a circle.
The most suitable antenna (a compromise between performance and costs) is the antenna with the most grey marks and without circle marks.

Of the two candidates (the last two columns of table 7.2), the choise is made in favour the 4x4-antenna composed of sequentially rotated and fed linearly polarized pathes, scanned on subarray level, with a dielectric constant $\varepsilon_r = 6$, because of the better axial ratio and VSWR bandwidth as well as the lower substrate cost.

This antenna meets the MSATX gain requirement (10dB). To meet the INMARSAT gain requirement (12dB), the number of patches should be increased. The antenna nearly meets the MSATX axial ratio requirement (AR ≤ 4dB for $\vartheta \leq 60^0$): the maximum scanangle is 55^0.

Table 7.2 - Characteristics scanned beam array antennas

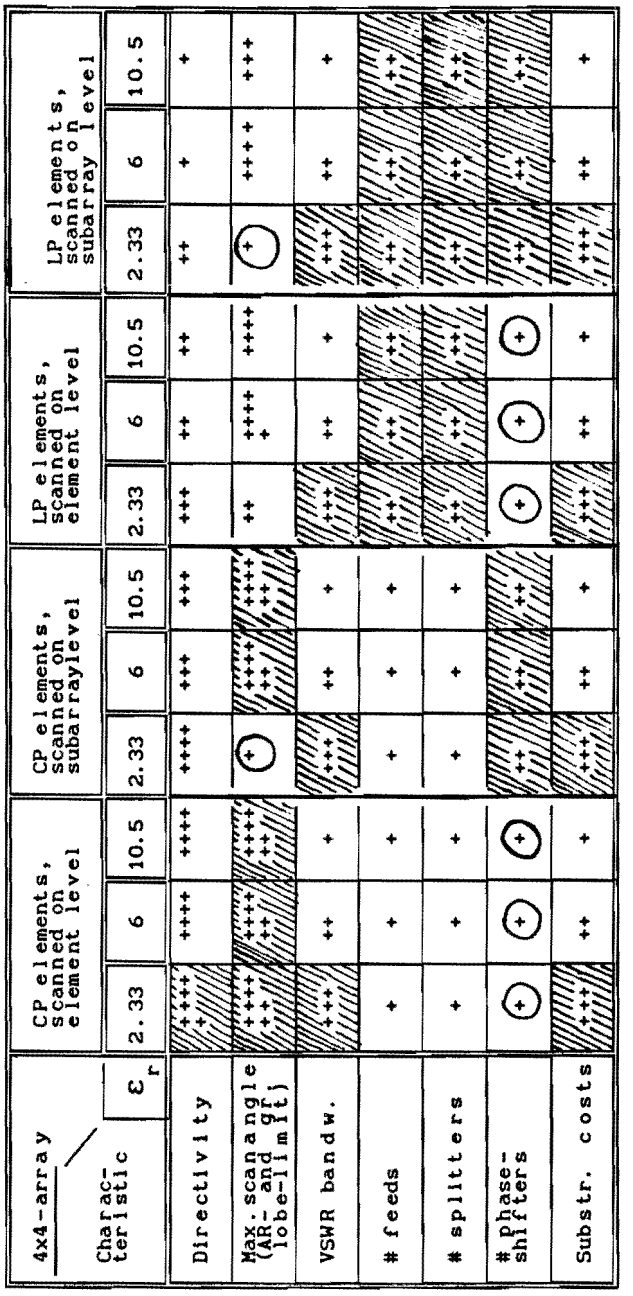

When applying the sequential rotation technique, one should be carefull in chosing the elementspacing. Exceeding an elementspacing of about 0.7*λ (corresponding to a diagonal spacing of about λ), results in the occcurance of grating lobes. This added to the high crosspolarized lobes in the diagonal planes (the crosspolarized lobes become higher as the elementspacing increases), results in a high gain loss, compared with an array composed of circularly polarized patches. For a 4x4-array this gain loss can exceed 6dB. It should be noted here that the results described in this research report are in close agreement with results elsewhere recently obtained [7-2].

For use in the antenna feeding network, Wilkinson power splitters are recommended, because of the good isolation between output ports and because of the low reflection coefficient at the input of the feeding network. This low reflection coefficient originates from the use of dissipating power splitters; the sequential rotation technique does not improve the VSWR bandwidth, as is recently published [7-2].

Not considered in the analysis of the arrays, is the effect of mutual coupling. Since this phenomenon can strongly affect the antenna performance, a mutual coupling analysis should be performed.

References

[7-1] Mosig J.R., Barlatey L., Gardiol F.E., ' *Stacked Microstrip Patches* ',
Proceedings of the COST 213 / KUL Phased Array Workshop at Leuven, Belgium, 26-27 October 1988, pp.37-45.

[7-2] Hall P.S., Huang J., Rammos E., Roederer A., ' *Gain of Circularly Polarized Arrays Composed of Linearly Polarized Elements* ',
Electronic Letters, January 1989, Vol.25, No.2, p.124.

Acknowledgements

At this place I wish to thank the following persons for their support during this work:
A.J.J Reijnders, for his help in selecting, testing and applying numerical procedures;
E.C. den Toom, for his help in developing and testing the software concerned with the microstrip patch analysis.
R. Caspers, for use of his personal computer for night-time calculations and for use of print facilities.

My special thanks go to the "Koninklijk Instituut van Ingenieurs" (Royal Dutch Institute of Engineers), that made it possible for me to attend the COST 213/ KUL Phased-Array Workshop in Leuven, Belgium, 25-26 October 1988.

APPENDIX A

It is to be proven that the $\bar{E}$-vector as a function of time describes an ellipse in the ϑ,φ-plane. The $\bar{E}$-vector is given by:

$$\bar{E} = |E_\vartheta| \cdot e^{j\psi_\vartheta} \cdot (\bar{a}_\vartheta + \rho \cdot \bar{a}_\varphi) \qquad \text{(A.1a)}$$

with

$$\rho = \frac{|E_\varphi|}{|E_\vartheta|} \cdot e^{j(\psi_\varphi - \psi_\vartheta)} \qquad \text{(A.1b)}$$

To trace the figure of the extremity of the electric field, the real part of the time dependent electric field is taken:

$$\begin{aligned} \bar{\mathcal{E}} &= \mathrm{Re}\{ \bar{E} \cdot e^{j\omega t} \} \\ &= |E_\vartheta| \cdot \{ \cos(\omega t + \psi_\vartheta) \cdot \bar{a}_\vartheta + |\rho| \cdot \cos(\omega t + \psi_\vartheta + \psi_\rho) \cdot \bar{a}_\varphi \} \end{aligned} \qquad \text{(A.2)}$$

The electric field in the ϑ,φ-plane can be represented by the relations:

$$\mathcal{E}_\vartheta = E_1 \cdot \cos(\omega t') \qquad \text{(A.3a)}$$

$$\mathcal{E}_\varphi = E_2 \cdot \cos(\omega t' + \psi_\rho) \qquad \text{(A.3b)}$$

with:

$$E_1 = |E_\vartheta| \tag{A.3c}$$

$$E_2 = |E_\vartheta| \cdot |\rho| = |E_\varphi| \tag{A.3d}$$

$$t' = t + \frac{\psi_\vartheta}{\omega t} \tag{A.3e}$$

Using the relations (A.3a) and (A.3b) to eliminate t':

$$\frac{\varepsilon_\varphi}{E_2} - \cos(\omega t') \cdot \cos(\psi_\rho) = -\sin(\omega t') \cdot \sin(\psi_\rho) = \frac{\varepsilon_\varphi}{E_2} - \frac{\varepsilon_\vartheta}{E_1} \cdot \cos(\psi_\rho) \tag{A.4}$$

This gives:

$$\left(\frac{\varepsilon_\varphi}{E_2} - \frac{\varepsilon_\vartheta}{E_1} \cdot \cos(\psi_\rho) \right)^2 = \sin^2(\omega t') \cdot \sin^2(\psi_\rho) =$$

$$= \left(1 - \left(\frac{\varepsilon_\vartheta}{E_1} \right)^2 \right) \cdot \sin^2(\psi_\rho) \tag{A.5}$$

or:

$$\left(\frac{\varepsilon_\vartheta}{E_1} \right)^2 + \left(\frac{\varepsilon_\varphi}{E_2} \right)^2 - \frac{2\varepsilon_\vartheta \varepsilon_\varphi}{E_1 E_2} \cdot \cos(\psi_\rho) = \sin^2(\psi_\rho) \tag{A.6}$$

This equation is of the form $ax^2 + bxy + cy^2 = 1$, with $a > 0$ and $b > 0$. It can be written as:

$$(A\bar{p}, \bar{p}) = 1 \tag{A.7a}$$

with:

$$\bar{p} = (x,\ y) \tag{A.7b}$$

$$A = \begin{pmatrix} a & b/2 \\ b/2 & c \end{pmatrix} \tag{A.7c}$$

The eigenvalues $\lambda_{1,2}$ of A are found out of:

$$\begin{vmatrix} a-\lambda b/2 \\ b/2c-\lambda \end{vmatrix} = 0 \tag{A.8}$$

or:

$$\lambda^2 - \lambda\cdot(a + c) + (ac - \frac{1}{4}\cdot b^2) \tag{A.9}$$

The roots are:

$$\lambda_{1,2} = \frac{1}{2}\cdot\left\{ a + c \pm \left[(a + c)^2 + (b^2 - 4ac) \right]^{1/2} \right\} \tag{A.10}$$

Because $a > 0$ and $c > 0$:

$$\lambda_1 > 0 \quad \text{and} \quad \lambda_2 > 0 \quad \text{if} \quad (b^2 - 4ac) < 0 \tag{A.11}$$

After transformation on the headaxis, for $ax^2 + bxy + cy^2 = 1$, is found the equation:

$$\lambda_1\cdot x'^2 + \lambda_2\cdot y'^2 = 1 \tag{A.12}$$

which is the equation of an ellipse with axis of length $\frac{1}{\sqrt{|\lambda_{1,2}|}}$

So the $\bar{\mathbf{E}}$-vector describes an ellipse in the ϑ,φ-plane if:

$$b^2 - 4ac < 0 \tag{A.13}$$

$$b^2 - 4ac = \left(-2 \cdot \frac{\cos(\psi_\rho)}{\sin^2(\psi_\rho)} \right)^2 - 4 \cdot \left(\frac{1}{\sin^2(\psi_\rho)} \right) \cdot \left(\frac{1}{\sin^2(\psi_\rho)} \right) =$$

$$= - \frac{4}{\sin^2(\psi_\rho)} < 0 \tag{A.14}$$

APPENDIX B

Considered is a magnetic dipole in the xy-plane. This dipole is created by a circular wire in the xz-plane [B-1] (see figure B.1).

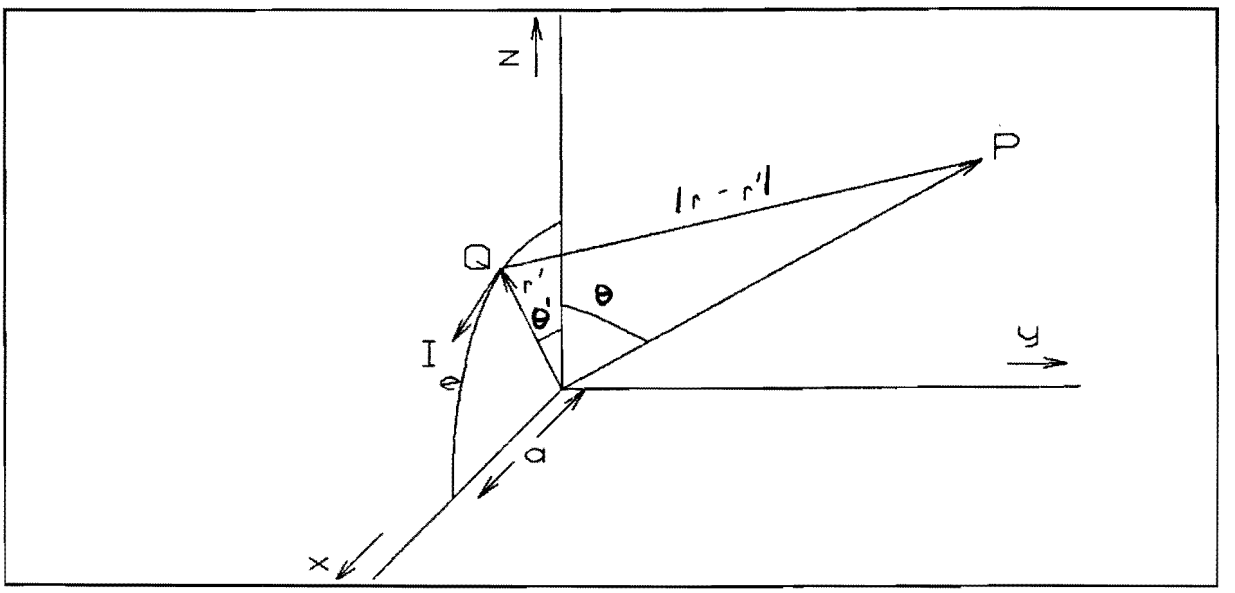

Fig. B.1 - Magnetic dipole

The current $\bar{I}_e$ is given by:

$$\bar{I}_e = I_0 \cdot \delta(\sqrt{x^2 + y^2} - a) \cdot \delta(y) \cdot \bar{a}_\vartheta \qquad (B.1)$$

This current is split up in the components I_{ex} and I_{ez} as depicted in figure B.2.

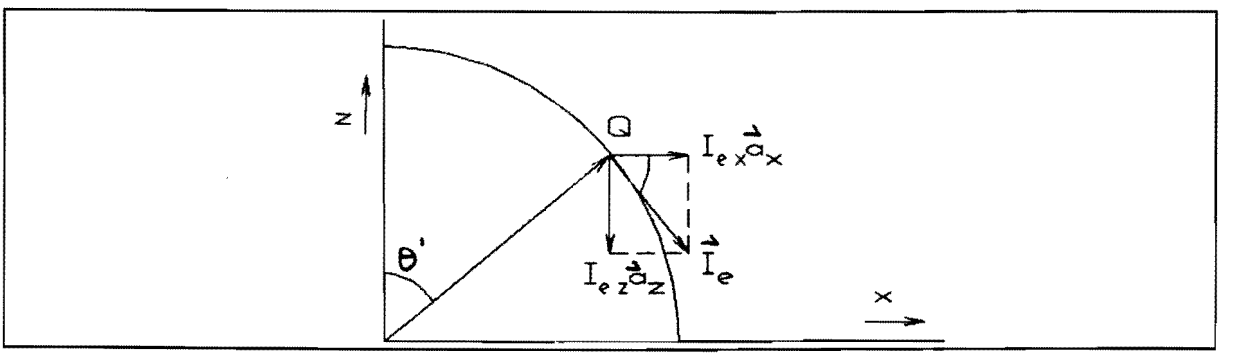

Fig. B.2 - Orthogonal current components

$$I_{ex} = |\bar{I}_e| \cdot \cos(\vartheta') \tag{B.2a}$$

$$I_{ez} = |\bar{I}_e| \cdot \sin(\vartheta') \tag{B.2b}$$

The vector potential is given by [B-1]:

$$\bar{A}_e(\bar{r}) = \frac{\mu_0}{4\pi} \cdot \int_V \bar{I}_e(\bar{r}') \cdot \frac{e^{-jk \cdot |\bar{r} - \bar{r}'|}}{|\bar{r} - \bar{r}'|} dV \tag{B.3}$$

with:

$$\bar{r}' = a \cdot \cos(\vartheta') \cdot \bar{a}_z + a \cdot \sin(\vartheta') \cdot \bar{a}_x \tag{B.4a}$$

$$\bar{r} = r \cdot \cos(\varphi) \cdot \sin(\vartheta) \cdot \bar{a}_x + r \cdot \sin(\varphi) \cdot \sin(\vartheta) \cdot \bar{a}_y + r \cdot \cos(\vartheta) \cdot \bar{a}_z \tag{B.4b}$$

So:

$$|\bar{r} - \bar{r}'| = \left\{ r^2 + a^2 - 2ar\left[\cos(\varphi)\sin(\vartheta)\sin(\vartheta') + \cos(\vartheta)\cos(\vartheta')\right] \right\}^{\frac{1}{2}} \tag{B.5}$$

The x- and z-component of the vector potential $\bar{A}_e$ can now be written as ($A_{ey} = 0$ because $I_{ey} = 0$):

$$A_{ex} = \frac{\mu_0}{4\pi} \cdot a \cdot \int_0^{2\pi} I_0 \cdot \cos(\vartheta') \cdot f(a) \cdot d\vartheta' \tag{B.6a}$$

$$A_{ez} = -\frac{\mu_0}{4\pi} \cdot a \cdot \int_0^{2\pi} I_0 \cdot \sin(\vartheta') \cdot f(a) \cdot d\vartheta' \tag{B.6b}$$

with:

$$f(a) = \frac{\exp\left\{-jk\left[r^2+a^2-2ra\left(\cos(\varphi)\sin(\vartheta)\sin(\vartheta')+\cos(\vartheta)\cos(\vartheta')\right)\right]^{\frac{1}{2}}\right\}}{\left[r^2+a^2-2ra\left(\cos(\varphi)\sin(\vartheta)\sin(\vartheta\,')+\cos(\vartheta)\cos(\vartheta\,')\right)\right]^{\frac{1}{2}}} \tag{B.7}$$

a is assumed to be small enough to expand f(a) in a Taylor series:

$$f(a) = f(0) + a\cdot f'(0) \tag{B.8}$$

with:

$$f(0) = \frac{\exp(-jkr)}{r} \tag{B.9a}$$

$$f'(0) = \frac{jk\cdot\left(\cos(\varphi)\sin(\vartheta)\sin(\vartheta')+\cos(\vartheta)\cos(\vartheta')\right)\cdot e^{-jkr}}{r} + \frac{\left(\cos(\varphi)\sin(\vartheta)\sin(\vartheta')+\cos\vartheta)\cos(\vartheta')\right)\cdot e^{-jkr}}{r} \tag{B.9b}$$

With the above Taylor expansion the x- and z-component of the vector potential turn out to be, after some calculations:

$$A_{ex} = \frac{\mu_0}{4\pi}\cdot a\cdot e^{-jkr}\cdot\left[\frac{jk}{r}+\frac{1}{r^2}\right]\cdot I_0\cdot a\cdot\pi\cdot\cos(\vartheta) =$$

$$= C(r)\cdot\cos(\vartheta)\cdot e^{-jkr} \tag{B.10a}$$

$$A_{ez} = - \frac{\mu_0}{4\pi} \cdot a \cdot e^{-jkr} \cdot \left[\frac{jk}{r} + \frac{1}{r^2} \right] \cdot I_0 \cdot a \cdot \pi \cdot \cos(\varphi) \sin(\vartheta) =$$

$$= - C(r) \cdot \cos(\varphi) \sin(\vartheta) \cdot e^{-jkr} \qquad \text{(B.10b)}$$

In spherical coordinates:

$$A_{er} = \sin(\vartheta)\cos(\varphi) \cdot A_{ex} + \sin(\vartheta)\sin(\varphi) \cdot A_{ey} + \cos(\vartheta) \cdot A_{ez} =$$

$$= 0 \qquad \text{(B.11a)}$$

$$A_{e\vartheta} = \cos(\vartheta)\cos(\varphi) \cdot A_{ex} + \cos(\vartheta)\sin(\varphi) \cdot A_{ey} - \sin(\vartheta) \cdot A_{ez} =$$

$$= C(r) \cdot \cos(\varphi) \cdot e^{-jkr} \qquad \text{(B.11b)}$$

$$A_{e\varphi} = - \sin(\varphi) \cdot A_{ex} + \cos(\varphi) \cdot A_{ey} =$$

$$= - C(r) \cdot \sin(\varphi)\cos(\vartheta) \cdot e^{-jkr} \qquad \text{(B.11c)}$$

$\bar{B}$ can be calculated with (in spherical coordinates):

$$\bar{B} = \nabla \times \bar{A} =$$

$$= \frac{1}{r\sin(\vartheta)} \cdot \left[\frac{\delta}{\delta\vartheta} \left(\sin(\vartheta) \cdot A_{e\varphi} \right) - \frac{\delta A_{e\varphi}}{\delta\varphi} \right] \cdot \bar{a}_r +$$

$$+ \frac{1}{r} \cdot \left[\frac{1}{\sin(\vartheta)} \cdot \frac{\delta A_{er}}{\delta\varphi} - \frac{\delta}{\delta r} \left(r \cdot A_{e\varphi} \right) \right] \cdot \bar{a}_\vartheta +$$

$$+ \frac{1}{r} \cdot \left[\frac{\delta}{\delta r} \left(r \cdot A_{e\vartheta} \right) - \frac{\delta A_{er}}{\delta\vartheta} \right] \cdot \bar{a}_\varphi \qquad \text{(B.12)}$$

In the far field only terms with a r^{-1} dependence are of interest and it can be found that:

$$B_r = 0 \tag{B.13a}$$

$$B_\vartheta \quad - jk \cdot \frac{e^{-jkr}}{r} \cdot \sin(\varphi)\cos(\vartheta) \tag{B.13b}$$

$$B_\varphi \quad - jk \cdot \frac{e^{-jkr}}{r} \cdot \cos(\varphi) \tag{B.13c}$$

With $\bar{E} \quad \nabla \times \bar{B}$ and only considering terms with a r^{-1} dependence, it is found that:

$$E_\varphi \quad \frac{1}{r} \cdot \frac{\delta}{\delta r} \left(r \cdot B_\vartheta \right) \quad - \frac{e^{-jkr}}{r} \cdot \sin(\varphi)\cos(\vartheta) \tag{B.14a}$$

$$E_\vartheta \quad - \frac{1}{r} \cdot \frac{\delta}{\delta r} \left(r \cdot B_\varphi \right) \quad + \frac{e^{-jkr}}{r} \cdot \cos(\varphi) \tag{B.14b}$$

Comparing the above formulas with (1.2) shows that for n=1 and small angles ϑ, the far field radiation pattern of a circular microstrip antenna can be thought to originate from a magnetic dipole in the plane of the antenna.

Reference:

[B-1] Jeuken, M.E.J., ' *Elektromagnetishe Golven en Antennes* ', Professional Group Electromagnetism & Circuit Theory, Department of Electrical Engineering, Eindhoven University of Technology, 1983, pp.4.1-4.3 (in Dutch).

APPENDIX C

With $\varphi = n \cdot \frac{360}{N}$:

$$\cos(\varphi - \varphi_i) = \cos\{ (-1 + 2n - 4i) \cdot \frac{360}{2N} \} \qquad \text{(C.1a)}$$

$$\cos(\varphi - \varphi_i - \frac{360}{N}) = \cos\{ (-3 + 2n - 4i) \cdot \frac{360}{2N} \} \qquad \text{(C.1b)}$$

and:

$$\sum_1 = \sum_{i=0}^{\frac{N-2}{2}} e^{j \cdot \alpha \cdot \cos(\varphi - \varphi_i)} \qquad \text{(C.2a)}$$

$$\sum_2 = \sum_{i=0}^{\frac{N-2}{2}} e^{j \cdot \alpha \cdot \cos(\varphi - \varphi_i - \frac{360}{N})} \qquad \text{(C.2b)}$$

with:

$$\alpha = r \cdot \frac{2\pi}{\lambda} \cdot \sin(\vartheta) \qquad \text{(C.2c)}$$

$\sum_1$ and $\sum_2$ can be written as:

$$\sum_1 = \sum_{i=0}^{\frac{N-2}{2}} \left\{ J_0(\alpha) + 2 \cdot \sum_{l=0}^{\infty} j^l \cdot J_l(\alpha) \cdot \cos\{ l \cdot (\varphi - \varphi_i) \} \right\} \qquad \text{(C.3a)}$$

$$\sum_2 = \sum_{i=0}^{\frac{N-2}{2}} \left\{ J_0(\alpha) + 2 \cdot \sum_{k=0}^{\infty} j^k \cdot J_k(\alpha) \cdot \cos\left\{ k \cdot (\varphi - \varphi_i - \frac{360}{N}) \right\} \right\} \quad \text{(C.3b)}$$

To prove is that $\sum_1 - \sum_2 = 0$.

$$\sum_1 - \sum_2 = 2 \cdot \left[\sum_{l=0}^{\infty} j^l \cdot J_l(\alpha) \cdot \sum_3 - \sum_{k=0}^{\infty} j^k \cdot J_k(\alpha) \cdot \sum_4 \right] \quad \text{(C.4a)}$$

with:

$$\sum_3 = \sum_{i=0}^{\frac{N-2}{2}} \cos\left\{ l \cdot (2n - 1 - 4i) \cdot \frac{360}{2N} \right\} =$$

$$= \mathrm{Re}\left\{ e^{j \cdot l \cdot (2n-1) \cdot \frac{360}{2N}} \cdot \sum_{i=0}^{\frac{N-2}{2}} e^{2j \cdot l \cdot i \cdot \frac{360}{N}} \right\} \quad \text{(C.4b)}$$

$$\sum_4 = \sum_{i=0}^{\frac{N-2}{2}} \cos\left\{ k \cdot (2n - 3 - 4i) \cdot \frac{360}{2N} \right\} =$$

$$= \mathrm{Re}\left\{ e^{j \cdot k \cdot (2n-3) \cdot \frac{360}{2N}} \cdot \sum_{i=0}^{\frac{N-2}{2}} e^{2j \cdot k \cdot i \cdot \frac{360}{N}} \right\} \quad \text{(C.4b)}$$

The summations in (C.4) can be worked out:

$$\sum_{i=0}^{\frac{N-2}{2}} e^{2j\cdot l\cdot i\cdot \frac{360}{N}} = \begin{cases} \dfrac{1 - e^{2j\cdot l\cdot \frac{360}{N}\cdot \frac{N}{2}}}{1 - e^{2j\cdot l\cdot \frac{360}{N}}} = 0 & l \neq \dfrac{N}{2} \\ \dfrac{N}{2} & l = \dfrac{N}{2} \end{cases}$$

(C.5a)

$$\sum_{i=0}^{\frac{N-2}{2}} e^{2j\cdot k\cdot i\cdot \frac{360}{N}} = \begin{cases} \dfrac{1 - e^{2j\cdot k\cdot \frac{360}{N}\cdot \frac{N}{2}}}{1 - e^{2j\cdot k\cdot \frac{360}{N}}} = 0 & k \neq \dfrac{N}{2} \\ \dfrac{N}{2} & k = \dfrac{N}{2} \end{cases}$$

(C.5b)

$\sum_3$ and $\sum_4$ can now be written as:

$$\sum_3 = \begin{cases} 0 & l \neq \frac{N}{2} \\ \frac{N}{2} \cdot \mathrm{Re}\left\{ e^{j \cdot \frac{N}{2} \cdot (2n - 1) \cdot \frac{360}{2N}} \right\} = & \\ = \frac{N}{2} \cdot \mathrm{Re}\left\{ e^{j \cdot n \cdot 180} \cdot e^{-j \cdot 90} \right\} = & \\ = \frac{N}{2} \cdot \mathrm{Re}\left\{ -j \cdot e^{j \cdot n \cdot 180} \right\} = 0 & l = \frac{N}{2} \end{cases} \qquad \text{(C.6)}$$

In the same way can be found:

$$\sum_4 = 0 \qquad \text{(C.7)}$$

Substitution of (C.6) and (C.7) in (C.4a) gives:

$$\sum_1 - \sum_2 = 0 \qquad \text{(C.8)}$$

Appendix D - DUROID Characteristics

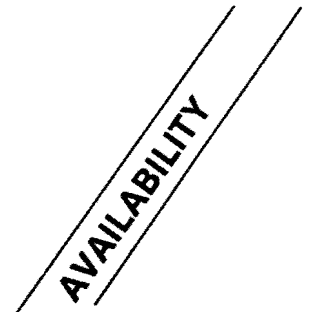

RT/duroid® 5870 AND 5880

DIELECTRIC CONSTANT

RT/D 5870: ϵ_r = 2,33 ± 0,02
RT/D 5880: ϵ_r = 2,20 ± 0,02
Specification MIL-P-13949F type GRN

CLADDING

COPPER: 1/8 oz ED Copper
1/4 oz ED Copper
1/2 oz Rolled or ED Copper
1 oz Rolled or ED Copper
2 oz Rolled or ED Copper

THICK METAL BACKING
On special request we can supply Aluminium, Brass or Copper backed material.

SHEET SIZE AND THICKNESS

Size:	inches	mm
	18 x 12	457 x 305
	18 x 24	457 x 610
	18 x 36	457 x 915
	18 x 48	457 x 1219
Thickness and tolerance:		
	0,005 ± 10%	0,13 ± 10%
	0,010 ± 7%	0,25 ± 7%
	0,015 ± 7%	0,38 ± 7%
	0,020 ± 0,001	0,51 ± 0,03
	0,031 ± 0,001	0,79 ± 0,03
	0,062 ± 0,002	1,57 ± 0,05
	0,125 ± 0,004	3,18 ± 0,10

Other sheetsizes and thicknesses available on request.

RT/duroid® 6010

DIELECTRIC CONSTANT

RT/D 6010.2: ϵ_r = 10,2 ± 0,25
RT/D 6010.5: ϵ_r = 10,5 ± 0,25
RT/D 6006 : ϵ_r = 6 ± 0,20

CLADDING

COPPER: 1/8 oz ED Copper
1/4 oz ED Copper
1/2 oz Rolled Copper or ED Copper
1 oz Rolled Copper or ED Copper
2 oz Rolled Copper or ED Copper

THICK METAL BACKING
On special request we can supply Aluminium, Brass of Copper backed material.

SHEET SIZE AND THICKNESS

Size:	inches	mm
	20 x 20	508 x 508
	10 x 20	254 x 508
	10 x 10	254 x 254
Thickness and tolerance:		
	0,010 ± 0,001*	0,25 ± 0,03*
	0,025 ± 0,001	0,64 ± 0,03
	0,050 ± 0,002	1,27 ± 0,05
	0,075 ± 0,004	1,91 ± 0,10
	0,100 ± 0,005	2,54 ± 0,13

* not available in **RT/duroid 6010.2**

RT/duroid® 5500

DIELECTRIC CONSTANT

RT/D 5500: ϵ_r = 2,5 ± 0,04

CLADDING

COPPER: 1 oz ED Copper
other copper claddings available on request.

THICK METAL BACKING
On special request we can supply Aluminium, Brass or Copper backed material.

SHEET SIZE AND THICKNESS

Size:	inches	mm
	18 x 12	457 x 305
	18 x 24	457 x 610
	18 x 36	457 x 915
	18 x 48	457 x 1219
Thickness and tolerance:		
	0,015 ± 0,001	0,38 ± 7%
	0,031 ± 0,001	0,79 ± 0,03
	0,062 ± 0,002	1,57 ± 0,05
	0,093 ± 0,003	2,36 ± 0,07
	0,125 ± 0,004	3,18 ± 0,10

Other sheetsizes and thicknesses available on request.

ROGERS

RT/duroid 5870

PROPERTY	TEST METHOD, CONDITION		UNITS[1]	DIRECTION	TYPICAL VALUE[2]	
Dielectric constant, εr	ASTM D1531	1 MHz	—	Z	2.35	
	ASTM D3380	10 GHz	—	Z	2.33 · .02 spec.	
Dissipation factor, tan δ	ASTM D1531	1 MHz	—	Z	.0005	
	ASTM D3380	10 GHz	—	Z	.0012	
Volume resistivity	ASTM D257	C96/23/95	Mohm cm	Z	2×10^7	
Surface resistivity	ASTM D257	C96/23/95	Mohm	X,Y	3×10^8	
					Test at 23°C	Test at 100°C
Tensile modulus	ASTM D638	A	MPa (kpsi)	X	1300 (189)	490 (71)
				Y	1280 (185)	430 (63)
ultimate stress			MPa (kpsi)	X	50 (7.3)	34 (4.8)
				Y	42 (6.1)	34 (4.8)
ultimate strain			%	X	9.8	8.7
				Y	9.8	8.6
Compressive modulus	ASTM D695	A	MPa (kpsi)	X	1210 (176)	680 (99)
				Y	1360 (198)	860 (125)
				Z	830 (120)	520 (76)
ultimate stress			MPa (kpsi)	X	30 (4.4)	23 (3.4)
				Y	37 (5.3)	25 (3.7)
				Z	54 (7.8)	37 (5.3)
ultimate strain			%	X	4.0	4.3
				Y	3.3	3.3
				Z	8.7	8.5
Deformation under load	ASTM D621				Test at 50°C	Test at 150°C
		24 hr/14MPa (2 kpsi)	%	Z	0.6	1.0
		24 hr/8.3MPa(1.2 kpsi)	%	Z	0.2	1.0
Water absorption	ASTM D570	D 24/23				
		Thickness = 0.8mm(.031 in.)	mg (%)		0.9 (.02)	
		Thickness = 1.6mm(.062 in.)	mg (%)		1.3 (.015)	
Specific gravity	ASTM D792		—		2.2	
Heat distortion temperature	ASTM D648	1.82MPa(264 psi)	°C(°F)	X,Y	>260 (>500)	
Specific heat	Calculated		J/g/K(BTU/lb/°F)		0.96 (.23)	
Thermal conductivity	Rogers TR2721		W/m/K(BTU in/ft²/hr/°F)	Z	0.26 (1.8)	
Thermal expansion	ASTM D3386 (10 K/min.)		mm/m	→	X	Y	Z
		−100°C			−5.0	−5.5	−11.6
		15			−0.6	−0.9	− 4.0
(Values given are total change from a base temperature of 35°C)		25			−0.3	−0.4	− 2.6
		75			0.7	0.9	7.5
		150			1.8	2.2	22.0
		250			3.4	4.0	58.9

[1] S1 units given first with other frequently used units in parentheses.

[2] References: Internal TR's 1430, 2224, 2854. Tests were at 23°C unless otherwise noted. Typical values should not be used for specification limits.

Printed in U.S.A. 0798 027 5.0 WA

Revised 3/81
Supersedes 1/78

RT/duroid® 6006

PROPERTY	TEST METHOD, CONDITION		UNITS [1]	DIRECTION	TYPICAL VALUE [2]
Dielectric constant, ϵ_r	Adapted ASTM D3380, 10 GHz	A	—	Z	6.00 ± 0.15, spec.
Dissipation factor, tanδ	Adapted ASTM D3380, 10 GHz	A	—	Z	0.0027 max. spec.
Tensile modulus	ASTM D638 (0.1/min. strain rate)	A	MPa (kpsi)	X	510(74)
				Y	627(91)
ultimate stress		—	MPa (kpsi)	X	20(2.8)
				Y	17(2.5)
ultimate strain		—	%	X	12 to 13
				Y	4 to 6
Compression modulus	ASTM D695 (0.05/min. strain rate)	A	MPa (kpsi)	Z	1069(155)
ultimate stress		—	MPa (kpsi)	Z	54(7.9)
ultimate strain		—	%	Z	33
Flexural modulus	ASTM D790	A	MPa (kpsi)	X	2634(382)
				Y	1951(283)
ultimate stress		—	MPa (kpsi)	X	43(6.3)
				Y	38(5.5)
Deformation under load	ASTM D621	24 hr/50°C/7MPa	%	Z	0.33
		24 hr/150°C/7MPa	%	Z	2.1
Water absorption	ASTM D570	24 hr/23°C, 0.050" (1.27 mm) thick	%		0.05
		48 hr/50°C, 0.050" (1.27 mm) thick	%		0.18
Specific gravity	ASTM D792	—	—		2.7
Specific heat	(Calculated)		J/g/K (BTU/lb./°F)		0.97(0.231)
Thermal conductivity	Rogers TR 3824 [3]	23 to 100° C	W/m/K (BTU in/ft²/hr/°F)	Z	0.48(3.3)

Thermal expansion (Values shown are total change from a base temperature of 35°C)	ASTM D3386		mm/m	X	Y	Z
		− 50° C		− 4.0		
		10		− 1.7	− 1.9	− 3.8
		75		1.2	1.3	1.9
		150		2.6	2.9	3.7
		250		4.7	5.4	8.7
		315		6.6	7.5	12.7

[1] SI units given first with other frequently used units in parentheses.

[2] References: APR 4022.44, DJS 4019-27-32, Internal TR 2610. Tests were 23°C unless otherwise noted. Typical values should not be used for specification limits.

[3] Using the Colora Thermoconductometer

ROGERS

Rogers Corporation
Microwave Materials Division, 100 S. Roosevelt Avenue, Chandler, AZ 85226

Revised 2/86
Supercedes 5/85
0871-117-10.0-HG

ROGERS

RT/duroid® 6010.5

PROPERTY	TEST METHOD, CONDITION		UNITS[1]	DIRECTION	TYPICAL VALUE [2]
Dielectric constant, ε_r	Adapted ASTM D3380, 10 GHz	A	—	Z	10.5 ± .25, spec.
Thermal coefficient of ε_r	Adapted ASTM D3380, 10 GHz	−50 to 170°C	ppm/°C	Z	−370
Dissipation factor, tan δ	Adapted ASTM D3380, 10 GHz	A	—	Z	0.0028 max., spec.
Tensile modulus	ASTM D638 (0.1/min. strain rate)	A	MPa (kpsi)	X	931 (135)
				Y	559 (81)
ultimate stress		A	MPa (kpsi)	X	17 (2.4)
				Y	13 (1.9)
ultimate strain		A	%	X	9 to 15
				Y	7 to 14
Compression modulus	ASTM D695 (0.05/min. strain rate)	A	MPa (kpsi)	Z	2144 (311)
ultimate stress			MPa (kpsi)	Z	47 (6.9)
ultimate strain			%	Z	25
Flexural modulus	ASTM D790	A	MPa (kpsi)	X	4364 (633)
				Y	3751 (544)
ultimate stress			MPa (kpsi)	X	36 (5.2)
				Y	32 (4.4)
Deformation under load	ASTM D621	24 hr/50°C/7MPa	%	Z	0.26
		24 hr/150°C/7MPa	%	Z	1.37
Water absorption	ASTM D570	24 hr/23°C, 0.050" (1.27mm) thick	%		0.1
		48 hr/50°C, 0.050" (1.27mm) thick	%		0.25
Specific gravity	ASTM D792	—	—		2.9
Specific heat	Calculated		J/g/K (BTU/lb/°F)		1.00 (0.239)
Thermal conductivity	Rogers TR 2721	23 to 100°C	W/m/K (BTU in/ft²/hr/°F)	Z	0.41 (2.87)

PROPERTY	TEST METHOD	CONDITION	UNITS	DIRECTION	X	Y	Z
Thermal expansion	ASTM D3386 (5 K/min.)	−100°C	mm/m	—	−2.8	−3.0	−3.4
		− 50			−2.0	−2.1	−2.6
	(Values given are total change from a base temperature of 35°C)	10			−0.8	−0.8	−1.1
		75			1.0	1.0	0.7
		150			2.2	2.2	1.7
		250			3.7	3.8	4.3
		315			5.0	5.1	8.4

[1] SI units given first with other frequently used units in parentheses.

[2] References: APR 4022-44 DJS 4019 27 32 Internal TR 2610. Tests were at 23°C unless otherwise noted. Typical values should not be used for specification limits.

RT/duroid® microwave laminate is a registered trademark of Rogers Corporation. Printed in U.S.A.
Made under the following U.S. patents 4,518,737, 4,335,180

Revised 2/86. Supercedes 3/83
0871-117-10.0-HG

Appendix E - Wilkinson Power Splitter

E1 - Relationship Between T- and S-matrix

In general the relationship between incoming and outgoing voltage waves of a threeport is given by:

$$\begin{pmatrix} b_1 \\ b_2 \\ b_3 \end{pmatrix} = \begin{pmatrix} S_{11} & S_{12} & S_{13} \\ S_{21} & S_{22} & S_{23} \\ S_{31} & S_{32} & S_{33} \end{pmatrix} \cdot \begin{pmatrix} a_1 \\ a_2 \\ a_3 \end{pmatrix} \quad , \qquad \bar{b} = S \cdot \bar{a} \tag{E.1}$$

S is called the scattering matrix. a_i and b_i $(i = 1, 2, 3)$ are incoming and outgoing voltage waves, that are normalized so that $a_i \cdot a_i^*$ is the average incoming power at port i and $b_i \cdot b_i^*$ is the average outgoing power at port i.
The scattering matrix is used when the threeport has equal impedance levels at all ports. However when the threeport has unequal impedance levels, as is the case for the Wilkinson power splitter, the unnormalized voltage scattering matrix T is used. The relationship between incoming and outgoing (unnormalized) voltage waves is given by:

$$\begin{pmatrix} d_1 \\ d_2 \\ d_3 \end{pmatrix} = \begin{pmatrix} T_{11} & T_{12} & T_{13} \\ T_{21} & T_{22} & T_{23} \\ T_{31} & T_{32} & T_{33} \end{pmatrix} \cdot \begin{pmatrix} c_1 \\ c_2 \\ c_3 \end{pmatrix} \quad , \qquad \bar{d} = T \cdot \bar{c} \tag{E.2}$$

The relationhip between $\bar{d}$ and $\bar{b}$ and between $\bar{c}$ and $\bar{a}$ is given by [E-1]:

$$d_i = g_i \cdot b_i \qquad (i = 1, 2, 3) \tag{E.3a}$$

$$c_i = g_i \cdot a_i \qquad (i = 1, 2, 3) \tag{E.3b}$$

$$g_i = \sqrt{z_0^{(i)}} \qquad (i = 1, 2, 3) \tag{E.3c}$$

With use of (E.1) to (E.3):

$$d_1 = g_1 \cdot b_1 = g_1 \cdot S_{11} \cdot a_1 + g_1 \cdot S_{12} \cdot a_2 + g_1 \cdot S_{13} \cdot a_3 =$$

$$= T_{11} \cdot c_1 + T_{12} \cdot c_2 + T_{13} \cdot c_3 =$$

$$= T_{11} \cdot g_1 \cdot a_1 + T_{12} \cdot g_2 \cdot a_2 + T_{13} \cdot g_3 \cdot a_3 \qquad \text{(E.4a)}$$

and so:

$$S_{11} = T_{11} \qquad \text{(E.4b)}$$

$$S_{12} = \frac{g_2}{g_1} \cdot T_{12} \qquad \text{(E.4c)}$$

$$S_{13} = \frac{g_3}{g_1} \cdot T_{13} \qquad \text{(E.4d)}$$

In the same way:

$$S_{21} = \frac{g_1}{g_2} \cdot T_{21} \qquad \text{(E.5a)}$$

$$S_{22} = T_{22} \qquad \text{(E.5b)}$$

$$S_{23} = \frac{g_3}{g_2} \cdot T_{23} \qquad \text{(E.5c)}$$

$$S_{31} = \frac{g_1}{g_3} \cdot T_{31} \qquad \text{(E.6a)}$$

$$S_{32} = \frac{g_2}{g_3} \cdot T_{32} \qquad \text{(E.6b)}$$

$$S_{33} = T_{33} \qquad \text{(E.6c)}$$

with:

$$g_1 = \sqrt{Z_0^{(1)}} = \sqrt{Z_0} \tag{E.7a}$$

$$g_2 = \sqrt{Z_0^{(2)}} = \sqrt{K \cdot Z_0} \tag{E.7b}$$

$$g_3 = \sqrt{Z_0^{(3)}} = \sqrt{\frac{Z_0}{K}} \tag{E.7c}$$

calculated at the terminals of the threeport.
Because of the reciprocity of the S-matrix [E-2]:

$$S_{12} = S_{21} \tag{E.8a}$$

$$\frac{g_2}{g_1} \cdot T_{12} = \frac{g_1}{g_2} \cdot T_{21} \tag{E.8b}$$

$$T_{12} = \left(\frac{g_1}{g_2}\right)^2 \cdot T_{21} \tag{E.8c}$$

$$T_{12} = \frac{T_{21}}{K} \tag{E.8d}$$

$$S_{13} = S_{31} \tag{E.9a}$$

$$T_{13} = \left(\frac{g_1}{g_3}\right)^2 \cdot T_{31} = K \cdot T_{31} \tag{E.9b}$$

$$S_{23} = S_{32} \tag{E.10a}$$

$$T_{23} = \left(\frac{g_2}{g_3}\right)^2 \cdot T_{32} = K^2 \cdot T_{32} \tag{E.10b}$$

For $K = 1$: $g_1 = g_2 = g_3$ and consequently $S = T$.

E.2 - Even And Odd Excitation

For the even excitation, the voltage generators are excited with $V_{2e} = V_{3e}$ and $V_{2o} = V_{3o} = 0$. The power splitter network is splitted up as shown in figure E.1 [E-3].

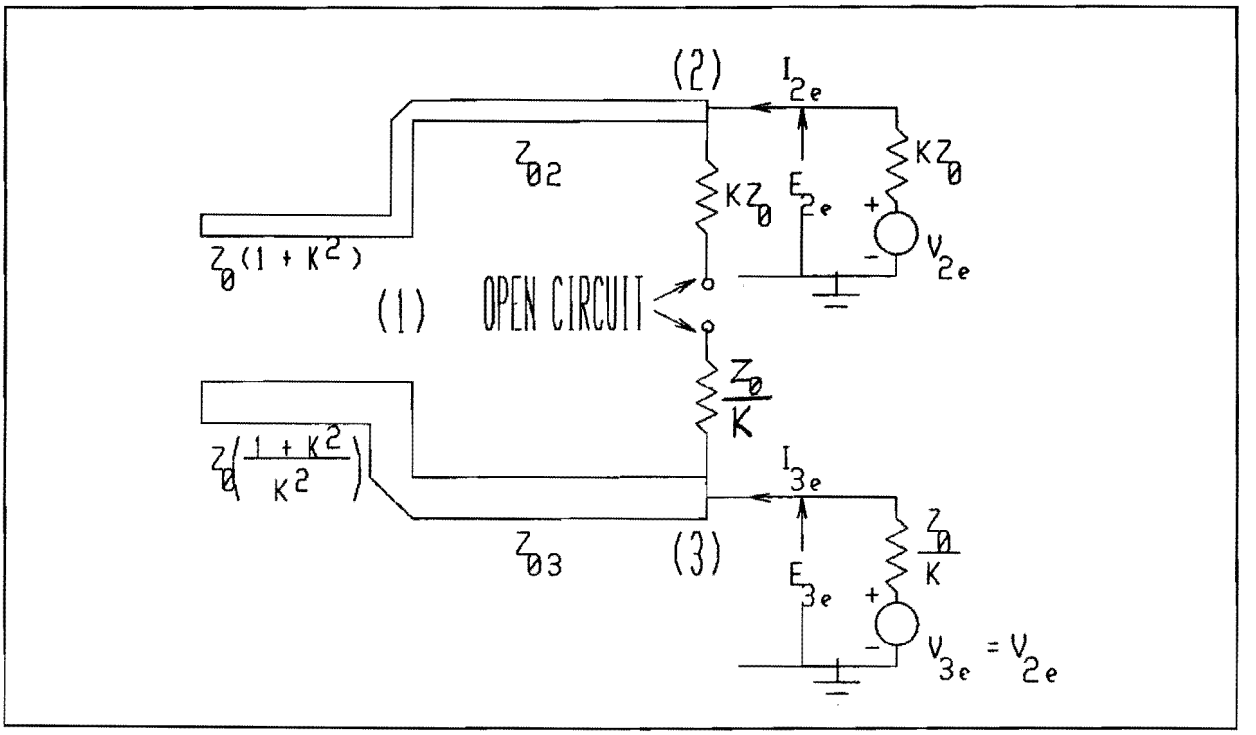

Fig. E.1 - Equivalent circuit for even excitation

The current I_{2e} is given by:

$$I_{2e} = \frac{V_{2e}}{K \cdot Z_0 + Z_{2e}} \tag{E.11}$$

with Z_{2e} the impedance seen looking into port 2. This impedance can be found from impedance seen at port 1 [E-4]:

$$z_{2e} = \frac{z_1 + j \cdot \tan(\vartheta)}{1 + j \cdot z_1 \cdot \tan(\vartheta)} \tag{E.12a}$$

$$Z_{2e} = Z_{02} \cdot z_{2e} = Z_{02} \cdot \frac{Z_{02} \cdot z_1 + j \cdot Z_{02} \cdot \tan(\vartheta)}{Z_{02} + j \cdot Z_{02} \cdot z_1 \cdot \tan(\vartheta)} =$$

$$= Z_{02} \cdot \frac{Z_0 \cdot (1 + K^2) + j \cdot Z_{02} \cdot \tan(\vartheta)}{Z_{02} + j \cdot Z_0 \cdot (1 + K^2) \cdot \tan(\vartheta)} \qquad \text{(E.12b)}$$

The voltage at port 2 is:

$$E_{2e} = Z_{2e} \cdot I_{2e} = \frac{Z_{2e} \cdot V_{2e}}{K \cdot Z_0 + Z_{2e}} \qquad \text{(E.13)}$$

In the same way can be found:

$$Z_{3e} = \frac{Z_{2e}}{K^2}, \quad I_{3e} = K^2 \cdot I_{2e} \quad , \quad E_{2e} = E_{3e} \qquad \text{(E.14)}$$

Since the impedance at every point along arm 2 is K^2 times the impedance at the corresponding point along arm 3, the voltage distribution in both networks is identical and the current in the lower impedance network is K^2 times that of the higher impedance network. Because the voltages along both arms are identical, the two networks in figure F.1 may be joined together and the voltages and currents for the even excitation are given by (E.11) to (E.14).

For the odd excitation, the voltage generators are excited so that $V_{2e} = V_{3e} = 0$ and $V_{20} = - K^2 \cdot V_{30}$. The power splitter network is splitted up as shown in figure E.2 [E-3].

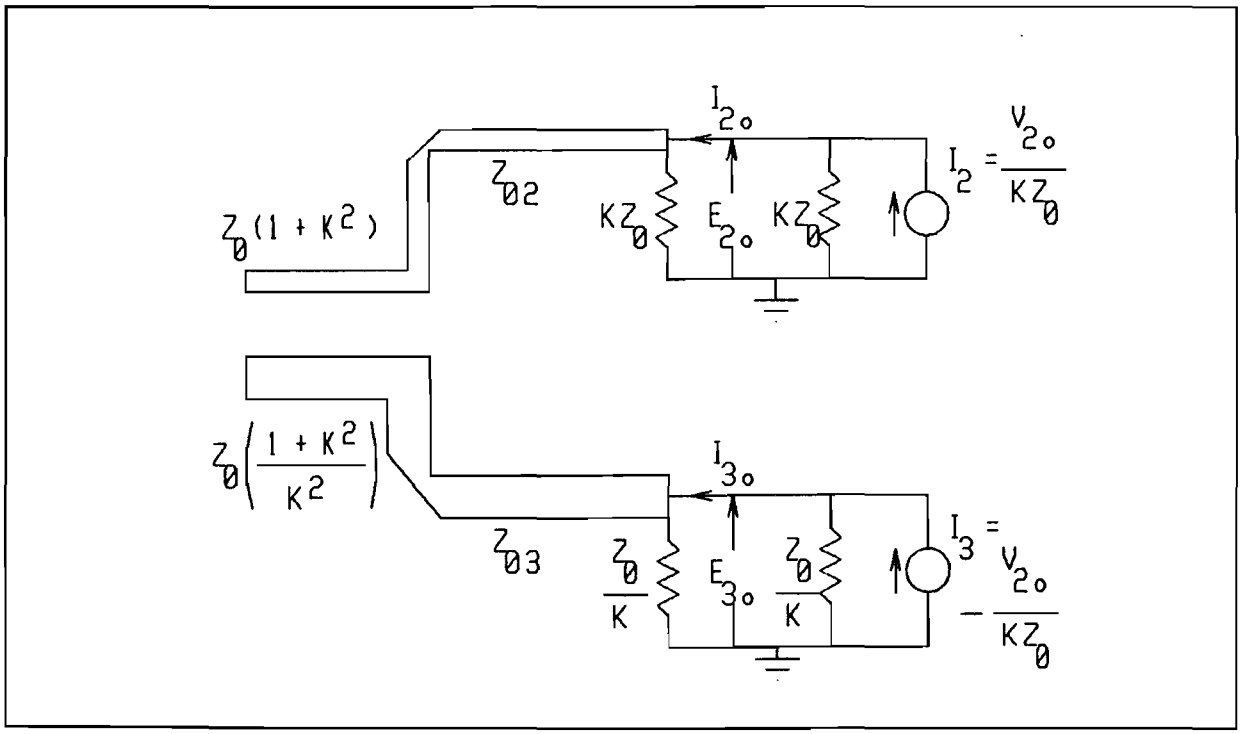

Fig. E.2 - Equivalent circuit for odd excitation

The voltage at port 2 is calculated as follows:

$$E_{2o} = (I_2 - I_{2o}) \cdot K \cdot Z_0 \qquad \text{(E.15a)}$$

$$E_{2o} = \frac{V_{2o}}{K \cdot Z_0} \cdot K \cdot Z_0 - E_{2o} \cdot Y_{2o} \cdot K \cdot Z_0 \qquad \text{(E.15b)}$$

$$E_{2o} = \frac{V_{2o}}{1 + K \cdot Y_{2o} \cdot Z_0} \qquad \text{(E.15c)}$$

with:

$$Y_{2o} = \frac{1}{K \cdot Z_0} + \frac{1}{Z_{2e}} \qquad \text{(E.15d)}$$

The admittance Y_{3o} is given by:

$$Y_{3o} = \frac{K}{Z_0} + \frac{1}{Z_{3e}} = \frac{K}{Z_0} + \frac{K^2}{Z_{2e}} = K^2 \cdot Y_{2o} \qquad (E.16)$$

and for the voltage at port 3 is found:

$$E_{3o} = - \frac{E_{2o}}{K^2} \qquad (E.17)$$

The current going into arm 2 is:

$$I_{2in} = I_{2o} - \frac{E_{2o}}{K \cdot Z_0} = E_{2o} \cdot Y_{2o} - \frac{E_{2o}}{K \cdot Z_0} = E_{2o} \cdot \left(Y_{2o} - \frac{E_{2o}}{K \cdot Z_0} \right) \qquad (E.18)$$

and the current going into arm 3 is:

$$I_{3in} = I_{3o} - \frac{E_{3o} \cdot K}{Z_0} = E_{3o} \cdot \left(Y_{3o} - \frac{K}{Z_0} \right) = - \frac{E_{2o}}{K^2} \cdot \left(K^2 \cdot Y_{2o} - \frac{K}{Z_0} \right) =$$

$$= - E_{2o} \cdot \left(Y_{2o} - \frac{1}{K \cdot Z_0} \right) = - I_{2in} \qquad (E.19)$$

So when the two circuits of figure F.2 are joined together, no current flows into port 1. When the two circuits are joined together, the admittance Y_{2o} has to change. Y_{2o} becomes, with equation (E.12) ($z_1 = 0$):

$$Y_{2o} = \frac{1}{K \cdot Z_0} + \frac{1}{j \cdot Z_0 \cdot \sqrt{K \cdot (1 + K^2)} \cdot \tan(\vartheta)} \qquad (E.20)$$

The voltage at the point where the resistors $R_1 = K \cdot Z_0$ and

$R_2 = \frac{Z_0}{K}$ are connected remains zero, so for the odd excitation, the voltages and currents are given by equations (E.15c), (E.17), (E.20) and:

$$I_{2o} = \frac{V_{2o} \cdot Y_{2o}}{1 + K \cdot Y_{2o} \cdot Z_0} \quad , \quad I_{3o} = - I_{2o} \tag{E.21}$$

E.3 - Short Transmission Line Between Generator Resistance and Load

Figure E.3 shows a generator with characteristic impedance Z_1, connected to a transmission line of length l with characteristic impedance Z_0. The transmission line is terminated with a load Z_L.

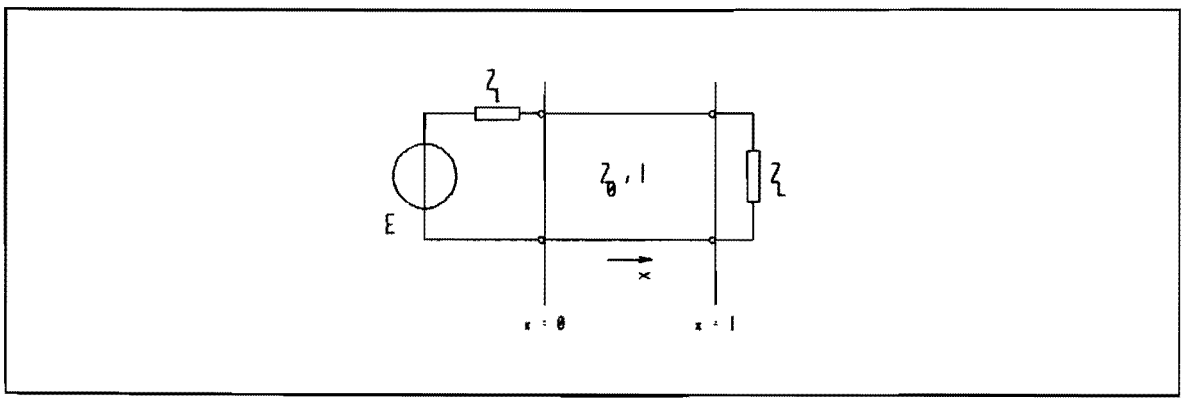

Fig. E.3 - Generator connected to terminated transmission line

The voltages at x = 0 and x = l are:

$$U(0) = E - Z_1 \cdot I(0) \tag{E.22a}$$

$$U(l) = Z_L \cdot I(l) \tag{E.22b}$$

The voltage and current at position x are given by [E-4]:

$$U(x) = A \cdot e^{-\gamma \cdot x} + B \cdot e^{+\gamma \cdot x} \qquad \text{(E.23a)}$$

$$I(x) = \frac{A}{Z_0} \cdot e^{-\gamma \cdot x} - \frac{B}{Z_0} \cdot e^{+\gamma \cdot x} \qquad \text{(E.23b)}$$

A is the amplitude of the voltage wave traveling in positive x-direction, B is the amplitude of the voltage wave traveling in negative x-direction.
Substitution of (E.22) in (E.23) leads to:

$$B = \frac{Z_L - Z_0}{Z_L + Z_0} \cdot e^{-2 \cdot \gamma \cdot l} = \Gamma \cdot e^{-2 \cdot \gamma \cdot l} \qquad \text{(E.24a)}$$

$$A = \frac{E}{\left(1 + \Gamma \cdot e^{-2 \cdot \gamma \cdot l}\right) + \frac{Z_l}{Z_0} \cdot \left(1 - \Gamma \cdot e^{-2 \cdot \gamma \cdot l}\right)} \qquad \text{(E.24b)}$$

For l approaching to zero:

$$\lim_{l \downarrow 0} A = \frac{E}{1 + \frac{Z_l}{Z_0}} \qquad \text{(E.25)}$$

If the characteristic impedance of the transmission line (that does not really exist) is chosen to be equal to the generator impedance, the amplitude of the voltage wave entering the load is E / 2.

E.4 - References

[E-1] Montgomery C.G., ' *Principles of Microwave Circuits* ', McGraw-Hill Book Company, Inc., 1948, pp.137-149.

[E-2] Ramo S., Whinnery J.R., Van Duzer T., ' *Fields and Waves in Communication Electronics* ', John Wiley, 1984, pp.528-529.

[E-3] Parad L.I., Moynihan R.L., ' *Split-Tee Power Divider* ', IEEE Trans. on Microwave Theory and Techniques, January 1965, pp.91-95.

[E-4] Versnel W., ' *Microgolftechniek* ', Professional Group Electromagnetism and Circuit Theory, Department of Electrical Engineering, Eindhoven University of Technology, Netherlands (in Dutch).

Appendix F - T Power Splitter

For the even and odd excitation, the results of the even and odd excitation of the Wilkinson power splitter can be used: Z_{02} is replaced by $\alpha \cdot Z_0$, the generator impedances are Z_0 and K=1. The isolation resistor is removed. This results in:

$$I_{2e} = \frac{V_{2e}}{Z_0 + Z_{2e}} \quad , \quad E_{2e} = \frac{Z_{2e} \cdot V_{2e}}{Z_0 + Z_{2e}} \tag{F.1a}$$

$$Z_{2e} = \alpha \cdot Z_0 \cdot \frac{2 + j \cdot \alpha \cdot \tan(\vartheta)}{\alpha + j \cdot 2 \cdot \tan(\vartheta)} \tag{F.1b}$$

$$I_{3e} = I_{2e} \quad , \quad E_{3e} = E_{2e} \tag{F.1c}$$

and for the odd excitation:

$$E_{2o} = \frac{V_{2o}}{1 + Y_{2o} \cdot Z_0} \quad , \quad I_{2o} = \frac{V_{2o} \cdot Y_{2o}}{1 + Y_{2o} \cdot Z_0} \tag{F.2a}$$

$$Y_{2o} = \frac{1}{j \cdot \alpha \cdot Z_0 \cdot \tan(\vartheta)} \tag{F.2b}$$

$$E_{3o} = - E_{2o} \quad , \quad I_{3o} = - I_{2o} \tag{F.2c}$$

Appendix G - Computer Program Listings

On the next pages the listings of the computer programs that are used to calculate antenna characteristics are stated. All programs are written in PASCAL. The programs developed at the start of the research are written in TURBO PASCAL 3.0 and converted to TURBOPASCAL 4.0. The programs developed later on during the research are written in MS-PASCAL. The advantages of MS-PASCAL over TURBO PASCAL are its better DOS-compatibility, its better error-reporting and its ability to emulate a numerical coprocessor.
All programs can be run on a (4.77MHz) XT. For the directivity calculations it is recommended to run the programs on a machine that is much faster, like the IBM PS-2 computer model 60 or model 80.
Since the programs are written in "standard" PASCAL (no specific TURBO PASCAL or MS PASCAL options are used), with little effort the programs can be converted for use on a micro computer (eg VAX).

G.1 Program FREQSCAN

The program FREQSCAN calculates the radiation pattern of an array of circular microstrip patches, excited in the TM_{11} mode, subdivided in co- and crosspolarization as function of the angle ϑ, for a given angle φ. It also calculates the axial ratio of the array as function of the angle ϑ, for a given angle φ.
If the array is elecronically scanned, the radiation pattern will be normalized to the unscanned boresight radiation, to visualise the scan loss.

For using the program, the user has to make a text file containing the array information. Every row of this text file contains the information of one microstrip patch:

x-coordinate (in m)	y-coordinate (in m)	rotation (in ^{0})	phase shift (in ^{0})

For example the array of figure G.1 is described by:

-0.10	0.10	0	0
0.10	0.10	90	90
-0.10	-0.10	90	90
0.10	-0.10	0	0

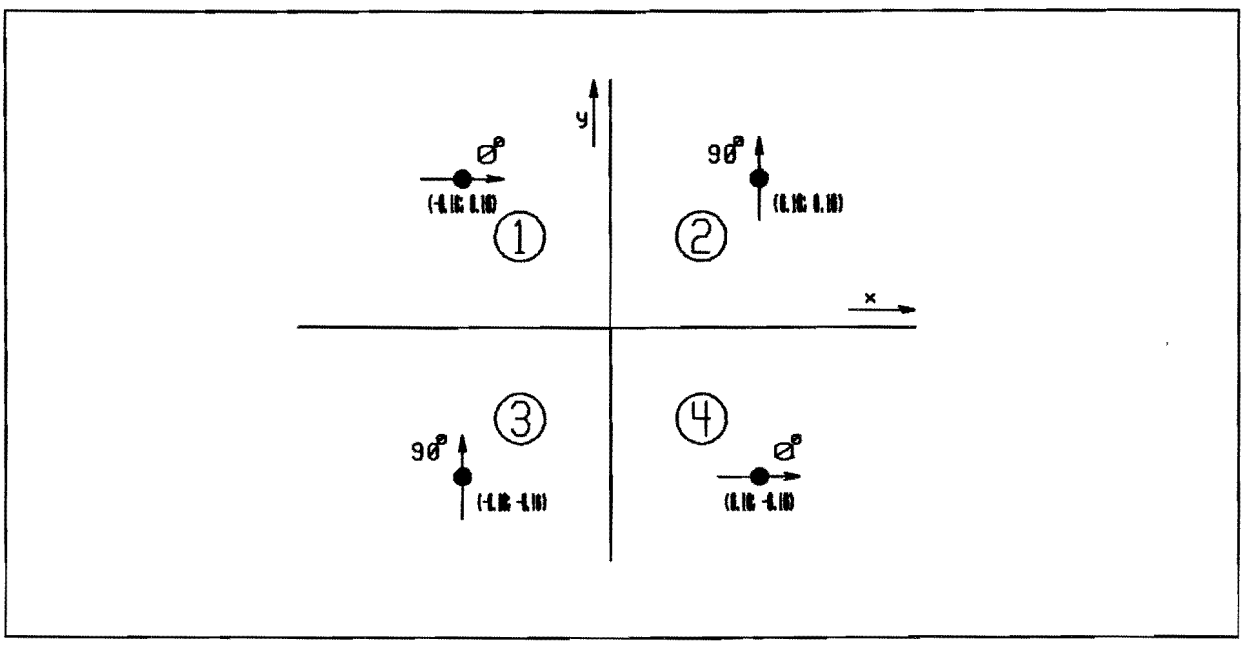

Fig. G.1 - 2x2 sequentially rotated array of linearly polarized elements

The results of the calculation are stored in a user defined output text file and can be shown in graphics on the screen.

The program will ask the user for the following information:

```
Lambda                          :
Epsr                            :
Input File                      :
Plane Phi in Degrees            :
Lowerbound Theta (Degrees)      :
Upperbound Theta (Degrees)      :
Step Size Theta  (Degrees)      :
Output File                     :
```

```
Plot Radiation Pattern (Y/N) :
Title                        :
Print (Y/N)                  :
Plot Axial Ratio (Y/N)       :
Print (Y/N)                  :
```

The calculations are as follows:

The angle dependent parts of E_ϑ and E_φ are given by:

$$E_\vartheta \quad - \cos(\varphi)\cdot\left\{J_0(\, k_0 a\sin(\vartheta)\,) - J_2(\, k_0 a\sin(\vartheta)\,)\right\} = - \cos(\varphi)\cdot F_1(\vartheta) \tag{G.1a}$$

$$E_\varphi \quad \cos(\vartheta)\sin(\varphi)\cdot\left\{J_0(\, k_0 a\sin(\vartheta)\,) + J_2(\, k_0 a\sin(\vartheta)\,)\right\} = \\ = \cos(\vartheta)\sin(\varphi)\cdot F_2(\vartheta) \tag{G.1b}$$

There are N elements, each having a position (x_i, y_i), a rotation ψ_i and a phase shift Ψ_i. The contribution of one element to the field is (see also figure G.2):

$$\bar{E}_i \quad \left[- \cos(\varphi - \psi_i)\cdot F_1(\vartheta)\cdot\bar{a}_\vartheta + \cos(\vartheta)\sin(\varphi - \psi_i)\cdot F_2(\vartheta)\cdot\bar{a}_\varphi\right]\cdot \\ \cdot e^{jk_0\cdot\sin(\vartheta)\cdot(x_i\cdot\cos(\varphi)+y_i\cdot\sin(\varphi))}\cdot e^{j\Psi_i} \tag{G.2}$$

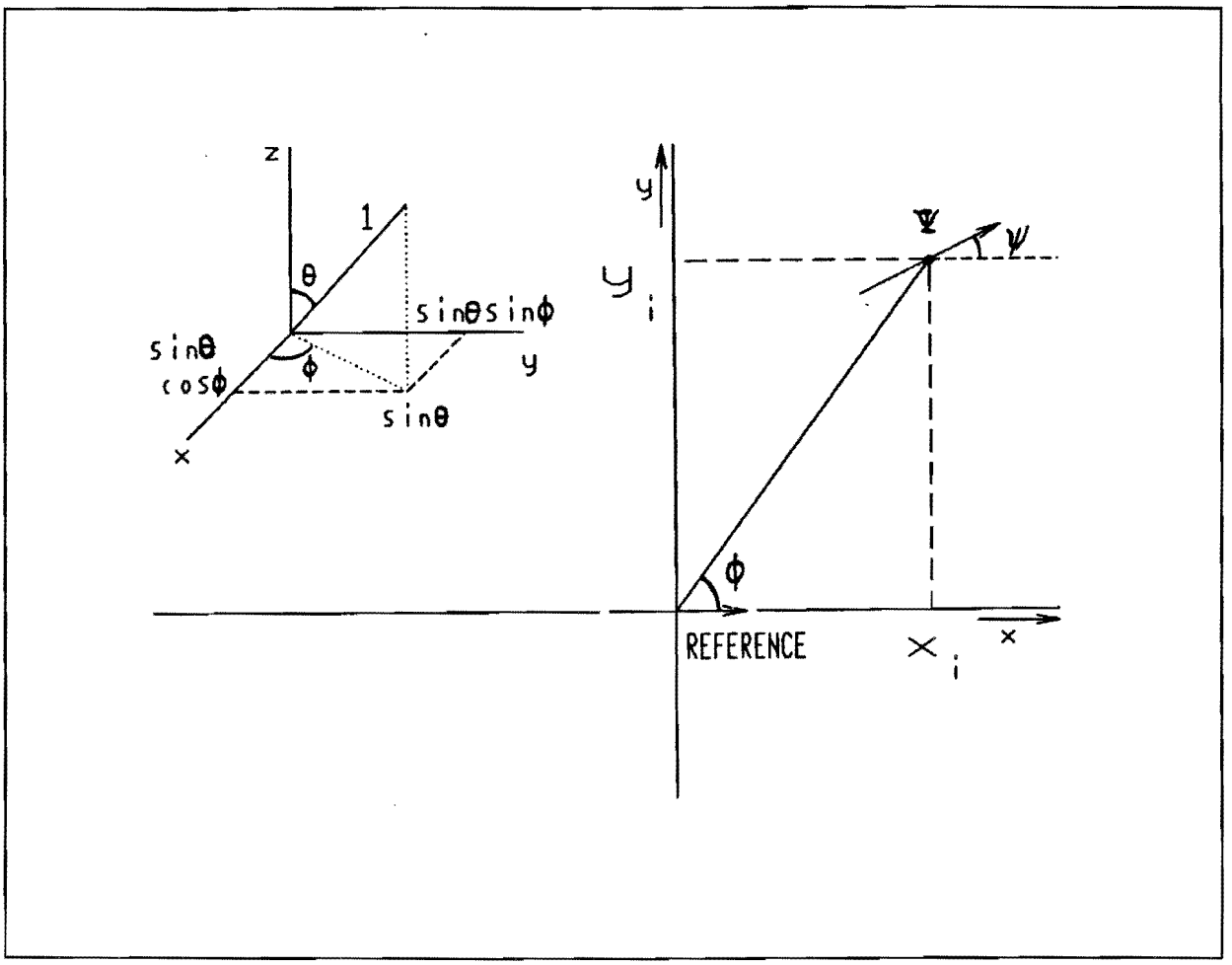

Fig. G.2 - Linear polarized element in coordinate system

The summed contributions, split up in ϑ- and φ-components are given by:

$$E_{\vartheta} \sum_{i=1}^{N} - F_1(\vartheta)\cdot\cos(\varphi - \psi_i)\cdot\cos\left\{k_0\sin(\vartheta)\left[x_i\cos(\varphi) + y_i\sin(\varphi)\right] + \Psi_i\right\}$$

$$+ j\cdot\sum_{i=1}^{N} - F_1(\vartheta)\cdot\cos(\varphi - \psi_i)\cdot\sin\left\{k_0\sin(\vartheta)\left[x_i\cos(\varphi) + y_i\sin(\varphi)\right] + \Psi_i\right\} \quad \text{(G.3a)}$$

$$E_{\varphi} \sum_{i=1}^{N} F_2(\vartheta)\cdot\cos(\vartheta)\cdot\sin(\varphi - \psi_i)\cdot$$

$$\cdot\cos\left\{k_0\sin(\vartheta)\left[x_i\cos(\varphi) + y_i\sin(\varphi)\right] + \Psi_i\right\} +$$

$$+ j\cdot\sum_{i=1}^{N} F_2(\vartheta)\cdot\cos(\vartheta)\cdot\sin(\varphi - \psi_i)\cdot$$

$$\cdot\sin\left\{k_0\sin(\vartheta)\left[x_i\cos(\varphi) + y_i\sin(\varphi)\right] + \Psi_i\right\} \qquad \text{(G.3b)}$$

In the above formulas the exponent is split up in real and imaginary part for the ease of programming.
The electric field can be written as a combination of a right hand circularly polarized part and a left hand circularly polarized part:

$$\bar{E} = E_R\cdot\bar{a}_R + E_L\cdot\bar{a}_L \qquad \text{(G.4a)}$$

with:

$$E_R = \frac{1}{\sqrt{2}}\cdot(E_\vartheta + jE_\varphi) \qquad \bar{a}_R = \frac{1}{\sqrt{2}}\cdot(\bar{a}_\vartheta - j\bar{a}_\varphi) \qquad \text{(G.4b)}$$

$$E_L = \frac{1}{\sqrt{2}}\cdot(E_\vartheta - jE_\varphi) \qquad \bar{a}_L = \frac{1}{\sqrt{2}}\cdot(\bar{a}_\vartheta + j\bar{a}_\varphi) \qquad \text{(G.4c)}$$

With (G.3) and (G.4) can be found:

$$|E_\vartheta \mp jE_\varphi|^2 \quad \left[\sum_{i=1}^{N} - F_1(\vartheta)\cdot\cos(\varphi - \psi_i)\cdot\right.$$

$$\cdot\cos\left\{k_0\sin(\vartheta)\cdot\left[x_i\cos(\varphi) + y_i\sin(\varphi)\right] + \Psi_i\right\} +$$

$$\pm F_2(\vartheta)\cdot\cos(\vartheta)\cdot\sin(\varphi - \psi_i)\cdot$$

$$\left.\cdot\sin\left\{k_0\sin(\vartheta)\cdot\left[x_i\cos(\varphi) + y_i\sin(\varphi)\right] + \Psi_i\right\}\right]^2 +$$

$$+\left[\sum_{i=1}^{N} - F_1(\vartheta)\cdot\cos(\varphi - \psi_i)\cdot \right.$$
$$\cdot\sin\left\{k_0\sin(\vartheta)\cdot\left[x_i\cos(\varphi) + y_i\sin(\varphi)\right] + \Psi_i\right\} +$$
$$\mp F_2(\vartheta)\cdot\cos(\vartheta)\cdot\sin(\varphi - \psi_i)\cdot$$
$$\left.\cdot\cos\left\{k_0\sin(\vartheta)\cdot\left[x_i\cos(\varphi) + y_i\sin(\varphi)\right] + \Psi_i\right\}\right]^2 \qquad (G.5)$$

This formula gives the co- and crosspolarization, with the crossspalarization being the smallest of the two for $(\vartheta = \vartheta_{scan},\ \varphi = \varphi_{scan})$.
The next pages give the (TURBO) PASCAL listing of the program that calculates (G.5). The radiation patterns are normalized to the copolarization for $\vartheta = 0$.
The radius of the patch will be calculated in a first approximation by:

$$a = 1.84118\cdot\frac{\lambda}{\sqrt{\varepsilon_r}\cdot 2\pi} \qquad (G.6)$$

The axial ratio is calculated with:

$$AR_{dB} = 20\cdot\log\left|\frac{|E_L| + |E_R|}{|E_L| - |E_R|}\right| \quad (dB) \qquad (G.7)$$

```
{$R-} {Range checking off}
{$B+} {Boolean complete evaluation on}
{$S+} {Stack checking on}
{$I+} {I/O checking on}
{$N-} {No numeric coprocessor}
{$M 65500,16384,655360} {Turbo 3 default stack and heap}

program FREQSCAN(input, output);

{************************************************************
 *                                                          *
 * Program to calculate the radiation pattern, divided in   *
 * copolarization ( full line ) en crosspolarization        *
 * ( dashed line ) and the axial ratio of an array          *
 * consisting of circular shaped microstrip patches.        *
 *                                                          *
 * The user is asked to generate an input-textfile with     *
 * the characteristics of the array in the following        *
 * format:                                                  *
 * A line for each patch/element containing:                *
 * 1) X-coordinate (m), 2) Y-coordinate (m),                *
 * 3) Element-rotation (degr.), 4) Element-phase-shift      *
 *    (degr.).                                              *
 *                                                          *
 * The program further asks for the wavelength, the die-    *
 * lectric constant, the plane Phi to be shown and the      *
 * boundaries and stepize of the angle Theta.               *
 *                                                          *
 * The results of the calculations are written to a text-   *
 * file and can be shown graphically.                       *
 *                                                          *
 ************************************************************}

   Uses   Dos, Crt, GDriver, GKernel, GWindow, GShell;

   Const
       Pi = 3.141592654;
       MaxArray = 256;
       Inf = 1000; {Infinite}

   Type
       ArrayType = array [1..MaxArray] of real;

       {Graphic specific types}
       LimitType =
           Record
               Left, bottom, right, top: integer
           end;
       Ttype = string [40];
       Str76 = string [76];
       {End Graphic specific types}

   Var
       Lambda, Epsr, A, Theta, Phi, Norm, Step, LowerB, UpperB, FF1,
       FF2: Real;
       N, i: integer;
       Xi, Yi, Ai, Bi, Ci: arrayType;  {Ai=rotation, Bi=phase}
       Invoer, Uitvoer: text;
       FName: string [40];

       {Graphic specific vars}
       PlotRHCPow, PlotLHCPow, PlotAxial, PlotTemp: PlotArray;
       Title: WrkString;
       Limits: LimitType;
       Print: boolean;
       C: char;
       {End Grphic Specific Vars}

   {$I Bessel.fnc}


   Function F1(Theta: Real): Real;
       Begin
           F1 := BessJ0(((2 * Pi) / Lambda) * A * Sin(Theta)) - BessJ(2,
                 ((2 * Pi) / Lambda) * A * Sin(Theta))
       End; {F1}
```

```
Function F2(Theta: Real): Real;
    Begin
        F2 := BessJ0(((2 * Pi) / Lambda) * A * Sin(Theta)) + BessJ(2,
              ((2 * Pi) / Lambda) * A * Sin(Theta))
    End; {F2}


Function Arg(i: Integer;
             Theta, Phi: Real): Real; {Element phase}
    Begin
        Arg := (2 * Pi / Lambda) * Sin(Theta) * (Xi[i] * Cos(Phi) +
               Yi[i] * Sin(Phi)) + Bi[i]
    End; {Arg}


Function RightHandArg1(i: Integer;
                       Theta, Phi: Real): Real; {First part RHC-argument}
    Begin
        RightHandArg1 := - FF1 * Cos(Phi - Ai[i]) * Cos(Arg(i, Theta,
                         Phi)) - FF2 * Cos(Theta) * Sin(Phi - Ai[i]) *
                         Sin(Arg(i, Theta, Phi))
    End; {RightHandArg1}


Function LefthandArg1(i: Integer;
                      Theta, Phi: Real): Real; {First part LHC-argument}
    Begin
        LeftHandArg1 := - FF1 * Cos(Phi - Ai[i]) * Cos(Arg(i, Theta,
                        Phi)) + FF2 * Cos(Theta) * Sin(Phi - Ai[i]) *
                        Sin(Arg(i, Theta, Phi))
    End; {LeftHandArg1}


Function RightHandArg2(i: Integer;
                       Theta, Phi: Real): Real; {2nd part RHC-argument}
    Begin
        RightHandArg2 := - FF1 * Cos(Phi - Ai[i]) * Sin(Arg(i, Theta,
                         Phi)) + FF2 * Cos(Theta) * Sin(Phi - Ai[i]) *
                         Cos(Arg(i, Theta, Phi))
    End; {RightHandArg2}


Function LeftHandArg2(i: Integer;
                      Theta, Phi: Real): Real; {2nd part LHC-argument}
    Begin
        LeftHandArg2 := - FF1 * Cos(Phi - Ai[i]) * Sin(Arg(i, Theta,
                        Phi)) - FF2 * Cos(Theta) * Sin(Phi - Ai[i]) *
                        Cos(Arg(i, Theta, Phi))
    End; {LeftHandArg2}


Function CalcNormRHC: Real; {RHC-power for Theta=0}

    Var
        i: Integer;
        Sum1, Sum2: Real;
    Begin
        Sum1 := 0;
        Sum2 := 0;
        FF1 := 1; {Theta:=0}
        FF2 := 1; {Theta:=0}
        For i := 1 To N Do
            Begin
                Ci[i] := Bi[i]; {Saving phaseshift}
                Bi[i] := Ai[i]; {No scanning}
                Sum1 := Sum1 + RightHandArg1(i, 0, Phi);
                Sum2 := Sum2 + RightHandArg2(i, 0, Phi);
                Bi[i] := Ci[i] {Restoring phaseshift}
            End;
        CalcNormRHC := Sqr(Sum1) + Sqr(Sum2)
    End; {CalcNormRHC}
```

```
Function CalcNormLHC: Real; {LHC-power for Theta=0}

    Var
        i: Integer;
        Sum1, Sum2: Real;
    Begin
        Sum1 := 0;
        Sum2 := 0;
        FF1 := 1; {Theta:=0}
        FF2 := 1; {Theta:=0}
        For i := 1 To N Do
            Begin
                Ci[i] := Bi[i]; {Saving phaseshift}
                Bi[i] := Ai[i]; {No scanning}
                Sum1 := Sum1 + LeftHandArg1(i, 0, Phi);
                Sum2 := Sum2 + LeftHandArg2(i, 0, Phi);
                Bi[i] := Ci[i] {Restoring phaseshift}
            End;
        CalcNormLHC := Sqr(Sum1) + Sqr(Sum2)
    End; {CalcNormLHC}


Function RHCPow(Theta, Phi: Real): Real; {RHC-power(Theta, Phi)}

    Var

        i: Integer;
        Sum1, Sum2: Real;
    Begin
        Sum1 := 0;
        Sum2 := 0;
        For i := 1 To N Do
            Begin
                Sum1 := Sum1 + RightHandArg1(i, Theta, Phi);
                Sum2 := Sum2 + RightHandArg2(i, Theta, Phi)
            End;
        RHCPow := 10 * ln((Sqr(Sum1) + Sqr(Sum2)) / Norm) / ln(10)
                  {Normalized RHC-power in dB}
    End; {RHCPow}


Function LHCPow(Theta, Phi: Real): Real; {LHC-power(Theta, Phi)}

    Var
        i: Integer;
        Sum1, Sum2, Temp: Real;
    Begin
        Sum1 := 0;
        Sum2 := 0;
        For i := 1 to N Do
            Begin
                Sum1 := Sum1 + LeftHandArg1(i, Theta, Phi);
                Sum2 := Sum2 + LeftHandArg2(i, Theta, Phi)
            End;
        Temp := (Sqr(Sum1) + Sqr(Sum2)) / Norm; {Nomalized LHC-power}
        If Temp <= 0 Then {In case of numerical round off error}
            LHCPow := - Inf
        Else
            LHCPow := 10 * ln(Temp) / ln(10)
            {Normalized LHC-power in dB}
    End; {LHCPow}
```

```
Procedure ReadTable(Var Xi, Yi, Ai, Bi: ArrayType;
                    Var N: Integer); {Read input file }

    Var
        FName: string [40];
        i: Integer;
    Begin
        Write('Input File                : ');
        Readln(FName);
        Assign(Invoer, FName);
        Reset(Invoer);
        i := 0;
        While Not Eof(invoer) Do
            Begin
                i := i + 1;
                ReadLn(Invoer, Xi[i], Yi[i], Ai[i], Bi[i]);
                Ai[i] := (Pi / 180) * Ai[i]; {Conversion degr.-rad}
                Bi[i] := (Pi / 180) * Bi[i]  {Conversion degr.-rad}
            End;
        N := i {Number of array-elements}
    End; {Readtable}


{Begin Graphic Specific Area}

Procedure PolygonDrawRad(Title: WrkString;
                         Limits: LimitType;
                         N: Integer); {Drawing of the radiation patterns}

    Var
        J: Integer;
        Ch: Char;
        X1, X2: Integer;
    Begin
        ClearScreen;
        DefineWindow(1, 0, 0, XMaxGlb, YMaxGlb);
        With Limits Do
            DefineWorld(1, Left - 2, Bottom, Right, Top + 5);

        SelectWorld(1);
        SelectWindow(1);
        SetBackground(0);
        DrawBorder;
        DrawAxis(5, 5, 0, 0, 0, 0, 0, 0, true); {Draw the axes}
        If CalcNormRHC >= CalcNormLHC Then  {In case of RHC polarization}
            SetLineStyle(0) {Full line}
        Else
            SetLinestyle(2); {Dashed line}
        DrawPolygon(PlotRHCPow, 1, - N, 0, 0, 0); {Draw the polygon}

        AxisGlb := true;


        If CalcNormRHC >= CalcNormLHC Then {In case of RHC polarization}
            SetLineStyle(2) {Dashed line}
        Else
            SetLinestyle(0); {Full line}
        DrawPolygon(PlotLHCPow, 1, - N, 0, 0, 0); {Draw the polygon}

        With Limits Do
            DrawTextW(Left + ((Right - Left - Length(Title)) div 2),
                      Bottom + 2, 1, Title)

    End; {PolygonDrawRad}
```

```
Procedure PolygonDrawAxRat(Title: WrkString;
                      Limits: LimitType;
                      N: Integer);

    Var
        J: Integer;
        Ch: Char;
        X1, X2: Integer;
    Begin
        ClearScreen;
        DefineWindow(1, 0, 0, XMaxGlb, YMaxGlb);
        With Limits Do
            DefineWorld(1, Left - 2, Bottom, Right, Top + 5);

        SelectWorld(1);
        SelectWindow(1);
        SetBackground(0);
        DrawBorder;
        DrawAxis(5, 5, 0, 0, 0, 0, 0, 0, true); {Draw the axes}
        SetLineStyle(0); {Full line}
        DrawPolygon(PlotAxial, 1, - N, 0, 0, 0); {Draw the polygon}
        With Limits Do
            DrawTextW(Left + ((Right - Left - Length(Title)) div 2),
                      Bottom + 2, 1, Title)

    End; {PolygonDrawAxRat}
{End Graphics specific area}

Begin
    Write('Lambda                    : ');
    Readln(Lambda);
    Write('Epsr                      : ');
    Readln(Epsr);
    Writeln;
    A := 1.841 * (Lambda / (Sqrt(Epsr) * 2 * Pi)); {Diameter patch}
    ReadTable(Xi, Yi, Ai, Bi, N); {Arraycharacteristics}
    Write('Plane Phi in Degrees      : ');
    ReadLn(Phi);
    Writeln;
    Phi := (Pi / 180) * Phi; {Rad}
    Write('Lowerbound Theta (Degrees) : ');
    ReadLn(LowerB);
    Write('Upperbound Theta (Degrees) : ');
    ReadLn(UpperB);
    Write('Step size Theta (Degrees)  : ');
    ReadLn(Step);
    Writeln;
    Write('Output file               : ');
    ReadLn(Fname);
    Assign(Uitvoer, FName);
    Rewrite(Uitvoer);
```

```
If CalcNormRHC > CalcNormLHC Then {In case of RHC polarization}
    Begin
        Norm := CalcNormRHC;
        Writeln(Uitvoer, 'Polarization Righthand Circular')
    End
Else If CalcNormRHC = CalcNormLHC Then {In case of linear polariz.}
    Begin
        Norm := CalcNormRHC; {Arbitrary}
        Writeln(Uitvoer, 'Polarization Linear')
    End
Else  {In case of LHC polarization}
    Begin
        Norm := CalcnormLHC;
        Writeln(Uitvoer, 'Polarization Lefthand Circular')
    End;
Writeln(Uitvoer);
Writeln(Uitvoer);
WriteLn(Uitvoer, 'Lambda          = ', Lambda: 6: 3, ' m');
WriteLn(Uitvoer, 'Epsr            = ', Epsr: 6: 3);
WriteLn(Uitvoer, 'Radius patch    = ', A: 6: 3, ' m');
WriteLn(Uitvoer);
Writeln(Uitvoer);
WriteLn(Uitvoer, 'Antenna': 8, ' ': 4, 'X', ' ': 8, 'Y', ' ': 7,
        'Rot', ' ': 5, 'Phase', ' ': 5, 'R');
WriteLn(Uitvoer);
Writeln(Uitvoer);
For i := 1 To N Do
    Begin
        WriteLn(Uitvoer, i: 3, ' ': 5, Xi[i]: 7: 3, '  ', Yi[i]: 7: 3,
                '  ', (180 / Pi) * Ai[i]: 7: 3, '  ',
                (180 / Pi) * Bi[i]: 7: 3, '  ', A: 7: 3)
    End;
WriteLn(Uitvoer);
Writeln(Uitvoer);
WriteLn(Uitvoer, 'Phi = ', Phi * (180 / Pi): 6: 3, ' Degrees');
WriteLn(Uitvoer);
Writeln(Uitvoer);
If CalcNormRHC >= CalcNormLHC Then {In case of RHC polarization}
    WriteLn(Uitvoer, 'Theta', ' ': 9, 'CoPol', ' ': 14, 'CrossPol',
            ' ': 11, 'Axial Ratio')
Else
    WriteLn(Uitvoer, 'Theta', ' ': 7, 'CrossPol', ' ': 14, 'CoPol',
            ' ': 13, 'Axial Ratio');
WriteLn(UitVoer, '(Degrees)', ' ': 4, ' (dB)', ' ': 17, '(dB)', ' ':
        17, '(dB)');
WriteLn(Uitvoer);
Theta := LowerB;
i := 1;
While (Theta <= UpperB) And (i <= MaxPlotGlb) Do
    Begin
        Writeln('Theta=', Theta: 7: 3);
        FF1 := F1((Pi / 180) * Theta);
        FF2 := F2((Pi / 180) * Theta);

        {begin Graphics Changed area}
        PlotRHCPow[i, 1] := Theta;
        PlotRHCPow[i, 2] := RHCPow((Pi / 180) * Theta, Phi);
        PlotLHCPow[i, 1] := Theta;
        PlotLHCPow[i, 2] := LHCPow((Pi / 180) * Theta, Phi);
        PlotAxial[i, 1] := Theta;
        If (Abs(exp(ln(10) * PlotRHCPow[i, 2] / 20)) - Abs(exp(ln(10) *
           PlotLHCPow[i, 2] / 20))) = 0 Then
            PlotAxial[i, 2] := Inf {Denominator AxRat = 0}
        Else
```

```
            Begin
                If PlotRHCPow[i, 2] ( - 200 Then {To big a Real}
                    PlotTemp[i, 2] := - 200
                Else
                    PlotTemp[i, 2] := PlotRHCPow[i, 2];
                    {Protection PlotRHCPow}
                PlotAxial[i, 2] := Abs((Abs(exp(ln(10) *
                                                PlotTemp[i, 2] /
                                        20)) + Abs(exp(ln(10) *
                                        PlotLHCPow[i, 2] / 20))) /
                                        (Abs(exp(ln(10) *
                                                PlotTemp[i, 2] /
                                             20)) - Abs(exp(ln(10) *
                                        PlotLHCPow[i, 2] / 20))));
                            { Abs( Abs(El)+Abs(Er)/Abs(El)-Abs(Er) ) }
                PlotAxial[i, 2] := 20 * ln(PlotAxial[i, 2]) / ln(10)
                {Axial Ratio in dB}
            End;
        WriteLn(Uitvoer, Theta: 5: 1, ' ': 5, PlotRHCPow[i, 2]: 10: 4,
                ' ': 10, PlotLHCPow[i, 2]: 10: 4, ' ': 10,
                PlotAxial[i, 2]: 10: 4);
        i := i + 1;
        {end graphics Changed area}

        Theta := Theta + Step
    End;

{Begin Graphics specific area 3}
Repeat
    Write('Plot Radiation Pattern (Y/N) : ');
    Readln(C);
    If C In ['y', 'Y'] Then
        Begin
            Write('Title                          : ');
            Readln(Title);
            Limits.left := round(LowerB);
            Limits.bottom := - 60; {dB}
            Limits.right := round(UpperB);
            Limits.top := 0;
            Write('Print (Y/N)                    : ');
            readln(C);
            Print := C In ['y', 'Y'];
            InitGraphic; {Initialize graphics}
            PolygonDrawRad(Title, Limits, i - 1);
            If Print Then
                HardCopy(False, 1);
            Repeat
            Until KeyPressed;
```

```
                LeaveGraphic;
                C := 'Y'
            End;
    Until C In ['n', 'N'];
    Repeat
        Write('Plot Axial Ratio (Y/N)       : ');
        Readln(C);
        If C In ['y', 'Y'] Then
            Begin
                Title := ' AXIAL RATIO ';
                Limits.left := round(LowerB);
                Limits.bottom := 0;
                Limits.right := round(UpperB);
                Limits.top := 15; {dB}
                Write('Print (Y/N)                  : ');
                readln(C);
                Print := C In ['y', 'Y'];
                InitGraphic; {Initialize graphics}
                PolygonDrawAxRat(Title, Limits, i - 1);
                If Print Then
                    HardCopy(False, 1);
                Repeat
                until KeyPressed;
                LeaveGraphic;
                C := 'Y'
            End;
    Until C in ['n', 'N'];
    {End Graphic specific area 3}

    Close(Uitvoer)
End.
```

G.2 - Program POLARAX

The program POLARAX is a modified version of program FREQSCAN. The Axial Ratio (dB) is calculated and for the polar plot the x-component becomes AR*Cos(Phi) and the y-component becomes AR*Sin(Phi).
The changed part of the program is shown on the next page.

```
Begin
    Write('Lambda                    : ');
    Readln(Lambda);
    Write('Epsr                      : ');
    Readln(Epsr);
    Writeln;
    A := 1.841 * (Lambda / (Sqrt(Epsr) * 2 * Pi)); {Diameter patch}
    ReadTable(Xi, Yi, Ai, Bi, N); {Arraycharacteristics}
    Write('Plane Theta in Degrees    : ');
    Readln(Theta);
    Writeln;
    Theta := (Pi / 180) * Theta; {Rad}
    Write('Lowerbound Phi   (Degrees) : ');
    ReadLn(LowerB);
    Write('Upperbound Phi   (Degrees) : ');
    ReadLn(UpperB);
    Write('Step size Phi    (Degrees)  : ');
    ReadLn(Step);
    Writeln;
    Write('Output file               : ');
    ReadLn(Fname);
    Assign(Uitvoer, FName);
    Rewrite(Uitvoer);
```

```
Begin
    If PlotRHCPow[i, 2] < - 200 Then {To big a Real}
        PlotTemp[i, 2] := - 200
    Else
        PlotTemp[i, 2] := PlotRHCPow[i, 2];
        {Protection PlotRHCPow}
    PlotAxTemp[i, 1] := Abs((Abs(exp(ln(10) *
                                PlotTemp[i, 2] /
                        20)) + Abs(exp(ln(10) *
                        PlotLHCPow[i, 2] / 20))) /
                        (Abs(exp(ln(10) *
                                PlotTemp[i, 2] /
                            20)) - Abs(exp(ln(10) *
                        PlotLHCPow[i, 2] / 20))));
            { Abs( Abs(El)+Abs(Er)/Abs(El)-Abs(Er) ) }
    PlotAxTemp[i, 2] := PlotAxTemp[i, 1];
    PlotAxial[i, 1] := (20 * ln(PlotAxTemp[i, 1]) / ln(10))
                    * Cos((Pi / 180) * Phi);
    {Horizontal component}
    PlotAxial[i, 2] := (20 * ln(PlotAxTemp[i, 2]) / ln(10))
                    * Sin((Pi / 180) * Phi);
    {Vertical component}
    {Axial Ratio in dB in polar coordinates}

    PlotAxTemp[i, 1] := Abs( Abs(FF1 + Cos(Theta) * FF2) +
                            Abs(FF1 - Cos(Theta) * FF2) )
                    /
                    Abs( Abs(FF1 + Cos(Theta) * FF2) -
                            Abs(FF1 - Cos(Theta) * FF2) ); {Axial Ratio element}
    PlotAxTemp[i, 2] := PlotAxTemp[i, 1];

    PlotAxel[i, 1] := (20 * ln(PlotAxTemp[i, 1]) / ln(10))
                    * Cos((Pi / 180) * Phi);
    {Horizontal component}
    PlotAxel[i, 2] := (20 * ln(PlotAxTemp[i, 2]) / ln(10))
                    * Sin((Pi / 180) * Phi);
    {Vertical component}
    {Axial Ratio element in dB in polar coordinates}
End;
WriteLn(Uitvoer, Phi: 5: 1, ' ': 9, PlotAxial[i, 1]: 10: 4,
        ' ': 11, PlotAxial[i, 2]: 10: 4, ' ': 5,
        PlotAxel[i, 1]: 10: 4, ' ':4, PlotAxel[i, 2]: 10: 4);
i := i + 1;
```

G.3 Program Directiv

The program DIRECTIV calculates the directivity or the gain of a rectangular array of circularly polarized microstrip antennas for different element spacings. The results are stored in a user defined output text file. The user is asked for the following information:

Frequency	:
Epsr	:
M	: Number of patches in one coordinate
N	: Number of patches in other coordinate
Efficiency	:1 for calculating the directivity
Output File	:
Number of iterations	:

The directivity of a rectangular array consisting of circularly polarized patches is given by:

$$D = \frac{4\pi \cdot \left(F_1^2(0) + F_2^2(0) \right) \cdot M^2 \cdot N^2}{\int_0^{\frac{\pi}{2}} \int_0^{2\pi} \left(F_1^2(\vartheta) + \cos^2(\vartheta) F_2^2(\vartheta) \right) \cdot \frac{\sin^2\left(\frac{\pi}{\lambda} M d_x T_x\right)}{\sin^2\left(\frac{\pi}{\lambda} d_x T_x\right)} \cdot \frac{\sin^2\left(\frac{\pi}{\lambda} N d_y T_y\right)}{\sin^2\left(\frac{\pi}{\lambda} d_y T_y\right)} \cdot \sin(\vartheta) \, d\vartheta \, d\varphi} \qquad (G.8)$$

The program DIRECTIV calculates the directivity for 10 steps of d/λ, starting at a d of two times the radius of the patch (the minimum possible element spacing) and ending for $d/\lambda = 1$ (the distance from which grating lobes start to occur).
The radius of the patch is calculated with:

$$a = 1.84118 \cdot \frac{\lambda}{\sqrt{\varepsilon_r} \cdot 2\pi} \qquad (G.9)$$

The double integral is calculated with the Monte Carlo Integration Method.
In this method N points are uniformly randomly chosen in the integration surface. Then the integral of a function f over the surface S is approximated by:

$$\iint f \cdot dS \approx S \cdot \langle f \rangle \pm S \cdot \sqrt{\frac{\langle f^2 \rangle - \langle f \rangle^2}{N}} \qquad (G.10a)$$

with:

$$\langle f \rangle = \frac{1}{N} \cdot \sum_{i=1}^{N} f(x_i) \qquad (G.10b)$$

and:

$$\langle f^2 \rangle = \frac{1}{N} \cdot \sum_{i=1}^{N} f^2(x_i) \qquad (G.10c)$$

The second term in (G.10a) is a one standard deviation error estimate for the integral and should be taken only as a rough indication of probable error.

The (MS) PASCAL program listing is given on the following pages.
The other directivities can be calculated by modified versions of this program. As an example the listing of the program that calculates the directivity of a circular array of linearly polarized patches is given too (DIRECTI3).

```
{$Real:8}
Program DIRECTIV (Input, Output);

Const
   Pi = 3.14159265;
   C0 = 3E8;

Var
   j, P : integer;
   gliy:integer4;
   idum : integer4;
   glir: ARRAY [1..97] OF integer4;
   sw, VarW, Phi, Theta, IntValue, IntErrorest, a, k0, dx, dy,
   M, N, Lambda, freq, Epsr, effic, D, Surf, Gain, Stepd: real;
   Uitvoer: Text;
   FName: String(40);

FUNCTION ran2(VAR idum: integer4): real; {Random generator}
(* Programs using RAN2 must declare the following variables
VAR
   gliy: integer;
   glir: ARRAY [1..97] OF integer;
in the main program. *)
CONST
   ia=1366;
   ic=150889;
   rm=1.400512e-6;      (* 1.0/m *)
VAR
   j: integer;
   m: integer4;

BEGIN
   m:=714025;
   IF (idum < 0) THEN BEGIN
      idum := (ic-idum) MOD m;
      FOR j := 1 to 97 DO BEGIN
         idum := (ia*idum+ic) MOD m;
         glir[j] := idum
      END;
      idum := (ia*idum+ic) MOD m;
      gliy := idum
   END;
   j := trunc(1 + (97*gliy) DIV m);
   IF ((j > 97) OR (j < 1)) THEN BEGIN
      writeln('pause in routine RAN2'); readln
   END;
   gliy := glir[j];
   ran2 := gliy*rm;
   idum := (ia*idum+ic) MOD m;
   glir[j] := idum
END; {Ran2}

{$INCLUDE: 'Bessel.fnc'}

Function F1(Theta: Real):Real;
Begin
  F1 := BessJ0(k0 * a * sin(Theta)) - BessJ(2, k0 * a * Sin(Theta))
End; {F1}

Function F2(Theta: Real):Real;
Begin
  F2 := BessJ0(k0 * a * sin(Theta)) + BessJ(2, k0 * a * Sin(Theta))
End; {F2}
```

```
Function f(Phi, Theta: Real): Real; {integrand}
Var
  T1, T2: Real;
Begin
  T1 := Sqr( Sin( (Pi / Lambda) * M * dx * Sin(Theta) * Cos(Phi) ) ) /
        Sqr( Sin( (Pi / Lambda)  * dx * Sin(Theta) * Cos(Phi) ) );
  T2 := Sqr( Sin( (Pi / Lambda) * N * dy * Sin(Theta) * Sin(Phi) ) ) /
        Sqr( Sin( (Pi / Lambda)  * dy * Sin(Theta) * Sin(Phi) ) );
  f := T1 * T2 * ( Sqr(F1(Theta)) + Sqr( Cos(Theta) * F2(Theta) )) *Sin(Theta);
End;


Begin

   Write('Frequency             : '); Readln(freq);
   Write('Epsr                  : '); Readln(Epsr);
   Write('M                     : '); Readln(M);
   Write('N                     : '); Readln(N);
   Write('Efficiency            : '); Readln(effic);
   Write('Output file           : '); Readln(FName);
   Assign(Uitvoer, Fname);
   Rewrite(Uitvoer);

   a:= (1.84118 * C0) / (2 * Pi * freq * Sqrt(Epsr) ); {radius patch}
   dx := 2 * a; {Minimum element spacing}
   dy := 2 * a; {Minimum element spacing}
   Lambda := C0 / freq;
   k0 := 2 * Pi / Lambda;
   Stepd := (Lambda - 2 * a) / 10; {10 distance steps}
   Writeln(Uitvoer, 'Frequency    = ',freq:9:5);
   Writeln(Uitvoer, 'Epsr         = ',Epsr:9:5);
   Writeln(Uitvoer, 'M            = ',M:3:2);
   Writeln(Uitvoer, 'N            = ',N:3:2);
   Writeln(Uitvoer, 'Efficiency   = ',effic:9:5);
   Writeln(Uitvoer, 'Radius patch = ',a:8:4);
   Writeln(Uitvoer);
   Writeln(Uitvoer);
   Writeln(Uitvoer, ' ':4, 'd/lmbda', ' ':4, 'Gain (dB)', ' ':6, 'Intvalue',
             ' ':8, 'Standev');

   Write('Number of iterations : '); Readln(P);
```

```
  While dx <= Lambda Do Begin
    dy := dx;

    {MONTE CARLO INTEGRATION}
    idum:= -1964;     {initialization Random Generator}
    sw := 0;
    VarW := 0;
    Surf := Sqr(Pi);  {integration 'surface'}
    For j := 1 To P Do Begin
      Write(j:3, ' ');
      Phi := 2 * Pi * Ran2(idum);
      Theta := (Pi / 2) * Ran2(idum);
      sw := sw + f(Phi, Theta);
      VarW := VarW + Sqr(f(Phi, Theta))
    End;
    IntValue := Surf * (sw / P);
    IntErrorest := Surf * Sqrt((VarW / P - Sqr(sw / P)) / P);
    {END MONTE CARLO INTEGRATION}

    D := 4 * Pi * Sqr(M) * Sqr(N) * ( (Sqr(F1(0)) + Sqr(F2(0))) / IntValue);

    Gain := 10 * ln(effic * D) / ln(10); {Gain in dB}
    Writeln(Uitvoer, ' ',(dx / Lambda):5:2, ' ':8, Gain:5:2, ' ':10, IntValue:8:4,
            ' ':7, IntErrorest:8:4);
    dx := dx + Stepd
  End;
  Close(Uitvoer)
End.
```

```
{$Real:8}
Program DIRECTI3 (Input, Output);

Const
   Pi = 3.14159265;
   C0 = 3E8;

Var
   j, P , counter, N: integer;
   gliy:integer4;
   idum : integer4;
   glir: ARRAY [1..97] OF integer4;
   sw, VarW, Phi, Theta, IntValue, IntErrorest, a, k0, d,
   Lambda, freq, Epsr, effic, DD, Surf, Gain, Stepd: Real;
   Uitvoer: Text;
   FName: String[40];

FUNCTION ran2(VAR idum: integer4): real; {Random generator}
(* Programs using RAN2 must declare the following variables
VAR
   gliy: integer;
   glir: ARRAY [1..97] OF integer;
in the main program. *)
CONST
   ia=1366;
   ic=150889;
   rm=1.400512e-6;      (* 1.0/m *)
VAR
   j: integer;
   m: integer4;

BEGIN
   m:=714025;
   IF (idum < 0) THEN BEGIN
      idum := (ic-idum) MOD m;
      FOR j := 1 to 97 DO BEGIN
         idum := (ia*idum+ic) MOD m;
         glir[j] := idum
      END;
      idum := (ia*idum+ic) MOD m;
      gliy := idum
   END;
   j := trunc(1 + (97*gliy) DIV m);
   IF ((j > 97) OR (j < 1)) THEN BEGIN
      writeln('pause in routine RAN2'); readln
   END;
   gliy := glir[j];
   ran2 := gliy*rm;
   idum := (ia*idum+ic) MOD m;
   glir[j] := idum
END; {Ran2}

{$INCLUDE: 'Bessel.fnc'}

Function F1(Theta: Real):Real;
Begin
  F1 := BessJ0(k0 * a * sin(Theta)) - BessJ(2, k0 * a * Sin(Theta))
End; {F1}

Function F2(Theta: Real):Real;
Begin
  F2 := BessJ0(k0 * a * sin(Theta)) + BessJ(2, k0 * a * Sin(Theta))
End; {F2}

Function Phii(i: Integer): Real;
Begin
  Phii := (1 + 4 * i) * (Pi / N)
End;   {Phii}
```

```
Function SumA(N: Integer; Phi, Theta, d: Real): Real;
Var
  i: Integer;
  r, SumHelp: Real;
Begin
  r := 0.5 * d * (1 / sin(Pi / N));
  SumHelp := 0;
  For i := 0 To ((N - 2) Div 2) Do
  SumHelp := SumHelp + Cos( (2 * Pi / Lambda) * r * Sin(Theta) *
             Cos(Phi - Phii(i)) );
  SumA := SumHelp
End;   {SumA}

Function SumB(N: Integer; Phi, Theta, d: Real): Real;
Var
  i: Integer;
  r, SumHelp: Real;
Begin
  r := 0.5 * d * (1 / sin(Pi / N));

  SumHelp := 0;
  For i := 0 To ((N - 2) Div 2) Do
  SumHelp := SumHelp + Sin( (2 * Pi / Lambda) * r * Sin(Theta) *
             Cos(Phi - Phii(i)) );
  SumB := SumHelp
End;   {SumB}


Function SumC(N: Integer; Phi, Theta, d: Real): Real;
Var
  i: Integer;
  r, SumHelp: Real;
Begin
  r := 0.5 * d * (1 / sin(Pi / N));
  SumHelp := 0;
  For i := 0 To ((N - 2) Div 2) Do
  SumHelp := SumHelp + Cos( (2 * Pi / Lambda) * r * Sin(Theta) *
             Cos(Phi - Phii(i) - (2 * Pi / N)) );
  SumC := SumHelp
End;   {SumC}


Function SumD(N: Integer; Phi, Theta, d: Real): Real;
Var
  i: Integer;
  r, SumHelp: Real;
Begin
  r := 0.5 * d * (1 / sin(Pi / N));
  SumHelp := 0;
  For i := 0 To ((N - 2) Div 2) Do
  SumHelp := SumHelp + Sin( (2 * Pi / Lambda) * r * Sin(Theta) *
             Cos(Phi - Phii(i) - (2 * Pi / N)) );
  SumD := SumHelp
End;   {SumD}

Function f(Phi, Theta: Real): Real; {integrand}
Var
  T1, T2, T3, T4, T5, T6: Real;
Begin
  T1 := Sqr(Cos(Phi)) * Sqr(F1(Theta)) + Sqr(Sin(Phi)) * Sqr(Cos(Theta)) *
        Sqr(F2(Theta));
  T2 := 2 * Sqr(SumA(N, Phi, Theta, d)) + 2 * Sqr(SumB(N, Phi, Theta, d));
  T3 := Sqr(Sin(Phi)) * Sqr(F1(Theta)) + Sqr(Cos(Phi)) * Sqr(Cos(Theta)) *
        Sqr(F2(Theta));
  T4 := 2 * Sqr(SumC(N, Phi, Theta, d)) + 2 * Sqr(SumD(N, Phi, Theta, d));
  T5 := Sqr(F1(Theta)) - Sqr(Cos(Theta)) * Sqr(F2(Theta));
  T6 := 4 * Sin(Phi) * Cos(Phi) * ( SumB(N, Phi, Theta, d) *
        SumC(N, Phi, Theta, d) - SumA(N, Phi, Theta, d) *
        SumD(N, Phi, Theta, d));
  f := (T1 * T2 + T3 * T4 + T5 * T6) * Sin(Theta)
  End;   {f}
```

```
Begin

   Write('Frequency            : '); Readln(freq);
   Write('Epsr                 : '); Readln(Epsr);
   Write('N                    : '); Readln(N);
   Write('Efficiency           : '); Readln(effic);
   Write('Output file          : '); Readln(FName);
   Assign(Uitvoer, Fname);
   Rewrite(Uitvoer);

   a:= (1.84118 * C0) / (2 * Pi * freq * Sqrt(Epsr) ); {radius patch}
   d := 2 * a; {Minimum element spacing}
   Lambda := C0 / freq;
   k0 := 2 * Pi / Lambda;
   Stepd := (Lambda - 2 * a) / 10; {10 distance steps}
   counter := 1; {initialization distance step counter}
   Writeln(Uitvoer, 'Frequency    = ',freq:9:5);
   Writeln(Uitvoer, 'Epsr         = ',Epsr:9:5);
   Writeln(Uitvoer, 'N            = ',N:2);
   Writeln(Uitvoer, 'Efficiency   = ',effic:9:5);
   Writeln(Uitvoer, 'Radius patch = ',a:8:4);
   Writeln(Uitvoer);
   Writeln(Uitvoer);
   Writeln(Uitvoer,' ':4, 'd/lambda', ' ':4, 'Gain (dB)', ' ':6, 'Intvalue',
           ' ':8, 'Standev');

   Write('Number of iterations : '); Readln(P);

   While d <= Lambda Do Begin

     {MONTE CARLO INTEGRATION}
     idum:= -1964;     {initialization Random Generator}
     sw := 0;
     VarW := 0;
     Surf := Sqr(Pi);  {integration 'surface'}


    For j := 1 To P Do Begin
      Write(counter:2, '-', j:3, ' ');
      Phi := 2 * Pi * Ran2(idum);
      Theta := (Pi / 2) * Ran2(idum);
      sw := sw + f(Phi, Theta);
      VarW := VarW + Sqr(f(Phi, Theta))
    End;
    IntValue := Surf * (sw / P);
    IntErrorest := Surf * Sqrt((VarW / P - Sqr(sw / P)) / P);
    {END MONTE CARLO INTEGRATION}

    DD :=2 * Pi * Sqr(N) * ( (Sqr(F1(0)) + Sqr(F2(0))) / IntValue);

    Gain := 10 * ln(effic * DD) / ln(10); {Gain in dB}
    Writeln(Uitvoer, ' ',(d / Lambda):5:2, ' ':8, Gain:5:2, ' ':10, IntValue:8:4,
            ' ':7, IntErrorest:8:4);
    d := d + Stepd;
    counter := counter + 1
   End;
   Close(Uitvoer)
End.
```

G.4 - Program FEEDLOC

The program feedloc, that calculates the input impedance of a microstrip patch as function of the feed location is given on the next pages. The calculation is performed as described in chapter 5.

The following programs also need no further explanation and are directly stated.

```
{$R-}    {Range checking off}
{$B+}    {Boolean complete evaluation on}
{$S+}    {Stack checking on}
{$I+}    {I/O checking on}
{$N-}    {No numeric coprocessor}
{$M 65500,16384,655360} {Turbo 3 default stack and heap}

Program FEEDLOC (Input, Output);

Uses    Dos, Crt, GDriver, GKernel, GWindow, GShell;

Const   Pi    = 3.141592654;
        C0    = 3E8;
        Mu    = 1.25664E-6;
        Sigma = 5.8E7;
        ka    = 1.84118;

{Graphic Specific Types}
Type    LimitType = Record
                      Left, Bottom, Right, Top: Integer
                    End;
        TType     = String[40];
        Str76     = String[76];
{End Graphic Specific Types}

Var     Lambda, f, Epsr, h, delta, k, a, Step, LowerB, UpperB, ro,
        ae, I1, k0     : Real;
        i              : Integer;
        Invoer, Uitvoer: Text;
        FName          : String[40];

{Graphic Specific Vars}
        PlotR : PlotArray;
        Title : WrkString;
        Limits: LimitType;
        Print : Boolean;
        C     : Char;
{End Graphic Specific Vars}

{$I Bessel.fnc}



Function F1(Theta: Real): Real;
Begin   F1:= BessJ0(k0*a*Sin(Theta))-BessJ(2,k0*a*Sin(Theta))
End;{F1}


Function F2(Theta: Real): Real;
Begin   F2:= BessJ0(k0*a*Sin(Theta))+BessJ(2,k0*a*Sin(Theta))
End;{F2}


Function fx(x: Real): Real;
Begin   fx:= x*Sqrt( (1+((2*h)/(Pi*x*Epsr))*(ln((Pi*x)/(2*h))+1.7726)) )-ae
End;{fx}
```

```
Function func(x: Real): Real;
Begin   func:= ( Sqr(F1(x))+Sqr(Cos(x))*Sqr(F2(x)) )*Sin(x)
End;{func}


{$I QGaus.pas}
{$I RtSec.pas}


Function R(ro: Real): Real;
Var     RR: Real;
Begin   RR:= (Sqr(h*k0*a)*I1)/(1920*(Sqr(ka)-1))+
             1/(8*Sqrt(Pi*Sigma*f*f*f*Mu*Mu*Mu))+
             (h*delta)/(8*Mu*f);
        RR:= 1/RR;
        R:= (RR*Sqr(h)*Sqr(BessJ1(k*ro)))/(2*(Sqr(ka)-1)*Sqr(BessJ1(ka)))
End;{R}


Procedure Polygondraw(Title: WrkString; Limits: LimitType; N: Integer);
Var     J     : Integer;
        Ch    : Char;
        X1, X2: Integer;
Begin   ClearScreen;
        DefineWindow(1, 0, 0, XMaxGlb, YMaxGlb);
        With Limits Do DefineWorld(1, Left-0.01, Bottom, Right, Top+5);
        SelectWorld(1);
        SelectWindow(1);
        SetBackground(0);
        DrawBorder;

        DrawAxis(5, 5, 0, 0, 0, 0, 0, 0, True);
        SetLineStyle(0);
        DrawPolygon(PlotR, 1, -N, 0, 0, 0);
        With Limits Do
        DrawTextW(Left+((Right-Left-Length(Title)) Div 2), Bottom+0.2, 1, Title)
End;{PolygonDraw}


Begin   Write('f  (in GHz)         : '); Readln(f);
        f:= f*1E9;
        Lambda:= C0/f;
        k0:=2*Pi/Lambda;
        Write('Epsr                : '); Readln(Epsr);
        k:=Sqrt(Epsr)*k0;
        Write('h  (in mm)          : '); Readln(h);
        h:= h/1000;
        Write('tan(delta)          : '); Readln(delta);
        Writeln;
        Write('Output file         : '); Readln(FName);
        Assign(Uitvoer, FName); Rewrite(Uitvoer);
        Writeln;
        Writeln;
        Writeln;

        ae:= (ka*C0)/(2*Pi*f*Sqrt(Epsr));
        a:= RtSec(0.001, 1.99*ae, 1E-6);
        Writeln('Succeeded in finding radius patch');
        Writeln;
```

```
        Writeln(Uitvoer);
        Writeln(Uitvoer,'frequency      : ', (f/1E9):8:4, ' GHz');
        Writeln(Uitvoer,'Epsr           : ', Epsr:8:4);
        Writeln(Uitvoer,'h              : ', (h*1000):8:4, ' mm');
        Writeln(Uitvoer,'tan(delta)     : ', delta:9:5);
        Writeln(Uitvoer);
        Writeln(Uitvoer,'Radius patch   : ', a:9:5, ' m');
        Writeln(Uitvoer);
        Writeln(Uitvoer);
        Writeln(Uitvoer);
        Writeln(Uitvoer);
        Writeln(Uitvoer,' ':3,'ro/a', ' ':16, 'R (Ohm)');
        Writeln(Uitvoer);

        QGaus(0, Pi, I1);
        Writeln('Integration completed');
        Writeln;
        Writeln;

        LowerB:= 0.01*a; UpperB:= a;
        Step:= 0.01*a;
        i:= 1;
        ro:= LowerB;
        While (ro <= UpperB) And (i <= MaxPlotGlb) Do
        Begin   PlotR[i, 1]:= ro/a;
                PlotR[i, 2]:= R(ro);
                Writeln(Uitvoer, PlotR[i, 1]:8:4, ' ':13, PlotR[i, 2]:8:4);
                Writeln('ro/a = ',PlotR[i,1]:8:4);
                i:= i+1;
                ro:= ro+Step
        End;

{Begin Graphic Specific Area}
        Repeat   Write('Plot R vs ro/a  (Y/N) : '); Readln(C);
                 If C in ['y', 'Y'] Then
                 Begin   Title:= 'R AS FUNCTION OF FEED LOCATION';
                         Limits.left:= 0;
                         Limits.bottom:= 0;
                         Limits.right:= 1;
                         Limits.top:= 100;
                         Write('Print  (Y/N)          : '); Readln(C);
                         Print:= C in ['y', 'Y'];
                         InitGraphic;
                         PolygonDraw(Title, Limits, i-1);
                         If Print Then HardCopy(False, 1);
                         Repeat Until KeyPressed;
                         LeaveGraphic;
                         C:= 'Y'
                 End;
        Until C in ['n', 'N'];
{End Graphic Specific Area}

        Close(Uitvoer)
End.
```

G.5 - Program STANWAVE

```
{$R-}    {Range checking off}
{$B+}    {Boolean complete evaluation on}
{$S+}    {Stack checking on}
{$I+}    {I/O checking on}
{$N-}    {No numeric coprocessor}
{$M 65500,16384,655360} {Turbo 3 default stack and heap}

Program STANWAVE (Input, Output);

Uses    Dos, Crt, GDriver, GKernel, GWindow, GShell;

Const   Pi    = 3.141592654;
        CO    = 3E8;
        Mu    = 1.25664E-6;
        Sigma = 5.8E7;
        ka    = 1.84118;

{Graphic Specific Types}
Type    LimitType = Record
                      Left, Bottom, Right, Top: Integer
                    End;
        TType     = String[40];
        Str76     = String[76];
{End Graphic Specific Types}

Var     Lambda, f, fr, Epsr, h, delta, k, a, Step, LowerB, UpperB, ro,
        ae, Il, w, RR, QQ, AA, BB, L, C, k0: Real;
        i                                   : Integer;
        Invoer, Uitvoer                     : Text;
        FName                               : String[40];

{Graphic Specific Vars}
        PlotRefl, PlotVSWR : PlotArray;
        Title              : WrkString;
        Limits             : LimitType;
        Print              : Boolean;
        D                  : Char;
{End Graphic Specific Vars}

{$I Bessel.fnc}



Function F1(Theta: Real): Real;
Begin   F1:= BessJ0(k0*a*Sin(Theta))-BessJ(2,k0*a*Sin(Theta))
End;{F1}


Function F2(Theta: Real): Real;
Begin   F2:= BessJ0(k0*a*Sin(Theta))+BessJ(2,k0*a*Sin(Theta))
End;{F2}


Function fx(x: Real): Real;
Begin   fx:= x*Sqrt( (1+((2*h)/(Pi*x*Epsr))*(ln((Pi*x)/(2*h))+1.7726)) )-ae
End;{fx}


Function func(x: Real): Real;
Begin   func:= ( Sqr(F1(x))+Sqr(Cos(x))*Sqr(F2(x)) )*Sin(x)
End;{func}


{$I QGaus.pas}
{$I RtSec.pas}


Function R(f: Real): Real;
Var     R1: Real;
Begin   R1:= (Sqr(h*k0*a)*Il)/(1920*(Sqr(ka)-1))+
             1/(8*Sqrt(Pi*Sigma*f*f*f*Mu*Mu*Mu))+
             (h*delta)/(8*Mu*f);
        R1:= 1/R1;
        R:= (R1*Sqr(h)*Sqr(BessJ1(k*ro)))/(2*(Sqr(ka)-1)*Sqr(BessJ1(ka)))
End;{R}
```

```
Function Q(f: Real): Real;
Var     Q1: Real;
Begin   Q1:= 1/(h*Sqrt(Pi*f*Mu*Sigma))+delta+
             (h*Mu*f*Sqr(k0*a)*I1)/(240*(Sqr(ka)-1));
        Q:= 1/Q1
End;{Q}



Function A1(w: Real): Real;

Begin   A1:= (Sqr(w*L)*RR)/(Sqr(RR-Sqr(w)*L*RR*C)+Sqr(w*L))
End;{A}



Function B(w: Real): Real;
Begin   B:= (w*L*RR*(RR-Sqr(w)*L*RR*C))/(Sqr(RR-Sqr(w)*L*RR*C)+Sqr(w*L))
End;{B}

Procedure Polygondraw1(Title: WrkString; Limits: LimitType; N: Integer);
Var     J     : Integer;
        Ch    : Char;
        X1, X2: Integer;
Begin   ClearScreen;
        DefineWindow(1, 0, 0, XMaxGlb, YMaxGlb);
        With Limits Do DefineWorld(1, Left-0.01, Bottom, Right, Top+0.25);
        SelectWorld(1);
        SelectWindow(1);
        SetBackground(0);
        DrawBorder;
        DrawAxis(5, 5, 0, 0, 0, 0, 0, 0, True);
        SetLineStyle(0);
        DrawPolygon(PlotRefl, 1, -N, 0, 0, 0);
        With Limits Do
        DrawTextW(Left+((Right-Left-Length(Title)) Div 2), Bottom+0.4, 1, Title)
End;{PolygonDraw1}

Procedure Polygondraw2(Title: WrkString; Limits: LimitType; N: Integer);
Var     J     : Integer;
        Ch    : Char;
        X1, X2: Integer;
Begin   ClearScreen;
        DefineWindow(1, 0, 0, XMaxGlb, YMaxGlb);
        With Limits Do DefineWorld(1, Left-0.01, Bottom, Right, Top+2);
        SelectWorld(1);
        SelectWindow(1);
        SetBackground(0);
        DrawBorder;
        DrawAxis(5, 5, 0, 0, 0, 0, 0, 0, True);
        SetLineStyle(0);
        DrawPolygon(PlotVSWR, 1, -N, 0, 0, 0);
        With Limits Do
        DrawTextW(Left+((Right-Left-Length(Title)) Div 2), Bottom+2, 1, Title)
End;{PolygonDraw2}


Begin   Write('fr  (in GHz)        : '); Readln(fr);
        fr:= fr*1E9;
        Write('Epsr                : '); Readln(Epsr);
        Write('h  (in mm)          : '); Readln(h);
        h:= h/1000;
        Write('tan(delta)          : '); Readln(delta);
        Write('ro (fraction of a)  : '); Readln(ro);
        Writeln;
        Write('Output file         : '); Readln(FName);
        Assign(Uitvoer, FName); Rewrite(Uitvoer);
        Writeln;
        Writeln;
        Writeln;

        ae:= (ka*C0)/(2*Pi*fr*Sqrt(Epsr));
        a:= RtSec(0.001, 1.99*ae, 1E-6);
        Writeln('Succeeded in finding radius patch');
        ro:= ro*a;
        Writeln;

        Writeln(Uitvoer);
        Writeln(Uitvoer,'frequency (res): ', (fr/1E9):8:4, ' GHz');
        Writeln(Uitvoer,'Epsr           : ', Epsr:8:4);
        k0:=(2*Pi*fr)/C0;
        Writeln(Uitvoer,'h              : ', (h*1000):8:4, ' mm');
        Writeln(Uitvoer,'tan(delta)     : ', delta:9:5);
```

```
        Writeln(Uitvoer);
        Writeln(Uitvoer,'Radius patch   : ', a:9:5, ' m');
        Writeln(Uitvoer,'ro             : ', (ro/a):9:5, '*a');
        Writeln(Uitvoer);
        Writeln(Uitvoer);
        Writeln(Uitvoer);
        Writeln(Uitvoer);
        Writeln(Uitvoer,' ':3,'f(GHz)', ' ':13, 'Refl', ' ':13, 'VSWR');
        Writeln(Uitvoer);

        LowerB:= 0.9*fr; UpperB:= 1.1*fr;

        Step:= 0.002*fr;
        f:= LowerB;
        i:= 1;
        While (f <= UpperB) And (i <= MaxPlotGlb) Do
        Begin   w:= 2*Pi*f;
                Lambda:= C0/(f*Sqrt(Epsr));
                k:=(2*Pi)/Lambda;
                QGaus(0, Pi, I1);
                Writeln('Integration completed');
                RR:= R(f);
                QQ:= Q(f);
                L:= RR/(2*Pi*fr*QQ);
                C:= QQ/(2*Pi*RR*fr);
                AA:= A1(w);
                BB:= B(w);

                PlotRefl[i, 1]:= (f/1E7);
                PlotRefl[i, 2]:= Sqrt(Sqr(AA-50)+Sqr(BB))/
                                 Sqrt(Sqr(AA+50)+Sqr(BB));
                PlotVSWR[i, 1]:= (f/1E7);
                PlotVSWR[i, 2]:= (1+PlotRefl[i, 2])/
                                 (1-PlotRefl[i, 2]);

                Writeln(Uitvoer,(f/1E9):9:5, ' ':10, PlotRefl[i, 2]:9:5,
                        ' ':10, PlotVSWR[i, 2]:9:5);

                Writeln('f(GHz) = ',(f/1E9):9:5);
                i:= i+1;
                f:= f+Step
        End;

{Begin Graphic Specific Area}
        Repeat   Write('Plot Reflection Factor  (Y/N) : '); Readln(D);
                 If D in ['y', 'Y'] Then
                 Begin   Title:= 'REFL AS FUNCTION OF F/Fr';
                         Limits.left:= Round(LowerB/1E7);
                         Limits.bottom:= 0;
                         Limits.right:= Round(UpperB/1E7);
                         Limits.top:= 1;
                         Write('Print  (Y/N)          : '); Readln(D);
                         Print:= D in ['y', 'Y'];
                         InitGraphic;
                         PolygonDraw1(Title, Limits, i-1);
                         If Print Then HardCopy(False, 1);
                         Repeat Until KeyPressed;
                         LeaveGraphic;
                         D:= 'Y'
                 End;
        Until D in ['n', 'N'];

        Repeat   Write('Plot Voltage Standing Wave Ratio  (Y/N) : ');
                 Readln(D);
                 If D in ['y', 'Y'] Then
                 Begin   Title:= 'VSWR';
                         Limits.left:= Round(LowerB/1E7);
                         Limits.bottom:= 0;
                         Limits.right:= Round(UpperB/1E7);
                         Limits.top:= 10;
                         Write('Print  (Y/N)          : '); Readln(D);
                         Print:= D in ['y', 'Y'];
                         InitGraphic;
                         PolygonDraw2(Title, Limits, i-1);
                         If Print Then HardCopy(False, 1);
                         Repeat Until KeyPressed;
                         LeaveGraphic;
                         D:= 'Y'
                 End;
        Until D in ['n', 'N'];
{End Graphic Specific Area}

        Close(Uitvoer)
End.
```

G.6 - Program WILKPOW1

```
{$Real:8}

Program WILKPOW1(Input, Output);

{*********************************************************************
 *                                                                   *
 *  This program calculates the outgoing powers of a Wilkinson       *
 *  Power Splitter as function of the frequency relative to the      *
 *  ingoing power with frequencydependant terminations.              *
 *  For every frequency the power balance will be checked.           *
 *                                                                   *
 *********************************************************************}

   Const
      Pi = 3.141592654;
      C0 = 3E8;
      Mu = 1.25664E-6;
      Sigma = 5.8E7;
      ka = 1.84118;
      MaxplotGlb = 256;

      {Graphic Specific Types}

   Type
      LimitType =
         Record
            Left, Bottom, Right, Top: Integer
         End;
      TType     = lString(40);
      Str76     = lString(76);
      PlotArray = Array [1..MaxPlotGlb, 1..2] of Real;
      {End Graphic Specific Types}

      Complex =
         Record
            r, j: real
         End;

   Var
      Lambda, f, fr, Epsr, h, delta, k, a, Step, LowerB, UpperB, ro, ae, I1,
      w, RR, QQ, AA, BB, L, C, k0: Real;
      i: Integer;
      Invoer, Uitvoer: Text;
      FName: String(40);
      S11, S12, S22, S23, Ro2, Ro3, RoA, d1, d2, d3, DelV, c2, c3: Complex;

      {Graphic Specific Vars}
      P1ret, P2, P3, Pdiss: PlotArray;
      {End Graphic Specific Vars}

      {$INCLUDE: 'Bessel.fnc'}


   procedure ComplAdd(C1, C2: Complex;
                      var Result: Complex);
      begin
         Result.r := C1.r + C2.r;
         Result.j := C1.j + C2.j
      end;


   procedure ComplSub(C1, C2: Complex;
                      var Result: Complex);
      begin
         Result.r := C1.r - C2.r;
         Result.j := C1.j - C2.j
      end;
```

```
procedure ComplMult(C1, C2: Complex;
                    var Result: Complex);
    begin
        Result.r := C1.r * C2.r - C1.j * C2.j;
        Result.j := C1.r * C2.j + C1.j * C2.r
    end;


procedure ComplDiv(C1, C2: Complex;
                   var Result: Complex);
    begin
        Result.r := (C1.r * C2.r + C1.j * C2.j) / (Sqr(C2.r) + Sqr(C2.j));
        Result.j := (C1.j * C2.r - C1.r * C2.j) / (Sqr(C2.r) + Sqr(C2.j))
    end;


function ComplMod(C: Complex): real;
    begin
        ComplMod := Sqrt(Sqr(C.r) + Sqr(C.j))
    end;


procedure ComplConj(var C: Complex);
    begin
        C.j := - C.j
    end;


Function F1(Theta: Real): Real;
    Begin
        F1 := BessJ0(k0 * a * Sin(Theta)) - BessJ(2, k0 * a * Sin(Theta))
    End; {F1}


Function F2(Theta: Real): Real;
    Begin
        F2 := BessJ0(k0 * a * Sin(Theta)) + BessJ(2, k0 * a * Sin(Theta))
    End; {F2}


Function fx(x: Real): Real;
    Begin
        fx := x * Sqrt((1 + ((2 * h) / (Pi * x * Epsr)) * (ln((Pi * x) /
                        (2 * h)) + 1.7726))) - ae
    End; {fx}


Function func(x: Real): Real;
    Begin
        func := (Sqr(F1(x)) + Sqr(Cos(x)) * Sqr(F2(x))) * Sin(x)
    End; {func}


Function Tan(X: Real): Real;
    Begin
        Tan := Sin(X) / Cos(X)
    End;

{$INCLUDE: 'QGaus.pas'}
{$INCLUDE: 'RtSec.pas'}


Function R(f: Real): Real;

    Var
        R1: Real;
    Begin
        R1 := (Sqr(h * k0 * a) * I1) / (1920 * (Sqr(ka) - 1)) + 1 / (8 *
              Sqrt(Pi * Sigma * f * f * f * Mu * Mu * Mu)) + (h * delta) /
              (8 * Mu * f);
        R1 := 1 / R1;
        R := (R1 * Sqr(h) * Sqr(BessJ1(k * ro))) / (2 * Sqr(BessJ1(ka)) *
             (Sqr(ka) - 1))
    End; {R}
```

```
Function Q(f: Real): Real;

    Var
        Q1: Real;
    Begin
        Q1 := 1 / (h * Sqrt(Pi * f * Mu * Sigma)) + delta + (h * Mu * f *
              Sqr(k0 * a) * I1) / (240 * (Sqr(ka) - 1));
        Q := 1 / Q1
    End; {Q}


Function A1(w: Real): Real;
    Begin
        A1 := (Sqr(w * L) * RR) / (Sqr(RR - Sqr(w) * L * RR * C) + Sqr(w *
              L))
    End; {A}


Function B(w: Real): Real;
    Begin
        B := (w * L * RR * (RR - Sqr(w) * L * RR * C)) / (Sqr(RR -
             Sqr(w) * L * RR * C) + Sqr(w * L))
    End; {B}


Procedure CalcS11(f: Real;
                  Var S11: Complex);

   Var
      T1, T2: Complex;
   Begin

      T1.r := - Sqrt(2);
      T1.j := 0;
      T2.r := 3 * Sqrt(2);
      T2.j := 4 * Tan((Pi / 2) * (f / fr));
      ComplDiv(T1, T2, S11)
   End;


Procedure CalcS22(f: Real;
                  Var S22: Complex);

   Var
      T1, T2: Complex;
   Begin
      T1.r := - 1;
      T1.j := 0;
      T2.r := 3 - 8 * Sqr(Tan((Pi / 2) * (f / fr)));
      T2.j := 8 * Sqrt(2) * Tan((Pi / 2) * (f / fr));
      ComplDiv(T1, T2, S22)
   End;


Procedure CalcS23(f: Real;
                  Var S23: Complex);

   var
      T1, T2: Complex;
   Begin
      T1.r := 2;
      T1.j := 2 * Sqrt(2) * Tan((Pi / 2) * (f / fr));
      T2.r := 3 - 8 * Sqr(Tan((Pi / 2) * (f / fr)));
      T2.j := 8 * Sqrt(2) * Tan((Pi / 2) * (f / fr));
      ComplDiv(T1, T2, S23)
   End;


Procedure CalcS12(f: Real;
                  Var S12: Complex);

   Var
      T1, T2, T3: Complex;
   Begin
      T2.r := 3 * Cos((Pi / 2) * (f / fr));
      T2.j := 2 * Sqrt(2) * Sin((Pi / 2) * (f / fr));
      T1.r := 2;
      T1.j := 0;
      ComplDiv(T1, T2, S12)
   End;
```

```
Procedure Calcd1(S11, S22, S23, S12, Ro2, Ro3: Complex;
                 Var d1: Complex);

    Var
        T1, T2, T3, T4, T5: Complex;
    Begin
        ComplMult(S22, S22, T4);
        ComplMult(S23, S23, T5);
        ComplSub(T4, T5, T1);
        ComplMult(Ro3, T1, T2);
        ComplMult(Ro2, T2, T1);
        ComplAdd(Ro2, Ro3, T2);
        ComplMult(S22, T2, T3);
        T2.r := - 1;
        T2.j := 0;
        ComplMult(T2, T3, T4);
        ComplAdd(T4, T1, T2);
        T1.r := 1;
        T1.j := 0;
        ComplAdd(T1, T2, T3);

        ComplSub(S22, S23, T1);
        ComplMult(Ro3, T1, T2);
        ComplMult(Ro2, T2, T1);
        T2.r := - 2;
        T2.j := 0;
        ComplMult(T2, T1, T4);
        ComplAdd(Ro2, Ro3, T1);
        ComplAdd(T1, T4, T2);
        ComplDiv(T2, T3, T1);

        ComplMult(S12, S12, T2);
        ComplMult(T2, T1, T3);

        ComplAdd(S11, T3, d1)
    End;

    Procedure Calcd2(S22, S23, S12, Ro2, Ro3: Complex;
                     Var d2: Complex);

        Var
            T1, T2, T3, T4, T5: Complex;
        Begin
            ComplMult(S22, S22, T4);
            ComplMult(S23, S23, T5);
            ComplSub(T4, T5, T1);
            ComplMult(Ro3, T1, T2);
            ComplMult(Ro2, T2, T1);
            ComplAdd(Ro2, Ro3, T2);
            ComplMult(S22, T2, T3);
            T2.r := - 1;
            T2.j := 0;
            ComplMult(T2, T3, T4);
            ComplAdd(T4, T1, T2);
            T1.r := 1;
            T1.j := 0;
            ComplAdd(T1, T2, T3);

            ComplSub(S22, S23, T1);
            ComplMult(T1, Ro3, T2);
            T1.r := 1;
            T1.j := 0;
            ComplSub(T1, T2, T4);
            ComplDiv(T4, T3, T1);
            ComplMult(T1, S12, d2)
        End;
```

```
Procedure Calcd3(S22, S23, S12, Ro2, Ro3: Complex;
                 Var d3: Complex);

    Var
        T1, T2, T3, T4, T5: Complex;
    Begin
        ComplMult(S22, S22, T4);
        ComplMult(S23, S23, T5);
        ComplSub(T4, T5, T1);
        ComplMult(Ro3, T1, T2);
        ComplMult(Ro2, T2, T1);
        ComplAdd(Ro2, Ro3, T2);
        ComplMult(S22, T2, T3);
        T2.r := - 1;
        T2.j := 0;
        ComplMult(T2, T3, T4);
        ComplAdd(T4, T1, T2);
        T1.r := 1;
        T1.j := 0;
        ComplAdd(T1, T2, T3);

        ComplSub(S22, S23, T1);
        ComplMult(T1, Ro2, T2);
        T1.r := 1;
        T1.j := 0;
        ComplSub(T1, T2, T4);
        ComplDiv(T4, T3, T1);
        ComplMult(T1, S12, d3)
    End;


Procedure CalcRoA(A, B: Real;
                  Var RoA: Complex);

    Var
        T1, T2, T3: Complex;
    Begin
        T1.r := A - 50;
        T1.j := B;
        T2.r := A + 50;
        T2.j := B;
        ComplDiv(T1, T2, RoA);
    End;


Procedure CalcDelV(d2, d3, Ro2, Ro3: Complex;
                   Var DelV: Complex);

    Var
        T1, T2, T3: Complex;
    Begin
        T1.r := 1;
        T1.j := 0;
        ComplAdd(T1, Ro2, T2);
        ComplMult(T2, d2, T1);
```

```
        T2.r := 1;
        T2.j := 0;
        ComplAdd(T2, Ro3, T3);
        ComplMult(T3, d3, T2);

        ComplSub(T1, T2, DelV)
    End;

Begin
    Writeln;
    Writeln;
    Writeln('*************************************************************');
    Writeln('*                                                           *');
    Writeln('*  This program calculates the outgoing powers of a         *');
    Writeln('*  Wilkinson Power Splitter and the dissipated power in     *');
    Writeln('*  the resistor, relative to the ingoing power, as          *');
    Writeln('*  function of the frequency.                               *');
    Writeln('*  For each frequencystep the power balance will be         *');
    Writeln('*  checked.                                                 *');
    Writeln('*  Port 3 has no additional transmission line of length     *');
    Writeln('*  Lambda(res)/4. Both output ports are terminated with     *');
    Writeln('*  microstrip patches, analysed by the cavity model         *');
    Writeln('*                                                           *');
    Writeln('*************************************************************');
    Writeln;
    Writeln;

    Write('fr  (in GHz)        : ');
    Readln(fr);
    fr := fr * 1E9;
    Write('Epsr                : ');
    Readln(Epsr);
    Write('h  (in mm)          : ');
    Readln(h);
    h := h / 1000;
    Write('tan(delta)          : ');
    Readln(delta);
    Write('ro (fraction of a)  : ');
    Readln(ro);
    Writeln;
    Write('Output file         : ');
    Readln(FName);
    Assign(Uitvoer, FName);
    Rewrite(Uitvoer);
    Writeln;
    Writeln;
    Writeln;
```

```
ae := (ka * C0) / (2 * Pi * fr * Sqrt(Epsr));
a := RtSec(0.001, 1.99 * ae, 1E-6);
Writeln('Succeeded in finding radius patch');
ro := ro * a;
Writeln;

Writeln(Uitvoer);
Writeln(Uitvoer, 'frequency (res): ', (fr / 1E9): 8: 4, ' GHz');
Writeln(Uitvoer, 'Epsr           : ', Epsr: 8: 4);
Writeln(Uitvoer, 'h              : ', (h * 1000): 8: 4, ' mm');
Writeln(Uitvoer, 'tan(delta)     : ', delta: 9: 5);
Writeln(Uitvoer);
Writeln(Uitvoer, 'Radius patch   : ', a: 9: 5, ' m');
Writeln(Uitvoer, 'ro             : ', (ro / a): 9: 5, '*a');
Writeln(Uitvoer);
Writeln(Uitvoer);
Writeln(Uitvoer);
Writeln(Uitvoer);
Writeln(Uitvoer, ' ': 2, 'f(GHz)', ' ': 6, 'Plret', ' ': 6, 'P2',
        ' ': 6, 'P3', ' ': 6, 'Pdiss', ' ': 6, 'Total P');
Writeln(Uitvoer);

LowerB := 0.9 * fr;
UpperB := 1.1 * fr;
Step := 0.002 * fr;
f := LowerB;
i := 1;
While (f <= UpperB) And (i <= MaxPlotGlb) Do
    Begin

        W := 2 * Pi * f;
        k0 := (2 * Pi * f) / C0;
        Lambda := C0 / (f * Sqrt(Epsr));
        k := (2 * Pi) / Lambda;
        QGaus(0, Pi, I1);
        Writeln('Integration completed');
        RR := R(f);
        QQ := Q(f);
        L := RR / (2 * Pi * fr * QQ);
        C := QQ / (2 * Pi * RR * fr);
```

```
            AA := A1(w);
            BB := B(w);

            CalcS11(f, S11);
            CalcS22(f, S22);
            CalcS23(f, S23);
            CalcS12(f, S12);
            CalcRoA(AA, BB, RoA);
            Ro2 := RoA;
            Ro3 := RoA;
            Calcd1(S11, S22, S23, S12, Ro2, Ro3, d1);
            Calcd2(S22, S23, S12, Ro2, Ro3, d2);
            ComplMult(Ro2, d2, c2);
            Calcd3(S22, S23, S12, Ro2, Ro3, d3);
            ComplMult(Ro3, d3, c3);
            CalcDelV(d2, d3, Ro2, Ro3, DelV);
            P1ret[i, 1] := f;
            P1ret[i, 2] := Sqr(ComplMod(d1));
            P2[i, 1] := f;
            P2[i, 2] := (Sqr(ComplMod(d2)) - Sqr(ComplMod(c2)));
            P3[i, 1] := f;
            P3[i, 2] := (Sqr(ComplMod(d3)) - Sqr(ComplMod(c3)));
            Pdiss[i, 1] := f;
            Pdiss[i, 2] := (Sqr(ComplMod(DelV))) / 2;

            Writeln(Uitvoer, (f / 1E9): 8: 4, ' ': 2, P1ret[i, 2]: 8: 4,
                    ' ': 2, P2[i, 2]: 8: 4, ' ': 2, P3[i, 2]: 8: 4, ' ':
                   2, Pdiss[i, 2]: 8: 4, ' ':2, (P1ret[i, 2] + P2[i, 2]
                   + P3[i, 2] + Pdiss[i, 2]));
            Writeln('f (GHz)              : ', (f / 1E9): 8: 4);

            If Abs(1 - P1ret[i, 2] - (P2[i, 2] + P3[i, 2] +
               Pdiss[i, 2])) <= 5E-2 Then
                Writeln('Power Balance OK')
            Else
                Writeln('!*!*!*!*!*!* POWER BALANCE WRONG !*!*!*!*!*!*');

            i := i + 1;
            f := f + Step
        End;

    Close(Uitvoer)
End.
```

G.7 - Program WILKPOW2, Modified Parts of WILKPOW1

```
Procedure CalcRo3(f: Real;
                  Var Ro3: Complex);

    Var
        T1, T2: Complex;
    Begin
        T1.r := Cos((Pi) * (f / fr));
        T1.j := -Sin((Pi) * (f / fr));
        T2.r := Roo3.r;
        T2.j := Roo3.j;
        ComplMult(T1, T2, Ro3)
    End;
```

```
Begin
    Writeln;
    Writeln;
    Writeln('************************************************************');
    Writeln('*                                                          *');
    Writeln('*  This program calculates the outgoing powers of a        *');
    Writeln('*  Tee Power Splitter and the dissipated power in          *');
    Writeln('*  the resistor, relative to the ingoing power, as         *');
    Writeln('*  function of the frequency.                              *');
    Writeln('*  For each frequencystep the power balance will be        *');
    Writeln('*  checked.                                                *');
    Writeln('*  Port 3 has an additional transmission line of length    *');
    Writeln('*  Lambda(res)/4. Both output ports are terminated with    *');
    Writeln('*  microstrip patches, analysed by the cavity model        *');
    Writeln('*                                                          *');
    Writeln('************************************************************');
    Writeln;
    Writeln;
```

```
CalcS11(f, S11);
CalcS22(f, S22);
CalcS23(f, S23);
CalcS12(f, S12);
CalcRoA(AA, BB, RoA);
Ro2 := RoA;
Roo3 := RoA;
CalcRo3(f, Ro3);
Calcd1(S11, S22, S23, S12, Ro2, Ro3, d1);
Calcd2(S22, S23, S12, Ro2, Ro3, d2);
ComplMult(Ro2, d2, c2);
Calcd3(S22, S23, S12, Ro2, Ro3, d3);
ComplMult(Ro3, d3, c3);
P1ret[i, 1] := f;
P1ret[i, 2] := Sqr(ComplMod(d1));
P2[i, 1] := f;
P2[i, 2] := (Sqr(ComplMod(d2)) - Sqr(ComplMod(c2)));
P3[i, 1] := f;
P3[i, 2] := (Sqr(ComplMod(d3)) - Sqr(ComplMod(c3)));
Pdiss[i, 1] := f;
Pdiss[i, 2] := 0;

Writeln(Uitvoer, (f / 1E9): 8: 4, ' ': 2, P1ret[i, 2]: 8: 4,
        ' ': 2, P2[i, 2]: 8: 4, ' ': 2, P3[i, 2]: 8: 4, ' ':
       2, Pdiss[i, 2]: 8: 4, ' ':2, (P1ret[i, 2] + P2[i, 2]
       + P3[i, 2] + Pdiss[i, 2]));
```

G.8 - Program DISTURBW, Modified Parts of WILKPOW1

```
Procedure CalcRoA(A, B: Real;
                  Var RoA: Complex);

    Var
        T1, T2, T3: Complex;
    Begin
        T1.r := A - 50;
        T1.j := B;
        T2.r := A + 50;
        T2.j := B;
        ComplDiv(T1, T2, RoA);
    End;

Procedure CalcRoA1(A, B: Real;
                  Var RoA1: Complex);

    Var
        T1, T2, T3: Complex;
    Begin
        T1.r := Factor * A - 50;
        T1.j := Factor * B;
        T2.r := Factor * A + 50;
        T2.j := Factor * B;
        ComplDiv(T1, T2, RoA1);
```

```
Begin
    Writeln;
    Writeln;
    Writeln('*************************************************************');
    Writeln('*                                                           *');
    Writeln('*  This program calculates the outgoing powers of a         *');
    Writeln('*  Wilkinson Power Splitter and the dissipated power in     *');
    Writeln('*  the resistor, relative to the ingoing power, as          *');
    Writeln('*  function of the frequency.                               *');
    Writeln('*  For each frequencystep the power balance will be         *');
    Writeln('*  checked.                                                 *');
    Writeln('*  Port 3 has no additional transmission line of length     *');
    Writeln('*  Lambda(res)/4. Both output ports are terminated with     *');
    Writeln('*  microstrip patches, analysed by the cavity model         *');
    Writeln('*  A match disturbance is made by taking Z3 = Factor*Z2     *');
    Writeln('*************************************************************');
    Writeln;
    Writeln;
    Writeln;

    Write('fr  (in GHz)        : ');
    Readln(fr);
    fr := fr * 1E9;
    Write('Epsr                : ');
    Readln(Epsr);
    Write('h  (in mm)          : ');
    Readln(h);
    h := h / 1000;
    Write('tan(delta)          : ');
    Readln(delta);
    Write('ro (fraction of a)  : ');
    Readln(ro);
    Writeln;
    Write('Output file         : ');
    Readln(FName);
    Assign(Uitvoer, FName);
    Rewrite(Uitvoer);
    Writeln('Z3 = Factor*Z2');
    Write('Factor              : ');
    Readln(Factor);
    Writeln;
    Writeln;
    Writeln;
```

G.9 - Program Teepow1, Modified Parts of WILKPOW1

```
Procedure CalcS11(f: Real;
                  Var S11: Complex);

    Var
        T1, T2: Complex;

    Begin
        T1.r := -(1 / 3) * Cos(2 * Pi * (f / fr));
        T1.j := (1 / 3) * Sin(2 * Pi * (f / fr));
        S11 := T1
    End;


Procedure CalcS22(f: Real;
                  Var S22: Complex);

    Var
        T1, T2: Complex;
    Begin
        T1.r := -1;
        T1.j := 4 * Tan(Pi * (f / fr));
        T2.r := 3;
        T2.j := 6 * Tan(Pi * (f / fr));
        ComplDiv(T1, T2, S22)
    End;


Procedure CalcS23(f: Real;
                  Var S23: Complex);

    var
        T1, T2: Complex;
    Begin
        T1.r := 2;
        T1.j := -2 * Tan(Pi * (f / fr));
        T2.r := 3;
        T2.j := 6 * Tan(Pi * (f / fr));
        ComplDiv(T1, T2, S23)
    End;

Procedure CalcS12(f: Real;
                  Var S12: Complex);

    Var
        T1, T2, T3: Complex;
    Begin
        T2.r := (2 / 3) * Cos(Pi * (f / fr));
        T2.j := -(2 / 3) * Sin(Pi * (f / fr));
        S12 := T2
    End;
```

G.10 - Bessel.Fnc

```
FUNCTION bessj0(x: real): real;
VAR
   ax,xx,z: real;  y,ans,ans1,ans2: real;
BEGIN
  IF x=0 THEN bessj0:=1 ELSE
   IF (abs(x) < 8.0) THEN BEGIN
      y := sqr(x);
      ans1 := 57568490574.0+y*(-13362590354.0+y*(651619640.7
         +y*(-11214424.18+y*(77392.33017+y*(-184.9052456)))));
      ans2 := 57568490411.0+y*(1029532985.0+y*(9494680.718
         +y*(59272.64853+y*(267.8532712+y*1.0))));
      bessj0 := ans1/ans2  END
   ELSE BEGIN
      ax := abs(x); z := 8.0/ax; y := sqr(z); xx := ax-0.785398164;
      ans1 := 1.0+y*(-0.1098628627e-2+y*(0.2734510407e-4
         +y*(-0.2073370639e-5+y*0.2093887211e-6)));
      ans2 := -0.1562499995e-1+y*(0.1430488765e-3
         +y*(-0.6911147651e-5+y*(0.7621095161e-6
         -y*0.934945152e-7)));
      ans := sqrt(0.636619772/ax)*(cos(xx)*ans1-z*sin(xx)*ans2);
      bessj0 := ans  END
END;

FUNCTION bessj1(x: real): real;
VAR
   ax,xx,z: real;  y,ans,ans1,ans2: real;
FUNCTION sign(x: real): real;
   BEGIN
    IF x=0 THEN bessj1:=0 ELSE
      IF x >= 0.0 THEN sign := 1.0
      ELSE sign := -1.0;
   END;
BEGIN
   IF (abs(x) < 8.0) THEN BEGIN
      y := sqr(x);
      ans1 := x*(72362614232.0+y*(-7895059235.0+y*(242396853.1
         +y*(-2972611.439+y*(15704.48260+y*(-30.16036606))))));
      ans2 := 144725228442.0+y*(2300535178.0+y*(18583304.74
         +y*(99447.43394+y*(376.9991397+y*1.0))));
      bessj1 := ans1/ans2  END
   ELSE BEGIN
      ax := abs(x); z := 8.0/ax; y := sqr(z); xx := ax-2.356194491;
      ans1 := 1.0+y*(0.183105e-2+y*(-0.3516396496e-4
         +y*(0.2457520174e-5+y*(-0.240337019e-6))));
      ans2 := 0.04687499995+y*(-0.2002690873e-3
         +y*(0.8449199096e-5+y*(-0.88228987e-6+y*0.105787412e-6)));
      ans := sqrt(0.636619772/ax)*(cos(xx)*ans1
         -z*sin(xx)*ans2)*sign(x);
      bessj1 := ans  END
END;
```

```
FUNCTION bessj(n: integer; x: real): real;
CONST
   iacc=40;
   bigno=1.0e10;
   bigni=1.0e-10;
VAR
   bj,bjm,bjp,sum,tox,ans: real;
   j,jsum,m: integer;
BEGIN
  IF x=0 THEN bessj:=0 ELSE
  BEGIN
   IF (n < 2) THEN BEGIN
      writeln('pause in BESSJ'); readln
   END;
   tox := 2.0/x;
   IF (x > 1.0*n) THEN BEGIN
      bjm := bessj0(x);
      bj := bessj1(x);
      FOR j := 1 to n-1 DO BEGIN
         bjp := j*tox*bj-bjm;
         bjm := bj;
         bj := bjp
      END;
      ans := bj
   END ELSE BEGIN
      m := 2*((n+trunc(sqrt(1.0*(iacc*n)))) DIV 2);
      jsum := 0;
      sum := 0.0;
      bjp := 0.0;
      bj := 1.0;
      FOR j := m DOWNTO 1 DO BEGIN
         bjm := j*tox*bj-bjp;
         bjp := bj;
         bj := bjm;
         IF (abs(bj) > bigno) THEN BEGIN
            bj := bj*bigni;
            bjp := bjp*bigni;
            ans := ans*bigni;
            sum := sum*bigni
         END;
         IF (jsum <> 0) THEN sum := sum+bj;
         jsum := 1-jsum;
         IF (j = n) THEN ans := bjp
      END;
      sum := 2.0*sum-bj;
      ans := ans/sum
   END;
   bessj := ans
  END
END;
```